EFFECTS OF EUGENOL ON THE CEREBRAL, CEREBELLAR CORTICES AND HIPPOCAMPUS FOLLOWING ORAL ADMINISTRATION OF ALUMINIUM CHLORIDE IN WISTAR RATS

BY

MESOLE SAMUEL BOLAJI

(B.Sc, Unilorin 2008; M.Sc Unilorin, 2011)

P13MDHA9002

Ph.D THESIS SUBMITTED TO THE DEPARTMENT OF HUMAN ANATOMY, FACULTY OF BASIC MEDICAL SCIENCES, COLLEGE OF MEDICAL SCIENCES AHMADU BELLO UNIVERSITY, ZARIA

April, 2020.

EFFECTS OF EUGENOL ON THE CEREBRAL, CEREBELLAR CORTICES AND HIPPOCAMPUS FOLLOWING ORAL ADMINISTRATION OF ALUMINIUM CHLORIDE IN WISTAR RATS

BY

MESOLE SAMUEL BOLAJI, B.Sc, M.Sc (Unilorin)

P13MDHA9002

A THESIS SUBMITTED TO THE SCHOOL OF POSTGRADUATE STUDIES, AHMADU BELLO UNIVERSITY, ZARIA IN PARTIAL FUFILLMENT OF THE REQUIREMENTS FOR THE AWARD OF DOCTOR OF PHILOSOPHY (Ph.D) DEGREE IN HUMAN ANATOMY

DEPARTMENT OF HUMAN ANATOMY
FACULTY OF BASIC MEDICAL SCIENCES
COLLEGE OF MEDICAL SCIENCES
AHMADU BELLO UNIVERSITY, ZARIA NIGERIA

APRIL, 2020.

DECLARATION

I Bolaji Samuel MESOLE, hereby declare that the work in this thesis entitled "EFFECTS OF EUGENOL ON THE CEREBRAL, CEREBELLAR CORTICES AND HIPPOCAMPUS FOLLOWING ORAL ADMINISTRATION OF ALUMINIUM CHLORIDE IN WISTAR RATS" has been carried out by me at the Department of Human Anatomy. The information derived from this literature has been duly acknowledged in the text and a list of references provided. No part of this thesis has been previously presented for another degree or diploma at this or any other institution.

Bolaji Samuel MESOLE _____ _____

Signature Date

CERTIFICATION

This Thesis titled "EFFECTS OF EUGENOL ON THE CEREBRAL, CEREBELLAR CORTICES AND HIPPOCAMPUS FOLLOWING ORAL ADMINISTRATION OF ALUMINIUM CHLORIDE IN WISTAR RATS" by Samuel Bolaji MESOLE meets the regulation governing the award of the degree of Doctor of Philosophy of the Ahmadu Bello University, Zaria and it's approved for it's contribution to knowledge and literary presentation.

Dr. Sunday Musa. B.Sc, M.Sc, Ph.D **Chairman** Supervisory Committee Department of Human Anatomy Faculty of Basic Medical Sciences Ahmadu Bello University Zaria.	Signature	Date
Prof. A.O Ibegbu. B.Sc, M.Sc, Ph.D Member Supervisory Committee Department of Human Anatomy Alex Ekwueme University Ndufu Alike, Ebonyi state.	Signature	Date
Dr. Zainab Bauchi B.Sc, M.Sc Ph.D Member Supervisory Committee Department of Human Anatomy Faculty of Basic Medical Sciences Ahmadu Bello University Zaria.	Signature	Date
Dr. Zainab Bauchi B.Sc M.Sc Ph.D Head of Department Department of Human Anatomy Faculty of Basic Medical Sciences Ahmadu Bello University Zaria.	Signature	Date
Prof. S.A Sani Dean, School of Postgraduate Studies Ahmadu Bello University, Zaria	Signature	Date

ACKNOWLEDGEMENTS

My sincere and profound appreciation first goes to Almighty God for his divine favour of wisdom and power, enduring goodness, mercy, and grace bestowed upon me throughout my educational pursuit for this degree in Zaria this dissertation.

My sincere gratitude goes to my competent supervisor: Prof A.O Ibegbu, 'thanks for been a wonderful father and mentor; Dr Sunday Musa and Dr Zainab Bauchi for their immense guidance, supervision, and professional advice throughout the duration of this study.

My heart felt gratitude goes to my parents, Chief and Mrs James O. Mesole for their immeasurable love, care, and support given to me. To my brothers Mr David O. Mesole, Mr Evans O. Mesole, Mr Oladipupo J. Mesole, and Mr Gbenga J. Mesole to you all I say a big thank you.

My Profound gratitude goes also to my wife, Mesole Y. Helen for being supportive and always right beside me. Your love is always a source of strength for me and a major pillar behind the success of this degree. You gave me the best gifts I could ever ask for our son and daughter, Mesole O. Jayden and Mesole A. Ifeoluwa who has always been a source of inspiration for me and a source of strength.

This section will not be complete without acknowledging the tireless effort of Dr. Abel N. Abgon and Mr Ivang Andrew who painstakingly worked with me tirelessly in the lab and your effort to make this study a success will not go unnoticed.

My gratitude goes to Prof. Sunday Adebisi, Dr. Buraimoh and also my brother in-law Kolawole, Tosin God bless you all.

TABLE OF CONTENTS

Contents Pages

Cover page i

Title page ii

DECLARATION iii

CERTIFICATION iv

ACKNOWLEDGEMENTS v

TABLE OF CONTENTS vi

LIST OF FIGURES xiv

LIST OF TABLES xvii

LIST OF PLATES xviii

ABSTRACT xxx

INTRODUCTION 1

1.1 Background Information 1

1.2 Aluminium 3

1.3 Statement of Research Problem 5

1.4 Justification of Study 6

1.5 Significance of the Study 6

1.6 Study Hypothesis 7

1.7 Aims and Objectives of the Study 7

1.7.1 Aim 7

1.7.2 Objectives 7

CHAPTER TWO 9

2.0 Literature Review 9

2.1 Aluminium 9

2.1.1 Definition 10

2.1.2 Chemistry 11

2.1.3 History 12

2.1.4 Toxicity 14

2.1.4.1 Sources of Aluminium Exposure 15

2.1.4.1.1 Aluminium in Food 15

2.1.4.1.2 Aluminium in Pharmaceutical Products 16

2.1.4.2.3 Aluminium-Triggered Immune and Inflammatory Responses in the CNS 17

2.1.4.1.4 Aluminium and Energy Metabolism 19

2.1.4.1.5 Aluminum and Oxidative Damage 20

2.1.4.1.6 Aluminium and Brain Inflammation 21

2.1.5 Absorption and Distribution of Bioavailable Aluminium 21

2.1.6 Eugenol 23

2.1.6.1 Pharmacological Actions of Eugenol 24

2.1.6.2 Local Anaesthesia 25

2.1.6.3 Antioxidant Function 25

2.1.6.4 Antibiotic Activity 26

2.1.6.5 Anticancer Activity 27

2.1.6.6 Antibacterial and Antiviral Effects 28

2.1.6.7 Anti-insect Activity 28

2.2 Brain 29
2.2.1 Embryology 30
2.2.1.1 Origin of the Nervous system 30
2.2.1.2 Development of the Brain 32
Midbrain 33
Hindbrain 34
Myelencephalon 34
Metencephalon 35
2.2.1.3 Gross Anatomy 36
2.2.1.3.1 Cerebrum 37
2.2.1.3.2 Hippocampus 37
Role in memory 38
Role in spatial memory and navigation 39
2.2.1.3.3 Midbrain 40
2.2.1.3.4 Pons 41
2.2.1.3.5 Medulla 41
2.2.1.3.6 Cerebellum 41
2.3.3 Brain Histology 43
2.3.3.1 Cerebrum 43
2.3.3.1.1 Neurone Types in the Cerebral cortex 43
2.3.3.1.2 Layers of the Neocortex 45
2.3.3.2 Hippocampus 47
2.3.3.3 Cerebellum 49

2.3.4 Histometry 51
2.3.5 Neurobehavioral testing 52
2.3.5.1 Learning and memory 53
Morris water maze 53
2.3.5.2 Anxiety-Like Behaviour 54
Elevated Plus maze 54
2.3.5.3 Forelimb grip Strength test time 54
CHAPTER THREE 55
MATERIALS AND METHODS 55
3.1 Materials 55
3.1.1 Experimental Animals 55
Drugs 55
Eugenol 55
Aluminium 56
3.1.3 Neurobehavioral Set-up 56
Animal Feed 56
Methodology 57
3.2.1 Dose Preparation of Eugenol. 57
3.2.2 Dose preparation of Aluminium 57
3.2.3 Experimental Design 57
Experimental Procedure 58
Neurobehavioral/Cognitive Studies 59
Elevated Plus Maze Test 59

Modified Elevated Plus Maze Open arm duration 60
Morris Water Maze Test 61
Procedure: 61
Sensori-motor Activity, Motor Coordination 62
Forelimb Grip Strength Time Test 62
Morphological Studies 64
3.2.4.4 Histometric Studies 64
3.2.4.5 Histological, Histochemical and Immunohistochemical studies 65
3.2.4.6 Neurochemical and Biochemical Studies 66
3.2.4.7 Oxidative Stress Markers 68
3.2.4.8 Isolation of Mitochondrial DNA (mtDNA) 68
3.2.4.9 Oxidative stress in Mitochondrial DNA 69
3.2.4.10 Determination of Apoptotic markers 70
Data Analysis 70
CHAPTER FOUR 71
Results 71
4.1 Physical Observation 71
4.2 Morphological Studies 73
4.2.1 Morphometry 73
4.3 Histometric Studies 75
4.3.1 Cerebral and Cerebellar Cortices Histometric Characteristics 75
4.3.2 Hippocampal Cell (CA1 and CA3) Histometric Characteristics 78
4.4 Histological and Histochemical Studies 81

4.4.1 Histological Features of the Cerebral Cortex 81
4.4.1.1 Histological and Histochemical Features of the Cerebral Cortex of Control (Untreated) and Treated Wistar Rats 81
4.4.2 Histological and Histochemical Features of the Cerebellar Cortex 107
4.4.2.1 Histological and Histochemical Features of the Cerebellar Cortex of Control 107
(Untreated) and Treated Wistar Rat 107
4.4.3 Histological and Histochemical Features of the Hippocampus 132
4.4.3.1 Histological, Histochemical and Immunohistochemical Features of the Hippocampus of the Control (Untreated), Wistar rat 132
4.4.3.2 Histological, Histochemical and Immunohistochemical Features of the Hippocampus of Treated Wistar Rats 133
4.5 Neurobehavioral Studies 159
4.5.1 Elevated plus Maze (EPM) Studies 159
4.5.1.1 EPM Open arm Duration 159
4.5.1.2 Modified Elevated Plus Maze (EPM) Close arm duration 161
4.5.1.3 Modified Elevated Plus Maze (EPM) Rearing Frequency 163
4.5.1.4 Grooming (cephalocaudal axis) 165
4.5.1.5 Forelimb grip Strength Time (FGST) 167
4.5.1.6 Morris Water Maze Studies (MWM) 170
4.6 Neurochemical and Biochemical Studies 175
4.6.1 Neurochemistry of Neuro-trace Elements 175
4.6.3 Intramitochondrial accumulation of 8-Hydroxy-2-deoxyguanosine (8-OHdG) 185

4.6.4 Effect of Eugenol on Caspase- 3 proteins following administration of aluminium chloride. 186
4.6.5 Effect of Eugenol on proapoptotic (Bax) and antiapoptotic (Bcl-2) protein following administration of aluminium chloride..... 188
4.6.6 Biochemistry of Endogenous Enzyme Activity..... 191
CHAPTER FIVE 193
5.1 Discussion..... 193
5.2 Physical Observation..... 193
5.3 Morphological Studies 194
5.4 Histological and Histochemical Studies..... 196
5.5 Neurochemical/ Biochemical Studies 209
5.6 Intramitochondrial accumulation of 8-OHdG..... 219
5.7 Proaoptotic and Antiapoptotic Proteins (Bax and Bcl-2)..... 220
5.8 Caspase -3 activation..... 221
5.9 Acetylcholinesterase 222
5.10 Immunohistological and Immunohistochemical Studies 224
CHAPTER SIX..... 227
Summary, Conclusion and Recommendation..... 227
6.1 Summary 227
6.2 Contribution to knowledge..... 228
6.3 Conclusion..... 230
6.4 Recommendation..... 230
REFERENCES..... 231

APPENDIX I 262

APPENDIX II 264

APPENDIX III 266

APPENDIX IV 270

APPENDIX V 271

APPENDIX VI 272

APPENDIX VII 273

APPENDIX VIII 274

APPENDIX IX 276

LIST OF FIGURES

Figure 2.1: Sections of the brain and spinal cord 30

Figure 2.2: Embryonic Development of the Neural Tube 32

Figure 2.3: Development of the Brain 33

Figure 2.4: Development of the Froebrain, Midbrain and Hind Brain 36

Figure 2.5 Midsagittal Section of the Brain 42

Figure 2.6: Histological Organization of the Cerebral cortex 47

Figure 2.7: Histological Photomicrograph of the Hippocampus 49

Figure 2.8: Histological PhotoMicrograph of the Cerebelar Cortex 51

Figure 3.1: Elevated Plus Maze set up 61

Figure 3.2: Morris Water Maze set up for memory and spatial navigation 62

Figure 4.1: Effect of eugenol on brain/body weight index following administration of aluminium chloride 74

Figure 4.1: Histological Photomicrograph of the Hippocampus showing different regioms 132

Figure 4.5a: Effect of Eugenol on Open arm duration (seconds) following administration of aluminium chloride. 160

Figure 4.5b: Effect of Eugenol on Close arm duration following administration of aluminium chloride 162

Figure 4.5c: Effect of Eugenol on rearing frequency in elevated plus maze following administration of aluminium chloride. 164

Figure 4.5d: Effect of Eugenol on Grooming following administration of aluminium chloride in Wistar rats elevated 166

Figure 4.5e: Effect of Eugenol on Forelimb grip strength following exposure to aluminium chloride in Wistar rats..... 169
Figure 4.5f: Transfer Latency of Wistar rats on Morris water maze habituation. 171
Figure 4.5g: Effect of Eugenol on Cognition (Morris water maze) following administration of aluminium chloride. 174
Figure 4.6a: Effect of Eugenol on Neurotrace Brain element (Iron Fe) following administration of aluminium chloride on Wistar rats. 176
Figure 4.6b: Effect of Eugenol on Neurotrace Brain element (Manganese Mn) following administration of aluminium chloride on Wistar rats. 177
Figure 4.6d: Effect of Eugenol on Neurotrace Brain element (Magnesium Mg) following administration of aluminium chloride on Wistar rats 178
Figure 4.6c: Effect of Eugenol on accumulation of aluminium in the Brain element following administration of aluminium chloride on Wistar rats. 179
Figure 4.6e: Effect of Eugenol on tissue (brain) MDA concentration following administration of aluminium chloride in Wistar rats. 181
Figure 4.6f: Effect of Eugenol on tissue (brain) SOD concentration following administration of aluminium chloride in Wistar rats. 182
Figure 4.6g: Effect of Eugenol on tissue (brain) CAT concentration following administration of aluminium chloride in Wistar rats. 183
Figure 4.6h: Effect of Eugenol on tissue (brain) GPx concentration following administration of aluminium chloride in Wistar rats. 184
Figure 4.7: Effect of eugenol on intramitochondrial accumulation of 8-OHdG levels following exposure to aluminium chloride (AC). 185

Figure 4.8: Effect of eugenol on brain caspase-3 levels following administration of aluminium chloride in Wistar rats..... 187

Figure 4.6I: Effect of Eugenol on tissue (brain) AchE concentration following administration of aluminium chloride in Wistar rats..... 192

LIST OF TABLES

Table 2.1: Chemical and Physical Properties of Aluminium 11

Table 3.0: Treatment of Experimental Animals 58

Table 4.1 Effects of Eugenol on body weight before and after administration of aluminium chloride 72

Table 4.2 Histometric analysis of the effect of Eugenol on cortical neurons of the cerebellum (Purkinje cells) and cerebrum (Pyramidal cells) of Wistar rats 77

Table 4.3 Histometric analysis of the effect of Eugenol on pyramidal neurons of the hippocampus (CA1 and CA3 regions) of Wistar rats 80

Table 4.4: Effect of eugenol on proapoptotic and antiapoptotic proteins following administration of aluminium chloride in wistar rats 190

LIST OF PLATES

Plate 3.1: Showing fore grip strength time set up 63

Plate 4.1: Section of the cerebral cortex 'A' (Layer III), 'B' (Layer V) of control (CTRL) group showing normal histology of the cerebral cortex: yellow arrow (Pyramidal cell); blue arrow (glial cell); White arrow (neuropil). (Mag x 250 H&E). 83

Plate 4.2: Section of the cerebral cortex 'A' (Layer III); B (Layer V) of aluminium treated group (AC) (100mg/kg of aluminium chloride) revealing a distorted histoarchitecture: (Yellow line Pyknotic Pyramidal cell 'P'), blue line (Chromatolysis (k) and green line 'perineuronal vacoulations PV) (Mag x 250 H&E) 84

Plate: 4.3: Section of Wistar rat cerebral cortex 'A' (Layer III) and 'B' (Layer V) of Group EGH+AC (300mg/kg Eugenol and 100mg/kg of Aluminium chloride) showing mild distortion and perineuronal vacoulations'PV' (blue line) in the cytoarchitecture when compared to the group administered 100mg/kg aluminium chloride only. Pyramidal cell 'P' yellow line (H&E x 250). 85

Plate 4.4: Section of Wistar rat cerebral cortex 'A' (Layer III) and 'B' (Layer V) of Group EGL+AC (150mg/kg of Eugenol and 100mg/kg of Aluminium chloride) showing mild distortion in the cytoarchitecture of the cerebral cortex with perineuronal vacoulations (PV) (blue line) when compared to the group that was administered 100mg/kg only. Pyramidal cell (P) (yellow line) (Mag x 250 H&E). 86

Plate 4.5: Section of the cerebral cortex 'A' (Layer III) and 'B' (Layer V) of Group (EGH) (300mg/kg of Eugenol) showing a normal cytoarchitecture of the cerebral cortex when compared to the control group. Pyramidal cell (P) (Yellow line) (Mag X 250 H&E). 87

Plate 4.6: Section of Wistar rat cerebral cortex ‘A’ (Layer III) and ‘B’ (Layer V) of Group (EGL) (150mg/kg of Eugenol) revealing a normal cytoarchitecture 0f the cerebral cortex when compared to the control group Pyramidal cell (P) (yellow line). (Mag x 250 H&E) 88

Plate 4.7: Section of the cerebral cortex ‘A ‘(layer III) and ‘B’ (layer V) of control (CTRL), showing the normal histology of the cerebral cortex. White line (Pyramidal cell (P); Red line (Neuropil) (Mag x 250 CFV)..... 89

Plate 4.8: Section of the cerebral cortex ‘A’ (layer III); ‘B’ (layer V) of aluminium treated group (AC) (100mg/kg of aluminium chloride), showing distortion in the histology of cerebral cortex.White line (Pyramidal cell ‘P’), black line (Chromatolysis ‘k’), with Pyknotic cells and perineuronal vacoulations (PV) (Mag x 250 CFV). 90

Plate: 4.9: Section of Wistar rat cerebral cortex ‘A’ (Layer III) and ‘B’ (Layer V) of Group EGH+AC (300mg/kg Eugenol and 100mg/kg of Aluminium chloride) showing mild distortion and perineuronal vacoulations ‘PV’ (blue line) in the cytoarchitecture when compared to the group administered 100mg/kg aluminium chloride only. Pyramidal cell ‘P’ (white line) (Mag x 250 CFV)..... 91

Plate 4.10: Section of the cerebral cortex ‘A’ (Layer III) and ‘B’ (Layer V) of Group EGL+AC (150mg/kg of Eugenol and 100mg/kg of aluminium chloride) showing mild distortion in the cytoarchitecture of the cerebral cortex with mild perineuronal vacoulations ‘PV’(blue line) when compared with the group administered 100mg/kg of aluminium chloride only. Pyramidal cell ‘P’ (white line) (Mag x 250 CFV)..... 92

Plate 4.11: Section of Wistar rat cerebral cortex ‘A’ (Layer III) and ‘B’ (Layer V) of Group (EGH) (300mg/kg of Eugenol) showing a normal cytoarchitecture of the cerebral cortex when compared with the control group. Pyramidal cell ‘P’ (white line) (Mag x 250 CFV)..... 93

Plate 4.12: Section Wistar rat cerebral cortex ‘A’ (Layer III) and ‘B’ (Layer V) of Group EGL (150mg/kg of eugenol) revealing a normal cytoarchitecture of the cerebral cortex when compared to the control. Pyramidal cell ‘P’ (black line) (Mag x 250 CFV). 94

Plate 4.13: Section of Wistar rat cerebral cortex ‘A’ (Layer III) and ‘B’ (Layer V) of control (CTRL) (Untreated) showing normal cytoarchitecture of the cerebral cortex; Pyramidal cell ‘P’ (black line). (Mag x 250 Congo red). 95

Plate 4.14: Section of Wistar rat cerebral cortex ‘A’ (Layer III) and ‘B’ (Layer V) of aluminium treated group (AC) (100mg/kg of aluminium chloride) with no visible amyloid plaques within the cerebral cortex. Pyramidal cell ‘P’ (black line). (Mag x 250 Congo). 96

Plate 4.15: Section of Wistar rat cerebral cortex ‘A’ (Layer III) and ‘B’ (Layer V) EGH+AC (300mg/kg Eugenol and 100mg/kg of aluminium chloride) with no visible amyloid plaques within the cerebral cortex. Pyramidal cell ‘P’ (yellow line). (Mag x 250 Congo). 97

Plate 4.16: Section of Wistar rat cerebral cortex ‘A’ (Layer III) and ‘B’ (Layer V) of Group EGL+AC (administered 150mg/kg Eugenol and 100mg/kg of aluminium chloride) with no visible amyloid plaques within the cerebral cortex. Pyramidal cell ‘P’ (yellow line). (Mag x 250 Congo). 98

Plate 4.17: Section of Wistar rat cerebral cortex ‘A’ (Layer III) and ‘B’ (Layer V) EGH (300mg/kg of Eugenol) with no visible amyloid plaques. Pyramidal cell ‘P’ (yellow line) (Mag x 250 Congo red). 99

Plate 4.18: Section of Wistar rat cerebral cortex ‘A’ (Layer III) and ‘B’ (Layer V). EGH (150mg/kg of Eugenol) revealing no amyloid plaques in the cerebral cortex. Pyramidal cell ‘P’ (yellow line) (Mag x 250 Congo). 100

Plate 4.19: Section of Wistar rat cerebral cortex ‘A’ (Layer III) and ‘B’ (Layer V) of control (CTRL) showing the normal cytoarchitecture of cerebral cortex with pyramidal cells with its neural processes (Neurites). Pyramidal cell ‘P’ (yellow line). (Mag x 250 Golgi stain)..... 101

Plate 4.20: Section of the cerebral cortex ‘A’ (layer III); ‘B’ (layer V) of aluminium treated group (AC) (100mg/kg of aluminium chloride), showing distortion in the cytoarchitecture of the cerebral cortex, Neuronal degeneration (loss of neuronal process); Pyramidal cell ‘P’ (yellow line) (Mag x 250 Golgi stain). 102

Plate 4.21: Section of the cerebral cortex ‘A’ (layer III); ‘B’ (layer V) of Group EGH+ AC (300mg/kg Eugenol and 100mg/kg of aluminium chloride) showing distortion in the cytoarchitecture of the cerebral cortex, Neuronal degeneration (loss of neuronal process); Pyramidal cell ‘P’(yellow line) (Mag x 250 Golgi stain). 103

Plate 4.22: Section of the cerebral cortex ‘A’ (layer III); ‘B’ (layer V) of Group EGL+AC (150mg/kg Eugenol and 100mg/kg of aluminium chloride) showing mild distortion in the cytoarchitecture of the cerebral cortex when compared with the group administered 100mg/kg of aluminium chloride; Neuronal degeneration (loss of neuronal process); Pyramidal cell ‘P (yellow line) (Mag x 250 Golgi stain). 104

Plate 4.23: Section of Wistar rat cerebral cortex ‘A’ (Layer III) and ‘B’ (Layer V) of Group (EGH) (300mg/kg of Eugenol). Showing a normal cytoarchitecture of the cerebral cortex showing neuronal process (Neurites); Pyramidal cell ‘P’ (yellow line) (Mag x 250 Golgi). 105

Plate 4.24: Section of Wistar rat cerebral cortex ‘A’ (Layer III) and ‘B’ (Layer V) of Group EGL (150mg/kg of Eugenol) showing a normal cytoarchitecture of the cerebral cortex with its Neuronal process (Neurites). Pyramidal cell ‘P’ (yellow line) (Mag x 250 Golgi). 106

Plate 4.25: Section of Wistar rat cerebellar cortex of Group I control (CTRL) untreated group showing normal histology of the cerebellar cortex. Purkinje cell 'PK' (yellow line); Granular layer (GL); Molecular layer (M); Stellate cells 'S' (blue line) (Mag x 250 H&E). 108
Plate 4.26: Section of Wistar rat cerebellar cortex of the aluminium treated group (AC) (100mg/kg of aluminium chloride) showing distortion in the histology of the cerebellar cortex. Purkinje cell 'PK' (green line); Granular layer (GL); Molecular layer (M); Perineuronal vacoulations 'PV' (Yellow line) (Mag x 250 H&E). 109
Plate 4.27: Section of Wistar rat cerebellar cortex of Group (EGH+AC) (300mg/kg of Eugenol and 100mg/kg of aluminium chloride) showing a mild distortion in the cytoarchitecture of the cerebellar cortex with Perineuronal vacoulations 'PV' (yellow line) when compared with the group the received aluminium chloride. Purkinje cell 'PK' (green line); Stellate cell (S); Granular Layer (GL); Molecular layer (M) (Mag x 250 H&E)..... 110
Plate 4.28: Section of Wistar rat cerebellar cortex of Group EGL+AC (150mg/kg of Eugenol and 100mg/kg of aluminium chloride) showing a mild distortion in the cytoarchitecture of the cerebellar cortex with mild Perineuronal vacoulations (PV) when compared with the group the received aluminium chloride. Purkinje cell (PK); Stellate cell (S); Granular Layer (GL); Molecular layer (M) (Mag x 250 H&E)..... 111
Plate 4.29: Section of Wistar rat cerebellar cortex of Group EGH (300mg/kg of Eugenol) showing a normal cytoarchitecture of the cerebellar cortex. Purkinje cell 'PK' (green line); Molecular layer (M); Stellate cell 'S' (yellow line); Granular layer (GL) (Mag x 250 H&E). ... 112
Plate 4.30: Section of Wistar rat Cerebellar cortex of Group EGL (150mg/kg of Eugenol) revealing a normal cytoarchitecture of the cerebellar cortex. Granular layer (GL); Molecular layer (M); Stellate cell 'S' (yellow line); Purkinje cell 'PK' (green line) (Mag x 250 H&E). 113

Plate 4.31: Section of Wistar rat cerebellar cortex of the control (CTRL) untreated group showing normal histology of the cerebellar cortex. Purkinje cell 'PK' (white line); Granular layer (GL); Molecular layer (M); Stellate cells 'S' (green line) (Mag x 250 CFV). 114

Plate 4.32: Section of Wistar of cerebellar cortex of the aluminium treated group (AC) (100mg/kg of aluminium chloride) showing distortion in the cytoarchitecture of the cerebellar cortex. Purkinje cell 'PK' (white line); Granular Layer (GL); Molecular layer (M), Chromatolysis (red line) 'k'; Neuronal degeneration (Perineuronal vacoulations PV 'black line') (Mag x 250 CFV). 115

Plate 4.33: Section of Wistar rat cerebellar cortex of Group EGH+AC (300mg/kg of Eugenol and 100mg/kg of aluminium chloride) showing mild distortion in the cytoarchitecture of the cerebellar cortex with perineuronal vacoulations. Purkinje cell (PK); Stellate cell (S); Molecular layer (M); Granular layer (GL) (Mag x 250 CFV). 116

Plate 4.34: Section of Wistar rat cerebellar cortex of Group EGL+AC (150mg/kg of Eugenol and 100mg/kg of aluminium chloride) revealing a mild distortion in the cytoarchitecture of the cerebellar cortex with perineuronal vacoulations (PV). Granular Layer (GL); Purkinje layer (PK); Molecular layer (Mag x 250 CFV). 117

Plate 4.35: section of the cerebellar cortex of Group EGH (300mg/kg of Eugenol) revealing a normal cytoarchitecture of the cerebellar cortex. Granular Layer (GL); Purkinje cell (PK); Molecular layer (M) (Mag x 250 CFV). 118

Plate 4.36: Section of Wistar rat Cerebellar cortex of Group EGL (150mg/kg of Eugenol) revealing a normal cytoarchitecture of the cerebellar cortex. Granular layer (GL); Molecular layer (M); Stellate cell(S); Purkinje cell (PK) (Mag x 250 CFV). 119

Plate 4.37: Section of Wistar rat cerebellar cortex of the control (CTRL) untreated group showing normal histology of the cerebellar cortex. Purkinje cell (PK); Granular layer (GL); Molecular layer (M); Stellate cells (S) (Mag x 250 Congo red). 120
Plate 4.38: Section of Wistar rat cerebellar cortex of Group the aluminium treated (AC) group (AC) (100mg/kg of aluminium chloride), showing distortion the cytoarchitecture of the cerebellar cortex but no visible amyloid plaques. Granular Layer (GL); Purkinje cell (PK); Molecular Layer (M); Stellate cell (S) (Mag x 250 Congo). 121
Plate 4.39: Section of Wistar rat cerebellar cortex of Group EGH+AC (300mg/kg of Eugenol and 100mg/kg of aluminium chloride) showing distortion the cytoarchitecture of the cerebellar cortex but no visible amyloid plaques. Granular Layer (GL); Purkinje cell (PK); Molecular Layer (M); Stellate cell (S) (Mag x 250 Congo). 122
Plate 4.40: Section of Wistar rat cerebellar cortex of Group EGL+AC (150mg/kg of Eugenol and 100mg/kg of aluminium chloride) with mild distortion in the histology of the cerebellar cortex but no visible amyloid plaques. Purkinje cell (PK); Stellate cell (S); Molecular layer (M); Granular layer (GL) (Mag x 250 Congo red). 123
Plate 4.41: Section of the cerebellar cortex of Group EGH (300mg/kg of Eugenol) revealing a normal cytoarchitecture of the cerebellar cortex with no visible amyloid plaques. Granular Layer (GL); Purkinje cell (PK); Molecular layer (M) (Mag x 250 Congo red). 124
Plate 4.42: Section of Wistar rat Cerebellar cortex of Group EGL (150mg/kg of Eugenol) revealing a normal cytoarchitecture of the cerebellar cortex and no visible amyloid plaques. Granular layer (GL); Molecular layer (M); Stellate cell(S); Purkinje cell (PK) (Mag x 250 Congo red). 125

Plate 4.43: Section of Wistar rat Cerebellar cortex of the control (CTRL) (Untreated), Showing a normal ACAT-1 Immunoreactivity of the Purkinje cells of the cerebellar cortex. Granular layer (GL); Molecular layer (M); Purkinje cell (PK) (ACAT x 250). 126
Plate 4.44: Section of Wistar rat Cerebellar cortex of the AC group (100 mg/kg Aluminium chloride) revealing a reduced ACAT-1 Immunoreactivity of the purkinje cells of the cerebellar cortex. Granular layer (GL); Molecular layer (M); Purkinje cell (PK) (ACAT x 250). 127
Plate 4.45: Section of Wistar rat Cerebellar cortex of the EGH+AC group (300 mg/kg Eugenol and 100 mg/kg Aluminium chloride) revealing a restored ACAT-1 Immunoreactivity of the purkinje cells of the cerebellar cortex when compared to AC. Granular layer (GL); Molecular layer (M); Purkinje cell (PK) (ACAT x 250). 128
Plate 4.46: Section of Wistar rat Cerebellar cortex of the EGL+AC group (150 mg/kg Eugenol and 100 mg/kg Aluminium chloride) revealing a restored ACAT-1 Immunoreactivity of the purkinje cells of the cerebellar cortex when compared to AC group. Granular layer (GL); Molecular layer (M); Purkinje cell (PK) (ACAT x 250). 129
Plate 4.47: Section of Wistar rat Cerebellar cortex of the EGH (300 mg/kg Eugenol) revealing a high ACAT-1 Immunoreactivity of the purkinje cells of the cerebellar cortex when compared to AC group. Granular layer (GL); Molecular layer (M); Purkinje cell (PK) (ACAT x 250). 130
Plate 4.48: Section of Wistar rat Cerebellar cortex of EGL group (150mg/kg Eugenol), Showing a high ACAT-1 Immunoreactivity of the purkinje cells of the cerebellar cortex when compared to AC group. Granular layer (GL); Molecular layer (M); Purkinje cell (PK) (ACAT x 250). 131
Plate 4.49: Sections of Wistar rat hippocampal regions (CA1 and CA3) of the control (CTRL) untreated group showing normal cytoarchitecture of the hippocampus. Pyramidal cell (P (Mag x 250 H&E). 135

Plate 4.50: Sections of Wistar rat hippocampal regions (CA1 and CA3) of of the aluminium treated group (AC) (100mgkg of aluminium) showing distortion (Neuronal degeneration N) in the cytoarchitecture of the hippocampus. Pyramidal cell (P), Chromatolysis (K) (Mag x 250 H&E). 136

Plate 4.51: Sections of Wistar rat hippocampal regions (CA1 and CA3) of Group EGH+AC (300mg/kg Eugenol and 100mg/kg of aluminium chloride) showing mild distortion in the cytoarchitecture of the hippocampus. Pyramidal cell (P) (Mag x 250 H&E). 137

Plate 4.52: Section of Wistar rat hippocampal regions (CA1 and CA3) of Group EGL+AC (150mg/kg Eugenol and 100mg/kg of aluminium chloride) showing mild distortion with Neuronal degeneration (N). Pyramidal cell (P) (Mag x 250 H&E). 138

Plate 4.53: Sections of Wistar rat hippocampal regions (CA1 and CA3) regions of Group EGH (300mg/kg Eugenol) Showing a normal cytoarchitecture of the hippocampus when compared to the untreated group. Pyramidal cell (P) (Mag x 250 H&E). 139

Plate 4.54: Sections of Wistar rat's hippocampal region (CA1 and CA3) of Group EGL (150mg/kg Eugenol) showing a normal cytoarchitecture when compared to the control group. Pyramidal cell (P) (Mag x 250 H&E). 140

Plate 4.55: Sections of rat hippocampal regions (CA1 and CA3) of Group control (CTRL) untreated group showing normal cytoarchitecture of the hippocampus. Pyramidal cell (P); Fusiform cell (F) (Mag x 250 CFV). 141

Plate 4.56: Sections of Wistar rat hippocampal regions (CA1 and CA3) of the aluminium treated group (AC) (100mg/kg of aluminium chloride) showing distortion in the cytoarchitecture of the hippocampus. Pyramidal cell (P) (Mag x 250 CFV). 142

Plate 4.57: Section of Wistar rat hippocampal regions (CA1 and CA3) of Group (EGH+AC) (300mg/kg of Eugenol and 100mg/kg of aluminium chloride) showing mild distortion (Neuronal degeneration with perineuronal vacoulations N). Pyramidal cell (P) (Mag x 250 CFV). 143
Plate 4.58: Sections of Wistar rat hippocampal regions (CA1 and CA3) of Group EGL+AC (150mg/kg Eugenol and 100mg/kg of aluminium chloride) showing mild distortion in the cytoarchitecture of the hippocampus. Pyramidal cell (P); (Mag x 250 CFV). 144
Plate 4.59: Sections of Wistar at hippocampal regions (CA1 and CA3) of Group EGH (300mg/kg of Eugenol) Showing a normal cytoarchitecture of the hippocampus when compared with the control (Untreated). Pyramidal cell (P) (Mag x 250 CFV). 145
Plate 4.60: Section of Wistar rat hippocampal regions (CA1 and CA3) of Group EGL (150mg/kg Eugenol) showing a normal cytoarchitecture of the hippocampal region. (Pyramidal cell (P) (Mag x 250 CFV). 146
Plate 4.61: Sections of Wistar rat hippocampal regions (CA1 and CA3) of the control (CTRL) Untreated group showing a normal cytoarchitecture of the hippocampus with no visible amyloid plaques. Pyramidal cell (P) (Mag x 250 Congo red). 147
Plate 4.62: Sections of Wistar rat hippocampal regions (CA1 and CA3) of the aluminium treated group (AC) (100mg/kg of aluminium chloride) showing distortions in the cytoarchitecture of the hippocampus, but no visible amyloid plaques. Pyramidal cell (P) (Mag x 250 Congo red). 148
Plate 4.63: Sections of Wistar rat hippocampal regions (CA1 and CA3) of Group (EGH+AC) (300mg/kg Eugenol and 100mg/kg of aluminium chloride) showing mild distortion but no visible amyloid plaques. Pyramidal cell (P) (Mag x 250 Congo red). 149
Plate 4.64: Sections of Wistar rat hippocampal regions (CA1 and CA3) regions of Group EGL+AC (150mg/kg Eugenol and 100mg/kg of aluminium chloride) with mild distortion in the

cytoarchitecture of the hippocampus with no visible amyloid plaques.(Pyramidal cell (P) (Mag x 250 Congo red). 150

Plate 4.65: Sections of Wistar rat hippocampal regions (CA1 and CA3) of Group EGH (300mg/kg Eugenol) showing a normal cytoarchitecture when compared with the control (Untreated) with no visible amyloid plaques. Pyramidal cell (P) (Mag x 250 Congo red). 151

Plate 4.66: Sections of Wistar rat hippocampal regions (CA1 and CA3) of Group EGL (150mg/kg of Eugenol) showing a normal cytoarchitecture of hippocampal regions with no visible amyloid plaques. Pyramidal cell (P) (Mag x 250 Congo red). 152

Plate 4.67: Section of Wistar rat hippocampal regions (CA1 and CA3) of Group VI (Untreated) showing a normal ACAT-1 immunoreactivity of the hippocampal region. (Pyramidal cell (P) (ACAT-1 x 250). 153

Plate 4.68: Section of Wistar rat hippocampal regions (CA1 and CA3) of Group V (100mg/kg $AlCl_{3)}$ showing a diminished ACAT-1 immunoreactivity of the Pyramidal cells of the hippocampal region. (Pyramidal cell (P). (ACAT-1 x 250). 154

Plate 4.69: Section of Wistar rat hippocampal regions (CA1 and CA3) of Group III (300mg/kg Eugenol and 100mg/kg $AlCl_3$) revealing a restored ACAT-1 immunoreactivity of the Pyramidal cells of the hippocampal region when compared to Group V. (Pyramidal cell (P) (ACAT-1 x 250). 155

Plate 4.70: Section of Wistar rat hippocampal regions (CA1 and CA3) of Group IV (150 mg/kg Eugenol and 100mg/kg Aluminium chloride) revealing a restored ACAT-1 immunoreactivity of the Pyramidal cells of the hippocampal region when compared to Group V. (Pyramidal cell (P) (ACAT-1 x 250). 156

Plate 4.71: Section of Wistar rat hippocampal regions (CA1 and CA3) of Group I (300 mg/kg Eugenol) showing a normal ACAT-1 immunoreactivity of the Pyramidal cells of the hippocampal region when compared to Group V. (Pyramidal cell (P) (ACAT-1 x 250). 157

Plate 4.72: Section of Wistar rat hippocampal regions (CA1 and CA3) of Group II (150 mg/kg Eugenol) revealing a normal ACAT-1 immunoreactivity of the Pyramidal cells of the hippocampal region when compared to Group V. (Pyramidal cell (P) (ACAT-1 x 250). 158

Plate 3.1a: Micrometer slide as captured by microscope at magnification x250 (using the x25 objective). 265

Plate 3.1b: Histometry using a Cresyl fast violet stained micrograph (digital microscopic images) with a computer running imaging software (AmScope MT version 3.0.0.5, USA)..... 265

ABSTRACT

Aluminium metal is a very potent neurotoxin that is capable of triggering various neuroinflammatory events in the brain and these include oxidative stress, production of biomarkers of neuroinflammation, apoptosis, cognitive decline and dementia. Sources of aluminium intoxication include vaccines, drugs, water, cooking utensils, etc. The use of aluminium as an adjuvant in vaccines has been linked to autism, autoimmunity, long-term brain inflammation and associated neurological complications. Eugenol, on the other hand, is a phenolic compound that belongs to the class Phenylpropanoids and a major component of many spice-derived plants which includes clove, cinnamon, and various species of Ocimum, coffee, Banana Soya bean and beans e.t.c. All plants listed above are known to possess antioxidant or anti-inflammatory properties and these properties are postulated to be performed by eugenol. This Study is aimed at evaluating the effect of eugenol on the cerebral (layers III and V), cerebellar cortices and hippocampus (CA1 and CA3 reregions) following administration of aluminium chloride; neurobehavioural studies using Morris water maze (MWM) for learning and memory, elevated plus maze (EPM) for anxiety like-behaviour and behaviour scored includes open and close duration, rearing and grooming; forelimb grip strength test to assess muscular strength; neurochemical analysis to assess the concentration of neuro-trace elements (Magnesium Mg, Manganese Mn, Iron Fe) and brain levels of Aluminium was also assessed. Brain tissue homogenates were used to assess levels of lipid peroxidation, Malondialdehyde (MDA), antioxidant enzymes Superoxide dismutase (SOD), glutathione peroxidase (GPx) and catalase (CAT); intramitochondrial accumulation of 8-Hydroxy-2-deoxyguanosine (8-OHdG), antiapoptotic (Bcl-2) and proapoptotic proteins Bax and Caspasce-3; endogenous enzymatic levels of aceylcholinestserase (AchE) and detect the presence of cholinergic neurons using

ACAT-1 stains; Routine hematoxylin and eosin (H&E) stains, cresyl fast violet (CFV) for Nissl bodies, Congo red for amyloidal plaques and Golgi stains for neuronal dendritic field. A total of thirty (30) apparently healthy adult Wistar Rats of either sex with a weight of 140-160 g was divided into six (6) groups with five (5) rats in each group. Group I served as control (CTRL), groups II-VI were designated as treatment groups. Group I served as the control was administered 0.6 ml distilled water. Neurotoxicity was induced in rats by oral administration of Aluminium Chloride ($AlCl_3$). Group II was administered 100 mg/kg $AlCl_3$ and was designated as AC. Group III was administered 300 mg/kg Eugenol and 100 mg/kg $AlCl_3$ and was designated as EGH+AC; Group IV was administered 150 mg/kg Eugenol and 100 mg/kg $AlCl_3$ and was designated as EGL+AC; Group V was administered 300 mg/kg Eugenol only and designated as EGH; Group VI was administered 150 mg/kg Eugenol only and designated as EGL. Eugenol was administered orally throughout the duration of this study for 21 days. On day 22 rats were euthanized using 0.8 ml of ketamine. Results revealed that exposure to $AlCl_3$ resulted in neurotoxicity in rats which were evident from Morphological, histometric, histologic, and histochemical alterations or changes in the brain; $AlCl_3$ resulted in an increase in anxiety like behaviour, cognitive impairments and motor deficits in the neurobehavioural assessment; significant ($p<0.05$) alterations in the levels of neurotrace elements; significant ($p<0.05$) increase in MDA levels, significant ($p<0.05$) reduction in antioxidant (SOD, CAT, GPx) enzyme activity, significant ($p<0.05$) increase in the level of 8-OHDG, proapoptotic protein (Bax, Caspasce-3) and endogenous acetlycholinesterase (AchE). Co-administration of Eugenol and $AlCl_3$ resulted in preserved histologic and histochemical alterations in the cerebral, cerebellar and hippocampal regions (CA1 and CA3) relative to the control; ameliorated anxiety like responses, prevented cognitive deficits produced by $AlCl_3$ relative to the control; alterations in the concentrations of

neurotrace metals (Mg, Mn and Fe); prevented alterations in the levels of biomarkers of lipid peroxidation (MDA), antioxidant enzymes (SOD, GPx and CAT) and endogenous acetylcholinesterase (AchE) activity. The result obtained from this study revealed that eugenol can protect the cerebral (Layers III and V), cerebellar cortices and hippocampus from pathological changes associated with oral administration of $AlCl_{3.}$ The protective properties of eugenol is due to its free radical scavenging property by maintaining the appropriate level of both enzymatic and non-enzymatic fortification in opposition to AlCl3 induced neurotoxicity. Results obtained revealed that eugenol is an effective treatment in attenuating the deleterious effects of $AlCl_3$ induced neurotoxicity.

INTRODUCTION

1.1 Background Information

Humans are said to live in what was described as an aluminium age (Exley, 2009). This is due to the fact that most of objects we use are made of aluminium; aluminium objects have been popular due to their physical properties which includes; durability, srtrenght corrosion resistant, and very light. Aluminium is an exceptional conductor of electric current. As a result of the above-mentioned properties, aluminium currently finds its way into virtually every aspect of our daily lives. The use of aluminium includes in cans, cookware, aluminium foil, housing materials, and components of electrical devices, airplanes, boats, cars and numerous hardware items of all descriptions (Carson, 2000; Hirata *et al.,* 2011).

Aluminium gains access into the body through drinking water and due to its action as flocculant in water treatment; it is also used as an additive in various processed foods; it can also be found with increasing usage in various pharmaceutical products (Hirata *et al.,* 2011). In vaccines, aluminium salts are used as adjuvants and this has increasingly exposed human systems to aluminium (Walton, 2007; Lori and Staff, 2017).

Aluminium is highly reactive with carbon and oxygen that are the two most abundant elements on earth. For this reason, the widespread use of bioavailable aluminium may have immense and far reaching implications for the health of humans and animals in general. Aluminium is known to be toxic to all forms of life on earth and hence aluminium is described as atoxin to all forms of life (Exley, 2009; Elif and Aylin, 2018).

The toxicity of aluminium ion (Al^{3+}) is well documented and food prepared or stored in aluminium containers yields soluble aluminium compounds that can be easily absorbed by the

gastrointestinal tract (GIT) and as a result they are absorbed into the blood stream (Thorsten *et al*, 2018).

Eugenol, also called 4-ally-2-methoxyphenol is a phenolic compound and a major component of several spice-derived plants with antioxidant and anti-inflammatory properties.

Eugenol can be obtained from *syzygium aromaticum* (clove) is used a flavoring agent, cosmetics, food industry and particularly in dentistry. Clove and other plants that contains eugenol is known to possess anti-ulcer activity using indomethacin and ethanol induced gastric lesion model (Pan and Dong, 2015). Plants rich in eugenol have been reported to suppress LPS- induced iNOS and COX-2 expression by downregulating NF-κB and AP-1 activity. The inhibition of NF-κB and AP-1 by plants containing eugenol has been correlated with the reduction in inflammatory cytokines such as TNF-α, MPO, and IL-1β. In rats model of LPS induced lung inflammation, these plants was found to possess anti-inflammatory properties. These plants also demonstrated potential in its use as an anticancer agent and potent antioxidant by increasing tissue activities of various antioxidants such as SOD, CAT, GPx, etc (Mnafgui et al., 2016).

Aluminium has been shown to severe consequences on the brain of rats in a study carried out by Kadour et al., 2016, revealing the ability of aluminium to change bodyweight, whole brain weight and cerebral weight. They further revealed that subacute treatment of aluminium resulted in spongiosis of the neuropil which resulted in growth retardation of the experimental animals. Yellamma et al., 2010, reported a spontaneous reduction in motor activity in rats treated with 500 mg/L of aluminium in drinking water. Memory impairment has been reported in ras treated with aluminium and this was assessed by the increase in latency time in morris water maze and elevated plus maze test (Abd-Elhady et al., 2013)

Exposure of humans and animals to aluminium from various sources can have deleterious consequences on the developing and adult nervous systems (Tomljenovic, 2011; Mathew *et al.* 2018). These impacts may depend in large part on various factors, for example, the form of aluminium, the route of administration, and the concentration and duration of exposure.

Included in this latter category is the issue of dietary versus injected aluminium, the latter a key component of many current vaccines (Exley, 2011). In addition, the final impact of aluminium will likely depend on a number of biological variables including age, gender, and potentially and largely yet unidentified genetic susceptibility factors enhancing aluminium toxicity (Exley, 2011).

1.2 Aluminium

Aluminium is a well-documented neurotoxin that enhances neuroinflammatory events in the brain by different mechanisms. Aluminium exacerbate oxidative stress, amyloid beta (Aβ) deposition, and plaque formation in the brain of mice (Pratico *et al.*, 2002). Aβ and aluminium are able to potentiate reactive oxygen species (ROS) formation that will lead to genotoxicity and DNA damage. The mammalian apurinic endonuclease 1, is an4 ubiquitous and remarkably multifunctional protein. It plays a central role in the base excision repair (BER) pathway for damaged bases and DNA single-strand breaks induced by ROS and alkylating agents (Izumi *et al,* 2003). Apurinic/apyrimidinic endonuclease 1 (APE1) was independently identified as a reductive activator factor and named redox effector factor 1 (Mitra *et al.,* 2002). A third and distinct function of APE1 as a transacting factor was also discovered (Tell *et al.*, 2005). Studies have shown that global cerebral ischemia or traumatic brain injury or cold injury-induced brain trauma (Fujimura *et al*, 1999; Shweta *et al*, 2014) induced oxidative stress decreases APE1

expression in the hippocampus and is associated with neuronal apoptosis in rats (Edwards *et al.* 1998). This specific inhibition of APE1 expression may affect the extent of apoptosis after ischemia.

An association between aluminium poisoning and memory disorder in humans was first reported in 1921 (Spofforth *et al,* 1921). Later, it was shown that the intracerebral administration of aluminium induced epilepsy in experimental animals (Chusid *et al*, 1951). As a component of dialysis solutions or aluminium containing pharmacological compounds, aluminium is known to cause various dialysis-related disorders, including osteomalacia (aluminium bone disease), microcytic anemia, β2-microglobulin-associated amyloidosis (Wills & Savory, 1989), and dialysis encephalopathy in hemodialysis patients (Alfrey *et al.*, 1976).

The accidental contamination of aluminium in drinking water occurred and more than 20,000 persons were exposed to high levels of aluminium at 1988 in Camelford North Cornwall, England. (Altmann *et al*, 1999). Residents exposed to contaminated aluminium exhibited various symptoms related to cerebral impairment such as loss of concentration and short-term memory in a 10-year follow-up study. (Altmann *et al*, 1999).

Martyn et al. (1989) reported a high incidence of Alzheimer's disease (AD) in areas with a high level of aluminium in the drinking water in England and Wales. A considerable number of studies have provided evidence to support an association between AD and Al in drinking water after this initial report (Flaten, 2002; Stephen and Arezoo, 2018). Frecker (1991) reported on a Norwegian area where high Al concentrations in drinking water were linked to high dementia-associated mortality. Relationship between Aluminium in drinking water and increased risk of Alzheimers disease was explored in Canada, and a significant increase in the incidence rate of Alzheimer disease as a result of aluminium poisoning was reported (Neri and Hewitt, 1991).

Greater risk of AD in Canadian areas where concentrations of Al are high and those of fluoride are low (Forbes and Mclachlan, 1996). Rondeau *et al*. (2009), demonstrated that high daily intake of Al was correlated with increased risk of dementia or cognitive decline in a 15-year follow-up French cohort study. These studies suggested that Aluminium has adverse effects on human memory and causes dementia when it enters the brain.

1.3 Statement of Research Problem

Aluminium salts have been used as pesticides for quite a long time and aluminium poisoning has been reported in countries such as Cameroon, Burkinafaso, Uganda, and Nigeria. Associated risks of aluminium based pesticides include multiple sclerosis, skin cancer, and cognitive decline. As a pesticide, aluminium is found more in raw unprocessed foods than in processed foods because majority of the foods are harvested and taken directly to the market for sale due to poor storage facilities. The use of aluminium as an adjuvant in vaccines has been linked to increase in the number of children with autism spectrum disorders. In Nigeria 1 out of every 125-150 children are autistic and this amounts to over 600,000 Nigerian children and this places a huge burden on the country's GDP. Currently in Nigeria there is no data on the levels of permissible content of aluminium in foods to be consumed by the regulatory body (NAFDAC) but high levels of aluminium has found in several processed foods in Nigeria and fresh farm produce with the most likely source of aluminium been from its use as a pesticide. Recommended daily exposure to aluminium by the United states of America Food and Drug Administration (FDA) is <5mcg/kg/d. Analysis of 30 parenteral nutrition infant formula was discovered to have contained three times higher permissible content of aluminium and all these infant formula finds its way to Nigerian markets.

Research carried out by Onainwa et al., 1995 revealed high levels of aluminium in fresh farm produce in the south western part of Nigeria but very little data exist in Nigeria about the mortality rate associated with aluminium. However, in the USA a link between infant mortality and high levels of aluminium adjuvants in Hepatitis B vaccine and infant formula contaminated with aluminium.

1.4 Justification of Study

Plants known to contain eugenol as active compounds are known to possess anti-inflammatory, antioxidative, anticancer and anxiolytic properties and as a result the need to investigate the active component of these plants becomes vital. Popular drug of choice used to treat aluminium toxicity such as deferoxamine and side effects associated with this drug include: itchy skin, blurred vision, dizziness, reddish coloured urine and pain at the sight of injection. The average cost of deferoxamine is 41 USD (#20,000) per dose. The cost of this drug makes it a substantial problem regarding the treatment of aluminium induced toxicity. As a result of this limitation associated with deferoxamine the need to explore a cheaper and more efficient drug with lesser side effects and as a result the need to explore the efficacy of eugenol becomes essential. The efficacy at which eugenol can attenuate neurotoxicity associated with aluminium chloride needs to be investigated. The paucity of data on the neuroprotective potential of eugenol makes this study very essential.

1.5 Significance of the Study

This present study is of great importance in identifying and evaluating available natural agents as an alternative to currently used drugs that are employed in combatting aluminium induced toxicity with sometimes life threatning side effects. As a result, this study will lead to the

identification of a safer and more effective agent with high affordability which is a vitalproblem of brain related disorders in developing countries. Finally knowledge gained from this study could provoke the minds of indigenous researchers to direct their research into the field of neuroscience, ethnopharmacology, and medicinal plants.

1.6 Study Hypothesis

Eugenol will posses protective properties in preventing, cerebral, cerebellar cortices toxicity associated with oral administration of aluminium chloride in Wistar rats.

1.7 Aims and Objectives of the Study

1.7.1 Aim

This study aimed at evaluating the effects of eugenol on the cerebral, cerebellar cortices and hippocampus following oral administration of aluminium chloride in Wistar rats.

1.7.2 Objectives

The objectives were to:

i. morphologically, histologically, histochemically, and immunohistochemically evaluate the protective effects of eugenol on aluminium-induced cerebellar, cerebral, and hippocampal neurotoxicity in Wistar rats.
ii. investigate the cognitive, anxiety-like behaviours and motor activities in Wistar rats.
iii. analyse of neurotrace metals such as magnesium (Mg), manganese (Mn), iron (Fe), and accumulation of aluminium in the brain of
iv. analyse the effect of eugenol on aluminium-induced neurotoxicity on the biomarkers of lipid peroxidation, Malondialdehyde (MDA), antioxidant enzymes superoxide dismutase (SOD),

catalase (CAT) and glutathione peroxidase (GPx), endogenous enzyme acetylcholinesterase (AchE) activities, and intramitochondrial accumulation of 8-hydroxy-2-deoxyguanosine

v. detect the levels of antiapoptotic (Bcl-2), proapoptotic proteins (Bax and Caspasce-3), cholinergic neurons within the brains of Wistar rats

CHAPTER TWO

2.0 Literature Review

2.1 Aluminium

Brain microglia can be activated by aluminium even in the absence of infectious agents within the brain. Aluminium can trigger and worsen brain inflammation. Aluminium is also a key factor in the pathology neurodegenerative diseases such as Alzheimer's disease (AD) and Parkinson disease (PD) due to its presence in the brain of patients with AD. (Cunningham *et al,* 2007; Dantzer and Kelley, 2007). Chronic exposure to aluminium can have a wide range of effects within the brain, such as impaired cognition and learning, attention deficits, social withdrawal, irritability, low food and water intake, and depression. Over the years, elevated levels of proinflammatory cytokines and glutamate have been revealed to be mediated by the activation of microglia cells within the brain (Peter *et al.....,* 2018; Couette *et al.*, 2009).

Human contact with aluminium increased tremendously over the last half of the nineteenth century when aluminium salts were used increasingly in the food preservation and textile industry (Walton and Wang, 2009). In infants formula aluminium can be present as a contaminant or a deliberate additive in the production process (Burrell & Exley, 2010). Aluminium can enter the body through various ways and this has increased in three folds with the use of aluminium wares for cooking and packaging food, cosmetics and medicinal formulations and antacids are known to contain very high levels of aluminium hydroxide (Pivnick *et al.*, 1995; Walton and Wang, 2009; Tomljenovic, 2011). The use of antiperspirantss provides a route for aluminium to enter the body through the skin and through food. These two routes allow aluminium faster route into the circulatory system at faster rate which is eliminated

by the kidneys (Tomljenovic, 2011). However, people with diminished kidney function, infants before the age of one and the elderly are very susceptible to the deleterious consequences of aluminium accumulation in the body (Tomljenovic & Shaw, 2011).

Experimental evidence reveals that long-term persistence of aluminium adjuvants in the human brain results in cognitive dysfunction affecting visual and verbal memory, as well as executive functions such as attention, working memory and planning (Couette et al., 2009).

2.1.1 Definition

Aluminium (Al) or aluminum is a chemical element with symbol Al and atomic number 13. It is a silvery-white, soft, nonmagnetic and ductile metal in the boron group. By mass, aluminium makes up about 8% of the Earth's crust; it is the third most abundant element after oxygen and silicon and the most abundant metal in the crust, though it is less common in the mantle . The chief ore of aluminium is bauxite. Al metal is so chemically reactive that native specimens are rare and limited to extreme reducing environments. Instead, it is found combined in over 270 different minerals (Shakhashiri, 2008).

Among all aluminium isotopes, only one is stable Al. This is consistent with the fact an atomic number is odd. It is the only isotope that has existed on Earth in its current form since the creation of the planet. It is essentially the only isotope representing the element on Earth, which makes a mononuclidic element and practically equates its standard atomic weight to that of the isotope. Such a low standard atomic weight of aluminium has some effects on the properties of the element (Van Ginkel *et al.,* 1993).

2.1.2 Chemistry

The chemical and physical properties of aluminium are shown in the table below.

Table 2.1: Chemical and Physical Properties of Aluminium

CHEMICAL PROPERTIES	
Atomic number	13
Standard atomic weight	26.9815384
Element Category	Post transition metal
Group, block	Group 13, p-block
Period	Period 3
Electronic configuration	[Ne] $3s^2$ $3p^1$
Per shell	2, 8, 3
ATOMIC PROPERTIES	
Oxidation states	−2, −1, +1,[2] +2,[3] +3 (an amphoteric oxide)
PHYSICAL PROPERTIES	
Phase	Solid
Melting point	933.47 K (660.32 °C, 1220.58 °F)
Boiling point	2743 K(2470 °C, 4478 °F)

(Van Ginkel *et al.*,1993)

2.1.3 History

The history of Al has been shaped by usage of alum. The first written record of *alum* was made by Greek historian Herodotus, dates to the 5th century BC. The ancients are known to have used alum as a dyeing mordant and for city defense. After the Crusades, alum became an indispensable good in the European fabric industry, was a subject of international commerce; it was imported to Europe from the eastern Mediterranean until the mid-15th century (Setton, 1976).

The nature of alum remains unknown. Around 1530, Swiss physician Paracelsus suggested alum was a salt of an earth of alum. In 1595, German doctor and chemist Andreas Libavius experimentally confirmed this; in 1754, German chemist Andreas Sigismund Marggraf synthesized alumina by boiling clay in sulfuric acid and subsequently adding potash (Holleman *et al.,* 1995).

However, attempts to produce Al metal date to 1760. The first successful attempt, however, was completed in 1824 by Danish physicist and chemist Hans Christian Ørsted, he reacted anhydrous aluminium chloride with potassium amalgam, yielding a lump of metal looking similar to tin. He presented his results and demonstrated a sample of the new metal in 1825. In 1827, German chemist Friedrich Wöhler repeated Ørsted's experiments but did not identify any Al. (Andersson, 1988).

Al became widely used in jewelry, everyday items, eyeglass frames, optical instruments, tableware, and foil in the 1890s and early 20th century. The ability to form hard yet light alloys

with other metals provided the metal has many uses at the time. During World War I, major governments demanded large shipments of Al for light strong airframes (Dohmeier *et al*., 1996).

By the mid-20th century, Al had become a part of everyday life and an essential component of housewares. During the mid-20th century, aluminium emerged as a civil engineering material, with building applications in both basic construction and interior finish work and increasingly being used in military engineering, for both airplanes and land armor vehicle engines. Earth's first artificial satellite, launched in 1957, consisted of two separate aluminium semispheres joined together and all subsequent space vehicles have been made of aluminium. The aluminium can was invented in 1956 and employed as storage for drinks in 1958 (Slanina *et al.*, 1986)

Throughout the 20th century, the production of aluminium rose rapidly, while the world production of aluminium in 1900 was 6,800 metric tons, the annual production first exceeded 100,000 metric tons in 1916; 1,000,000 tons in 1941; 10,000,000 tons in 1971. In the 1970s, the increased demand for aluminium made it an exchange commodity; it entered the London Metal Exchange, the oldest industrial metal exchange in the world, in 1978.The output continued to grow: the annual production of aluminium exceeded 50,000,000 metric tons in 2013 (Durrant and Durrant, 2014)

The real price for aluminium declined from $14,000 per metric ton in 1900 to $2,340 in 1948 Extraction and processing costs were lowered over technological progress and the scale of the economy. However, the need to exploit lower-grade poorer quality deposits and the use of fast increasing input costs (above all, energy) increased the net cost of aluminium. The real price

began to grow in the 1970s with the rise of energy cost. Production moved from the industrialized countries to countries where production was cheaper (Darbre, 2006).

2.1.4 Toxicity

Al is not as toxic as heavy metals. Aluminium is classified as a non-carcinogen by the United States Department of Health and Human Services. There is little evidence that normal exposure to aluminium presents a risk to a healthy adult and there is evidence of no toxicity if it is consumed in amounts not greater than 40 mg/day per kg of body mass (Dolara, 2014).

Most Al consumed will leave the body in feces, the small part of it that enters the body will be excreted via urine. Al that does stay in the body is accumulated in bone and apart from that in brain, liver, and kidney. All metals cannot pass the blood–brain barrier and natural filters before the brain, but some compounds, such as fluoride, sulphides, and chlorides can pass through the blood-brain barrier (Bingham and Cohrssen, 2012).

Al can interact with transition metals; in particular, the interaction with iron and copper enhances the production of reactive oxygen species by these two redox-active metal ions, leading to the exacerbation of cell oxidative stress and neuronal cell death. Recently, the interaction between Al and iron, regarding the evidence on toxicity and pathological consequences in humans, has been proposed as one of the main molecular mechanisms underlying toxicity in humans (Becaria *et al*, 2003). The potential toxic effects of Al as an enhancer of reactive oxygen species production, catalysed by transition metal ions, have been recently confirmed in a study on emerging strategies for the prevention of Alzheimer ’s disease progression . The intimate mechanism underlying this activity of Al on transition ions has not, to the best of our knowledge,

been clarified yet. Whereas the vast majority of reports regarding aluminium toxicity are related to chronic events, acute intoxication is uncommon in clinical practice.

Nevertheless, acute aluminium intoxication is a well-known event because of the incidence of fatal cases. Alum bladder irrigation is one of the most frequently reported causes of encephalopathy due to acute aluminium toxicity (Savory *et al*, 1996; Nakamura *et al*.., 2000; Percy *et al*, 2011).

Aluminium is unquestionably neurotoxic, this has been well demonstrated in multiple experimental animals and in clinical practice (Ambreen *et al*., 2017; Mathew *et al*., 2018). Aluminium deposits in the brain would be of little interest, given their small size and low impact on the brain upon aluminium metabolism, if it were not for the widely accepted link between aluminium and dialysis-related dementia. The report that some cognition/neuro-behavioral deficits could be associated with an increased aluminium body burden has stimulated research interest. Aluminium may enter the brain through multiple routes: from the blood, either through the choroid plexus or across the blood-brain barrier (BBB) and from the nasal cavity into the olfactory nerves, followed by direct distribution into the brain (Campbel, 2002).

2.1.4.1 Sources of Aluminium Exposure

2.1.4.1.1 Aluminium in Food

Aluminium is ubiquitous in the hearth environment. As a consequence, food is the primary source for aluminium intake under physiological conditions (Yokel and McNamara, 2001). The widespread presence of aluminium, both in the environment and in foodstuffs, makes it virtually impossible to avoid exposure to this metal ion (Hewitt *et al*., 1990). In fact, aluminium is a component of many items used daily, including personal hygiene products and medications. The

concentration of aluminium in food is extremely variable, due both to the original content and to food interaction with the material it contacts in storage or in cooking. For example, the aluminium content of a variety of beverages contained in aluminium cans is five to seven times higher compared to the same type of beverage in bottles. Most plant food has a low aluminium content, normally < 25 μ g/g of dry weight. At the extremes of the spectrum, we find tomatoes, showing very low aluminium levels, from 0.2 to 1.1 μ g/g, and marjoram and thyme, which show very high aluminium concentrations, ranging from 500 to 1000 μ g/g. Soy-based milk formulas provide a potentially high aluminium source to infants (Burrell and Exley, 2010).

2.1.4.1.2 Aluminium in Pharmaceutical Products

Aluminium hydroxide, contained in numerous antacids, is generally considered the most common cause of iatrogenic aluminium toxicity in the Western countries.

A normal therapeutic regimen of antacids contains 5 g of aluminium hydroxide per day, a dosage several hundred times higher than the amount normally ingested from food. In particular, when associated with oral citrate, the administration of aluminium hydroxide has been reported to cause acute aluminium intoxication, clinically characterized by the development of rapid progressive encephalopathy. This condition presents with marked confusion, myoclonic seizures, and coma and in rare cases, death (Kirschbaum and Schoolwerth, 1989; Gordon, 2005). Aluminium storage and toxicity has been reported in children affected by renal insufficiency and receiving aluminium hydroxide as a phosphate binder, who later developed encephalopathy with myoclonic seizures (Griswold *et al*, 1983). Various studies have demonstrated that children affected by chronic renal failure under aluminium hydroxide therapy develop aluminium storage, revealed by serum albumin > 100μ g/L and increased bone aluminium concentration (Griswold

et al., 1983; Salusky et al., 1984). Preterm infants submitted to prolonged intravenous feeding have been found at risk of aluminium intoxication, developing neurotoxicity clinically manifested in childhood with a mental development index < 85 and subsequent educational problems (Bishop *et al.*, 1997). The contamination of parenteral solutions with aluminium has been reported as one of the main factors responsible for the development of metabolic bone disease in parenteral nutrition of patients, particularly in preterm newborns and leading to osteopenic bone disease (Klein, 1995; Marcus and Mathew., 2007). Elevated concentrations of aluminium have been reported in infants receiving intravenous therapy and in children undergoing protracted regimens of parenteral nutrition, caused by parenteral drug products containing aluminium as an ingredient (Koo *et al*, 1986; Robert *et al.,* 2008).

2.1.4.2.3 Aluminium-Triggered Immune and Inflammatory Responses in the CNS

Experimental observations demonstrate that aluminium levels relevant to human exposure to vaccines can directly activate both microglia and astrocytes as well as induce significant Inflammatory changes in the brain of rodent species (Shaw & Petrik, 2009; Mjad *et al*., 2018).

A strong indication that aluminium can activate glial cells in humans comes from an autopsy case of aluminium encephalopathy. In this case, a 59-year old woman died following a nine months history of disorientation, loss of emotional control, and memory. General convulsions and disturbed consciousness. She was a chronic renal patient who took 3 g of hydroxy-aluminium gel per day for 15 years to control her serum phosphorus. X-ray microanalysis demonstrated aluminium deposits in neurons of her cerebral cortex (Shirabe *et al.*, 2002).

Notably, neuropathological examination of the brain showed nerve cell atrophy and mild loss with stromal spongiosis, proliferation of astrocytes and microglia in the cerebral cortex, basal

ganglia and thalamus. No neurofibrillary tangles (NFT) were seen (Shirabe *et al.*, 2002). The slow evolution of this case suggests a progressive accumulation of aluminium within neurons and glia. Other aluminium forms such as aluminosilicates have also been reported in diseased brains, that is, in the cores of senile plaques of AD patients. Furthermore, Evans *et al.*,(1992) using purified murine microglia exposed to aluminosilicate particles observed the generation of ROS, indicating microglial activation. There is evidence that systemically administered aluminium in drinking water can specifically activate tumor necrosis factor –α (TNF-α) without activating other cytokines. Exposed male mice to aluminium sulphate-containing drinking water *ad libitum* at concentrations of 0, 5, 25, and 125 ppm aluminium for one month and found significant expression of TNF-α mRNA in the cerebral cortex (Tsunoda & Sharma, 1992). Elevations in this cytokine followed a dose-dependent response.

The source of the TNF- α was likely from activated microglia, importantly, these changes occurred at aluminium concentrations commonly encountered in public drinking water, the study, indicated that even very small amounts of aluminium can activate microglia in a pro-inflammatory mode (Tsunoda & Sharma, 1992).

Brain inflammation was reported in animals that were exposed to aluminium lactate via drinking water *ad libitum* (Campbell *et al.*, 2004). The lowest concentration used in their study (0.01nM) was equivalent to that associated with AD and aluminium containing public drinking water. Unlike the previous study, they found elevations in nuclear factor (NF)-kB and IL-1ß in the brain of rats, but no elevation in β-amyloid. Both studies found that systemic exposure to aluminium produced selective inflammation of the brain (Tsunoda & Sharma, 1992).

It has also been shown that aluminium in combination with other metals (e.g. Copper) additively increases brain inflammation (Becaria *et al.*, 2006). Interestingly, much like aluminium, other

neurotoxic metals commonly found in the environment such as mercury, lead and manganese, have also been shown to activate glial cells, promote both inflammation and oxidative stress in the brain (Burton and Guilarte, 2009). It is worth emphasizing that all of these metal-induced neurotoxic effects are indicative of an excitotoxic process, it is of significant concern that low levels of environmental aluminium are sufficient to induce neurotoxic outcomes (Campbell *et al.,* 2004). Moreover, experimental evidence shows that aluminium preferentially accumulates in the mitochondria and cell nucleus, which makes this metal very resistant to removal by chelation obviously, long-term intracellular persistence of aluminium is likely to exacerbate its toxic effects. (Kruck *et al.,* 2004). The difficulty of removing brain intracellular aluminium will lead to its progressive accumulation over a lifetime, eventually reaching a neurotoxic threshold sufficient to trigger neurodegenerative disease processes (Walton & Wang, 2009).

2.1.4.1.4 Aluminium and Energy Metabolism

Aluminium is known to accumulate in the mitochondria and disrupt a number of mitochondrial functions leading to an energy deficit (Mohan *et al.*, 2009; Feibo *et al.*, 2017), which by itself may not result in sufficient neuronal dysfunction or damage. However, several studies show that reductions in neuronal energy can dramatically amplify excitotoxic injury. Impairment of mitochondrial function and energy metabolism by aluminium would thus be expected to increase the sensitivity of neurons to excitotoxicity and accelerate and potentiate neuronal damage (Kumar *et al.*, 2008; Yasmin *et al*., 2019).

2.1.4.1.5 **Aluminum and Oxidative Damage**

Additional link between aluminium toxicity and excitotoxicity is found in the observation by Exley (2004). For example, while aluminium in a non-redox metal, under certain conditions it can act as a pro-oxidant. Moreover, aluminium appears to react with the superoxide radical thus facilitating its destructive potential (Exley, 2004). Experimental observations also indicate that the formation of superoxide plays a critical step in triggering excitotoxicity-mediated neuronal death through generation of peroxynitrite (Mander and Brown, 2005). One of the primary destructive reactions in the excitotoxic cascade is the building up of peroxynitrite, formed when elevated levels of superoxide react with nitric oxide (NO), which is also produced during excitotoxicity (Exley, 2004). Aluminium could also enhance excitotoxicity by inducing apoptosis of astrocytes, which are considered a primary site of aluminium accumulation (Suarez-Fernandez *et al.*, 1999). Indeed, research evidence shows that, apart from providing trophic support to neurons, astrocytes also play a crucial role in protecting neurons from excitotoxic damage, by mediating the clearance of excess glutamate (Aremu and Meshitsuka, 2006).

Moreover, Al has been shown to dramatically lower neuronal reduced glutathione levels and astrocytes are the major source of glutathione for neurons (Murakami and Yoshino, 2004)

High levels of glutamate also inhibit glutathione production intracellularly by inhibiting the cystine/glutamate antiporter (Blaylock and Maroon, 2011). In addition, aluminium has been shown to impair gap junctional intercellular communication between astrocytes in culture (Theiss and Meller, 2002).

2.1.4.1.6 Aluminium and Brain Inflammation

The relationship between Al, chronic brain inflammation and excitotoxicity revealed that Al produces a profound general decrease in nicotine binding involving all brain areas (Gulya *et al.*, 1990). The nicotinic receptor (alpha7 nicotinic acetylcholine receptor- nAchR) plays an important role in dampening brain inflammation and interference with cholinergic neurotransmission can increase brain inflammation (Tyagi *et al.,* 2009). This may be a major mechanism linking aluminium accumulations in the AD brain and chronic inflammation that goes beyond the neurotransmitter functions of acetylcholine. Taken together, all the above experimental observations indicate that by promoting oxidative damage and inflammation in the CNS, exacerbating excitotoxic damage by:

(i) Increasing the levels of excitotoxic mediators

(ii) Impeding their clearance, aluminium can both trigger and promote neuronal injury.

Aluminium-induced microglial/astrocyte-mediated immunoexcitotoxicity combined with its direct neurotoxic effects, makes this element a strong candidate for at least enhancing neurodegeneration associated with such disorders as Alzheimer's disease (AD), Parkinson disease (PD), Amyotrophic lateral sclerosis (ALS), Huntington's disease (HD), Multiple sclerosis (MS), viral encephalopathies and Chronic traumatic encephalopathy (CTE) (Tyagi *et al.*, 2009).

2.1.5 Absorption and Distribution of Bioavailable Aluminium

When assessing aluminium's potential toxicity, one must also consider absorption and distribution. While absorption from foods is considered quite small, under certain conditions, this

can be increased substantially. For example, organic acids and some amino acids increase aluminium absorption significantly. Increasing absorption is as follows:

aluminium citrate> aluminium tartrate> aluminium gluconate> aluminium lactate> aluminium glutamate> $AlCl_3$, $AlSO_4$,aluminium nitrate (Cunat *et al*,2000). Forms of aluminium are of special concern: aluminium-L-glutamate and nanoscaled aluminium, both of which have high absorption from the gut and passage into the brain, as well as higher toxicity profiles than aluminium alone. Adding to this concern is the fact that glutamate, both as a food additive and naturally occurring in foods, is common in the Western diet. Deloncle *et al.,* 1995. injected Al-*L*-glutamate subcutaneously and intravenously for 5 weeks and demonstrated a significant increase in aluminium content in several areas of the animals' brain, including the hippocampus, occipito-parietal cortex, cerebellum and striatum (Deloncle *et al.,* 1995). It is of considerable interest that 50% of the animals given subcutaneous injections of aluminium glutamate developed neurological disturbances such as trembling, equilibrium disturbances, and convulsions leading to death. This is suggestive of an excitotoxic effect, supporting this conclusion, Deloncle *et al*. (1995) found significant elevations in glutamate in the occipito-parietal cortex of Al-*L*-glutamate-treated animals. These observations suggest that the Al-*L*-glutamate complex is capable of crossing the Blood brain barrier (BBB).

Nanoscaled aluminium has higher absorption rates than naturally found aluminium. Li *et al.* (2009) compared nanoscaled aluminium oxides with non-nanoscaled aluminium oxide in terms of their ability to activate microglia and astrocytes and found that nanoscaled aluminium oxide produced significantly greater activation of glial cells than did nonnanoscaled aluminium oxide (Li *et al*., 2009). Of note, nano-particulate aluminium compounds are being used in a growing number of products as well as vaccines (Frey *et al.,* 1997).

It is important to know what proportion of absorbed aluminium reaches the brain in comparison to other organs. To answer this question, Flarend *et al*., (1997). Injected New Zealand White rabbits intramuscularly with 26Al radiolabeled aluminium hydroxide and aluminium phosphate and traced aluminium distribution at 28 days post-injection in blood and urine samples as well as tissues, by utilizing accelerator mass spectrometry. The Al isotope appeared in the first blood sample at one hour for both adjuvants, but the levels were 3x higher for the aluminium phosphate than aluminium hydroxide. Tissue distribution profiles were the same for both compounds (kidney>spleen>liver>heart>lymph nodes>brain). Even though brain levels were low following a single injection, children are receiving multiple injections repeatedly during early life in addition to a lifetime of aluminium exposure from other environmental sources. Furthermore, Substantial evidence shows that bio-available aluminium tends to accumulate in the brain over a lifetime (Tomljenovic, 2011).

2.1.6 Eugenol

Eugenol (4-allyl-2-methoxyphenol), with a molecular formula of $C_{10}H_{12}O_2$ and a molecular weight of 164.21, mainly exists in clove oil, camphorated oil, cinnamon leaf oil, and nutmeg oil. In normal temperatures, eugenol is a pale yellow viscous oily liquid with a strong clove flavour and a special hot taste or brown powder in dried form. Eugenol oil is slightly soluble in water and easily dissolved in organic solvents while food grade eugenol powder is highly soluble in water. Eugenol is widely applied in dentistry, anaesthetics, analgesics, anti-inflammatory agents, and flavouring agents (Chaieb *et al*., 2007).

In recent years, the pharmacodynamics of eugenol has been developed on immunological function, central nervous regulation, reproductive effects, cardiovascular system, digestive system, blood biochemistry, and urinary system (Prakash and Gupta, 2005).

2.1.6.1 Pharmacological Actions of Eugenol

Low doses of eugenol can inhibit the activity of peripheral nerves and have local analgesic and anaesthetic effects. However, high doses of eugenol can cause coma. Studies found that eugenol can significantly inhibit the generation of prostaglandin E2 (PGE-2), exogenous prostaglandin (PG) can cause pain response or improve the sensitivity of a model organism to the sense of touch (Liu *et al.,* 2001). Prostaglandin E1 (PGE-1) and PGE-2 in exogenous PG have stronger effects than in other types of PG, and eugenol elicits analgesic activity by inhibiting PGE-2 generation. Yang *et al* (2008). Used eugenol as a compound nano-emulsion transdermal agent and observed wriggle frequency of mouse after injection of chemical irritants and hot plate-induced pain model, respectively. They found that compound nano-emulsion can reduce the wriggle frequency of mice and that the inhibitory rates to the chemical irritant pain are 37.9% and 60.5%, respectively, whereas the effective rates of the hot plate-induced pain model are 54.4% and 96.5%, respectively. Obvious differences were observed among the compound nano-emulsion, ordinary mixture, and positive control. Its active ingredient, eugenol, can increase the pain threshold of the mouse model and has a clear analgesic function (Yang *et al.,* 2008).

In the study of Kurian et al. (2006) on the analgesic activity of eugenol, the efficiency of eugenol on induced pain mouse model in the inflammatory stage is better than that in the neurological stage. Guenette *et al.* (2007) also found that 40 mg/kg eugenol can extend the response time of Sprague-Dawley mice to pain.

2.1.6.2 Local Anaesthesia

Eugenol is widely applied to current local nerve anaesthesia. As an herbal anaesthetic, eugenol is becoming increasingly used by patients and researchers. Studies on the adjustment of eugenol on the excitability of sciatic nerve of mouse. They found that eugenol mainly inhibits Na^+-dependent channel receptor, activates transient receptor potential vanilloid receptor 1 (TRPV1) subfamily of ion channel receptors, and inhibits the flow of sodium ions, thus, blocking nerve conduction and decreasing the conduction rate gradually. Low eugenol content can inhibit complex action potential and decrease nerve excitability (Moreira-Lobo *et al.*, 2010).

2.1.6.3 Antioxidant Function

The antioxidant function of eugenol has gained universal acceptance in academia. Increasing scientific researchers have made in-depth studies on eugenol. It was revealed that eugenol can avoid functional disorders of endothelial cells resulting from oxidized low-density lipoprotein (LDL) and increase antioxidant activity to inhibit active oxygen generation (Ou *et al.*, 2006; Nagababu *et al.*, 2010).

It was believed that eugenol, butylated hydroxyanisole, and other phenols have important antioxidant activity because they can capture the oxygen atom from alkyl radical over the oxidation group by devoting a hydrogen atom of the phenolic hydroxyl group. Its reaction rate is significantly higher than that of the substrate of over-oxidized groups to attack the organs (Fujisawa *et al.*, 2001).

Studies on the inhibition of eugenol on iron-dependent lipid peroxidation and oxidation of copper-dependent LDL. They believed that its mechanism reduces transition metal ions,

particularly divalent copper ions, thus delaying the generation of hydrogen peroxide and alkoxy from polyunsaturated fatty acids in the body.

This research results of the antioxidant function of eugenol show that its antioxidant function is similar to that of most phenols. Eugenol captures oxygen atoms by devoting hydrogen atoms and reducing free radical generation to achieve its antioxidant function. However, further studies are needed to determine the mechanism of eugenol that is related to some enzymes and the electron transport system and to reveal further its antioxidant function (Masae *et al.*, 2005).

2.1.6.4 Antibiotic Activity

Numerous studies on the antimycotic, antiviral, desinsection, and antiparasitic activities of eugenol and other volatile oils were implemented. Meija *et al*. (1960) studied the structure of antibiotic substances in flavouring agents. Results showed that the benzene ring compound containing hydroxyl group has antibacterial efficacy even when diluted to more than 2000 times (Pandey *et al.*, 2004). Eugenol also contains this structure, but (2004) studied the antibiotic mechanism of eugenol and other flavouring agents, in which the cell wall becomes degraded, which damages the plasma membrane and membrane protein and exposes the cell contents.

The cytoplasm coagulates, causing the proton-motive force to move far away. Investigation on the in vitro antibacterial activity of eugenol by micro-dilution test, found that eugenol has better antibacterial action on 12 common bacteria.

The hydrophobicity of eugenol oil is an important factor affecting its antibacterial activity. The hydrophobic property of eugenol can separate the lipids of cell membrane and mitochondria of bacteria and change its structure to increase the penetrability of the cell membrane.

Eugenol also has antibiotic activity because it can block the proton-motive force, electron stream, and active transport, and cause coagulation of cell contents (Lu *et al.*, 2008).

2.1.6.5 Anticancer Activity

The anti-cancer activity of eugenol has become an important research topic in recent years. Chemically synthesized anti-cancer drugs have toxic side effects and usually cause potential damage to normal cells. Eugenol shows better application potential in the prevention and treatment of some cancers. Studies on the effect of eugenol combined with gemcitabine on cervical carcinoma. It was discovered that the combination of eugenol and gemcitabine can inhibit cancer cell growth, even in low concentrations. In addition, eugenol can reduce the toxic side effect of gemcitabine on normal cells. Studies on the related gene also found that eugenol can reduce the possibility of apoptosis of B-cell lymphoma-2 (Bcl-2), Cyclooxygenase-2 (COX-2), and interleukin-1β (IL-1β), reduce inflammation, and increase the treatment efficacy of gemcitabine (Hussain *et al.*, 2011).

Studies showing the treatment effect of eugenol on gastric cancer in Wistar rats caused by N-methyl-N'-nitryl-N-nitrosoguanidine by regarding apoptosis, cancer cell invasion, and angiogenesis as the main indices. It revealed that eugenol inhibits cell apoptosis, cancer cell invasion, and cancer angiogenesis by regulating the Bcl-2 protein family, apoptotic protease-activating factor-1 (Apaf-1), cytochrome C, and cysteine aspartic protease, and changes the activity of mesenchymal metalloprotease and the expression of Matrix Metalloproteinase-2 (MMP-2), Matrix Metalloproteinase-9 (MMP-9), vascular endothelial growth factor (VEGF), vascular endothelial growth factor receptor 1 (VEGFR-1), and tissue metalloprotease inhibitor (TIMP-2). MMP, VEGF, and TIMP are important observations indicating tumorigenesis.

Studies on the curative effect of the combination of eugenol and 2-methoxyestradiol on non-androgen-dependent prostate cancer. They found that this combination can effectively inhibit the proliferation of prostate cancer cells and enhance the expression of apoptosis precursor proteins to prevent prostate cancer. Moreover, Eugenol shows better curative effects in skin cancer and melanoma (Rita *et al.*, 2009).

2.1.6.6 Antibacterial and Antiviral Effects

Several bacterial infections are associated with the risk of certain cancer, and viruses are now recognized as the second most important cause of human cancer. Given that many chemicals are produced in plants as antimicrobial and antiviral agents, these compounds are being examined for their potential to inhibit human pathogens. A preliminary screening of 35 different Indian spices and herbs indicated that clove, cinnamon, bishop's weed, chili (Capsicumannum), horseradish, cumin, tamarind, black cumin, pomegranate seeds, nutmeg, garlic, onion, tejpat, celery, and cambodge had potent antimicrobial activities against the test organisms Bacillus subtilis (ATCC 6633), Escherichia coli (ATCC 10536), and Saccharomyces cerevisiae (ATCC 9763) (Lu *et al.*, 2008).

2.1.6.7 Anti-insect Activity

The anti-insect activity of eugenol depends on the structure of its phenolic hydroxyl. Studies showed the inhibition of eugenol on small ruminants of *Haemonchus contortus* by ovum hatching test and obtained the highest inhibition rate when the concentration was 0.5%. Furthermore, Studies on the effect of eugenol on the growth, activity, adherence, and ultrastructure of *Giardia lamblia*. Their results showed that eugenol inhibits the adherence of trophosome after being administered for 3hours and does not cause cytolysis. They also found

that eugenol can affect the cell shape and cause the coagulation of cytoplasm and autophagy in cells (Machado *et al*, 2011; Pessoa *et al*, 2002).

2.2 Brain

The nervous system, for the purposes of description is divided into two main parts: the central nervous system (CNS), which consists of the brain and spinal cord, and the peripheral nervous system (PNS), which consist of the cranial and spinal nerves and their associated ganglia.

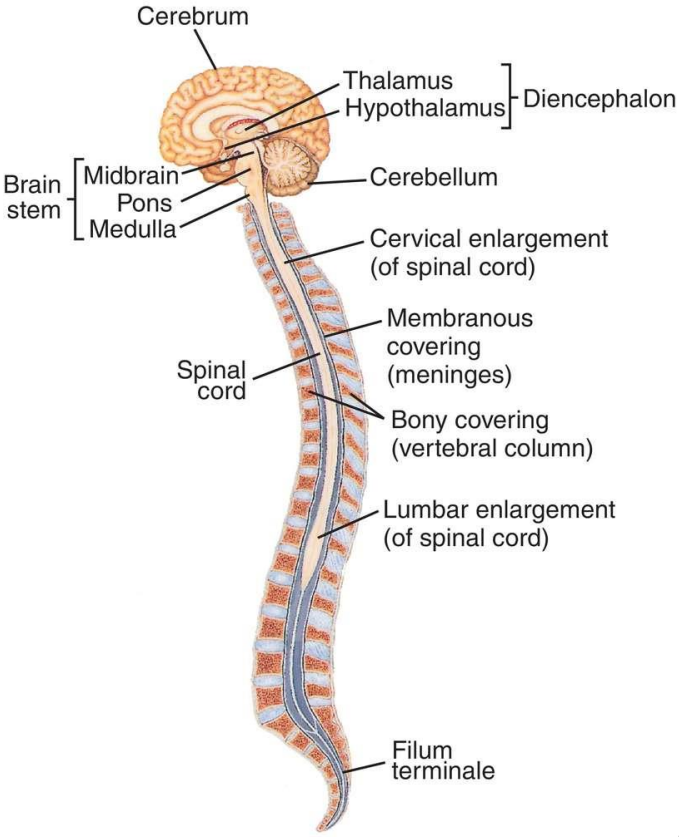
In the CNS, the brain and spinal cord are the main centres where correlation and integration of nervous information occur. Both the brain and the spinal cord are covered with a system of membranes, called the meninges and are suspended in the cerebrospinal fluid; they arefurther protected by bones of the skull and vertebral column. The CNS is composed of excitable nerve cells and their processes, called neurones which are supported by a specialized tissue called neuroglia. The long processes of a nerve cell are called axons or nerve fibers.

The interior of the CNS is organized into gray and white matter. Gray matter consist of nerve fibers embedded in neuroglia, it has a white color due to the presence of lipid material in the myelin sheaths of many of the nerve fibers (Snell, 2010).

The interior of the central nervous system is organized into gray and white matter. Gray matter consists of nerve cells embedded in neuroglia; it has a gray color. White Matter consists of nerve fibers embedded in neuroglia; it has a white color due to the Presence of lipid material in the myelin sheaths of many of the nerve fibers.

In the peripheral nervous system, the cranial and spinal nerves, which consist of bundles Of nerve fibers or axons, conduct information to and from the central nervous system.

Although the nerves are surrounded by fibrous sheaths as they run to different parts of the body, they are relatively unprotected and are commonly damaged by trauma (Snell, 2010)



(Snell, 2010)

Figure 2.1: Sections of the brain and spinal cord

2.2.1 Embryology

2.2.1.1 Origin of the Nervous system

The nervous system develops from the neural plate, a thickened area of the embryonic ectoderm.

It is the notochord and paraxial mesenchyme that induce the overlying ectoderm to differentiate into the neural plate.

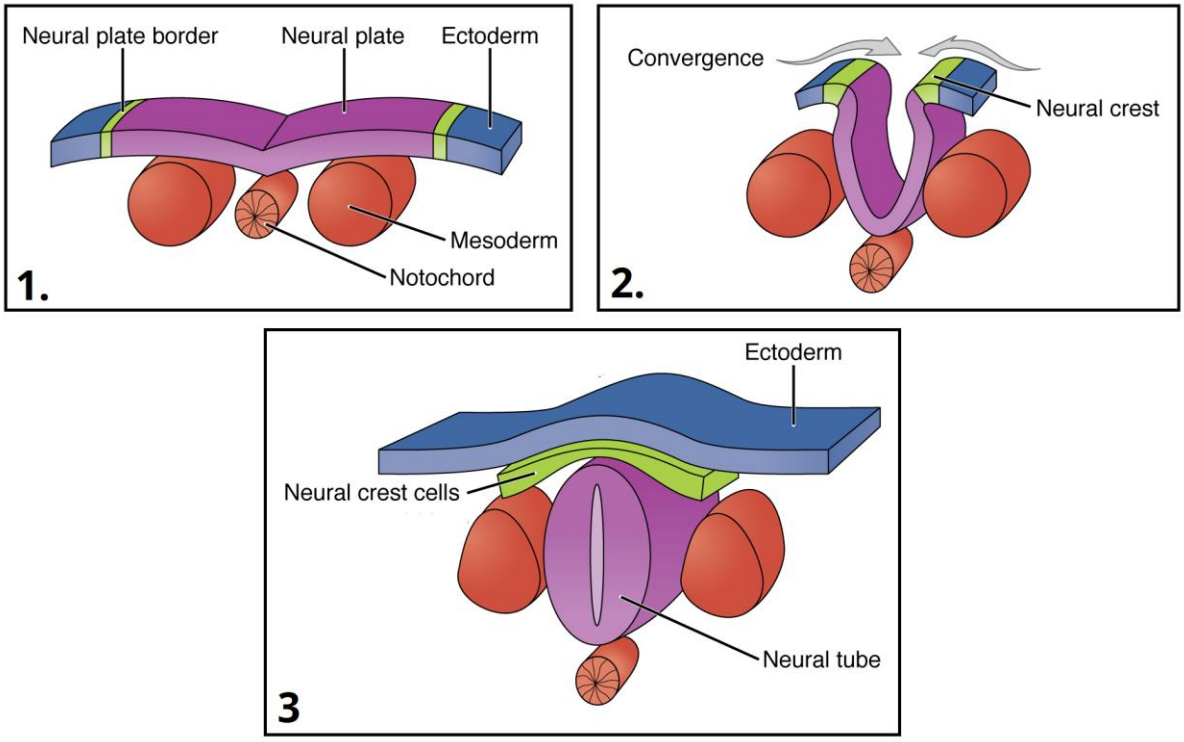
The neural folds, neural tube, and neural crest are formed from the neural plate.

- The neural tube differentiates into the CNS (Brain and spinal cord)

- The neural crest cells give rise to cells that form most of the PNS and ANS, consisting of the cranial, spinal, and autonomic ganglia.

- Neurulation formation of the neural plate and neural tube begins during stage 10 of development (22-23 days) in the region of the forth to sixth pair of somites. At this stage, the cranial two-thirds of the neural plate and tube, as far caudal as the fourth pair of somites, represent the future brain and the caudal one-third of the neural plate and tube represent the future spinal cord. Fusion of the neural folds and formation of the neural tube proceeds in the cranial and caudal directions until only small areas of the tube remain open at both ends. Here the lumen of the neural tube canal communicates freely with the amniotic cavity. The cranial opening, the rostral neuropore, closes on the 25^{th} day (approximately) and the caudal neuropore closes 2 days later.

Closure of the neuropores coincides with the establishment of a blood vascular circulation in the neural tube. The walls of the neural tube thicken to form the brain and spinal cord. The neural canal forms the ventricular system of the brain and the central canal of the spinal cord (Moore and Persaud, 2008).



(Inderbir Singh, 2018).

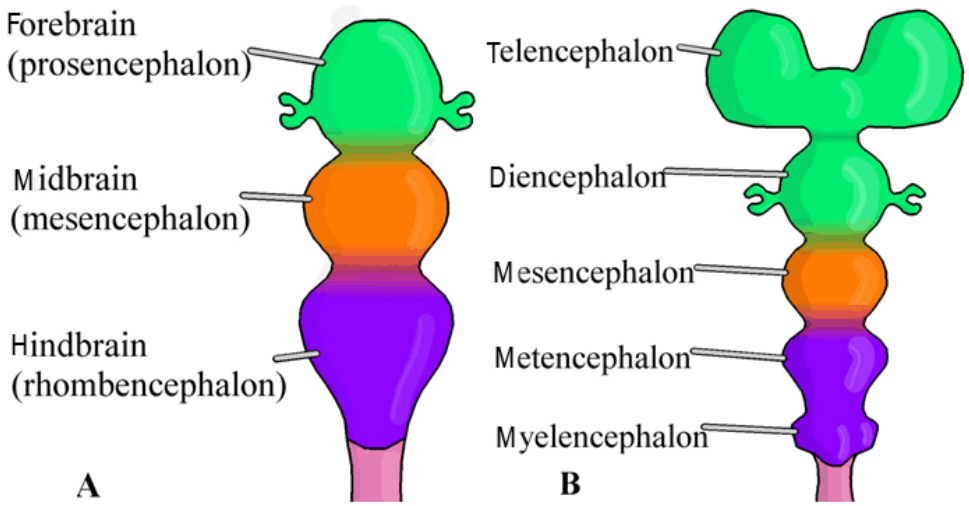
Figure 2.2: Embryonic Development of the Neural Tube

2.2.1.2 Development of the Brain

The neural tube cranial to the fourth pair of somites develops into the brain. Fusion of the neural folds in the cranial region and closure of the rostral neuropore form three primary brain vesicles from which the brain develops. The three primary brain vesicles form:

- The forebrain (prosencephalon)
- The Midbrain (mesencephalon)
- The hindbrain (rhombencephalon)

During the fifth week, the forebrain partly divides into two secondary brain vesicles, the telencephalon and diencephalon; the midbrain does not divide; the hindbrain partly divides into metencephalon and myelencephalon, consequently, there are five secondary brain vesicles.



(Indebir Singh, 2018).

Figure 2.3: Development of the Brain

Midbrain

The Midbrain undergoes less change than any other part of the developing brain, except for the caudal part of the hindbrain. The neural canal narrows and becomes the cerebral aqueduct, a channel that connects the third and fourth ventricles.

Neuroblast migrate from the alar plates of the mid brain into the tectum and aggregate to form four large groups of neurones, the paired superior and inferior colliculi, which are connected with the visual and auditory reflexes, respectively. Neuroblasts from the basal plates may give rise to groups of neurons in the tegmentum of the midbrain.

The substatia nigra, a broad layer of gray matter adjacent to the cerebral peduncle, may also differentiate from the basal plate that migrate ventrally. Fibers growing from the cerebrum form the stem like cerebral peduncles anteriorly. The cerebral peduncles become progressively more prominent as more descending fiber groups pass through the developing midbrain on their way to the brainstem and spinal cord (Moore and Persaud, 2008).

Hindbrain

The cervical flexure demarcates the hindbrain from the spinal cord. Later, this junction is arbitrarily defined as the level of the superior rootlet of the first cervical nerve, which is located roughly at the foramen magnum. The pontine flexure, located in the future pontine region, divides the hindbrain into caudal (myelencephalon) and rostral (metencephalon) parts. The myelencephalon becomes the medulla oblongata and the metencephalon becomes the pons and cerebellum. The cavity of the hindbrain becomes the fourth ventricle and the central canal in the medualla (Moore and Persaud).

Myelencephalon

The caudal part of the myelencephalon resembles the spinal cord, both developmentally and structurally. The neural canal of the the neural tube forms the small central canal of the myelencephalon. Unlike those of the spinal cord, neuroblasts from the alar plates in the myelencephalon migrate into the marginal zone and form isolated areas of gray matter – the gracile nuclei and nuclei laterally. These nuclei are associated with the correspondingly named tracts and enter the medulla from the spinal cord.

The ventral area of the medulla contains a pair of fiber bundles (Pyramids) that consist of the corticospinal fibers descending from the developing cerebral cortex (Moore and persaud, 2008)

Metencephalon

The walls of the metencephalon form the pons and cerebellum, and cavity of the metencephalon forms the superior part of the fourth ventricle. As in the rostral part of thr myelencephalon, the pontine flexure causes divergence of the lateral walls of the pons, which spreads the gray matter in the floor of the fourth ventricle. As in the myelencephalon, neuroblasts in each basal plate develop into motor nuclei and organize into three columns on each side. (Moore and Persaud., 2008).

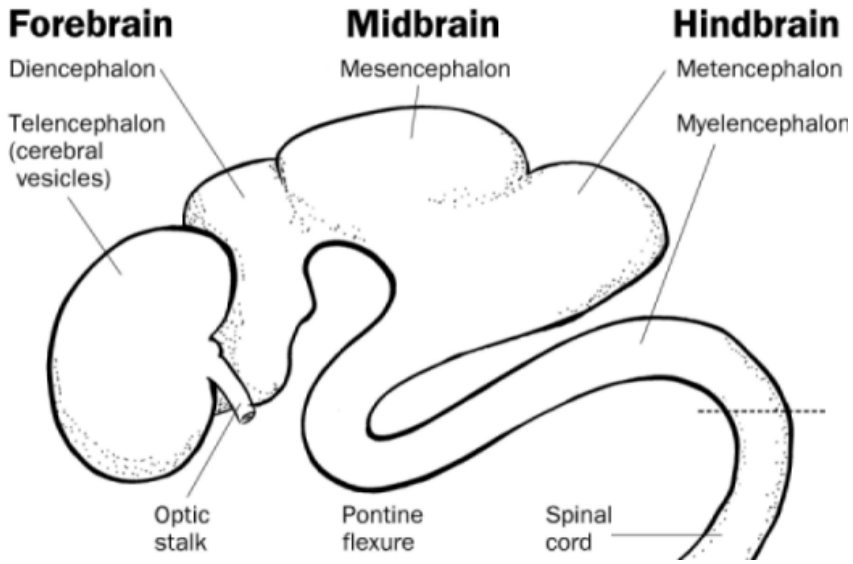
The cerebellum develops from the thickenings of dorsal parts of alar plates. Initially, the cerebellar swellings project into the fourth ventricle. As the swellings enlarge and fuse in the median plane, they overgrow the rostral half of the fourth ventricle and overlap the pons and medulla. Some neuroblast in the intermediate zone of the alar plates migrates to the marginal zone and differentiates into the neurones of the cerebral cortex. Other neuroblasts from these plates give rise to the pontine nuclei, the cochlear and vestibular nuclei and the sensory nuclei of the trigeminal nerve.

The structure of the cerebellum reflects it phylogenetic (evolutionary) development:

- The archicerebellum (flocculonodular lobe), the oldest part part phlogenetically, has connections with the vestibular apparatus
- The paleocerebellum (Vermis and anterior lobe), of more recent development is associated with sensory data from the limbs.

- The neocerebellum (posterior lobe), the newest part phylogenetically, is concerned with selective control of limb movement.

Nerve fibers connecting the cerebral and cerebellar cortices with the spinal cord pass through the marginal layer of the ventral region of the metencephalon. This region of the brainstem is called the pons (L.bridge) because of the robust band of nerve fibers that crosses the median plane and forms a bulky ridge on its anterior and lateral aspects (Moore and Persaud, 2008).



(Moore and Persaud, 2008)

Figure 2.4: Development of the Froebrain, Midbrain and Hind Brain

2.2.1.3 Gross Anatomy

The brain lies in the cranial cavity and is continuous with the spinal cord through the foramen magnum. It is surrounded by three meninges, the dura mater, the arachnoid mater, and the pia mater; these are continuous with the corresponding meninges of the spinal cord.

The cerebrospinal fluid surrounds the brain in the subarachnoid space. The brain is conventionally divided into three major divisions. These are, in ascending order from the spinal

cord, the hindbrain, the midbrain, and the forebrain. The hindbrain may be subdivided into the medulla oblongata, the pons, and the cerebellum. The forebrain may also be subdivided into the diencephalon (brain), which is the central part of the forebrain, and the cerebrum. The brainstem (a collective term for the medulla oblongata, pons, and midbrain) is that part of the brain that remains after the cerebral hemispheres and cerebellum are removed (Snell, 2010).

2.2.1.3.1 Cerebrum

The cerebrum, the largest part of the brain, consists of two cerebral hemispheres,

Which are connected by a mass of white matter called the corpus callosum. Each hemisphere extends from the frontal to the occipital bones in the skull, superior to the anterior and

Middle cranial fossae; posteriorly, the cerebrum lies above the tentorium cerebelli. The hemispheres are separated by a deep cleft, the longitudinal fissure, into which projects the falx cerebri. (Snells, 2010).

2.2.1.3.2 Hippocampus

The hippocampus (named after its resemblance to the seahorse, "seahorse" "sea monster") is a major component of the brains of humans and other vertebrates. Humans and other mammals have two hippocampi, one in each side of the brain. The hippocampus belongs to the limbic system and plays important roles in the consolidation of information from short-term memory to long-term memory, and in spatial memory that enables navigation. The hippocampus is located under the cerebral cortex (allocortical) and in primates in the medial temporal lobe. It contains two main interlocking parts: the hippocampus proper (also called Ammon's horn) and the dentate gyrus (Martin, 2003).

In Alzheimer's disease (and other forms of dementia), the hippocampus is one of the first regions of the brain to suffer damage; short-term memory loss and disorientation are included among the early symptoms. Damage to the hippocampus can also result from oxygen starvation (hypoxia), encephalitis, or medial temporal lobe epilepsy. People with extensive, bilateral hippocampal damage may experience anterograde amnesia (the inability to form and retain new memories).

In rodents as model organisms, the hippocampus has been studied extensively as part of a brain system responsible for spatial memory and navigation.

Many neurons in the rat and mouse hippocampus respond as place cells: that is, they fire bursts of action potentials when the animal passes through a specific part of its environment. Hippocampal place cells interact extensively with head direction cells, whose activity acts as an inertial compass, and conjecturally with grid cells in the neighbouring entorhinal cortex.

Since different neuronal cell types are neatly organized into layers in the hippocampus, it has frequently been used as a model system for studying neurophysiology. The form of neural plasticity known as long-term potentiation (LTP) was initially discovered to occur in the hippocampus and has often been studied in this structure. LTP is widely believed to be one of the main neural mechanisms by which memories are stored in the brain (amaral and Lavenex, 2007).

Role in memory

Psychologists and neuroscientists generally agree that the hippocampus plays an important role in the formation of newmemories about experienced events (episodic or autobiographical memory). Part of this function is hippocampal involvement in the detection of new events, places, and stimuli (Gluck *et al.,* 2014), Some researchers regard the hippocampus as part of a

larger medial temporal lobe memory system responsible for general declarative memory (memories that can be explicitly verbalized—these would include, for example, memory for facts in addition to episodic memory). The hippocampus also encodes an emotional context from the amygdala. This is partly why returning to a location where an emotional event occurred may evoke that emotion. There is a deep emotional connection between episodic memories and place (Vanelzakker *et al., 2008*).

Role in spatial memory and navigation

Studies conducted on moving rats and mice have shown numerous hippocampal neurons acting as place cells that cluster in place fields, these fire bursts of action potentials when the animal passes through a particular location. This place-related neural activity in the hippocampus has been reported in monkeys that were moved around a room while on a restraint chair (Schiller *et al,* 2015).

However, the place cells may have fired in relation to where the monkey was looking rather than that to its actual location in the room. Place cell responses are marked by pyramidal cells in the hippocampus and by granule cells in the dentate gyrus. Other cells in smaller proportion are inhibitory interneurons and these often show place-related variations in their firing rate which are much weaker. The size of place fields varies in gradient along the length of the hippocampus, with cells at the dorsal end showing the smallest fields, cells near the centre showing larger fields, and cells at the ventral tip showing fields that cover the entire environment the firing rate of hippocampal cells depends not only on place but also on the direction the rat is moving, the destination toward which it is traveling, or other task-related variables In humans, cells with location-specific firing patterns have been reported during a study of patients with drug-resistant

epilepsy. They were undergoing an invasive procedure to localize the source of their seizures, with a view to surgical resection. The patients had diagnostic electrodes implanted in their hippocampus and then used a computer to move around in a virtual reality town. Similar brain imaging studies in navigation have shown the hippocampus to be active (O'Keefe and Recce, 1993).

A study was carried out on taxi drivers. London's Black Cab Drivers need to learn the locations of a large number of places and the fastest routes between them to pass a strict test known as The Knowledge to gain a license to operate. A study showed that the posterior part of the hippocampus is larger in these drivers than in the general public, and that a positive correlation exists between the length of time served as a driver and the increase in the volume of this part. It was also discovered the total volume of the hippocampus was unchanged, as the increase seen in the posterior part was made at the expense of the anterior part, which showed a relative decrease in size. There have been no reported adverse effects from this disparity in hippocampal proportions. Another study showed opposite findings in blind individuals. The anterior part of the right hippocampus was larger and the posterior part was smaller, compared with sighted individuals (Karl *et al.,* 2006).

2.2.1.3.3 Midbrain

The midbrain is the narrow part of the brain that connects the forebrain to the hindbrain. The narrow cavity of the midbrain is the cerebral aqueduct, which connects the third and fourth ventricles. The midbrain contains many nuclei and bundles of ascending and descending nerve fibers (Snell, 2010). The midbrain, the rostral part of the brainstem, lies at the junction of the

middle and posterior cranial fossae. Cranial nerves (CN) III and IV are associated with the brain. (Moore *et al.*, 2014).

2.2.1.3.4 Pons

The pons is situated on the anterior surface of the cerebellum, inferior to the midbrain and superior to the medulla oblongata. The pons, or bridge, derives its name from the large number of transverse fibers on its anterior aspect connecting the two cerebellar hemispheres. It also contains many nuclei and ascending and descending nerve fibers (Snell, 2010)

Cranial nerve (CN) V is associated with pons (Moore *et al.*, 2014).

2.2.1.3.5 Medulla

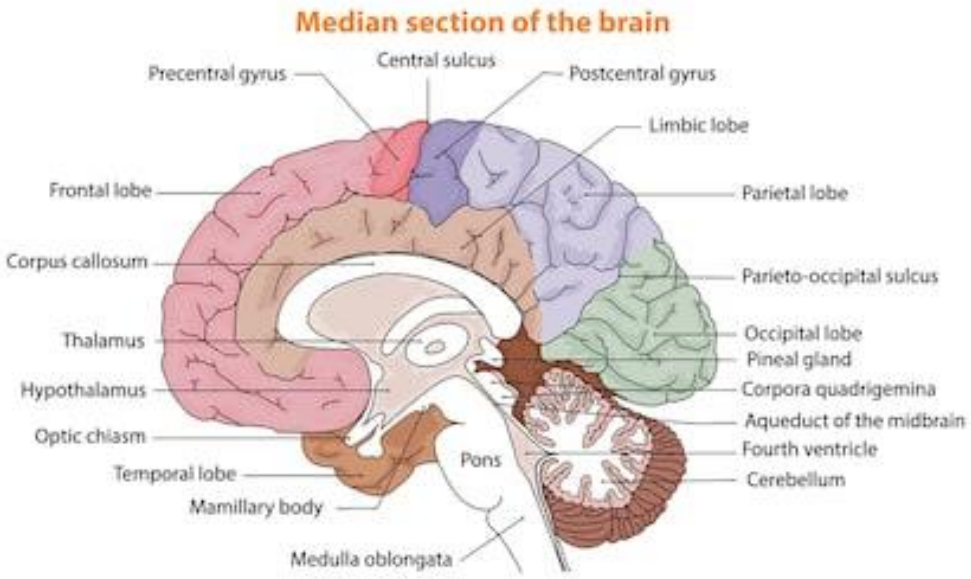
The medulla oblongata is conical in shape and connects the pons superiorly to the spinal cord inferiorly. It contains many collections of neurons, called nuclei, and serves as a conduit for ascending and descending nerve fibers. CN IX, X, and XII are associated with the medulla, whereas CN VI-VIII are associated with the junction of the pons and medulla (Snell, 2010; Moore et al, 2014).

2.2.1.3.6 Cerebellum

The cerebellum lies within the posterior cranial fossa of the skull posterior to the pons and the medulla oblongata. It consists of two laterally placed hemispheres connected by a median portion, the vermis. The cerebellum is connected to the midbrain by the superior cerebellar peduncles, to the pons by the middle cerebellar peduncles, and to the medulla by the inferior cerebellar peduncles the peduncles are composed of large bundles of nerve fibers connecting the cerebellum to the remainder of the nervous system.

The surface layer of each cerebellar hemisphere is called the cortex and is composed of gray matter. The cerebellar cortex is thrown into folds, or folia, separated by closely set transverse fissures. Certain masses of gray matter are found in the interior of the cerebellum, embedded in the white matter; the largest of these is known as the dentate nucleus.

The medulla oblongata, the pons, and the cerebellum surround a cavity filled with cerebrospinal fluid, called the fourth ventricle. This is connected superiorly to the third ventricle by the cerebral aqueduct; inferiorly, it is continuous with the central canal of the spinal cord. It communicates with the subarachnoid space through three openings in the inferior part of the roof. It is through these openings that the cerebrospinal fluid within the central nervous system can enter the subarachnoid space (Snell, 2010; Moore *et al.*, 2014).



(Snells, 2010).

Figure 2.5 Midsagittal Section of the Brain

2.3.3 Brain Histology

2.3.3.1 Cerebrum

Cerebral hemispheres consist of a convoluted cortex of grey matter overlying the central medullary mass of white matter, which conveys fibres between different parts of the cortex and to and from other parts of the CNS.

Histologically, the neurons of the cerebral cortex are divided into five different morphological types which are arranged in several layers. In submammalian species, the major function of the cortex concerns the sense of olfaction (smell) and the neurons are arranged into three layers. In mammals, there has evolved the so-called neocortex consisting of six (6) layers of neurones.

The neocortex as well as the association cortex and in humans constitutes about 90% of the cerebral cortex. The primitive three-layered patterns persist only in the olfactory cortex and the cortical part of the limbic system in the temporal lobe (Young *et al.,* 2007)

2.3.3.1.1 Neurone Types in the Cerebral cortex

There are five characteristics types of cortical neurones; pyramidal cells are by far the most common type.

i. **Pyramidal cells:** as the name implies, they have pyramidal-shaped cell bodies, the apex being directed towards the cortical surface. A slender axon arises from the base of the cell and passes into the underlying white matter, although in the case of small superficially placed cells, axon may synapse in the deep layers of the cortex. From the apex, a thick branching dendrite passes towards the surface where it has an array of fine dendritic branches, in addition, short dendrites arise from the edges of the base and ramify laterally. The size of the pyramidal cells

varies from small to large, the smallest tending to lie more superficially. The huge upper motor neurones of the motor cortex known as Betz cells, which are the largest of the pyramidal cells in the cortex.

ii. **Stellate cells:** stellate cells are any neuron in the central nervous system that have a star-like shape formed by dendritic processes radiating from the cell body. Many Stellate cells are GABAergic and are located in the molecular layer of the cerebellum. Stellate cells are derived from dividing progenitors in the white matter of postnatal cerebellum. Dendritic trees can vary between neurons. There are two types of dendritic trees in the cerebral cortex, which include pyramidal cells, which are pyramid shaped and stellate cells which are star shaped (Rubenstein, 2013)

iii. Cells of Martinotti: they are small polygonal cells with a few short dendrites; the axon extends towards the surface and bifurcates to run horizontally, usually in the most superficial layer.

iv. **Fusiform cells:** are spindle-shaped cells oriented at right angles to the surface of the cerebral cortex. The axon arises from the side of the cell body and passes superficially. Dendrites extend from each end of the cell body branching into deeper and more superficial layers.

v. **Horizontal cells of cajal:** are small spindle shaped but oriented parallel to the surface. They are the least common cell type and are only found in the most superficial layer where their axons pass laterally to the synapse with the dendrites of the pyramidal cells.

In addition to neurones, the cortex contains supporting neuroglial cells such as astrocytes, oligodendroglia and microglia (Young *et al.*, 2007).

2.3.3.1.2 Layers of the Neocortex

The neurones of the neocortex are arranged into six layers, layers differing in neurone morphology, size, and population density. The layers merge with one another rather than being highly demarcated and vary somewhat from one region of the cortex to another depending on cortical thickness and function. The characteristics of each layer are as follows:

I. **Plexiform (molecular) Layer:** The most superficial layer mainly contains dendrites and axons of cortical neurones, making synapse with one another; the sparse nuclei are those of neuroglia and occasional horizontal cells of Cajal.

II. **Outer granular layer:** A dense population of small pyramidal cells increases in size deeper in the layer. Martinotti cells are also present.

III. **Pyramidal cell layer:** Pyramidal cells of moderate size predominate in this broad layer, the cells increasing in size deeper in the layer. Martinotti cells are also present.

IV. **Inner granular layer:** This layer consists mainly of dense packed stellate cells.

V. **Ganglionic Layer:** Large pyramidal cells and smaller numbers of stellate cells and cells of Martinotti make up this layer, the name of the layer originating from the huge pyramidal Bertz cells of the motor cortex.

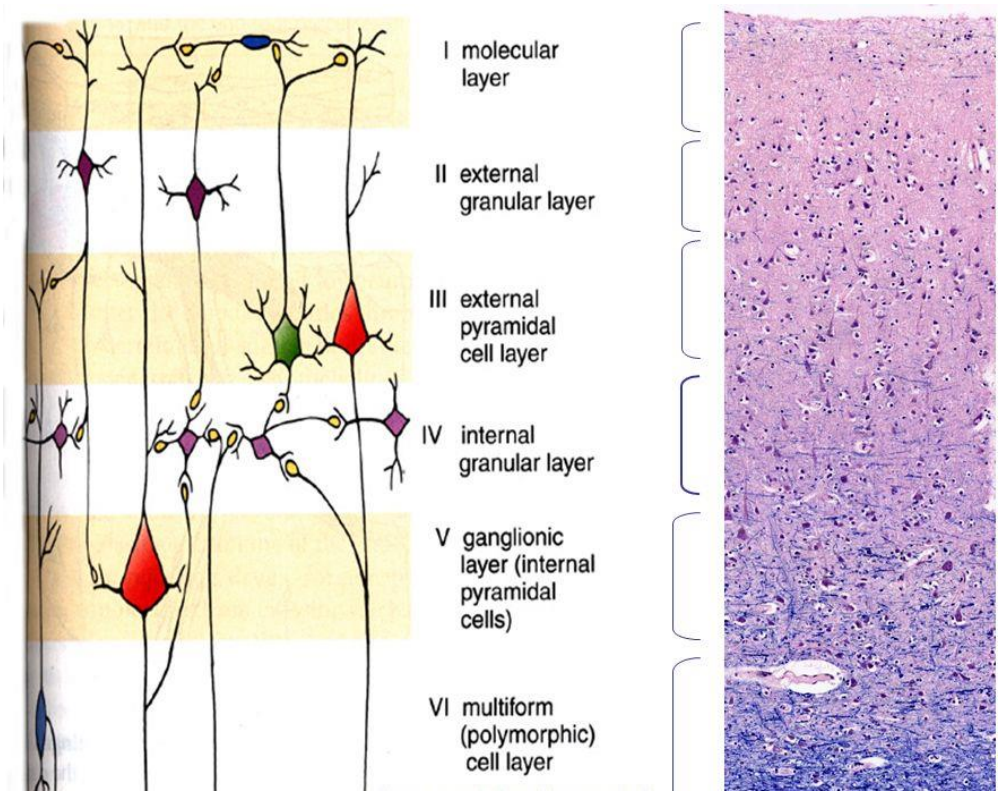
VI. **Multiform cell layer:** This is so named for the wide variety of differing morphological forms found in this layer. It contains numerous small pyramidal cells and cells of Martinotti, as well as stellate cells, especially superficially and cells in the deeper part.

The synaptic interconnections within the cortex are exceedingly complex, with anyone neuron synapsing with several hundred others. However, there are several basic principles of cortical organisation and function:

i. Functional units are disposed of vertically, corresponding to the general orientation of axons and major dendrites.

ii. Afferent fibers (their cell bodies lying elsewhere in the CNS) generally synapse high in the cortex with dendrites of efferent neurons, the cell bodies of which lie in deeper layers of the cortex.

Efferent pathways, typically the axons of pyramidal cells, tend to give off branches that pass back into more superficial layers to communicate with their dendrites via interneuronal connections involving other cortical cell types (Young *et al*., 2007).



(Ross and Pawlina, 2019)

Figure 2.6: Histological Organization of the Cerebral cortex

2.3.3.2 Hippocampus

Hippocampus contains two parts: Cornu ammonis (hippocampus proper) and dentate gyrus. Both of these parts are separated by hippocampal sulcus and curve into each other. Below the sulcus lies the subiculum. Since hippocampus is a part of allocortex (archicortex), there is a zone that separates it from neocortex. Some anatomists divide it into hippocampus proper (Cornu ammonis; CA), dentate gyrus (DG), subiculum, and entorhinal area (EC). The entire set is called as hippocampal formation (Gilbert and Brushfield, 2009).

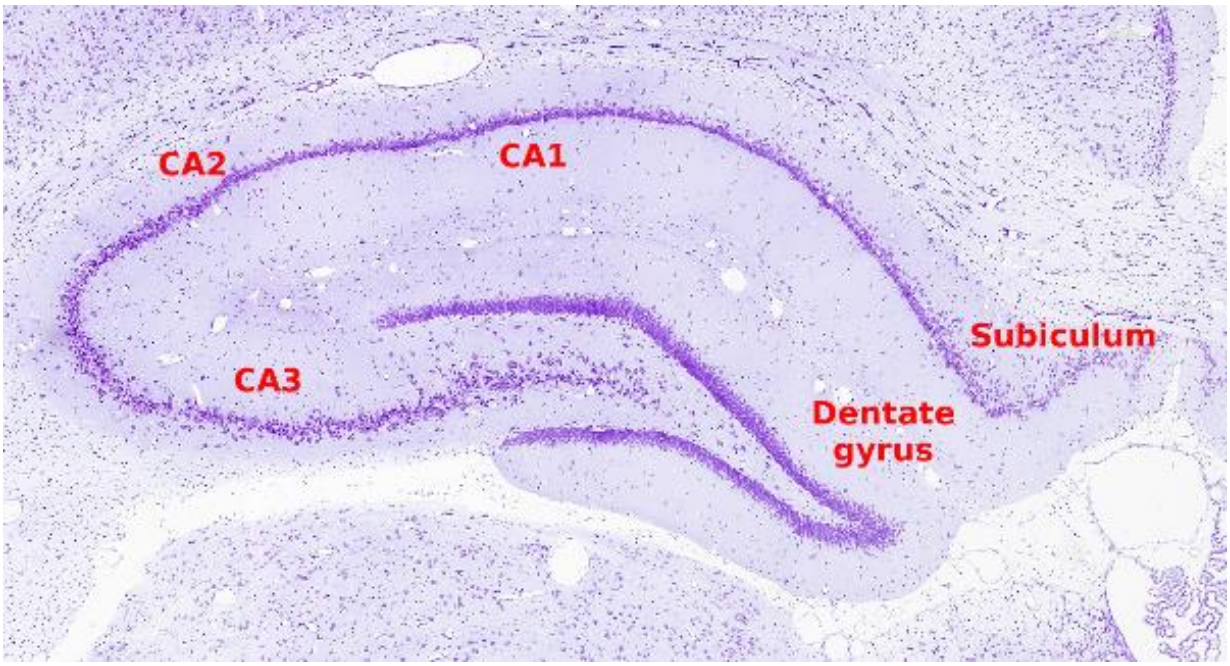
Hippocampus is divided into the the head, body, and tail; head is expanded part while tail is a thin curved part. Based upon histology, the hippocampus proper (Cornu ammonis) is divided into

CA1, CA2, CA3, and CA4 Just opposite CA1, a subiculum is located that connects the hippocampus with the entorhinal cortex in the ventricle; hippocampus is covered by choroid plexus. Hippocampus is supplied by posterior cerebral artery, which has three branches: Anterior, middle, and posterior. Blood Supply is also reinforced by the anterior choroidal artery (Soudry *et al*., 2011).

Cornu Ammonis (CA1, CA2, CA3, and CA4): CA1 contains pyramidal cells principally, and it plays an important role in matching and mismatching of information obtained from CA3. CA2 is a small area and is not considered very important hippocampal subfield, except for its high resistance to hippocampal sclerosis due to epileptic damage. Pyramidal cells are also seen in dentate gyrus of hippocampus (Toyoda *et al*., 2011).

Hippocampus is now known not just to be important in learning and memory but also in:

a. Spatial navigation
b. Emotional behavior
c. Regulation of hypothalamic functions (Koehl and Abrous, 2011).



(Ross and Pawlina, 2019)

Figure 2.7: Histological Photomicrograph of the Hippocampus

2.3.3.3 Cerebellum

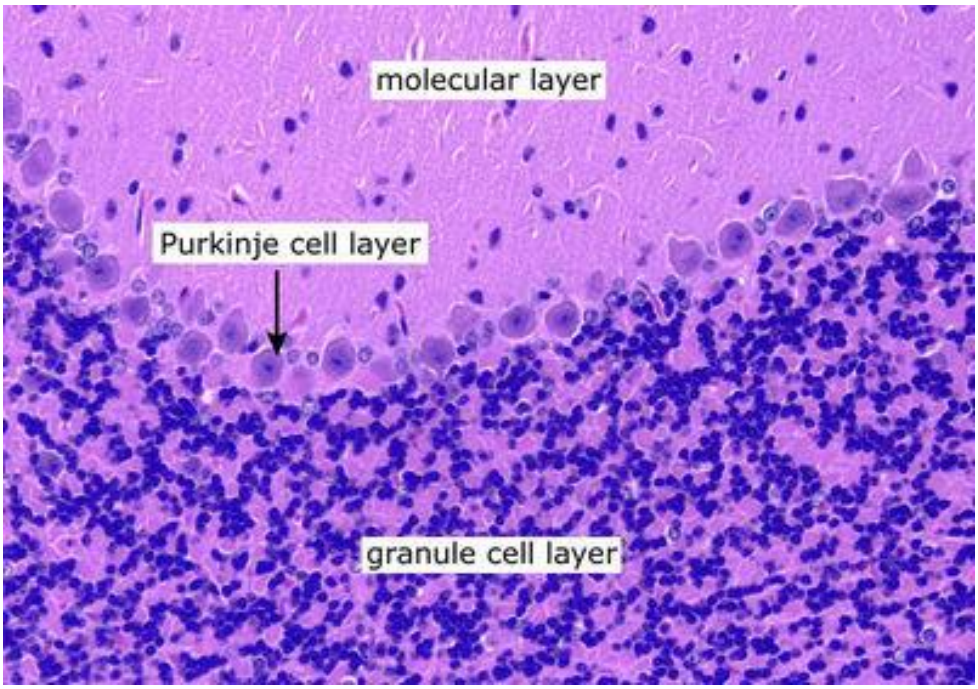
The cerebellum, which coordinates muscular activity and maintains posture and equilibrium, consists of a cortex of grey matter with a central core of white matter containing four pairs of nuclei. Afferent and efferent fibers pass to and from the brainstem via the inferior, middle and superior cerebellar peduncles linking the medulla, pons, and midbrain respectively.

The cerebellar cortex forms a series of deeply convoluted folds or folia supported by a branching central medulla of white matter. At higher magnification, the cortex is seen to consist of three layers. The outer molecular layer contains relatively few neurones and large number of unmyelinated fibers. The inner granular cell layer is extremely cellular. Between the two is a single layer of huge neurones called Purkinje cells.

- Purkinje cells have very large cell bodies, a relatively fine axon extending down through the granular cell layer, and an extensively branching dendritic system which arborises into the outer molecular layer.
- The deep granular cell layer of the cortex contains numerous small neurones, the non-myelinated axons of which pass outwards to the molecular layer where they bifurcate to run parallel to the surface to synapse with the dendrites of the Purkinje cells.

In addition to the Purkinje and granular cells, there are three other types of small neurones in the cerebellar cortex, namely cortex, namely stellate cells and basket cells scattered in the molecular layer and Golgi cells scattered in the superficial part of the granular cell layer.

In simple terms, afferent fibers enter the cerebellum from the brain stem and then pass via the white matter core to make complex connections with granular cells, these in turn connect with the Purkinje dendrites via basket cells and other neurones of the cerebellar cortex. Only efferent fibers from the cerebellar cortex and the purkinje cell axons, which pass down through the granular cell layer into the white matter where they synapse in the central nuclei of the cerebellum (Young et al., 2007).



(Ross and Pawlina, 2019)

Figure 2.8: Histological PhotoMicrograph of the Cerebelar Cortex

2.3.4 Histometry

Verbal descriptions of tissues have been greatly relied upon and a mathematical approach of tissues have received less attention. Recently, measurements of microscopic images of tissues and cells have been on the increase in both research and diagnostic labs.

Histologist, traditionally have relied on verbal descriptions of tissue structure and have seldom favored a mathematical approach. However, in recent years, measurements of the microscopic images of tissues and cells have increasingly been used in research and diagnostic work. Histometry has been used as a method of obtaining numerical quantification of both macroscopic and microscopic anatomical structures in terms of its volume, surface area, perimeter etc. (Machmud *et al*., 2019).

Histological sections can be used to define the normal or pathologic appearance of tissues. Descriptions such as large, small, many, few, absent or present are often sufficient to describe different sections when there is a distinct difference between pathologic and and physiologic conditions are very distinct. But when significant statistical changes in appearance which is as a result of a pathogen or toxin are required, verbal descriptions are not valid enough (Schmitz and Holf, 2005). Therefore, histometry provides a very sound basis for comparison of various histological observations. It gives objectivity, increases precision when compared with direct visual appraisal and statistical analysis becomes easier. It improves assessment of certain histological change, which, though may be recognizable by the eye, are accurately graded and their progression better appreciated by histometric quantization (Huda and Zaid, 2007; Ahmed Saad et al., 2018).

2.3.5 Neurobehavioral testing

Neurobehavioral testing is a noninvasive method used to evaluate different aspects of the functioning of the central nervous system. Test batteries consist of task that measure the performance of particular neurologic functions such as ability to learn, reaction time, memory, and coordination (Broadwater, 2010).

Additionally, neurobehavioral evaluations are an important component of screening for neurotoxicological effects. A neurobehavioral test battery were chosen to assess a variety of endpoints, including autonomic, neuromuscular, and sensory and excitability functions (Moser, 1991; 2001).

2.3.5.1 Learning and memory

Morris water maze

Studies of learning and memory play an important role in the study of neurological disorders with cognitive components, such as schizophrenia and Alzheimer's disease. The Most Common spatial navigation task is the Morris water maze (Morris, 1984; Brandies *et al.*, 1989), which can be used for both rats and mice. In this task, a rodent is placed in a tank of opaque water containing a hidden escape platform. Over the course of repeated trials, the animal learns to locate the platform using visual cues placed around the room. The rate at which the rats learn to locate the platform can be measured and learning is confirmed using a probe trial, in which the platform is removed and the amount of time the rat spends investigating the area of the tank that formerly contained the platform is measured (D'hooge and De Deyn, 2001), which can be used for both rat and mice (Pool size scaled appropriately). In this task, a rodent is placed in a tank of opaque water containing a hidden escape platform. Over the course of repeated trials, the animal Learns to locate the platform using visual cues placed around the room. The rate at which the animal learns to locate the platform can be measured and learning is confirmed using a probe trial, in which the platform is removed and the amount of time the animal spends investigating the area of the tank that formerly contained the platform is measured. The Morris water maze was initially used to show that lesions of the hippocampus impair spatial learning (Morris *et al*., 1982). A variation of the Morris water maze is the Barnes maze, in which rats must locate a hidden escape box on an open platform, which may be less stressful; than swimming in a water maze (Harrison *et al*., 2006).

2.3.5.2 Anxiety-Like Behaviour

Elevated Plus maze

The most commonly used tests of anxiety like behaviour assess exploratory behaviour in different novel environments and were initially developed based on the efficacy of anxiolytic drugs in altering behaviour in rats, although they have since been adapted for use in mice (Cryan and Holmes, 2005). As a foraging species subject to predation, rodents have a natural tendency to explore a novel area, but are also inclined to avoid open brightly lit areas. Rats tend to avoid more aversive areas of the arena (the center of the open field, open arms of the elevated plus maze), but this behaviour can be altered using using drugs or mutations that affect innate anxiety (Cryan and Holmes, 2005). The elevated plus maze is suitable for both rats and mice (Size of the maze may vary depending on the size of the species). The maze consists of two perpendicular arms, one of which is open and other with high walls, located 40-60cm above the ground.

The animal is placed in the center, facing an open arm, the amount of time spent in each arm and entrance into each arm is recorded over 5mins. Anxiolytic drugs will increase the time spent in open arms (Pellow *et al*., 1985; Lister, 1987; Cotstall *et al*., 1989).

2.3.5.3 Forelimb grip Strength test time

Forelimb grip strength test is a measure of the muscular strength in the forelimbs (Olopade *et al*., 2012). In this test, the rat's forepaws are placed on a horizontally suspended metal wire 2mm in diameter and placed 1m above a landing area filled with soft bedding. The length of time the rat was able to stay suspended before falling off the wire is recorded in seconds (Tamashiro *et al.,* 2000).

CHAPTER THREE

MATERIALS AND METHODS

3.1 Materials

3.1.1 Experimental Animals

A total of thirty (30) apparently healthy Wistar rats of both sex (males and females were kept in separate cages) with an average weight of 140 to 160g were obtained from the Animal House of the Department of Human Anatomy, Faculty of Basic Medical Sciences, Ahmadu Bello University, Zaria, Kaduna State Nigeria and housed in wired cages in the Animal House of the Department of Human Anatomy, Ahmadu Bello University, Zaria and they were acclimatized in two weeks prior to the commencement of the experiments. All rats were given food (rat chow – vital feeds) and water *ad libitum*. Treatment groups were administered Eugenol/Aluminium Chloride in addition to water and rat chow. Rats were weighed at the beginning and end of the study.

Drugs

Eugenol

500 g of Eugenol powder was obtained from Wuhan JCJ Logis, Wuchang District, Wuhan, Hubei, China and was used as a neuroprotective agent for the experiment. The product was manufactured by Yueyang Jiazhiyuan Biological Co, Ltd, Hunan China, with product number 5823-4 and 99.9% purity level.

Aluminium

500 g of aluminium chloride was obtained and used as a neurotoxic agent for this experiment. The product is manufactured by Guandong Guanghua Sci-Tech Co. Ltd., Shantou, Guandong, China with product number 7446-70-0 and 99.9% purity level.

Other Materials used in the course of study include:

Digital weighing balance, digital venire calliper, centrifuging machine, spectrophotometer and atomic absorption, spectrophotometer (ASS), cages, water bottles, saw dust (animal bedding), animal feed, distiiled water, microscope, glass slides, cover slips, stains, fixative (Bouin's fliud and formol saline), cylinders, beakers, syringes, tissue paper, gloves, methylated spirit, Phosphate buffer, pH meter.

3.1.3 Neurobehavioral Set-up

The set-ups used for the neurobehavioral studies are as follows:

1. Morris water Maze
2. Elevated plus Maze
3. Forelimb grip strength.

Animal Feed

Pelletized vital feed was obtained and used to feed the rats for the experiment. The product is manufactured by Grand Cereals and Oil Mills Limited (GCOML), Plateau state, Nigeria.

Methodology

3.2.1 Dose Preparation of Eugenol.

50 g of Eugenol was measured and dissolved in 1000 mls of distilled water. This makes up the working solution with a concentration of 0.05 g/ml. From freshly prepared working solution, a little portion was measured out for animal administration.

Eugenol was administered to the experimental animals by oral gavages using an orogastric tube for the treatment period. The method for computing the dosage is indicated in **appendix I**

3.2.2 Dose preparation of Aluminium

50g of aluminium chloride was dissolved in 1000mls of distilled water to form a solution of aluminium chloride with a concentration of 0.05 g/ml as a stock solution. The method for calculating the dosage is indicated in **appendix I**

3.2.3 Experimental Design

Thirty (30) Wistar rats (2 males and 3 females per group) were divided into six (6) groups (I-VI). Group I was the control (CTRL) administered 0.7 ml/kg distilled water, group II administered 100 mg/kg aluminium chloride (AC) (Anil *et al;* 2009) (LD_{50} 3500 mg/kg) group III and IV and II were co-administered 300 mg/kg (EGH) and 150 mg/kg (EGL) Eugenol and 100 mg/kg of aluminium chloride (AC) respectively. Neurotoxicity was induced in rats by administration of aluminium (aluminium chloride). Group V and VI was administered 300mg/kg eugenol (EGH) and 150 mg/kg eugenol (EGL) (LD_{50} of Eugenol 6000 mg/kg).

Administration was for a period of 21 days (three weeks). All administration was via oral route (Table 3.0)

Table 3.0: Treatment of Experimental Animals

Group	Treatment
CTRL(control)	Distilled water (0.6 ml/kg)
AC ($AlCl_3$)	100 mg/kg
EGH+AC	300 mg/kg Eugenol + $Alcl_3$ 100 mg/kg
EGL+AC	150 mg/kg eugenol + $Alcl_3$ 100 mg/kg
EGH	300 mg/kg eugenol
EGL	150 mg/kg eugenol

n = 5; **$Alcl_3$** = Aluminium chloride (AC). All administration was via oral route. Eugenol high dose (EGH), Eugenol low dose (EGL).

Experimental Procedure

All experimental procedures were conducted in the Department of Human Anatomy, Faculty of Basic Medical Sciences, Ahmadu Bello University Zaria, except otherwise specified. Administration was carried out in the morning at 0700 hrs and behavioural tests were carried out at 1600 hrs with elevated plus maze coming first followed by foregrip strength time and lastly by Morris water maze test with one hour test time between each test.

Neurobehavioral/Cognitive Studies

The following neurobehavioral tests were conducted:

Elevated Plus Maze Test

The elevated plus maze (EPM) is a widely used behavioural assay for rodents and it has been validated to asses anti-anxiety effects and to define brain regions and mechanism underlying anxiety-related behaviour (Walf and Frye, 2007; He *et al;* 2011).

The EPM set-up was built according to the description of Lister (1987) as reported by John (2010). The apparatus is in the configuration of a **'+'** and comprised of two open arms (50 x 10cm) across from each other perpendicular to two closed arms (50 x 10 x 20cm) with a center platform (10 x 10cm). The closed arms had a high wall (20cm) to enclose the arm. The entire apparatus was 50cm above the floor. The apparatus was made of wooden materials, painted black.

Procedure: Wistar rats were placed in the central square of the Plus-Maze facing the open arm and was then allowed to explore the apparatus for 5 minutes. The maze was then cleaned with methylated spirit and allowed to dry between tests. Behaviour scored and how these were measured include:

I. **Open arm duration:** Length of time (in seconds) the rat spent in the open arms this was measured using a stop watch to determine the time duration spent in the open arm
II. **Close arm duration:** Length of time (in seconds) the rat spent in close arms this was measured using a stop watch to determine the time duration spent in the open arm

III. **Rearing:** Frequency with which the rat stands on its hind legs or leans against walls of the maze with front paws this was measured by observing the number of times the animals carry out this activity.

IV. **Grooming (cephalocaudal axis):** This refers to the number of times the rat licks fur (from the head to the tail region), grooms with forepaws, and scratches any limb, and this was measured by observing the number of times the animals carry out this activity.

Note: Prior to the test (before treatment), rats were habituated (accustomed) to the EPM set up daily for three (3) days.

Modified Elevated Plus Maze Open arm duration

The elevated plus maze served as an exteroceptive behavioral model to assess anxiety-like behaviour in Wistar rats (Chakravarthi *et al.;* 2012; Khare *et al*; 2014). The apparatus, as described above was used for this study.

Procedure: On the first day, before treatment, each rat was placed on the open arm of the EPM, facing away from the central platform. Transfer latency (TL) was defined as the time (in seconds) taken by the rat to move from the open arm to anyone of the closed arms with all its four paws. TL was recorded on the first day (training session) for each animal. The rat was allowed to explore the maze for another two minutes and returned to its home cage. (Plate 3.1).



Figure 3.1: Elevated Plus Maze set up

Morris Water Maze Test

This method described by Morris *et al.*, (1982), as reported by Drapeau *et al.*, (2003), for spatial memory and learning was adopted for this study. Rats were tested in a Morris water maze (180 cm diameter, 60 cm height) filled with water. An escape platform was hidden 2cm below the surface of the water in a fixed location in one of the four quadrants halfway between the wall and the middle of the pool.

Procedure:

Before the commencement of the treatment, the rats were trained in the pool daily for four (4) days. During the training, animals were required to locate the submerged platform by using distal extra-maze cues which included different shaped objects on the walls around the maze. They were tested for four trials per day (90 seconds with an inter trial interval of 30 seconds and beginning from different start points that varied randomly each day). Rats were tested after seven

(7), fourteen (14), and twenty-one (21) days of treatment. At 21 days of treatment, the test was done 24 hours after the last dose of treatment.



Figure 3.2: Morris Water Maze set up for memory and spatial navigation

Sensori-motor Activity, Motor Coordination

Forelimb Grip Strength Time Test

Forelimb grip strength time (seconds) test was assessed using a modified procedure described by Olopade *et al;* (2012).

Procedure: The rat's forepaws were placed on a horizontally suspended metal wire 2.5mm in diameter, 1m in length and placed 1m above a landing area filled with soft bedding. The length

of time each rat was able to stay suspended before falling off the wire was recorded; a maximum of 2 minutes was given to each rat (Plate 3.1)



Plate 3.1: Showing fore grip strength time set up

Note: Prior to the test (before treatment), rats were habituated (accustomed) to the set up daily for 2 days to determine the muscular strength before the commencement of the treatment. Upon commencement of treatment muscular strength was assessed on day seven (7), day fourteen (14) and day twenty-one (21).

Morphological Studies

Rats were weighed before the commencement of the treatment and at the end of the study. Rats were Euthanized with Ketamine (0.8 ml/kg) used as anaesthesia, which was injected intraperitoneally. Rat brains were harvested (by decapitating the rats and the skull was carefully opened using scissors and a forceps) for morphometric analysis. Morphometry involved taking brain weight using a digital weighing scale, brain-body weight ratio computed.

3.2.4.4 Histometric Studies

Histometric studies involved measuring the cell area and perimeter of pyramidal cells (neurones) of the cerebral cortex layers III and V using a light microscope (HM-LUX, Leitz Wetzlar, Germany) with a x 250 magnification and a micrometer slide (1mm graduated in 0.01mm units; that is divided 10x into 100 µm units) and software (AmScope MT version 3.0.0.5, USA) according to the manufacturer's instruction. (See **appendix II**). Cresyl fast violet micrographs (digital microscopic images) were used for histometry. Three micrographs were randomly captured (Lai *et al.*....., 2001; Kaizaki *et al.*; 2013) in each of the brain regions (cerebral cortex Layers III and V (Toft et al., 2005; Lai et al., 2011) and Cerebellar cortex – purkinje cell layer (Andersen and Pakkenberg, 2003; Jelsing *et al.,* 2006)) and 5 – 20 cells were randomly selected, measured and averaged in three micrographs. Layer III contains medium sized pyramidal cells while Layer V contains large size pyramidal cells.

This is briefly described below:

- Using a light microscope with a x25 objective (x 250 magnification) and computer running image processing software (Amscope MT *version* 3.0.0.5, USA) for microscopy, digital microscopic images were captured.

1. Histometry and calibration (Using the Amscope Microscope Cameras; Psi Wave function, 2009)

- Firstly, a micrometer slide (microscope slide with scale on it), which come as 1 mm graduated in 0.01 mm units (that is divided 10x into 100 µm units) is captured at the same magnification and quality (pixels) as the micrograph was photographed
- A line tool was selected and this was used to carefully measure from the start of one major line (of the captured microscope slide) tot the start of the next, or end to end.
- Recorded length in pixels; in this study it was 408 pixels/ 100µm or 4.08 pixel/µm.
- Next use a polygon tool to measure the area and perimeter of the desired cells. Values are computed and presented automatically by the software. (**Plate 3.1b in appendix II**).

3.2.4.5 Histological, Histochemical and Immunohistochemical studies

At the end of the experiment, harvested brain organs (under ketamine anaesthesia, the rats were decapitated and the skull was opened using scissors and carefully opened with a forceps to carefully remove the brain) were fixed in Bouin's fluid and tissues processed (see **Appendix III**) for light microscopic examination, stained with routine Heamatoxylin and Eosin (H & E), histochemical (Cresyl fast violet – CFV and Golgi) stains and Immunohistochemical (ACAT-1) satins. ACAT-1 staining protocol is shown below:

1. Sections were sectioned at 4 microns thick with the microtome

2. Sections were placed on electrostatically charged the the slides and slides were baked at 70°C for 10 minutes

3. Slides were taken in distilled water

4. Slides were blocked in hydrogen peroxide for 5 minutes

5. Slides were washed in distilled water

6. Slides were retrieved in citrate buffer pH 6.0 for 20 minutes at 95°C

7. Slides were washed in distilled water

8. Slides were covered with PBS pH 7.4

9. Slides were incubated with ACAT antibody (1/100) at RT for 90minutes

10. Slides were washed in PBS pH 7.4

11. Slides were incubated in Mouse + Rabbit HRP (DBBiotech, Slovakia), for 30 minutes

12. Slides were washed in PBS for 10 minutes

13. Slides were incubated in DAB + substrate mixture (DBBiotech, Slovakia) for 5 minutes

14. Slides were washed in distilled water

15. Slides were counter stained with Haematoxylin for 1 minute

16. Slides were washed in distilled water

17. Slides were dehydrated, cleared, and mounted in DPX. **(See appendix IV).**

3.2.4.6 Neurochemical and Biochemical Studies

At the end of the experiment, euthanized rats (under ketamine anaesthesia) were decapitated and the skull was carefully opened to expose the brain) weighed, and homogenized in 0.1M

Phosphate buffer (pH 7.4) (1g tissue/ 4ml (Ige *et a*l., 2011). The homogenates were then centrifuged and aliquots of the supernatant were obtained for neurochemical/biochemical analysis.

Neurochemical analysis for (Fe, Mn, Mg. and Al) estimation in the in the tissue (brain) homogenate was conducted using atomic Absorption Spectrophotometer (AAS – AA240FS, Varian) at the Multiuser Laboratory, Department of Chemistry Ahmadu Bello University, Zaria. The analytical method for determining metals in biological tissues as the reported Monitoring methods index, EMMI (1997) was adopted and is summarized below (see **Appendix V for full procedure).**

1. **Tissue preparation/digestion** (EMMI, 1997)

- Take 1 ml (0.25g) of sample (homogenized tissue; 1g in 4ml of phosphate buffer) into a boiling tube and add 2 ml of concentrated HNO_3
- Heat (100°C) for 2 hours and allow to cool
- Add 0.3 ml of 30% H_2O_2
- Heat (100°C) for 1-2 hours and allow to cool
- Filter using Whatmann's filter paper.

2. **Dilution/ Deionization**

- Make volume (of digested sample) into 20ml using deionized water

3. **Analytical method:** Atomic Absorption Spectrophotometry (AAS)**.**

3.2.4.7 Oxidative Stress Markers

Lipid Peroxidation level was detected using malondialdehyde (MDA) as a biomarker. Antioxidant enzymatic activity was assayed using superoxide dismutase (SOD), catalase (CAT), and glutathione peroxidease (GPx) as biomarkers using tissue homogenate. Endogenous enzymatic activity of acetylcholinesterase (AchE) was assayed using brain homogenate and conducted in the department of Human Anatomy, Ahmadu Bello University.

The concentration of thiobarbituric acid-reactive substance malondialdehyde (MDA) as an index of lipid peroxidation, was evaluated in the brain sample using an assay kit (Rat Malondialdehyden(MDA) ELISA Kit; WKEA Med Supplies corp, China) as stated by the manufacturer's instructions.

Superoxide dismutase activity was analysed using Rat Super Oxide Dismutase (SOD) ELISA Kit (WKEA Med Supplies corp, China) as stated by the manufacturer.

Glutathione peroxidase was analysed using Glutathione Peroxidase (GPx) ELISA KIT (WKEA Med Supplies corp, China) as stated by the manufacturer.

Acetylcholinesterase activity was analysed using Acetylcholinesterase activity Assay Kit (Sigma-Aldrich, USA) as stated by the manufacturer.

3.2.4.8 Isolation of Mitochondrial DNA (mtDNA)

mtDNA isolations were carried out as described by meccoci et al., 1984. In brief, cerebral tissue was homogenized. The nDNA was extracted from the pellet by the initial low-speed centrifugation. mtDNA was isolated by high-speed centrifugation of the supernatant followed by

repelleting. The resulting material was treated with both RNase a and DNase I prior to lysing the mitochondria by addition of 2% sodium-dodecyl sulfate and 400 pg/ml proteinase K. Pretreating the preparations with DNase I largely eliminated nDNA contamination as assessed by using the polymerase chain reaction for a 439 nucleotide pair fragment of the dystrophin gene and a 475 nucleotide pair fragment of mtDNA.

3.2.4.9 Oxidative stress in Mitochondrial DNA

Intra-mitochondrial accumulation of (*8*-hydroxydeoxyguanosine) 8-OHdG was measured as an indicator of mtDNA oxidative damage using highly Sensitive 8-OHdG Check ELISA Kits. Mitochondrial DNA was isolated using the method of Mecocci et al. (1994) and reported by Ding and Yang (2010). Frontal lobe of the cerebral cortex was homogenized in buffer (pH 7.5) containing 0.21 M mannitol, 0.07 M sucrose, 0.05 M Tris–HCl, 0.2 M EDTA and 3mM CaCl2. A centrifugation at 1500 ×g for 15 min was performed, the supernatant was collected and centrifuged at 1500 ×g for 10 min again, and then the resulting supernatant was again centrifuged at 14,000 ×g for 20 min. The deposit was collected and re-suspended in Tris–EDTA buffer (pH 7.4). SDS (2%) and 400 μg/ml proteinase K were added to lyse the cells. Samples were incubated at 37 °C for 4 h. After three extractions with high purity distilled phenol and chloroform isoamyl alcohol, mtDNA was precipitated with 1/10 volume of 3 M sodium acetate (pH 7.4) and 2 volumes of ethanol at −20 °C overnight. Isolated mtDNA was digested with DNase I (200 U/mg DNA),Nuclease P1 and alkaline phosphatase (10 U/mg DNA) in the presence of 40mM Tris–HCl (pH 8.5) containing 10mM MgCl2. Samples were incubated for 4 h at 37 °C, then the kits were used to determine the level of 8-OHdG **(see Appendix VI).**

3.2.4.10 Determination of Apoptotic markers

Brain homogenates were made in lysis buffer and these brain homogenates were analysed using a colorimetric caspase-3 assay kit (supplied by WKEA Med Supplies Corp, China, and manufactured by Fine test china), and these assay kits was used with strict compliance to the manufacturer's instructions. Bcl-2 protein and Bax protein levels were measured/assayed in brain tissue lysates by the appropriate ELISA kit (supplied by WKEA Med Supplies corp, China and manufactured by Fine test china), and the procedure for the assay was performed according to the manufacturer's instructions and the results was expressed as ng/mg **(See appendix VII).**

Data Analysis

Results obtained were analysed using statistical software, statistical package for social sciences (SPSS version 18.0) and Microsoft Office Excel 2007 for charts. Results were expressed as mean ± standard error of mean (S.E.M), and presence of significant differences among means of the groups were determined using one-way analysis of variance (ANOVA) with repeated measures with least significant difference (LSD) *post hoc test* for significance. Paired sample t-test was employed for comparison of means as appropriate. Values were considered significant when $p \leq 0.05$.

CHAPTER FOUR

Results

4.1 Physical Observation

During the period of administration of eugenol and aluminium chloride, the physical activities of Wistar rats were observed. Rats in the control or untreated group were observed to exhibit normal physical activities such as movements and playfulness, rats that received Eugenol did not exhibit reduced physical activity, but the group administered aluminium chloride only showed some decreased physical activity such as movements and playfulness.

The weights of the rats in all groups were observed to have increased when the initial and final weights were compared. Statistically significant ($p<0.05$) weight change differences were observed when EGH, EGL, EGH+AC, EGL+AC when compared to Control (CTRL) (Untreated) as shown in **(Table 4.1).** But a non-significant ($p>0.05$) weight change was observed when the groups are compared with aluminium treated group (AC) (100mg/kg Aluminium chloride) as shown in **(Table 4.1).**

Table 4.1 Effects of Eugenol on body weight before and after administration of aluminium chloride

Groups	IW (g)	FW (g)	*T*	p-value	FW-IW (g)
CTRL (0.6 ml)	157.20±10.15	198.34±13.47	-9.790	0.001	41.14±4.20
AC (100 mg/kg)	141.00±9.21	147.82±6.41	1.335	0.253	6.82±5.11*
EGH+AC (300 mg/kg + 100 mg/kg)	159.00±17.18	163.72±6.02	0.397	0.711	4.72±11.88*
EGL+AC (150 mg/kg + 100 mg/kg)	154.20±7.06	156.06±7.74	0.677	0.535	1.86±2.75*
EGH (300 mg/kg)	158.80 ± 6.34	170.48±7.95	1.669	0.170	11.68±7.00*
EGL	155.60±15.56	158.88±16.46	0.392	0.715	3.28±8.37*

n = 5; mean ± SEM, One way ANOVA *LSD post hoc test*: *p<0.05 when weight change difference **(FW-IW)** when compared to the control. **CTRL** (control), **AC** (aluminium chloride) **EG** (Eugenol), Initial weight **(IW)**, Final weight **(FW),** Weight change difference **(FW-IW).**

4.2 Morphological Studies

4.2.1 Morphometry

Morphological studies involved the morphometry of brain (brain weight). The relative organ weights (brain weight/ body ratio and index) were computed and compared with the control. Relative to the control, there was a Significant ($p<0.05$) increase in the relative organ weight of the groups groups that was administered 300 mg/kg eugenol and 100 mg/kg aluminium chloride (EGH+AC) and 150 mg/kg eugenol and 100 mg/kg aluminium chloride (EGL+AC) **(Figures 4.1).**

The result showed a Significant ($p<0.05$) difference in the relative organ weight (brain weight/ body ratio and index) was observed in 300 mg/kg eugenol and 100 mg/kg aluminium chloride (EGH+AC), 150 mg/kg eugenol and 100 mg/kg aluminium chloride (EGL+AC), 300 mg/kg eugenol (EGH) and 150 mg/kg eugenol (EGL) when compared to aluminium (AC) treated group respectively.

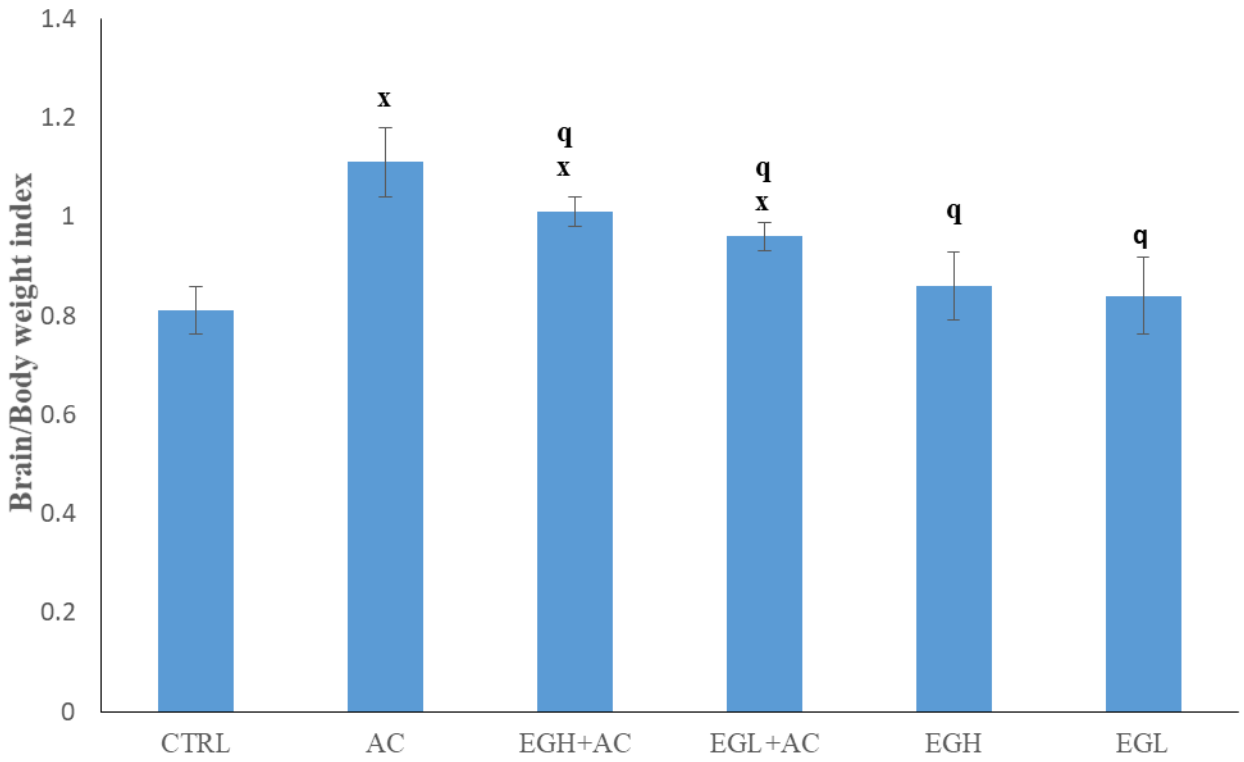


Figure 4.1: Effect of eugenol on brain/body weight index following administration of aluminium chloride

n = 5; mean ± SEM One way ANOVA *LSD post hoc test*: q=p<0.05 when compared to the aluminium (AC) treated group. x=p<0.05 when compared to the control (CTRL).

4.3 Histometric Studies

Histometry involved measuring the cell area and perimeter of neurones (pyramidal cells of the cerebral cortex- Layer III, V, CA1 and CA3 hippocampal regions, Purkinje cells of the cerebellar cortex) of the Wistar rats. The Purkinje cells are found at the boundary between the molecular layer and the granular cell layer

4.3.1 Cerebral and Cerebellar Cortices Histometric Characteristics

The histometric analysis of the cerebral cortex (layer III) pyramidal cell soma revealed a significant ($p<0.05$) increase in neuronal cell soma area when aluminium (AC) treated group is compared to the control (CTRL) and a significant change ($p<0.05$) when EGH+ AC, EGL+AC, EGH and EGL is compared to the AC group. But when compared to the control (CTRL), there was a non-significant change. Neuronal cell soma perimeter revealed a significant ($p<0.05$) increase in the perimeter when AC, EGH+AC, EGL+AC were compared to the control group (CTRL). When EGH+AC, EGH and EGL groups is compared to the AC treated group, there was a significant ($p<0.05$) difference in the neuronal cell soma perimeter as shown in table 4.2. Within layer V of the cerebral cortex, the result shows a nonsignificant ($p>0.05$) neuronal cell soma area of AC, EGH+AC, and EGL+AC is compared to the control (CTRL). When EGH+AC and EGL+AC were compared to the AC treated group, there was a nonsignificant ($p>0.05$) difference. However EGH and EGL showed a significant ($p<0.05$) when compared to control and aluminium treated group (AC), respectively, as shown in table 4.2.

Neuronal Purkinje cell soma area revealed a significant ($p<0.05$) increase when the AC treated compared to the control. When EGH+AC, EGL,+AC, EGH and EGL were compared to the control, there was a non-significant difference in neuronal cell soma area compared to control,

but when compared to the AC treated group there was a significant ($p<0.05$) difference as shown in table 4.2. However, Neuronal soma cell perimeter of purkinje cells showed a significant ($p<0.05$) increase when AC and EGH+AC and EGL+AC compared to control. EGH and EGL showed a significant ($p<0.05$) when compared to AC group as shown in figure 4.2 below.

Table 4.2 Histometric analysis of the effect of Eugenol on cortical neurons of the cerebellum (Purkinje cells) and cerebrum (Pyramidal cells) of Wistar rats

Groups	Cerebellum (Purkinje cells)		Cerebrum LIII (Pyramidal cell)		Cerebrum LV (Pyramidal cells)	
	Area (μm^2)	Perimeter (µm)	Area(μm^2)	Perimeter (µm)	Area (μm^2)	Perimeter (µm)
CTRL (0.6 ml/kg)	1.79 ± 0.14	5.28± 0.13	0.82 ± 0.04	3.69±0.07	1.05 ± 0.08	4.14 ± 0.10
AC (100 mg/kg)	2.50 ± 0.11^{x}	3.38±0.61^{z}	1.59 ± 0.09^{z}	4.70 ± 0.13^{z}	1.17 ± 0.08	4.23 ± 0.09
EGH + AC (300 mg/kg + 100 mg/kg)	1.99 ± 0.10^{q}	5.48±0.13^{s}	0.62 ± 0.09^{s}	3.09 ± 0.10^{ys}	1.06 ± 0.08	4.01 ± 0.13
EGL +AC (150 mg/kg/ 100 mg/kg)	1.78 ± 0.19^{q}	5.21±0.22^{s}	1.03 ± 0.10^{s}	4.36 ± 0.18^{y}	0.98 ± 0.06	4.11 ± 0.10
EGH (300 mg/kg)	1.80 ± 0.07^{q}	5.39±0.09^{s}	1.04 ± 0.17^{s}	4.10 ± 0.32^{q}	1.79 ± 0.34^{rz}	5.22 ± 0.42^{sz}
EGL (150 mg/kg)	1.84 ± 0.12^{q}	5.20±0.16^{s}	0.67 ± 0.09^{s}	3.29 ± 0.21^{s}	0.68 ± 0.05^{xq}	3.52 ± 0.09^{ry}

n = 5; mean ± SEM One way ANOVA *LSD post hoc test*: q, r, s=$p<0.05$ when compared to the AC treated group. x, y,z=$p<0.05$; when compared to the control (CTRL).

4.3.2 Hippocampal Cell (CA1 and CA3) Histometric Characteristics

Within the CA1, there was a significant decrease ($p<0.05$) decrease in the cell soma area of the pyramidal cells when the aluminium (AC) treated group is compared to the control. When the EGH+AC, EGH and EGL were compared with the AC treated group, there was a significant ($p<0.05$) in the pyramidal cell soma area. EGH+AC and EGL+AC when compared to the control (CTRL), there was a statistical ($p<0.05$) when compared to the control (CTRL). Pyramidal cell soma perimeter within the CA1 region of the hippocampus revealed a significant ($p<0.05$) reduction in perimeter when compared to the control. Treatment with eugenol, however, was able to increase the perimeter but this increase was not statistically significant ($p>0.05$) when compared to the AC treated group. Neuronal cell perimeter among EGH+AC and EGL+AC groups was not statistically significant ($p>0.05$) when compared to the AC treated group. However, comparison of EGH and EGL treated revealed a significant ($p<0.05$) difference in neuronal cell soma perimeter when compared to the AC treated group as shown in table 4.3.

Within the CA3, The aluminium (AC) treated group showed a statistically ($p<0.05$) decrease in the area of pyramidal cells when compared to the control (CTRL).

However, treatment with eugenol within the EGH+AC, EGL+AC, and EGH revealed a statistical difference ($p<0.05$) when compared with the aluminium treated group (AC) and this difference was nonsignificant ($p>0.05$) when compared to the control (CTRL) group. Within the EGL treated group, group the neuronal cell soma area revealed a nonsignificant ($p>0.05$) when compared to the aluminium (AC) and control groups respectively as shown in figure 4.3

The Cell perimeter of the CA3 region revealed a significant ($p<0.05$) reduction in the cell perimeter of pyramidal cell soma of the aluminium treated group (AC) when compared to the

control. However within the groups EGH+AC, EGL+AC, and EGH revealed a significant ($P<0.05$) difference when compared to the AC treated group, when compared to the control (CTRL), there was a non-significant difference ($p>0.05$). Cell soma perimeter in the EGL group revealed a nonsignificant ($p>0.05$) when compared to the control (CTRL) and aluminium treated group (AC) as shown in figure 4.3.

Table 4.3 Histometric analysis of the effect of Eugenol on pyramidal neurons of the hippocampus (CA1 and CA3 regions) of Wistar rats

Groups	CA1(Pyramidal cell)		CA3 Area(Pyramidal cell)	
	Area (μm^2)	Perimeter (µm)	Area (μm^2)	Perimeter (µm)
CTRL (0.6 ml/kg)	2.07±0.15	5.59±0.23	2.10±0.10	5.41±0.12
AC (100 mg/kg)	1.42±0.06^{z}	4.52±0.10^{x}	1.77±0.05^{x}	5.05±0.07^{x}
EGH + AC (300 mg/kg + 100 mg/kg)	1.70±0.11^{qx}	4.87±0.17^{x}	2.19±0.12^{q}	5.69±0.14^{q}
EGL +AC (150 mg/kg + 100 mg/kg)	1.61±0.0^{x}	4.76±0.06^{x}	2.05±0.08^{q}	5.55±0.14^{q}
EGH (300 mg/kg)	1.99±0.12^{q}	5.20±0.17^{q}	2.16±0.09^{q}	5.50±0.09^{q}
EGL (150 mg/kg)	1.96±0.07^{q}	5.31±0.10^{q}	1.96±0.06	5.27±0.08

n = 5; mean ± SEM One way ANOVA LSD post hoc test: q = $p<0.05$ when compared to the aluminium treated group (AC); x = $p<0.05$ when compared to the control (CTRL).

4.4 Histological and Histochemical Studies

Histological sections of Wistar rat brain regions (cerebral cortex layers III and V; cerebellum and hippocampus-CA1 and CA3) stained with routine histological (Haematoxylin and Eosin H&E) and histochemical (Cresyl Fast Violet, Congo red and Golgi) stains and examined under the light microscope revealed the following:

4.4.1 Histological Features of the Cerebral Cortex

4.4.1.1 Histological and Histochemical Features of the Cerebral Cortex of Control (Untreated) and Treated Wistar Rats

The cerebral sections of Wistar rats in the control group showed normal histoarchitecture of the cerebral cortex; the characteristic appearance of the neurons arranged into six (6) layers, differing in neuron morphology, size, and population density. Particularly, the ganglionic layer (Layer V) reveals large pyramidal (ganglion) cells of the motor cortex and and stellate cells. Unlike the Layer III which is composed of medium sized pyramidal cells. The cerebral sections of the cerebral cortex of Wistar rats treated with aluminium chloride revealed distortion in the cytoarchitecture of the cerebral cortex (Layer III and Layer V); neuronal degenerative changes such as neuronal shrinkage and perineuronal vacoulations, satelliotosis and Chromatolysis.

Histological and histochemical examination of the cerebral sections of the Wistar rats treated with eugenol, which was followed by administration of aluminium chloride revealed mild distortion of the cytoarchitecture of the cerebral cortex (Layers III and V). The histological features of the Eugenol treated group were comparable to the control (untreated). Histochemical (Golgi) staining revealed loss of pyramidal neuronal processes, CFV staining revealed necrosis and Chromatolysis.

Congo red staining revealed no amyloidal plaques across all groups at the stated dose that was administered to the Wistar rats**.** Histochemical (cresyl fast violet, CFV) staining for Nissl substances revealed normal appearance of distinctly stained large pyramidal neurons and Golgi staining for neurites revealed normal appearance of large pyramidal neurons, axonal and dendritic processes**.**

Congo red stain used to show amyloidal plaques showed no amyloid plaques with the layers of the cerebral cortex **(Plate 4.1-4.24)**

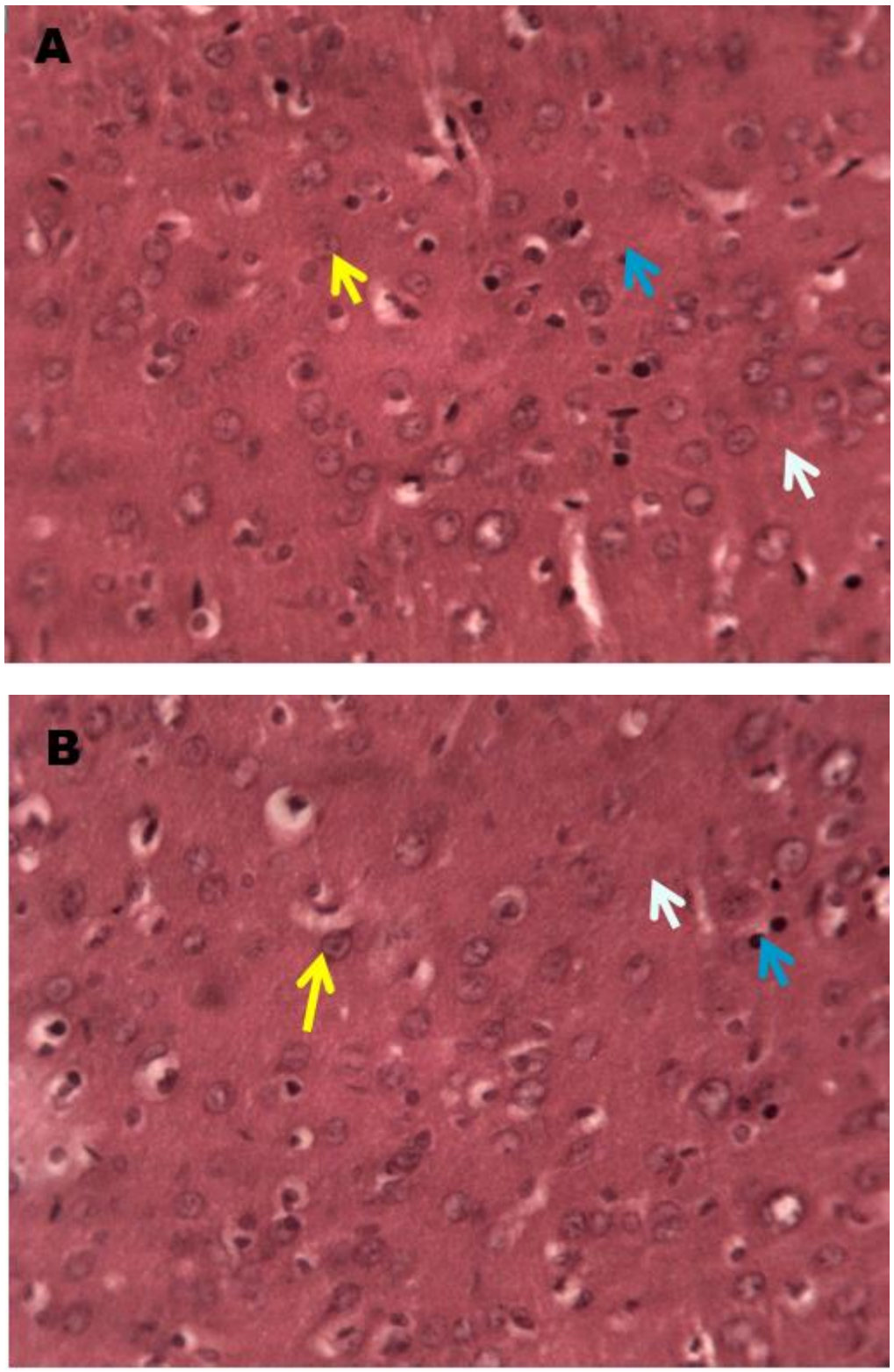


Plate 4.1: Section of the cerebral cortex 'A' (Layer III), 'B' (Layer V) of control (CTRL) group showing normal histology of the cerebral cortex: yellow arrow (Pyramidal cell); blue arrow (glial cell); White arrow (neuropil). (Mag x 250 H&E).

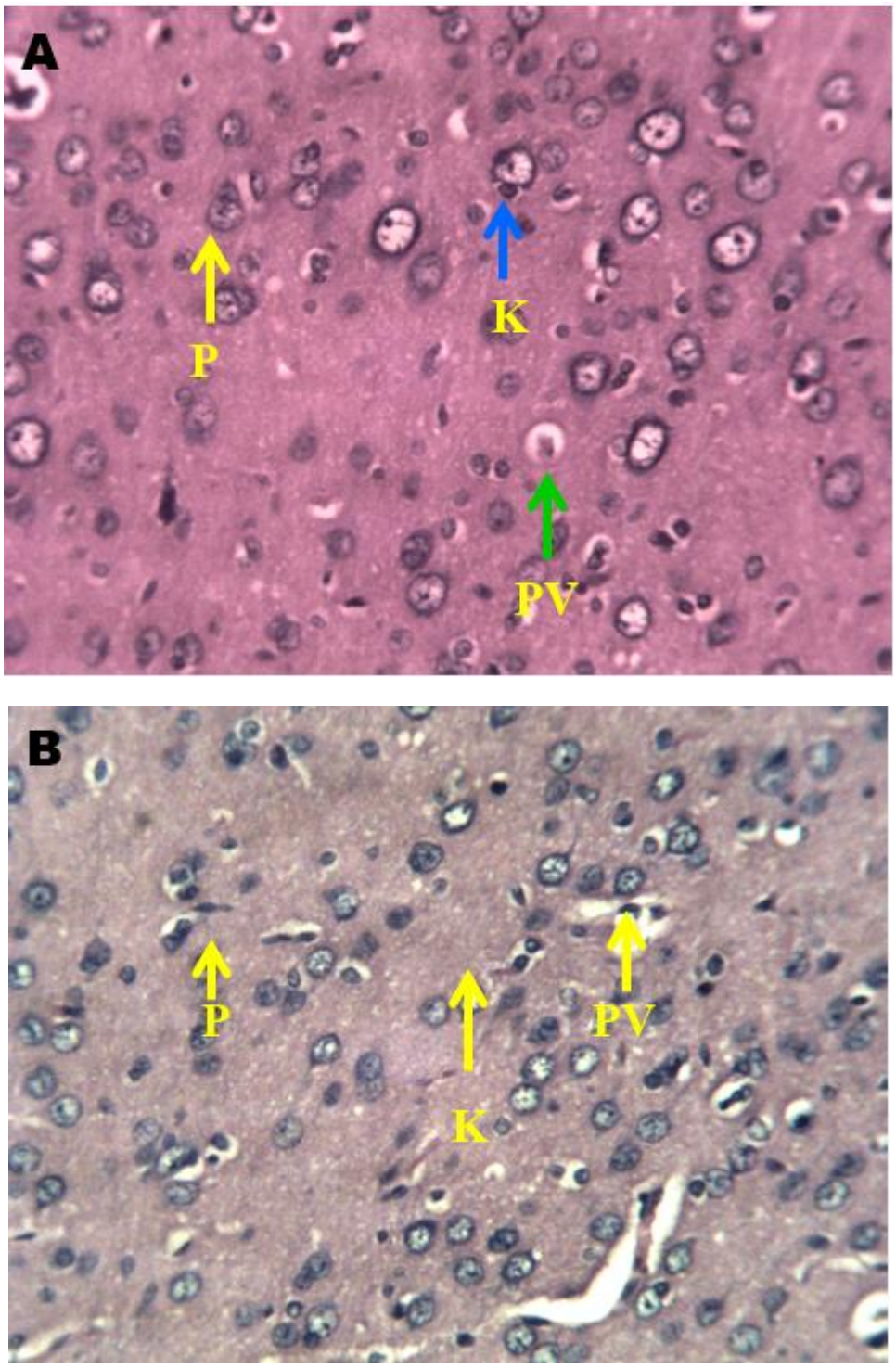


Plate 4.2: Section of the cerebral cortex 'A' (Layer III); B (Layer V) of aluminium treated group (AC) (100mg/kg of aluminium chloride) revealing a distorted histoarchitecture: (Yellow line Pyknotic Pyramidal cell 'P'), blue line (Chromatolysis (k) and green line 'perineuronal vacoulations PV) (Mag x 250 H&E)

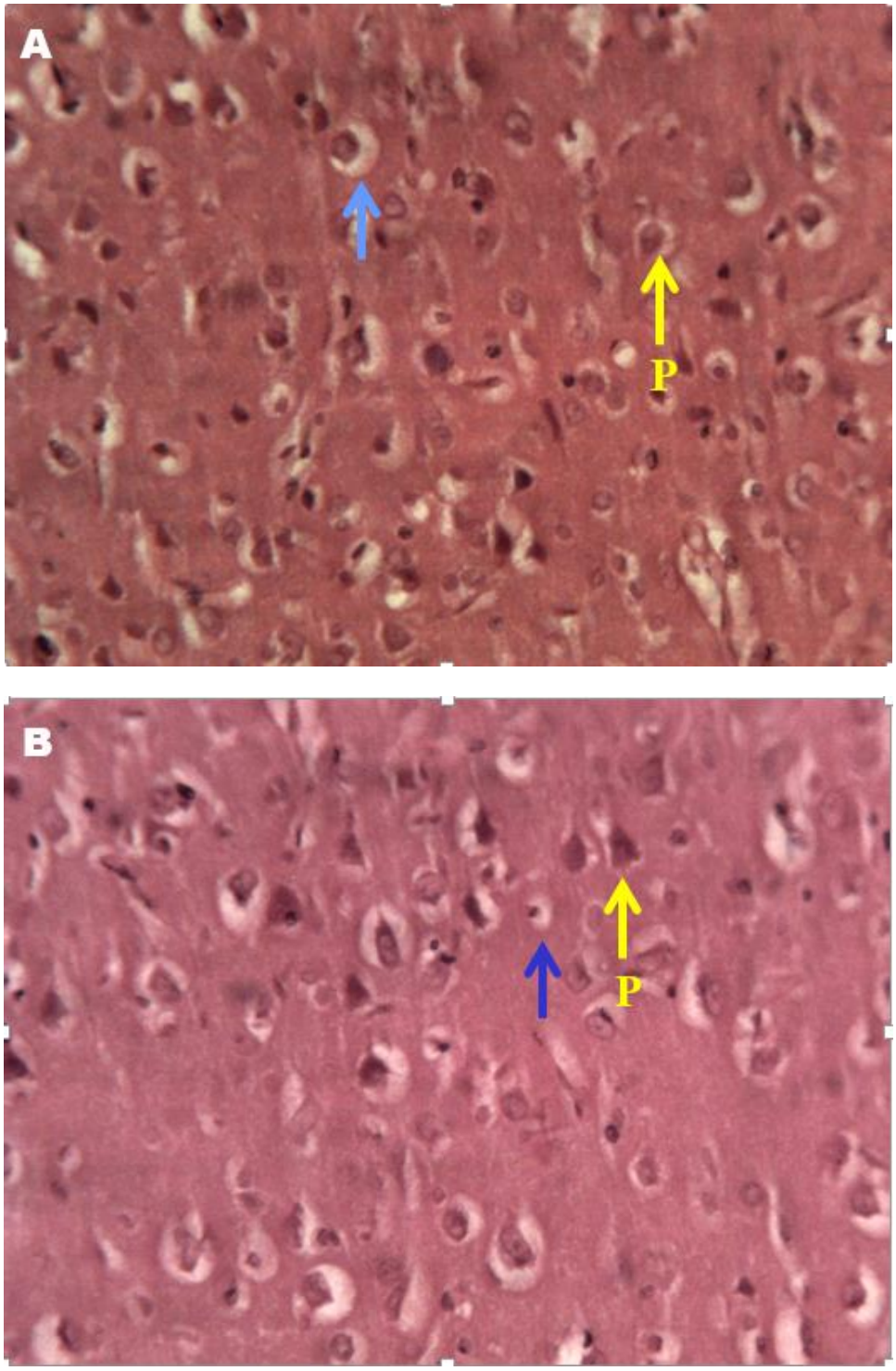


Plate: 4.3: Section of Wistar rat cerebral cortex 'A' (Layer III) and 'B' (Layer V) of Group EGH+AC (300mg/kg Eugenol and 100mg/kg of Aluminium chloride) showing mild distortion and perineuronal vacoulations'PV' (blue line) in the cytoarchitecture when compared to the group administered 100mg/kg aluminium chloride only. Pyramidal cell 'P' yellow line (H&E x 250).

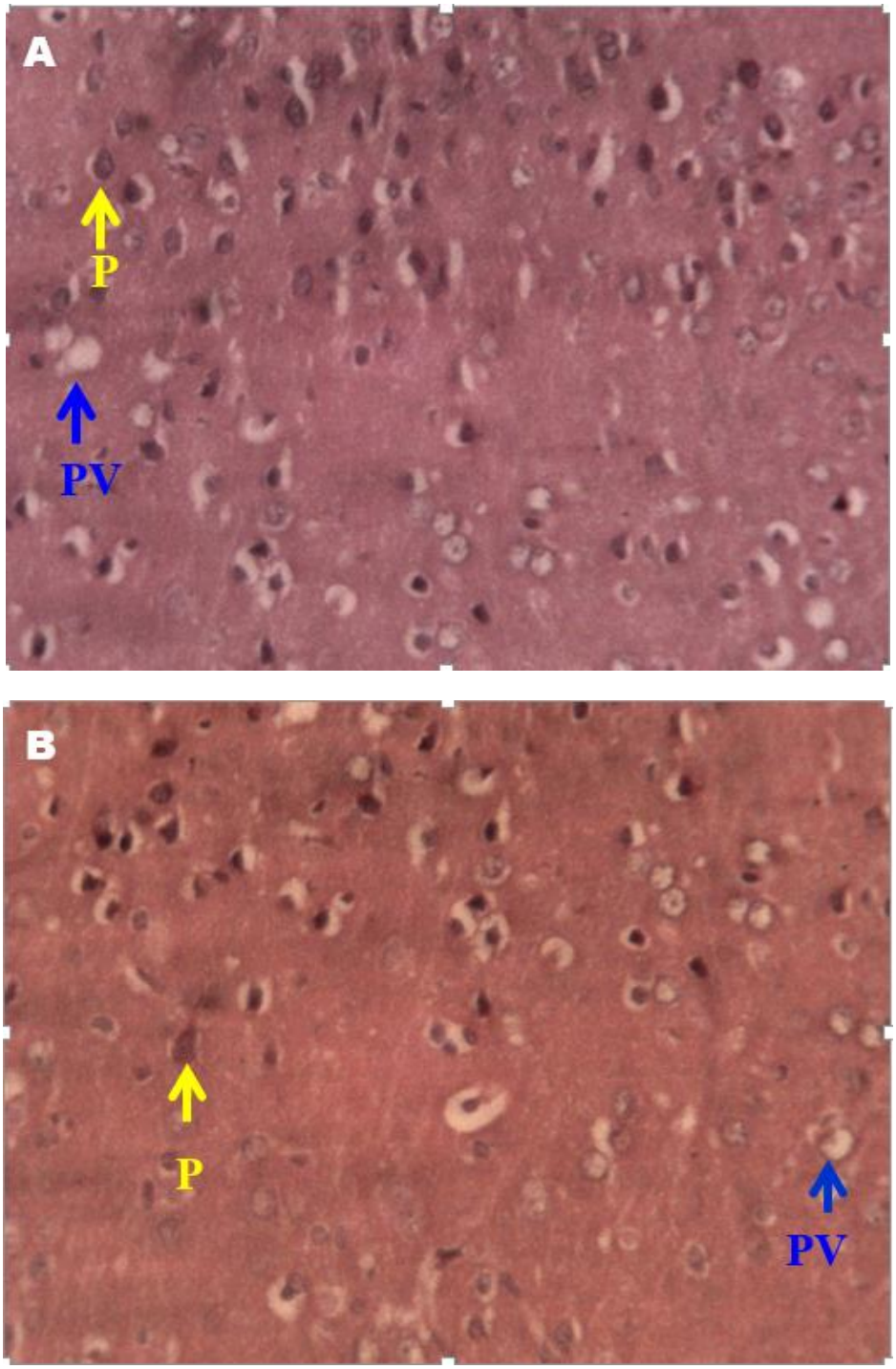


Plate 4.4: Section of Wistar rat cerebral cortex 'A' (Layer III) and 'B' (Layer V) of Group EGL+AC (150mg/kg of Eugenol and 100mg/kg of Aluminium chloride) showing mild distortion in the cytoarchitecture of the cerebral cortex with perineuronal vacoulations (PV) (blue line) when compared to the group that was administered 100mg/kg only. Pyramidal cell (P) (yellow line) (Mag x 250 H&E).

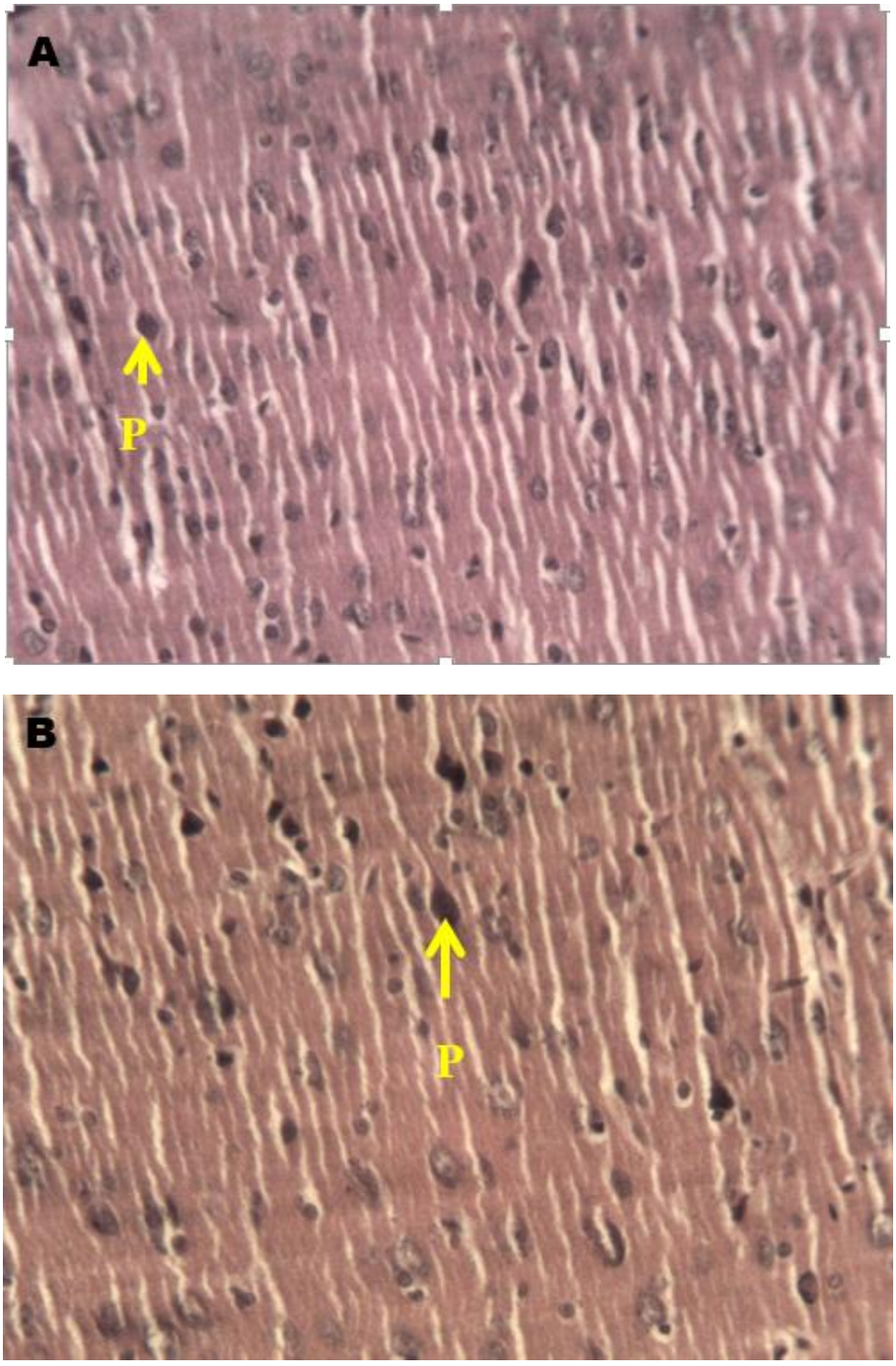


Plate 4.5: Section of the cerebral cortex 'A' (Layer III) and 'B' (Layer V) of Group (EGH) (300mg/kg of Eugenol) showing a normal cytoarchitecture of the cerebral cortex when compared to the control group. Pyramidal cell (P) (Yellow line) (Mag X 250 H&E).

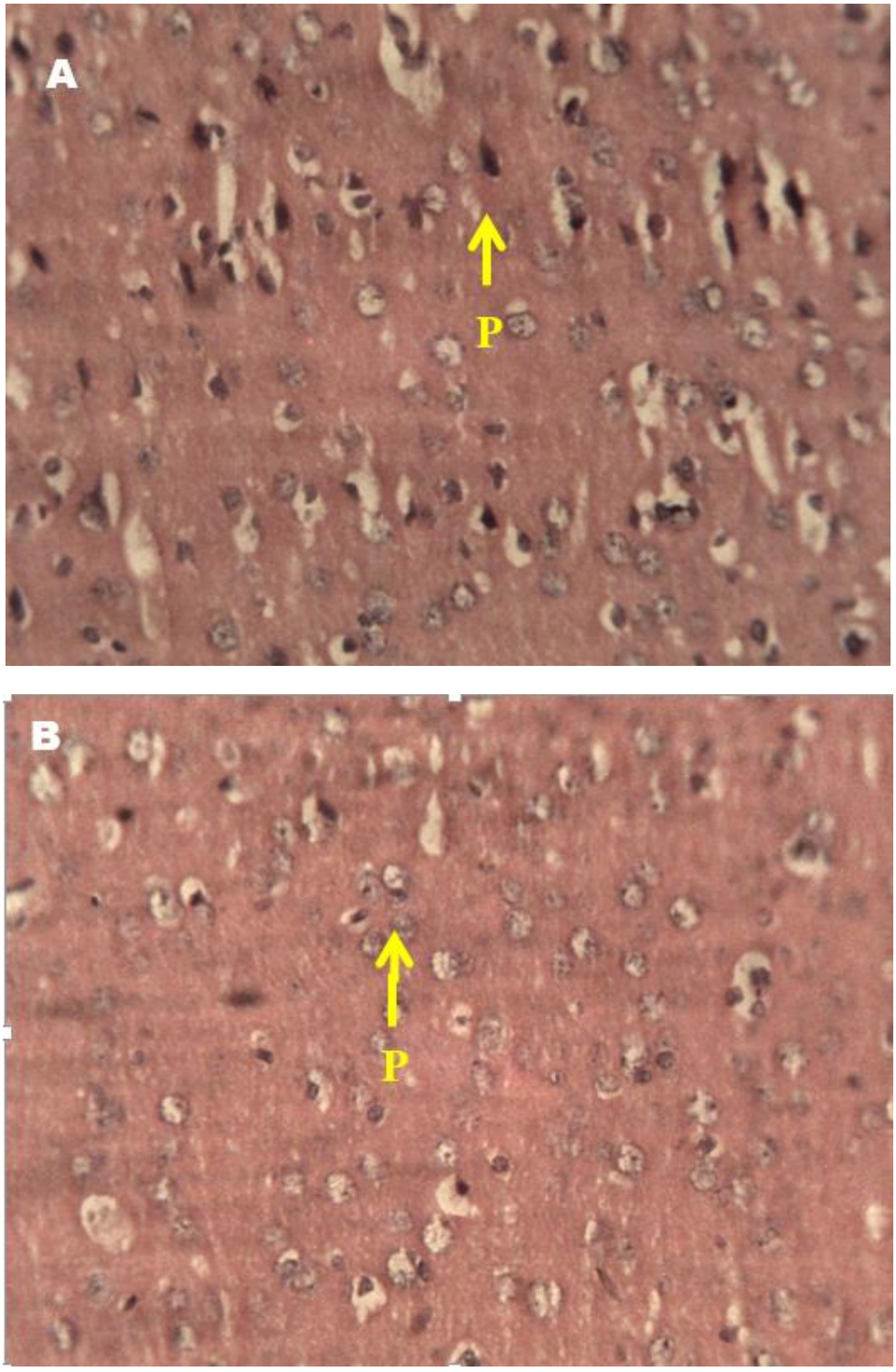


Plate 4.6: Section of Wistar rat cerebral cortex 'A' (Layer III) and 'B' (Layer V) of Group (EGL) (150mg/kg of Eugenol) revealing a normal cytoarchitecture 0f the cerebral cortex when compared to the control group Pyramidal cell (P) (yellow line). (Mag x 250 H&E)

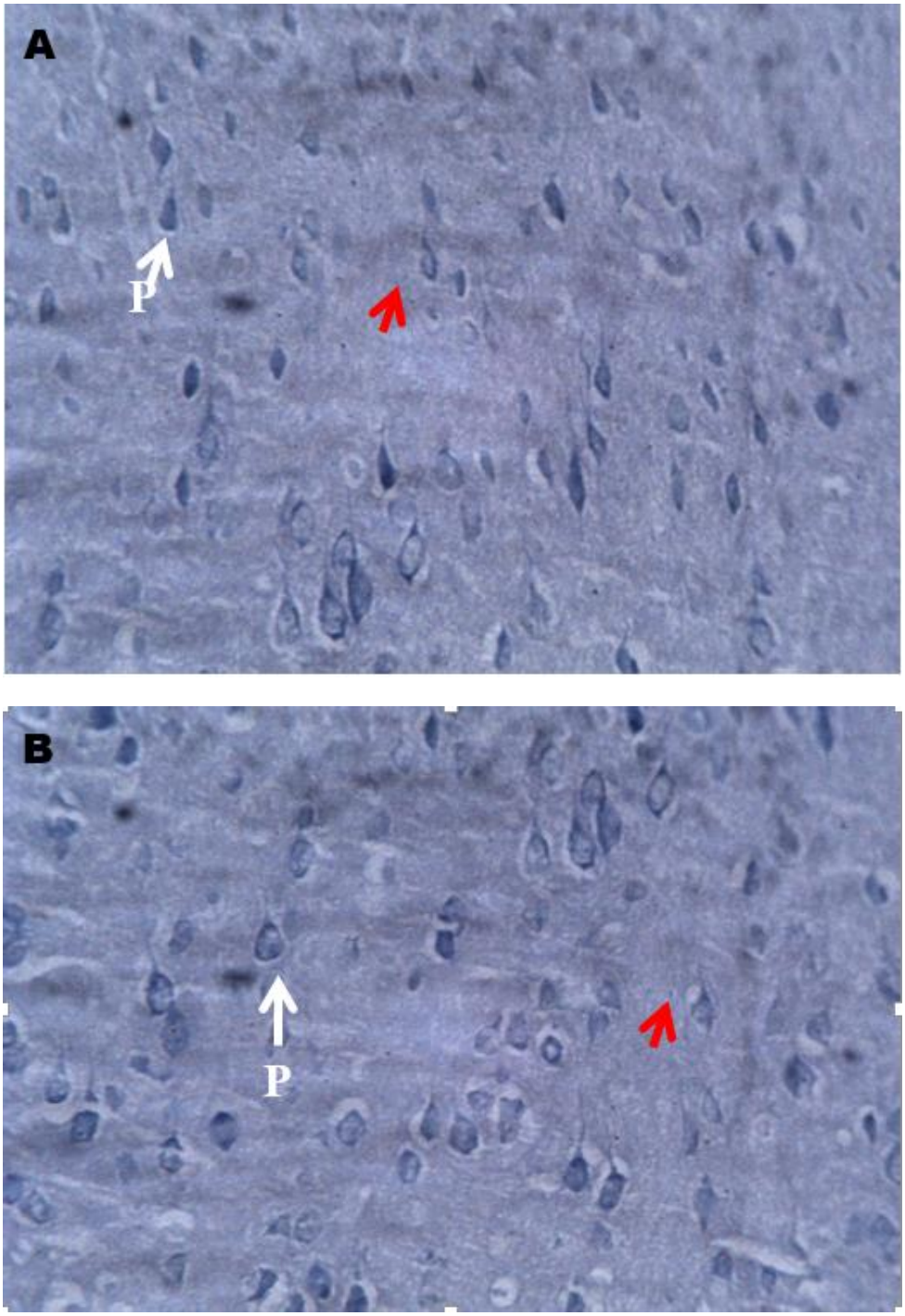


Plate 4.7: Section of the cerebral cortex 'A '(layer III) and 'B' (layer V) of control (CTRL), showing the normal histology of the cerebral cortex. White line (Pyramidal cell (P); Red line (Neuropil) (Mag x 250 CFV)

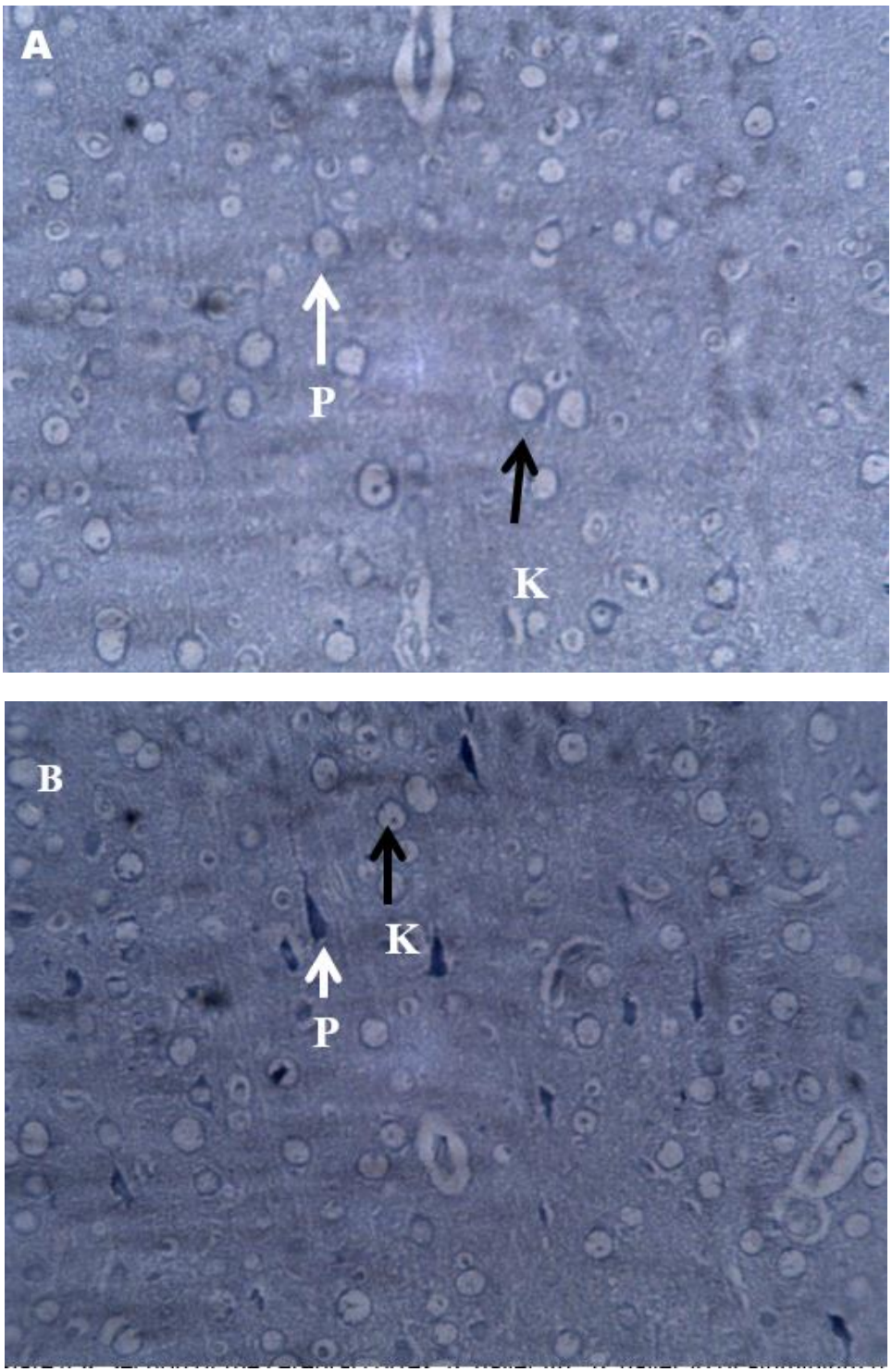


Plate 4.8: Section of the cerebral cortex 'A' (layer III); 'B' (layer V) of aluminium treated group (AC) (100mg/kg of aluminium chloride), showing distortion in the histology of cerebral cortex.White line (Pyramidal cell 'P'), black line (Chromatolysis 'k'), with Pyknotic cells and perineuronal vacoulations (PV) (Mag x 250 CFV).

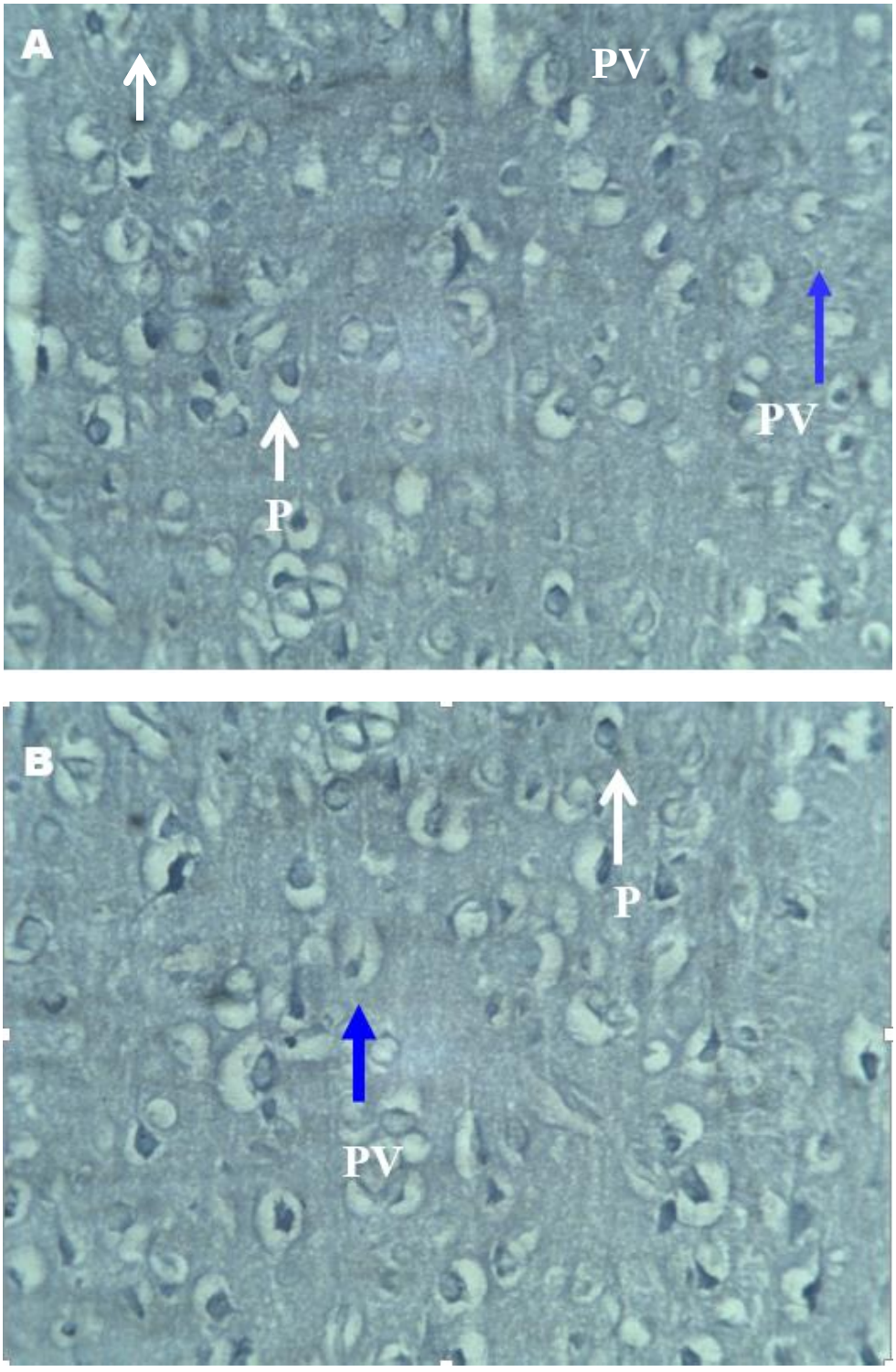


Plate: 4.9: Section of Wistar rat cerebral cortex 'A' (Layer III) and 'B' (Layer V) of Group EGH+AC (300mg/kg Eugenol and 100mg/kg of Aluminium chloride) showing mild distortion and perineuronal vacoulations 'PV' (blue line) in the cytoarchitecture when compared to the group administered 100mg/kg aluminium chloride only. Pyramidal cell 'P' (white line) (Mag x 250 CFV).

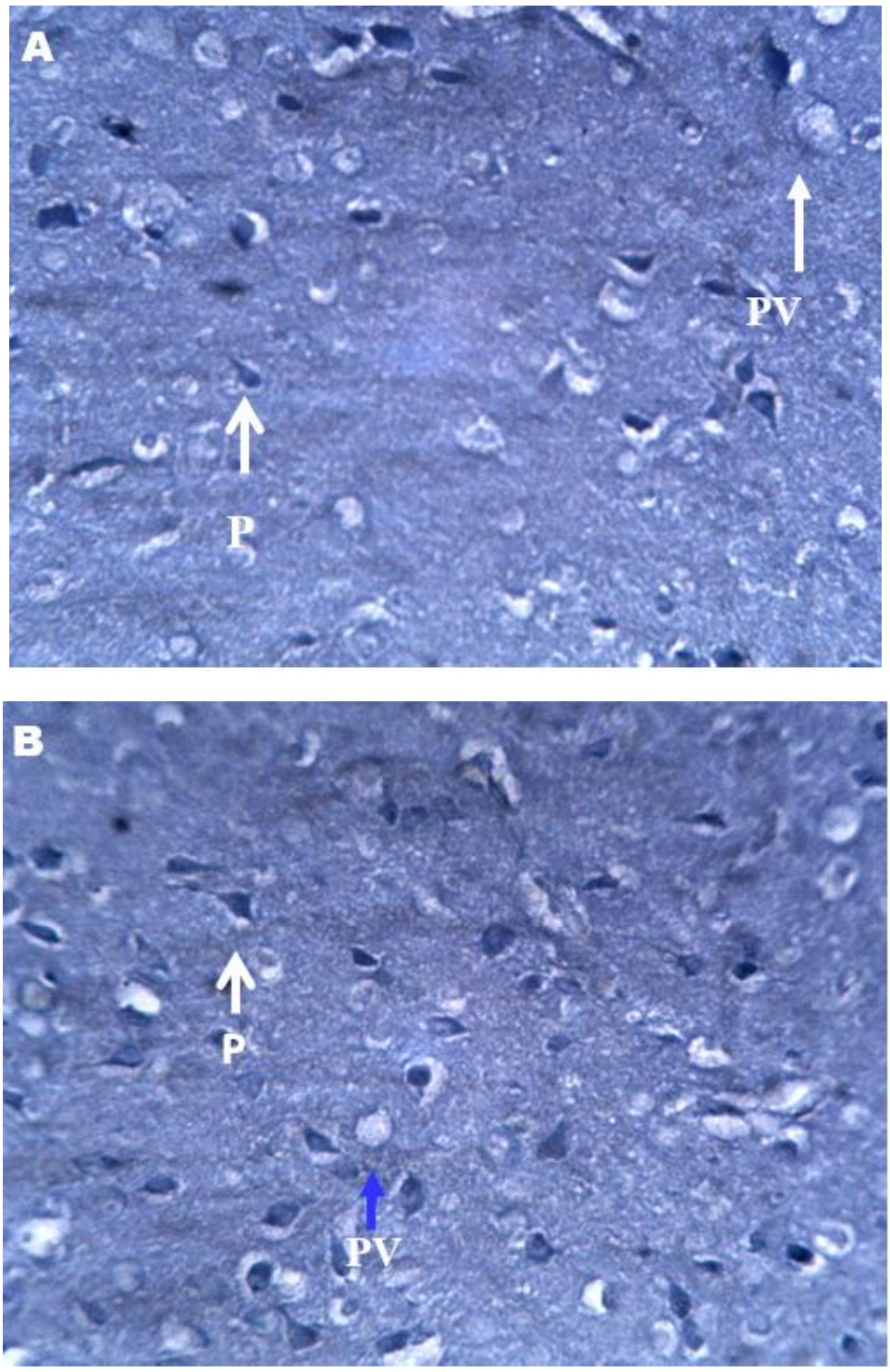


Plate 4.10: Section of the cerebral cortex 'A' (Layer III) and 'B' (Layer V) of Group EGL+AC (150mg/kg of Eugenol and 100mg/kg of aluminium chloride) showing mild distortion in the cytoarchitecture of the cerebral cortex with mild perineuronal vacoulations 'PV'(blue line) when compared with the group administered 100mg/kg of aluminium chloride only. Pyramidal cell 'P' (white line) (Mag x 250 CFV).

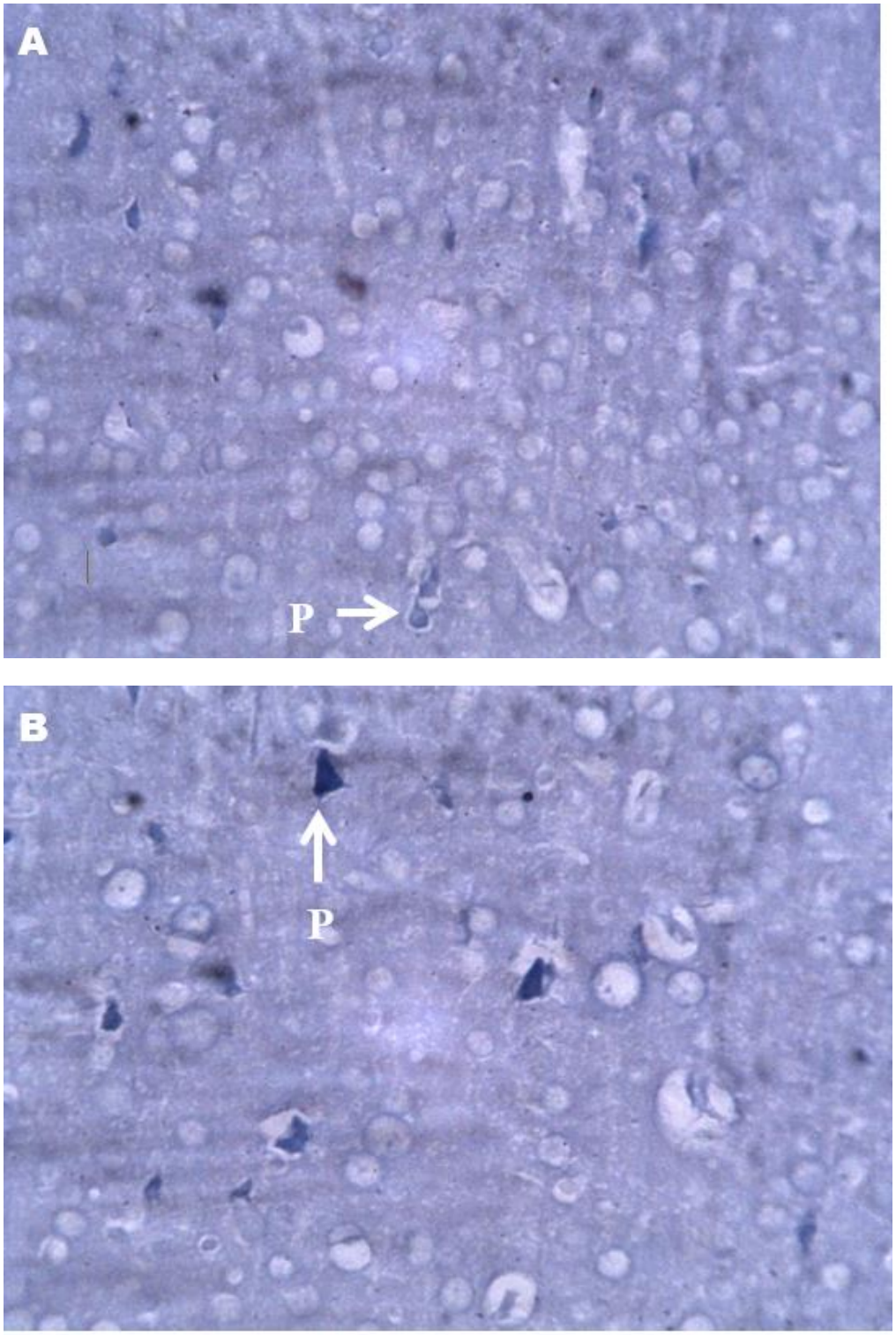


Plate 4.11: Section of Wistar rat cerebral cortex 'A' (Layer III) and 'B' (Layer V) of Group (EGH) (300mg/kg of Eugenol) showing a normal cytoarchitecture of the cerebral cortex when compared with the control group. Pyramidal cell 'P' (white line) (Mag x 250 CFV).

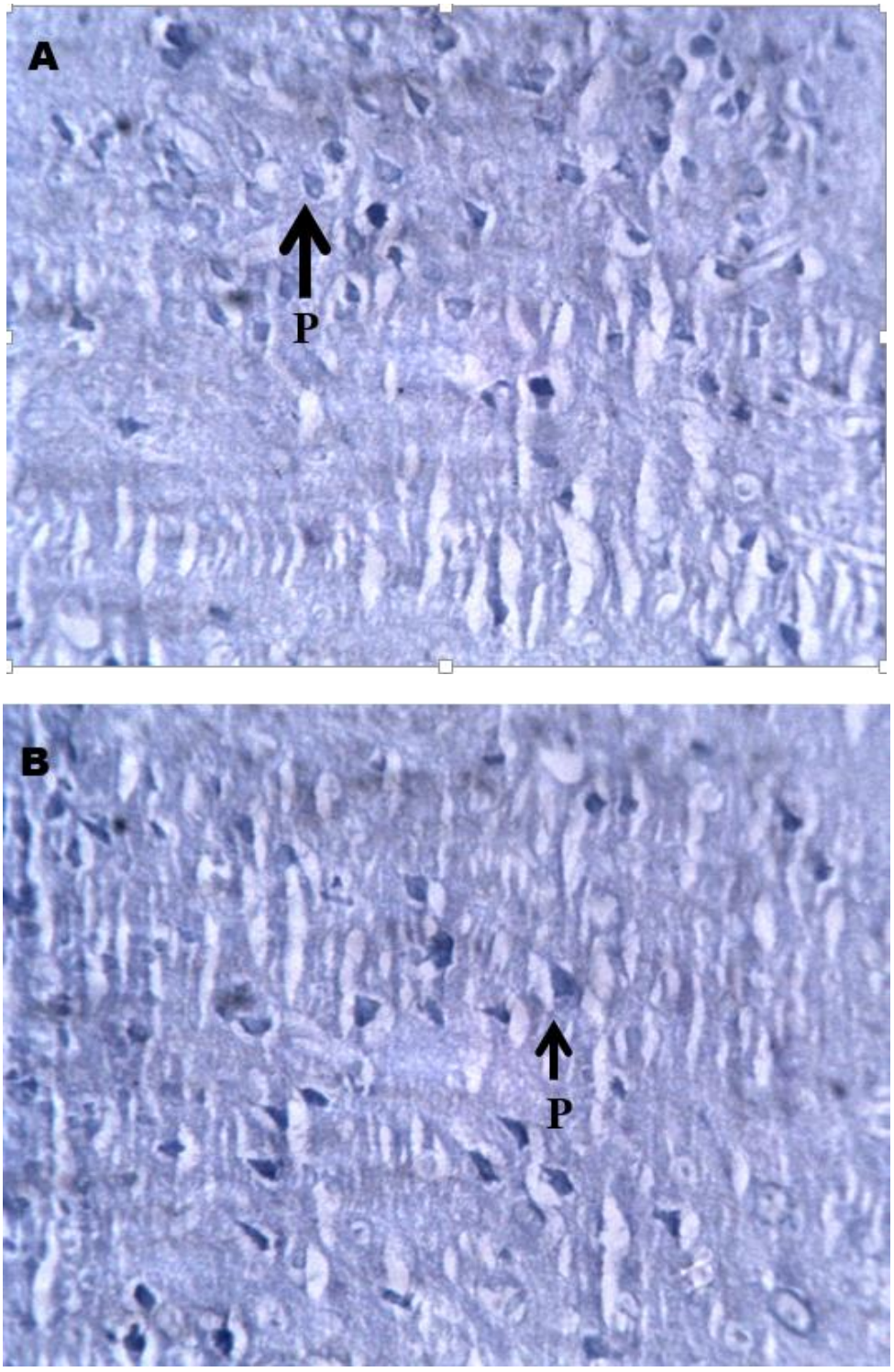


Plate 4.12: Section Wistar rat cerebral cortex 'A' (Layer III) and 'B' (Layer V) of Group EGL (150mg/kg of eugenol) revealing a normal cytoarchitecture of the cerebral cortex when compared to the control. Pyramidal cell 'P' (black line) (Mag x 250 CFV).

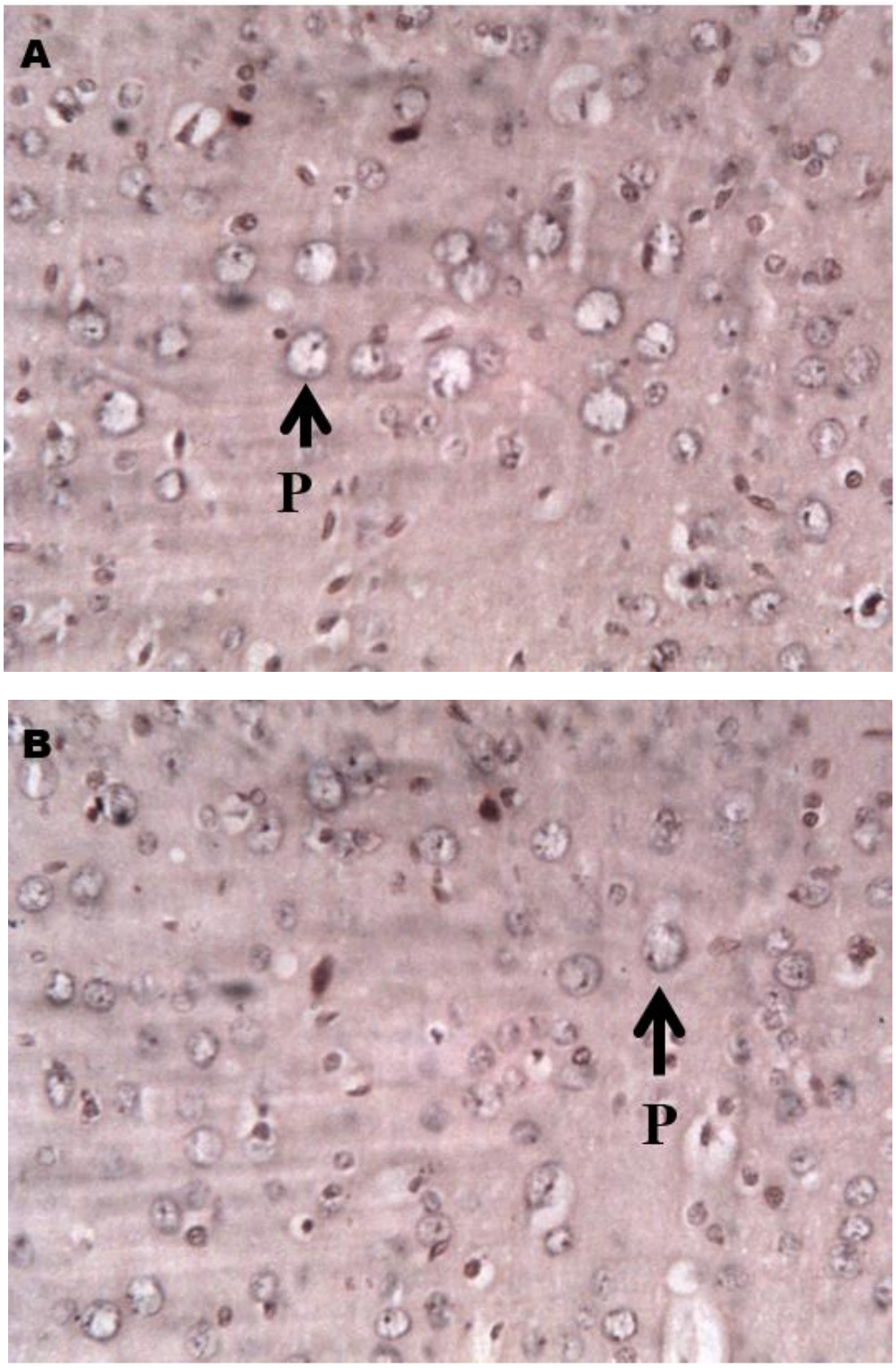


Plate 4.13: Section of Wistar rat cerebral cortex 'A' (Layer III) and 'B' (Layer V) of control (CTRL) (Untreated) showing normal cytoarchitecture of the cerebral cortex; Pyramidal cell 'P' (black line). (Mag x 250 Congo red).

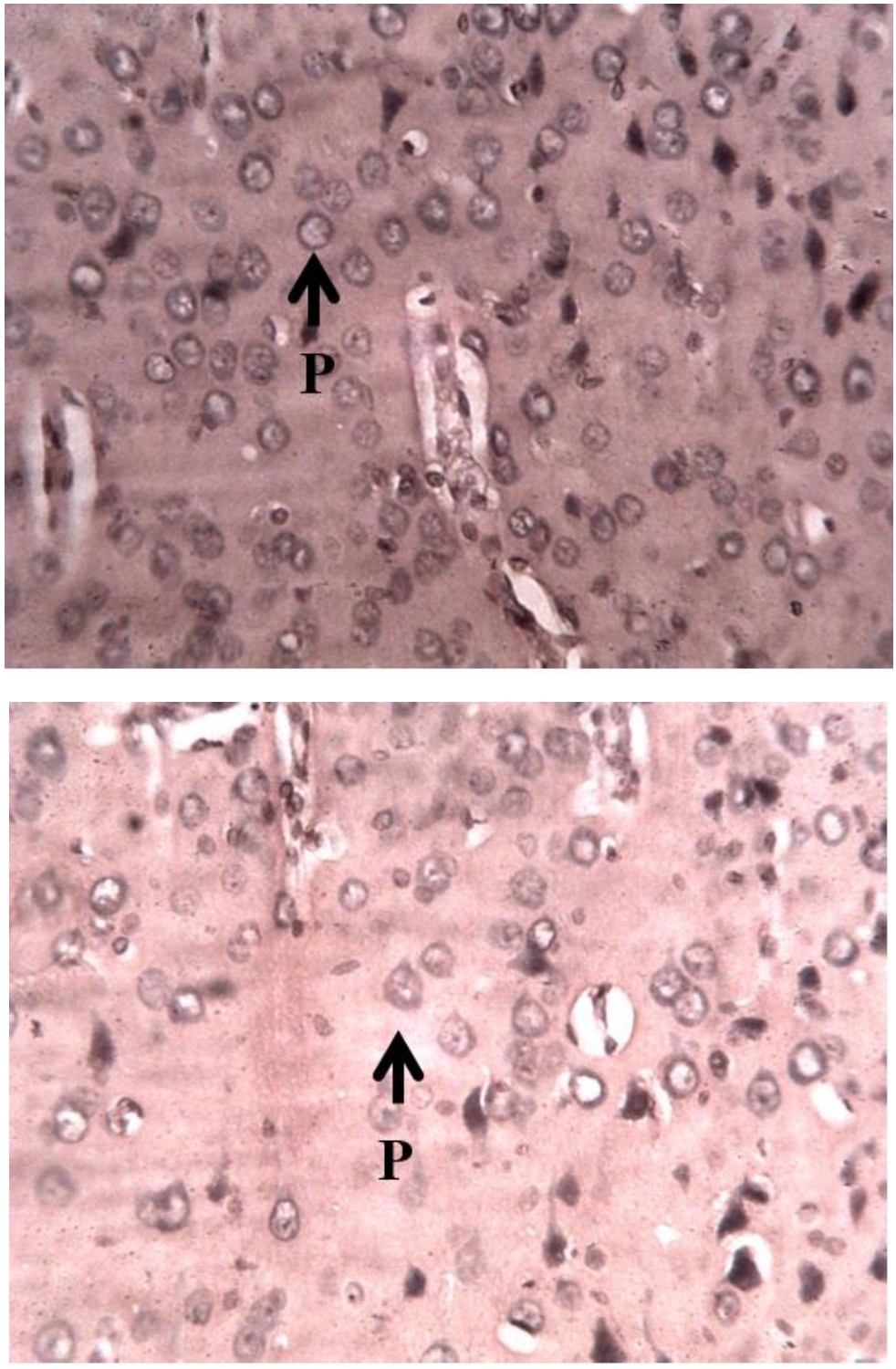


Plate 4.14: Section of Wistar rat cerebral cortex 'A' (Layer III) and 'B' (Layer V) of aluminium treated group (AC) (100mg/kg of aluminium chloride) with no visible amyloid plaques within the cerebral cortex. Pyramidal cell 'P' (black line). (Mag x 250 Congo).

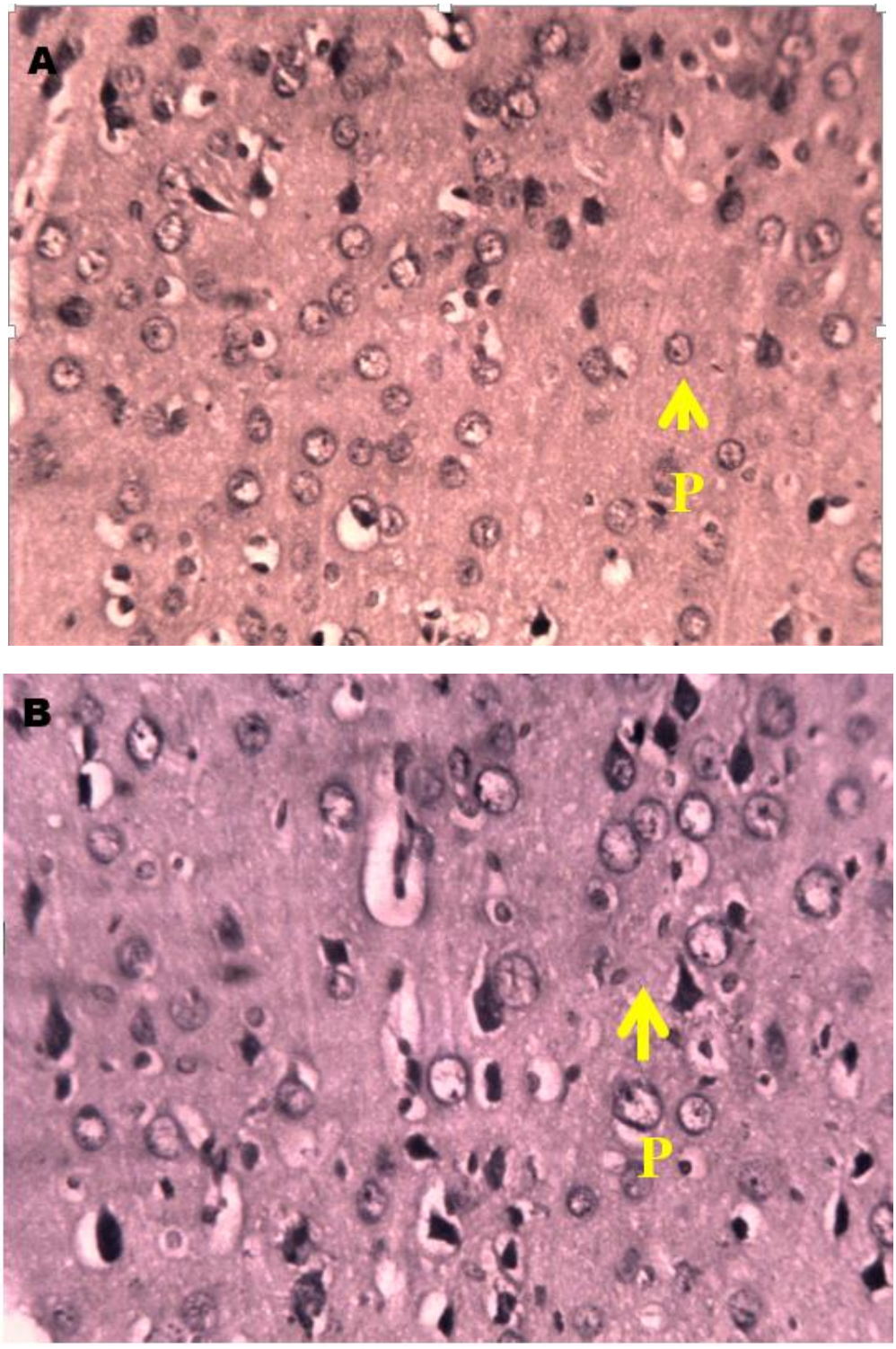


Plate 4.15: Section of Wistar rat cerebral cortex 'A' (Layer III) and 'B' (Layer V) EGH+AC (300mg/kg Eugenol and 100mg/kg of aluminium chloride) with no visible amyloid plaques within the cerebral cortex. Pyramidal cell 'P' (yellow line). (Mag x 250 Congo).

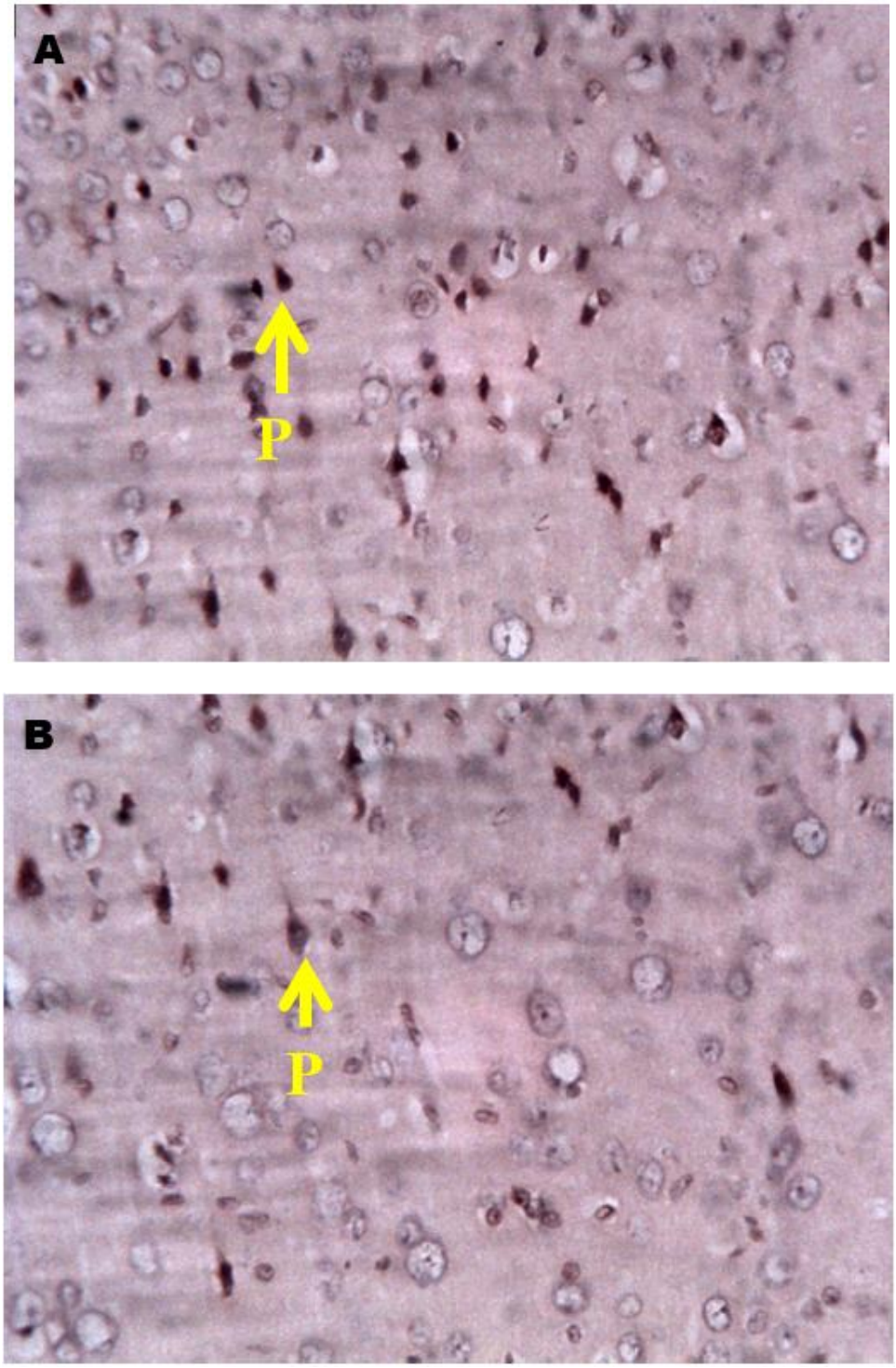


Plate 4.16: Section of Wistar rat cerebral cortex 'A' (Layer III) and 'B' (Layer V) of Group EGL+AC (administered 150mg/kg Eugenol and 100mg/kg of aluminium chloride) with no visible amyloid plaques within the cerebral cortex. Pyramidal cell 'P' (yellow line). (Mag x 250 Congo).

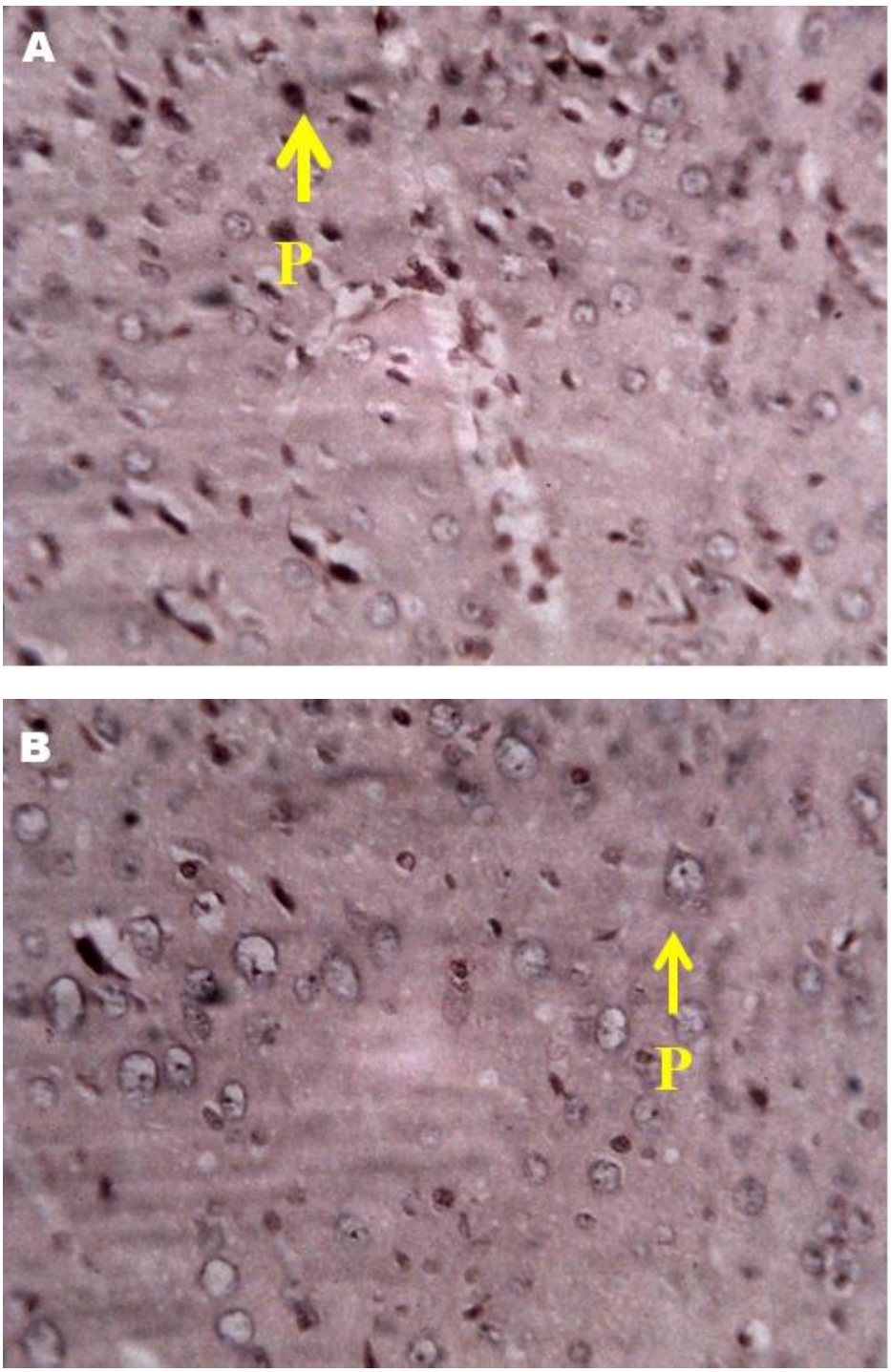


Plate 4.17: Section of Wistar rat cerebral cortex 'A' (Layer III) and 'B' (Layer V) EGH (300mg/kg of Eugenol) with no visible amyloid plaques. Pyramidal cell 'P' (yellow line) (Mag x 250 Congo red).

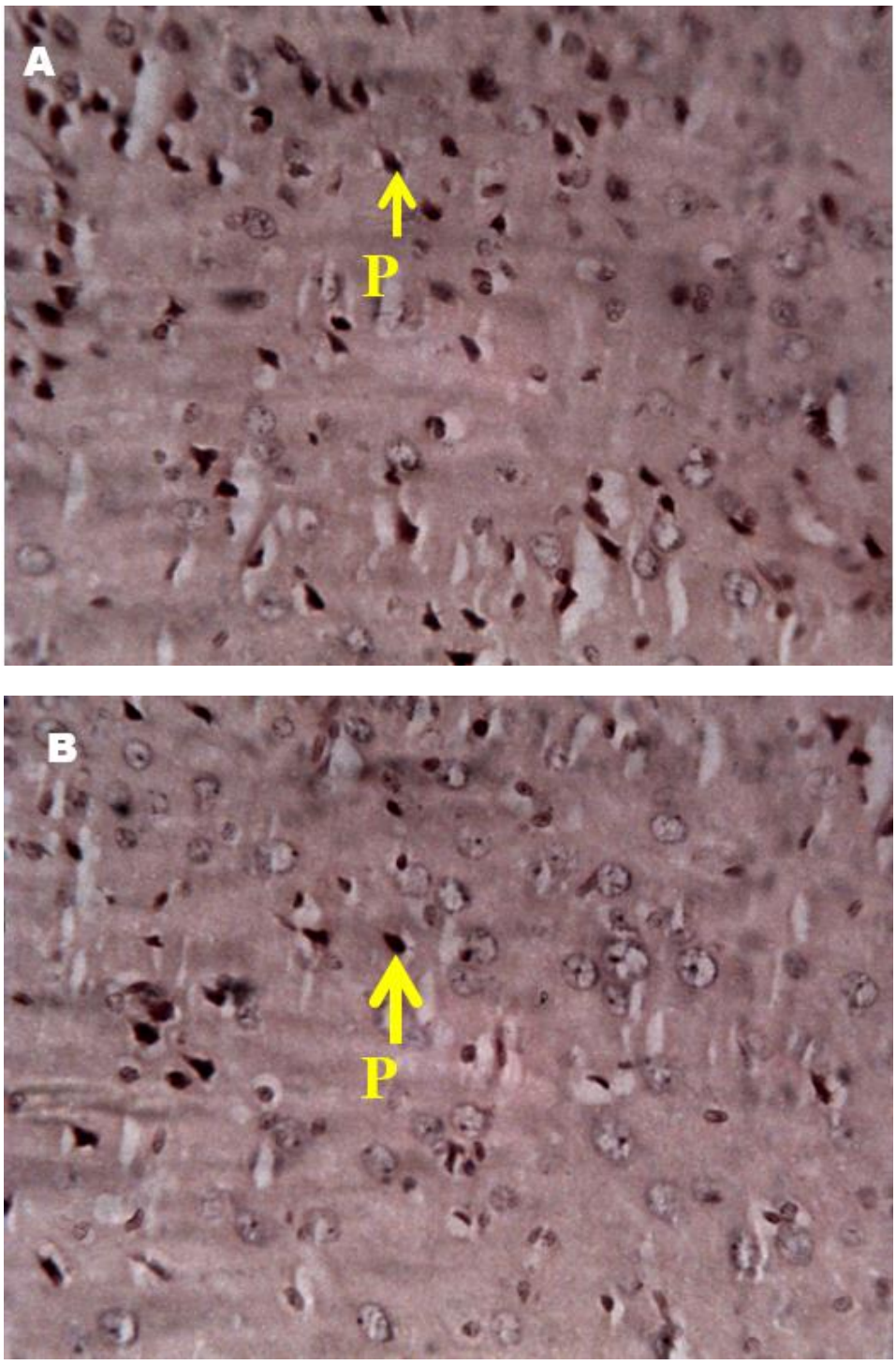


Plate 4.18: Section of Wistar rat cerebral cortex 'A' (Layer III) and 'B' (Layer V). EGH (150mg/kg of Eugenol) revealing no amyloid plaques in the cerebral cortex. Pyramidal cell 'P' (yellow line) (Mag x 250 Congo).

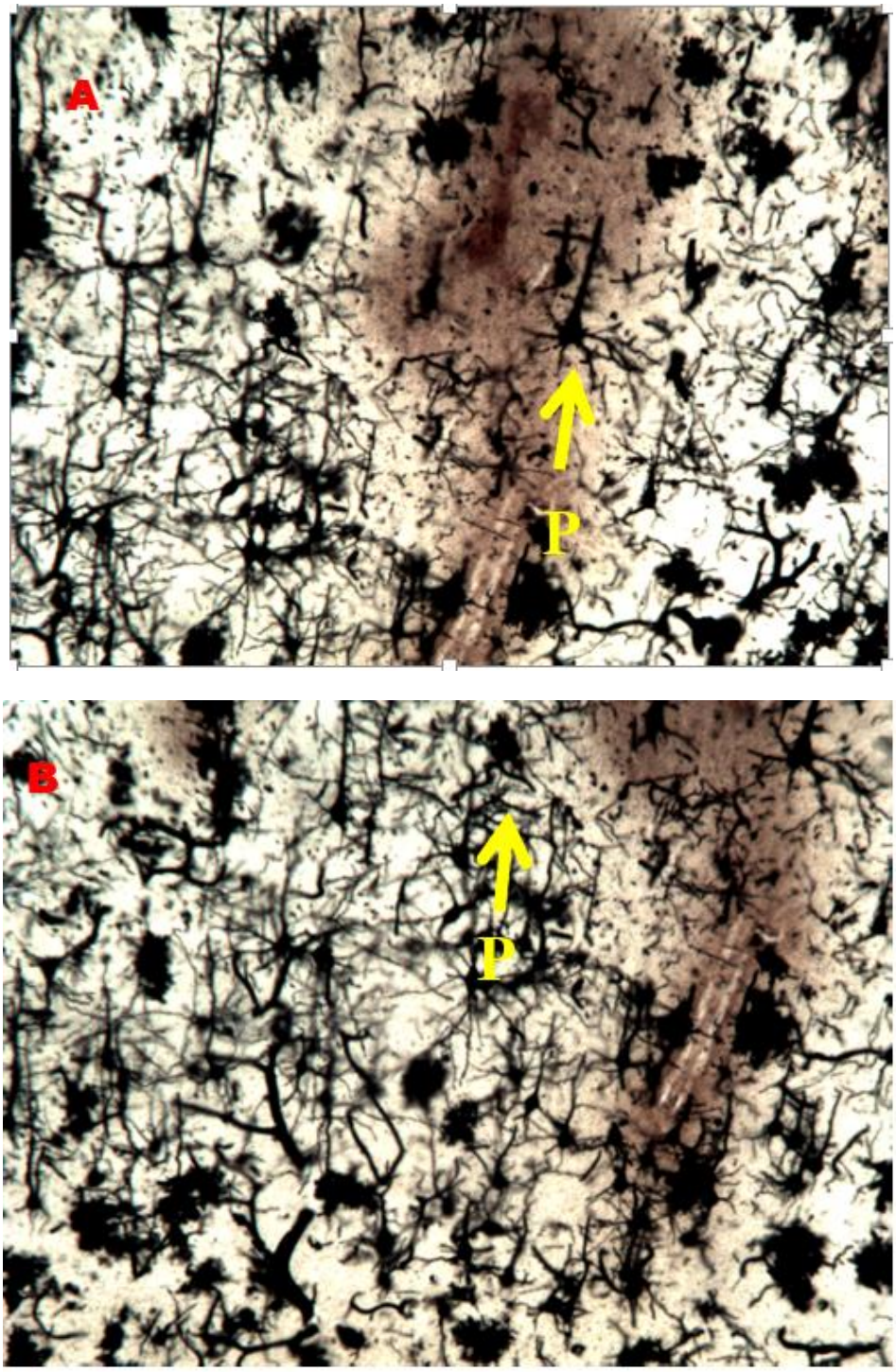


Plate 4.19: Section of Wistar rat cerebral cortex 'A' (Layer III) and 'B' (Layer V) of control (CTRL) showing the normal cytoarchitecture of cerebral cortex with pyramidal cells with its neural processes (Neurites). Pyramidal cell 'P' (yellow line). (Mag x 250 Golgi stain).

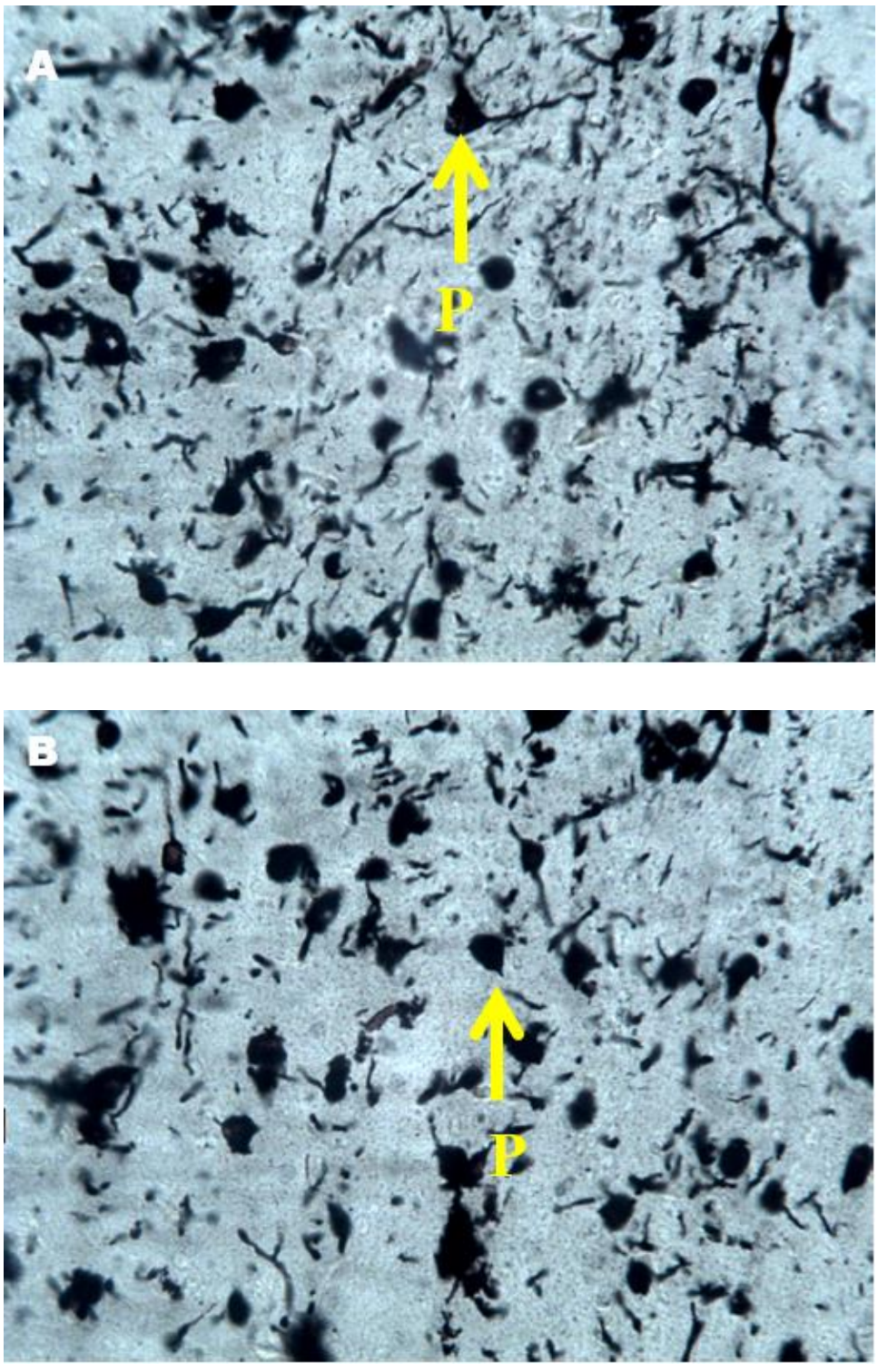


Plate 4.20: Section of the cerebral cortex 'A' (layer III); 'B' (layer V) of aluminium treated group (AC) (100mg/kg of aluminium chloride), showing distortion in the cytoarchitecture of the cerebral cortex, Neuronal degeneration (loss of neuronal process); Pyramidal cell 'P' (yellow line) (Mag x 250 Golgi stain).

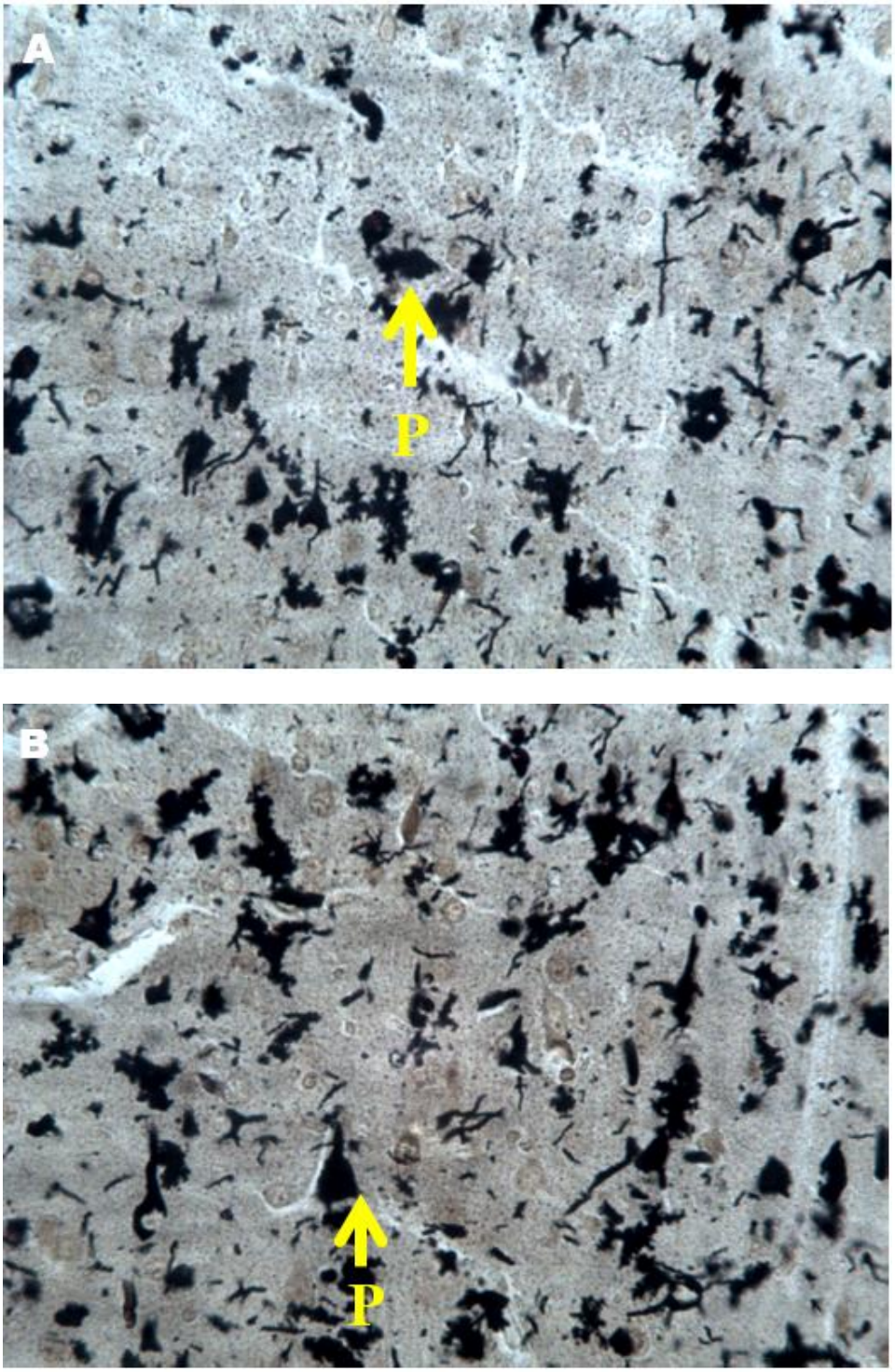


Plate 4.21: Section of the cerebral cortex 'A' (layer III); 'B' (layer V) of Group EGH+ AC (300mg/kg Eugenol and 100mg/kg of aluminium chloride) showing distortion in the cytoarchitecture of the cerebral cortex, Neuronal degeneration (loss of neuronal process); Pyramidal cell 'P'(yellow line) (Mag x 250 Golgi stain).

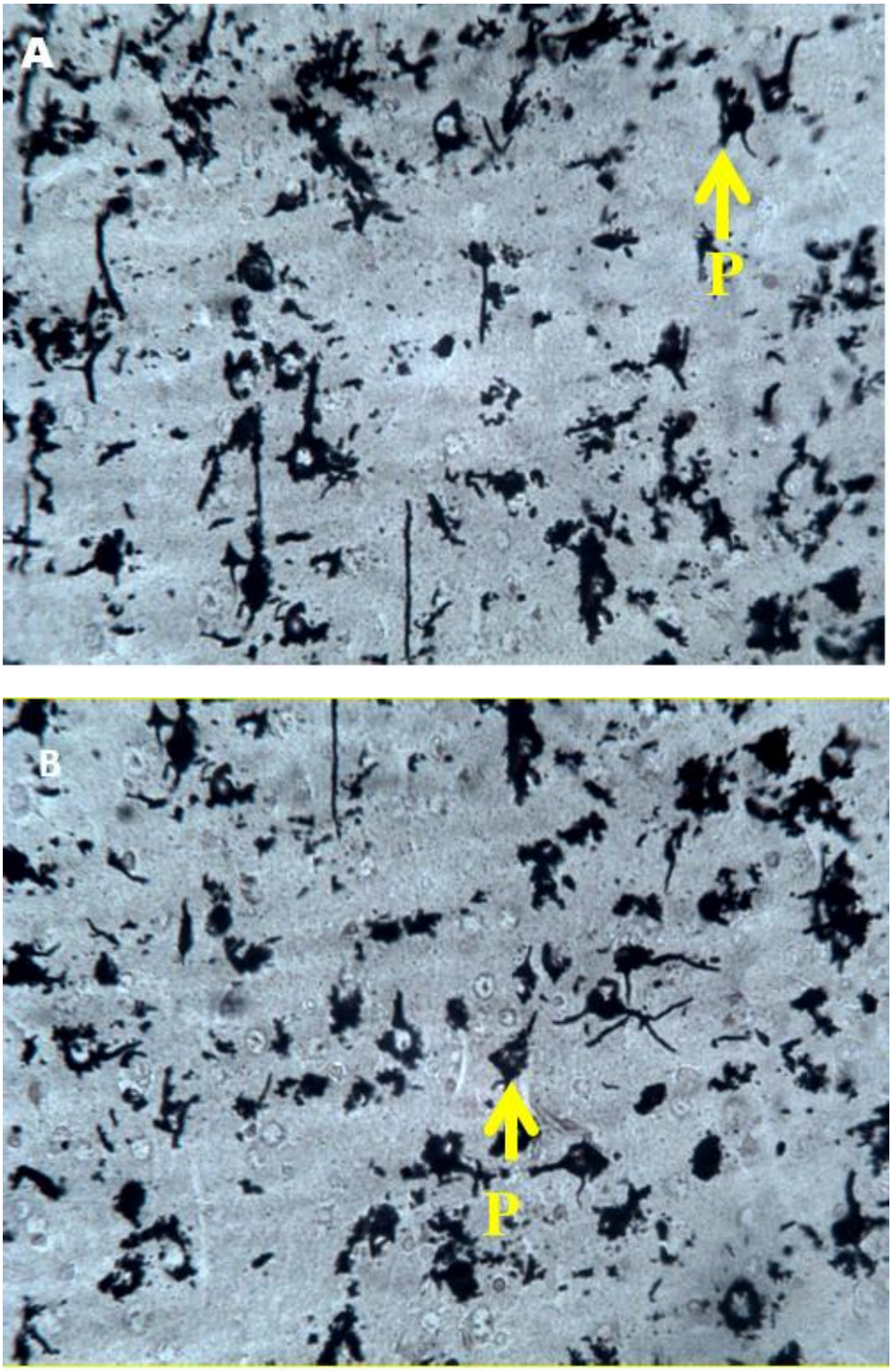


Plate 4.22: Section of the cerebral cortex 'A' (layer III); 'B' (layer V) of Group EGL+AC (150mg/kg Eugenol and 100mg/kg of aluminium chloride) showing mild distortion in the cytoarchitecture of the cerebral cortex when compared with the group administered 100mg/kg of aluminium chloride; Neuronal degeneration (loss of neuronal process); Pyramidal cell 'P (yellow line) (Mag x 250 Golgi stain).

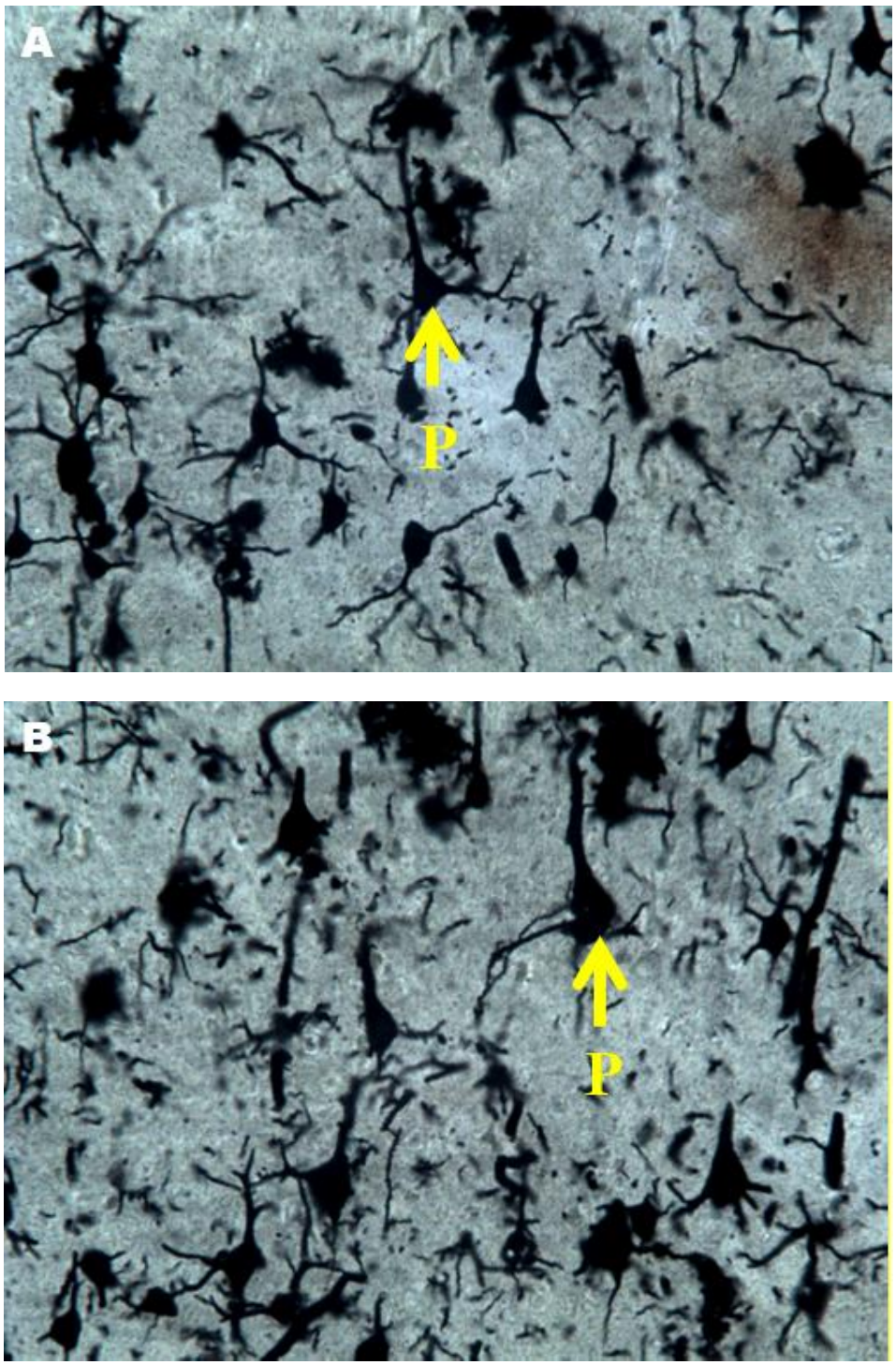


Plate 4.23: Section of Wistar rat cerebral cortex 'A' (Layer III) and 'B' (Layer V) of Group (EGH) (300mg/kg of Eugenol). Showing a normal cytoarchitecture of the cerebral cortex showing neuronal process (Neurites); Pyramidal cell 'P' (yellow line) (Mag x 250 Golgi).

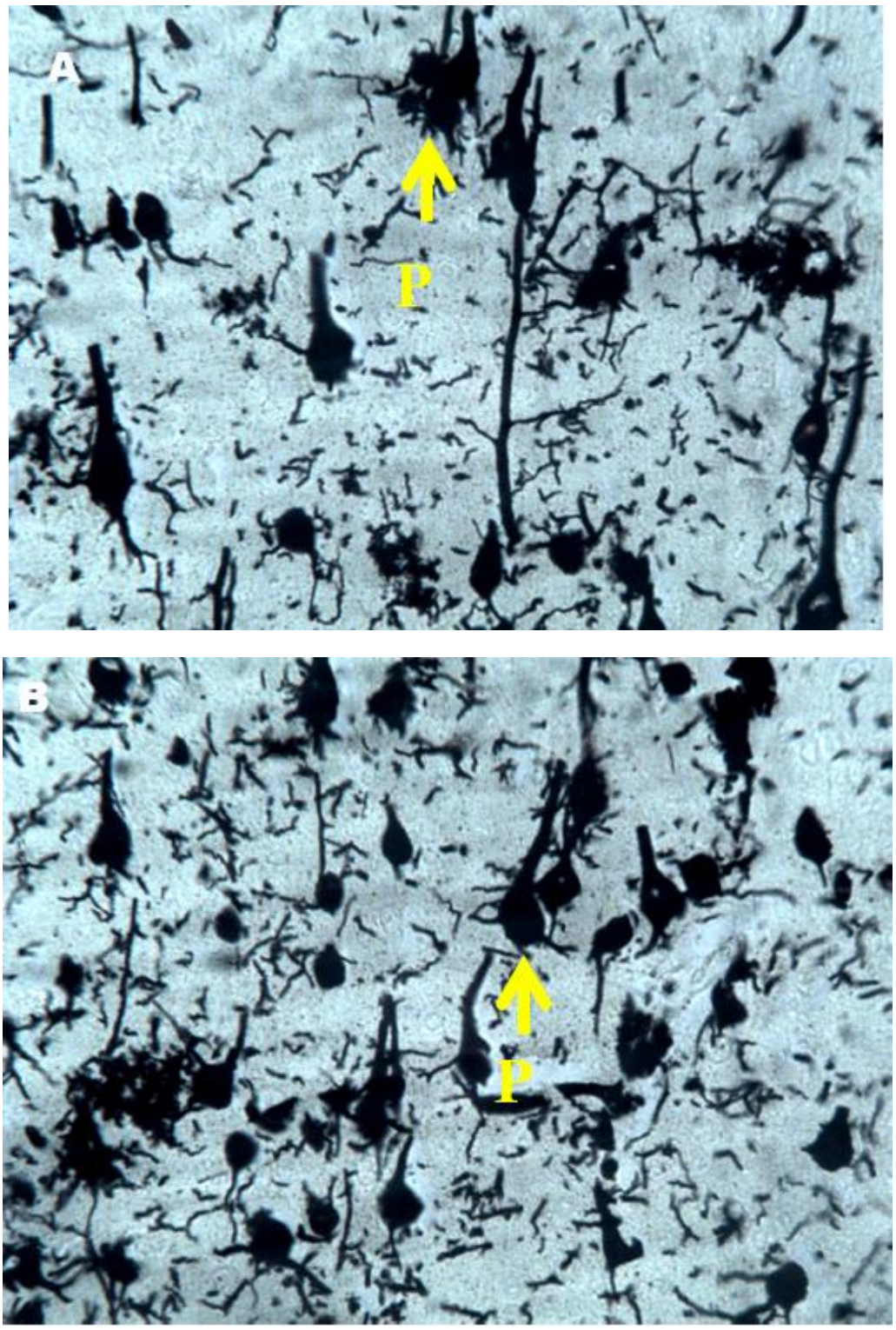


Plate 4.24: Section of Wistar rat cerebral cortex 'A' (Layer III) and 'B' (Layer V) of Group EGL (150mg/kg of Eugenol) showing a normal cytoarchitecture of the cerebral cortex with its Neuronal process (Neurites). Pyramidal cell 'P' (yellow line) (Mag x 250 Golgi).

4.4.2 Histological and Histochemical Features of the Cerebellar Cortex

4.4.2.1 Histological and Histochemical Features of the Cerebellar Cortex of Control (Untreated) and Treated Wistar Rat

The cerebellar sections of rats in the control group showed normal cytoarchitecture of the cerebellar cortex; the characteristic appearance of the three cortical layers: an outer molecular layer with distinct neurons and inner granular layer. Sandwiched between these layers is a monolayer of flask-shaped Purkinje cells, the Purkinje cell layer.

Heamatoxylin and Eosin (H&E) showed the normal cytoarchitecture of the cerebellar cortex in all three layers **(Plate 4.25)**.

Histochemical (CFV) staining for Nissil substances revealed normal appearance of distinct intensely stained cortical neurons **(Plate 4.31).**

Histochemical (Congo red) for amyloid plaques revealed normal appearance with no amyloid plaques **(Plates 4.37).**

The cerebellar sections of aluminium-treated Wistar rats revealed cytoarchitectural distortion of the cerebellar cortex; neurodegenerative changes such as Chromatolysis and perineuronal vacoulations, neuronal cytoplasmic shrinkage and gliosis. Histochemical CFV staining revealed Purkinje cells and internal granule cells and necrosis due to reduced staining intensity **(Plate 4.32)**

While Histochemical Congo red stain showed a distorted cytoarchitecture, but no visible amyloid plaques across all groups **(Plates 4.37-4.42)**

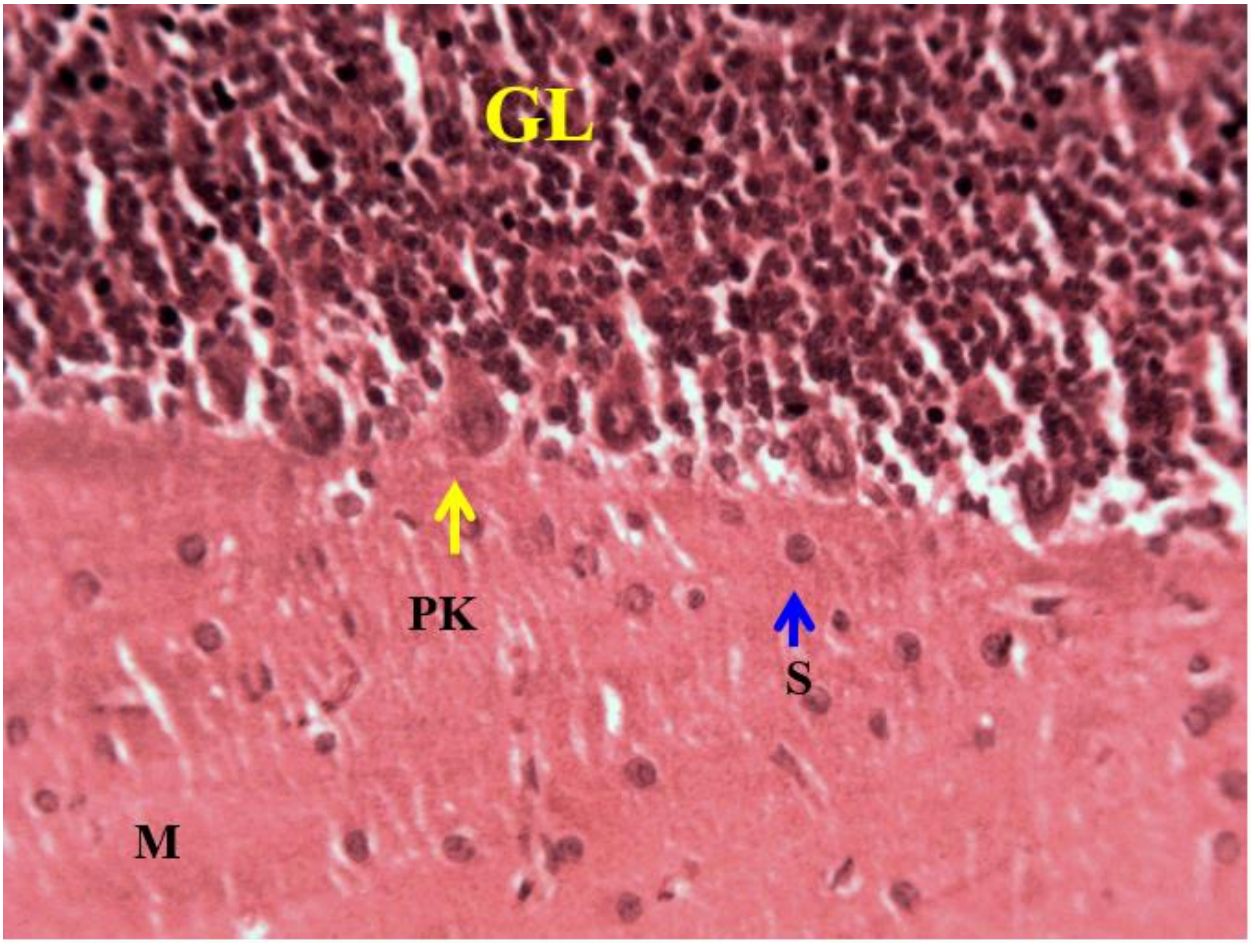


Plate 4.25: Section of Wistar rat cerebellar cortex of Group I control (CTRL) untreated group showing normal histology of the cerebellar cortex. Purkinje cell 'PK' (yellow line); Granular layer (GL); Molecular layer (M); Stellate cells 'S' (blue line) (Mag x 250 H&E).

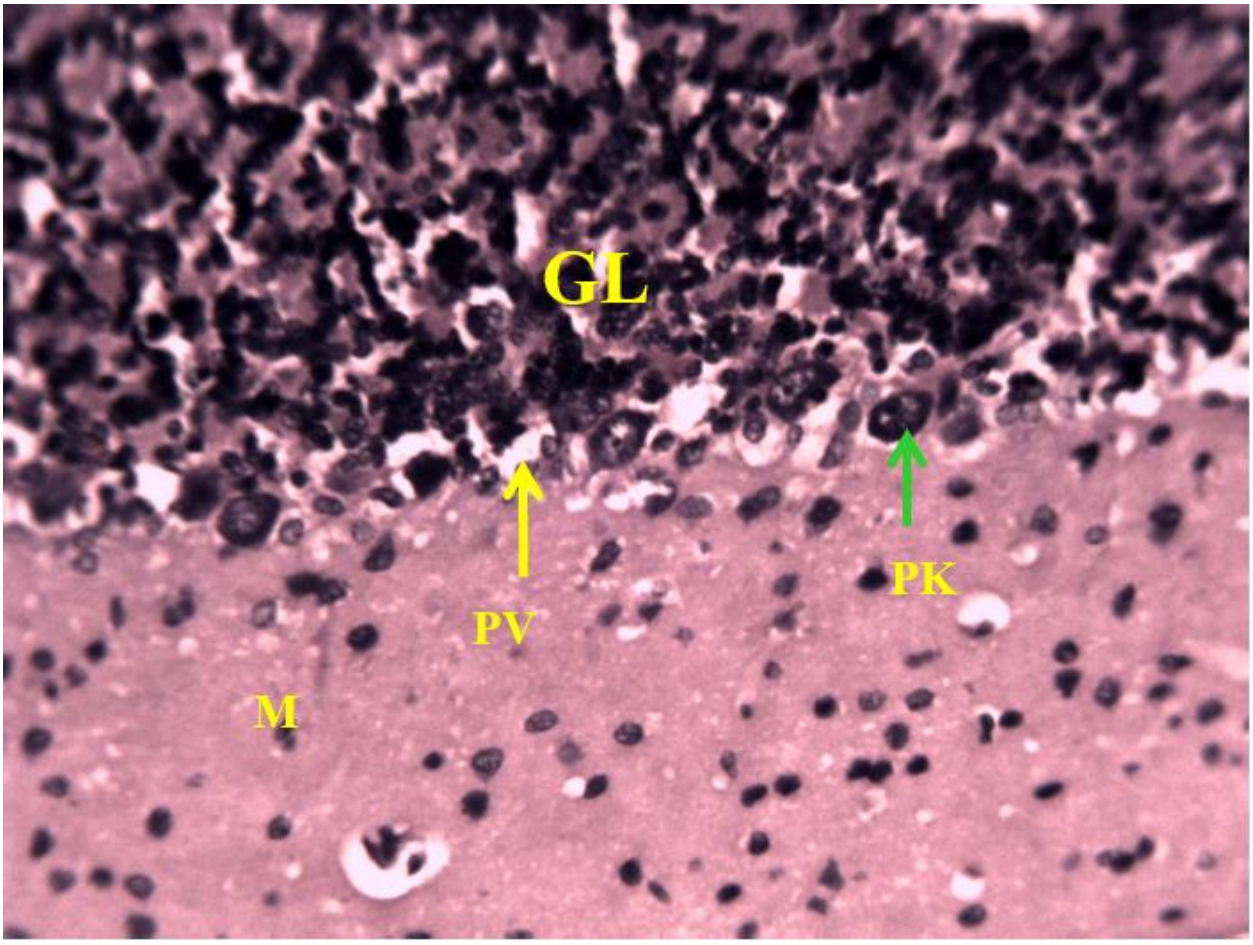


Plate 4.26: Section of Wistar rat cerebellar cortex of the aluminium treated group (AC) (100mg/kg of aluminium chloride) showing distortion in the histology of the cerebellar cortex. Purkinje cell 'PK' (green line); Granular layer (GL); Molecular layer (M); Perineuronal vacoulations 'PV' (Yellow line) (Mag x 250 H&E).

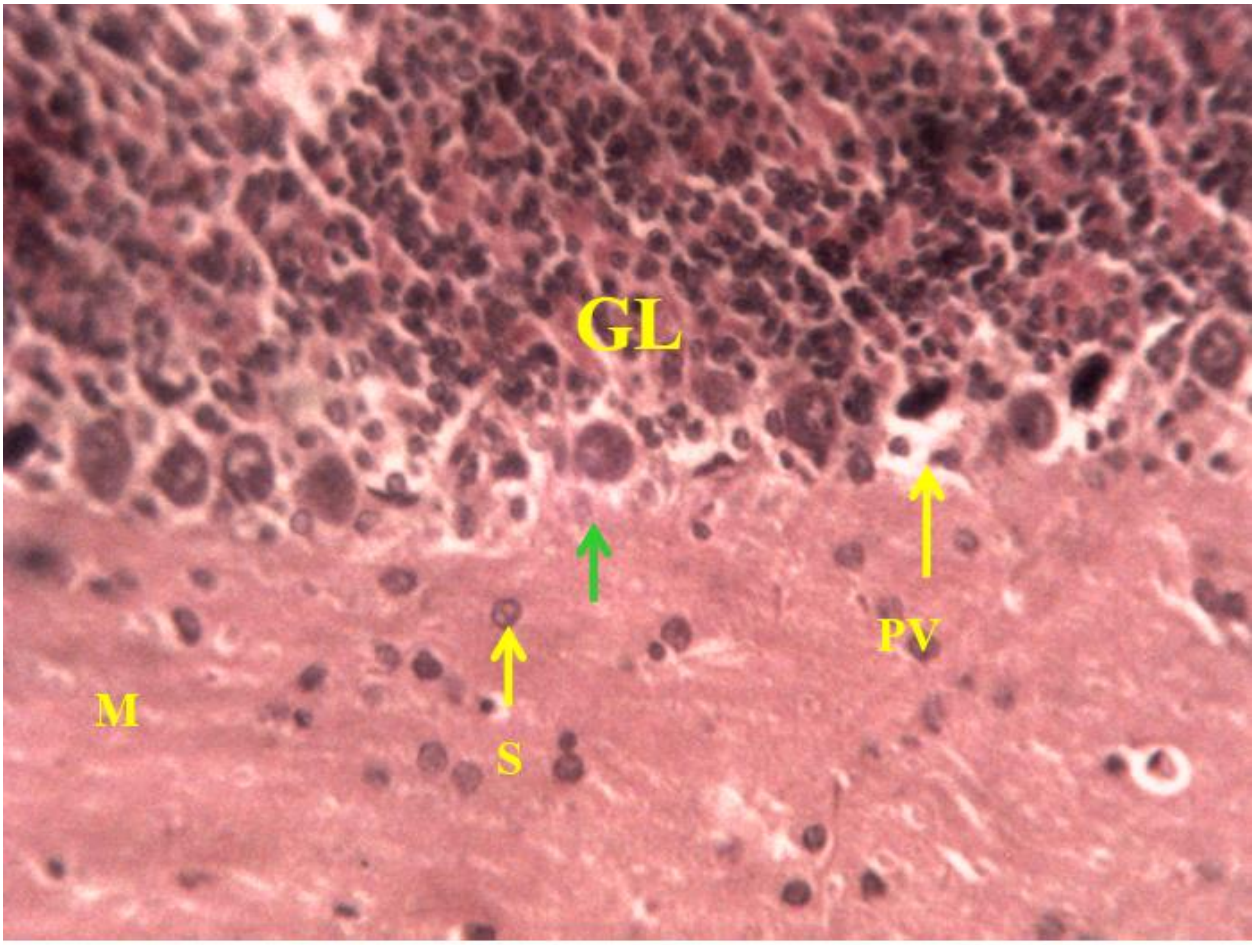


Plate 4.27: Section of Wistar rat cerebellar cortex of Group (EGH+AC) (300mg/kg of Eugenol and 100mg/kg of aluminium chloride) showing a mild distortion in the cytoarchitecture of the cerebellar cortex with Perineuronal vacoulations 'PV' (yellow line) when compared with the group the received aluminium chloride. Purkinje cell 'PK' (green line); Stellate cell (S); Granular Layer (GL); Molecular layer (M) (Mag x 250 H&E).

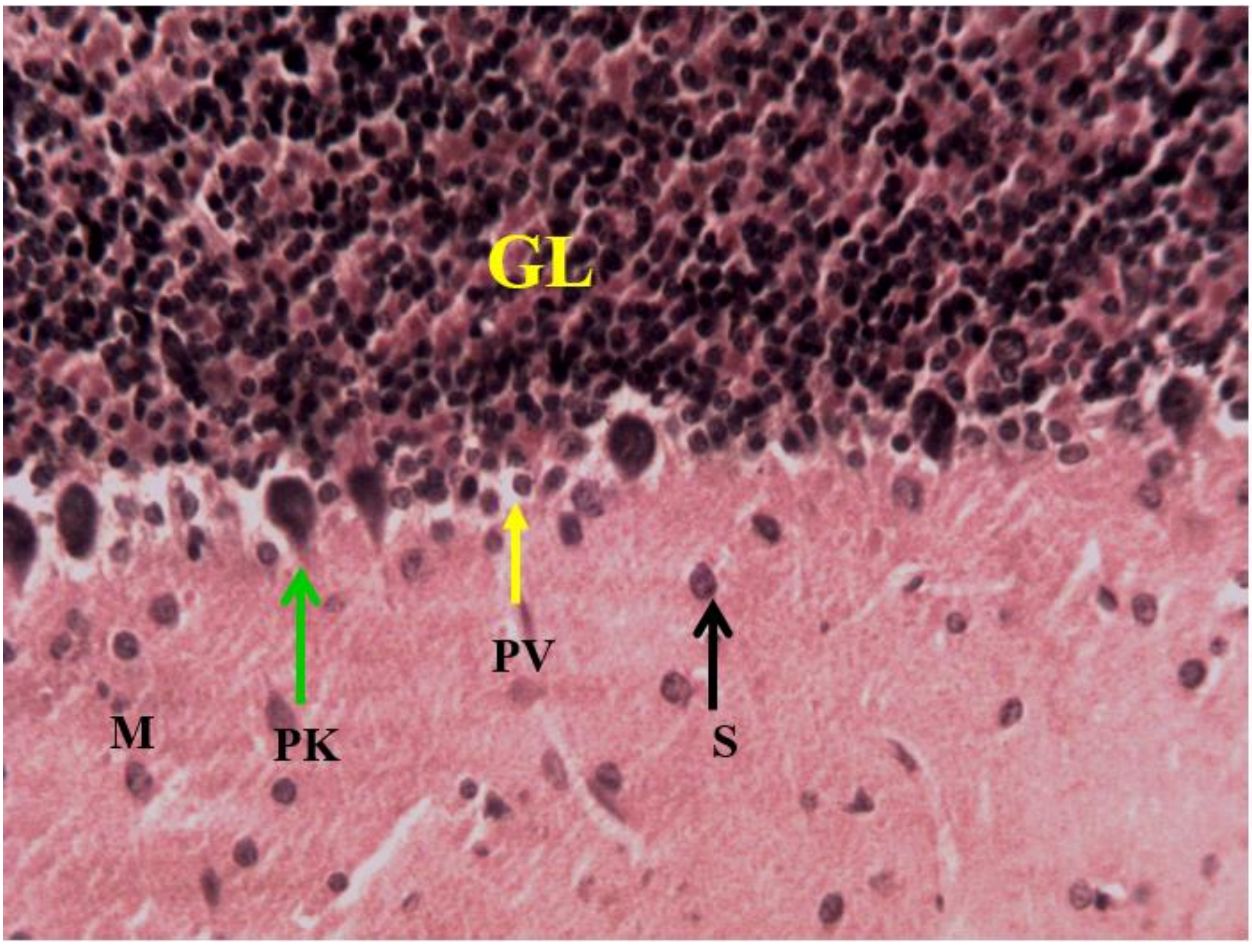


Plate 4.28: Section of Wistar rat cerebellar cortex of Group EGL+AC (150mg/kg of Eugenol and 100mg/kg of aluminium chloride) showing a mild distortion in the cytoarchitecture of the cerebellar cortex with mild Perineuronal vacoulations (PV) when compared with the group the received aluminium chloride. Purkinje cell (PK); Stellate cell (S); Granular Layer (GL); Molecular layer (M) (Mag x 250 H&E).

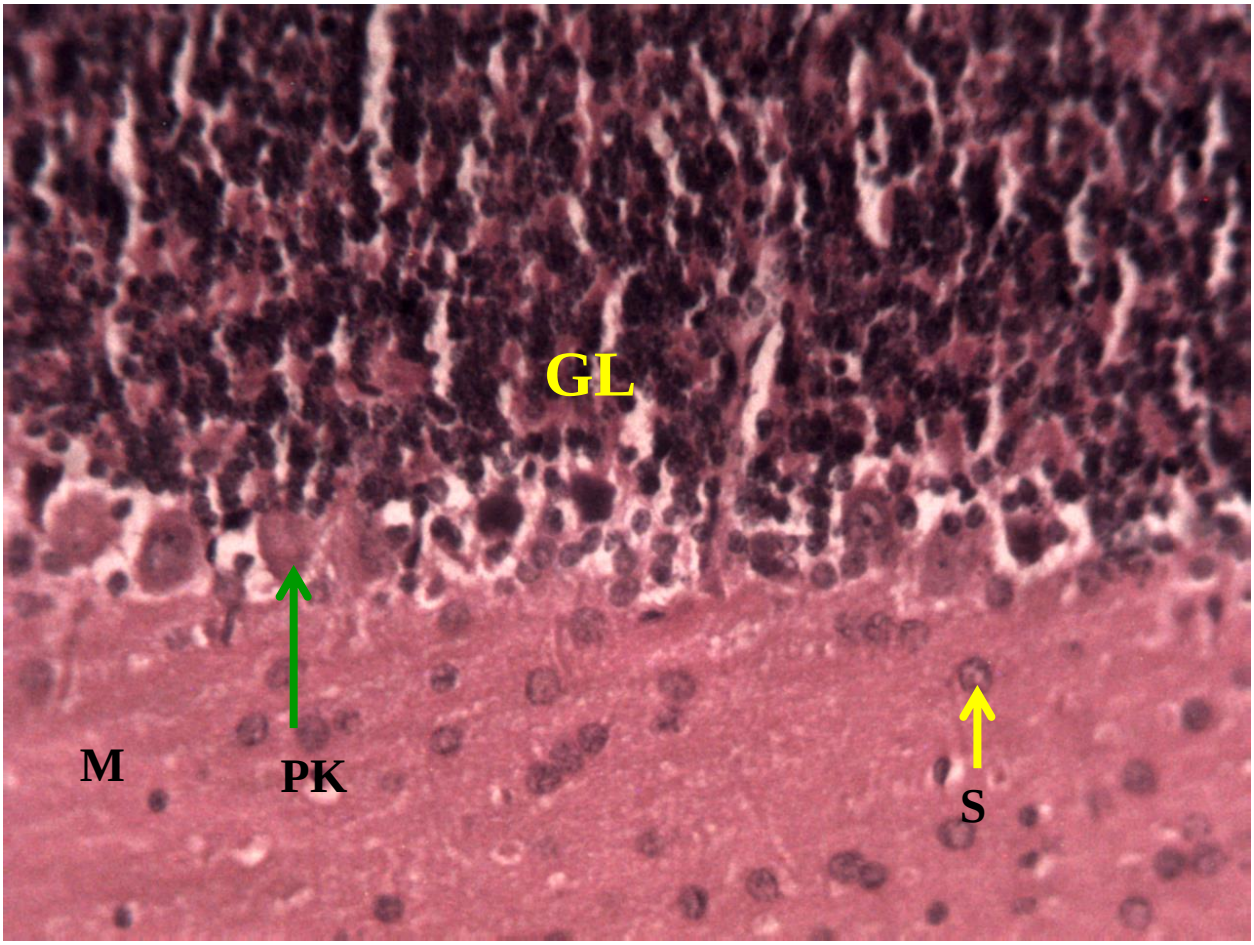


Plate 4.29: Section of Wistar rat cerebellar cortex of Group EGH (300mg/kg of Eugenol) showing a normal cytoarchitecture of the cerebellar cortex. Purkinje cell 'PK' (green line); Molecular layer (M); Stellate cell 'S' (yellow line); Granular layer (GL) (Mag x 250 H&E).

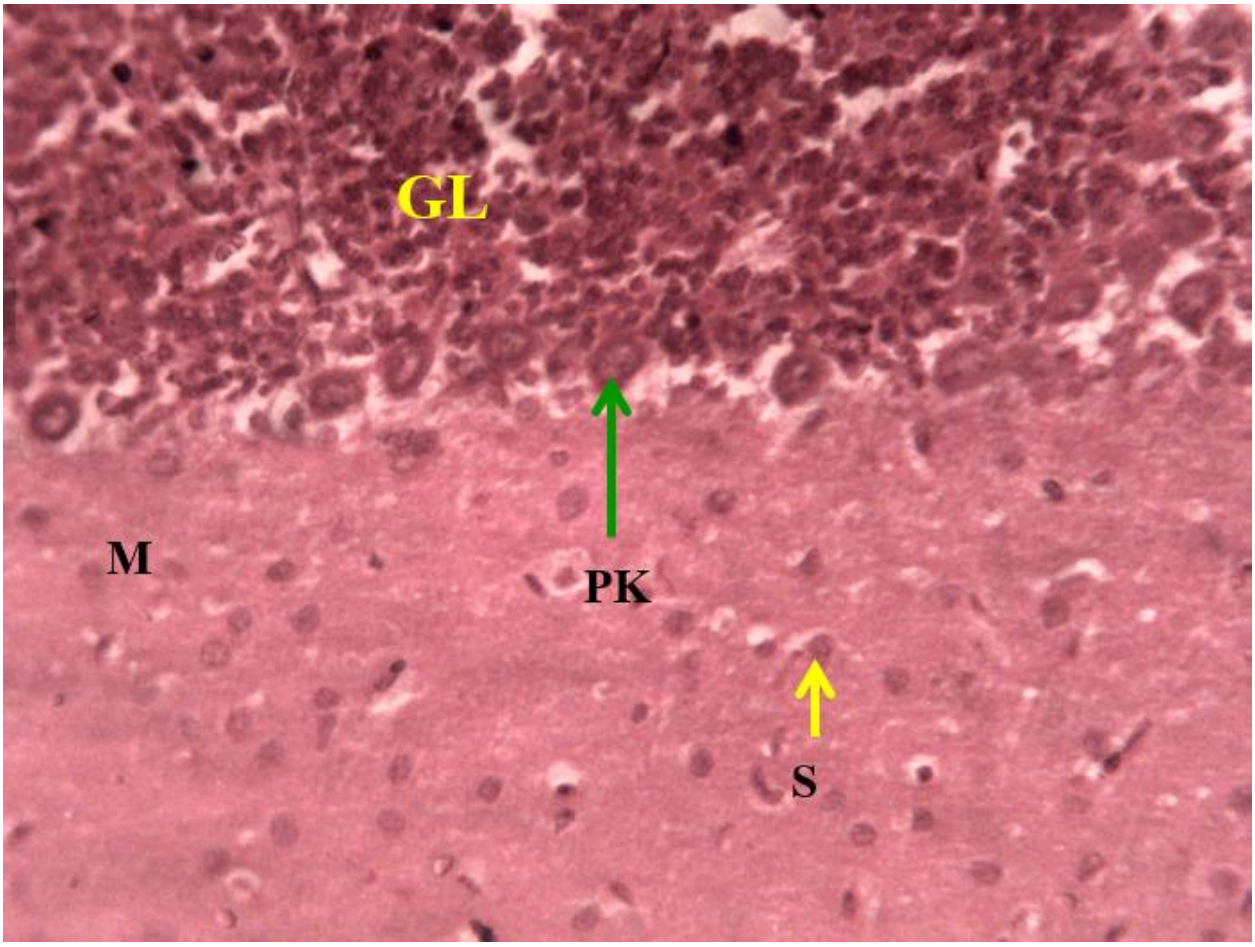


Plate 4.30: Section of Wistar rat Cerebellar cortex of Group EGL (150mg/kg of Eugenol) revealing a normal cytoarchitecture of the cerebellar cortex. Granular layer (GL); Molecular layer (M); Stellate cell 'S' (yellow line); Purkinje cell 'PK' (green line) (Mag x 250 H&E).

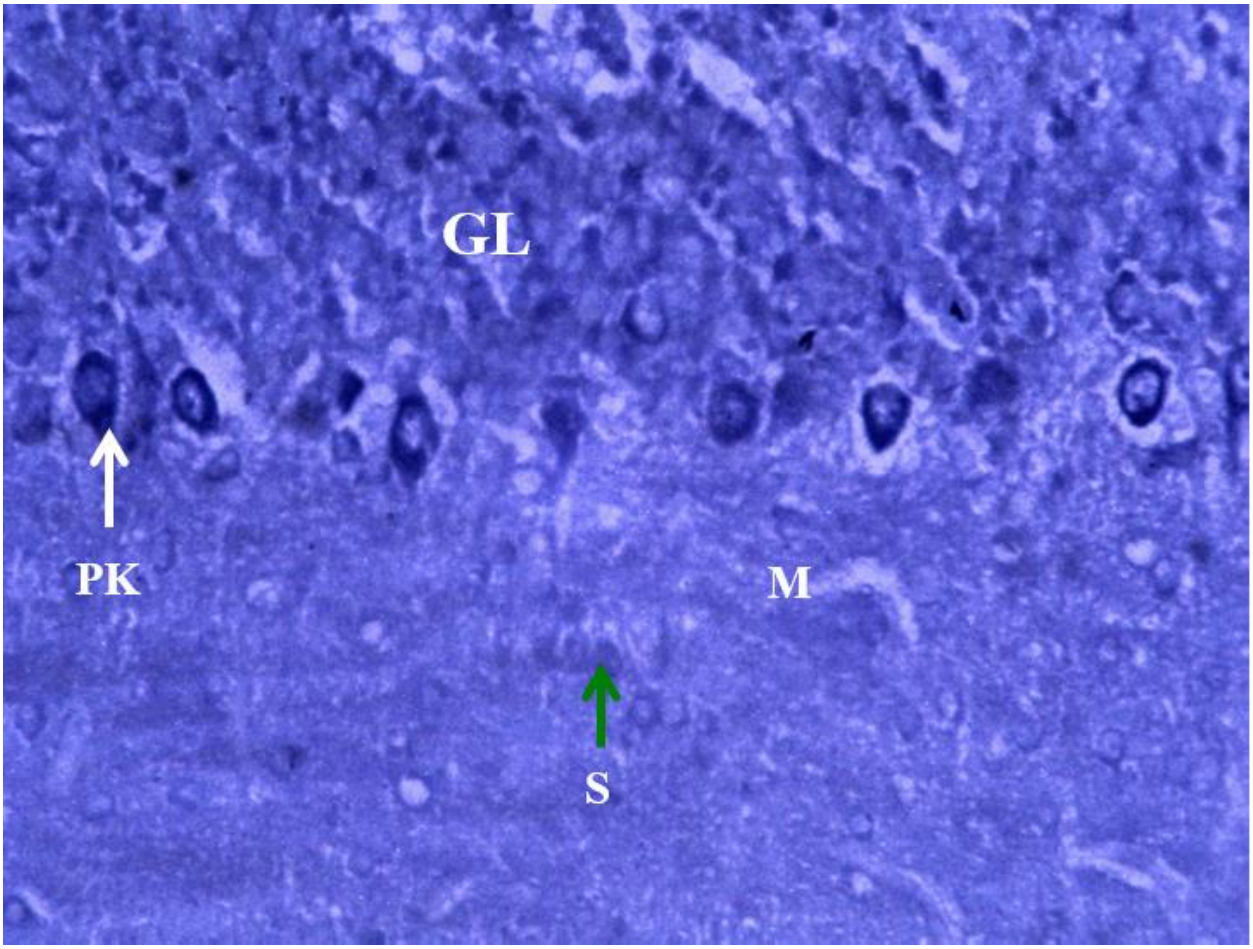


Plate 4.31: Section of Wistar rat cerebellar cortex of the control (CTRL) untreated group showing normal histology of the cerebellar cortex. Purkinje cell 'PK' (white line); Granular layer (GL); Molecular layer (M); Stellate cells 'S' (green line) (Mag x 250 CFV).

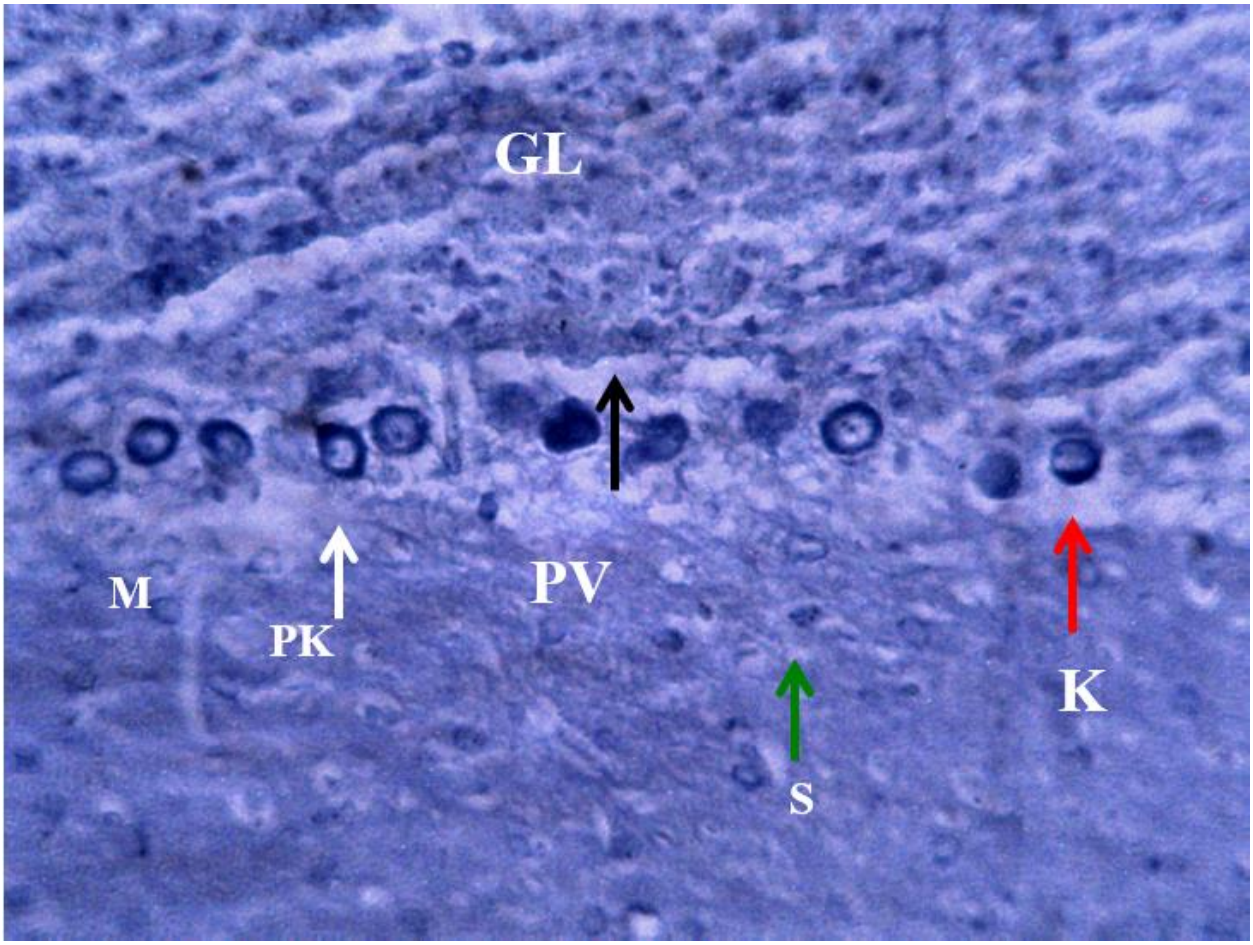


Plate 4.32: Section of Wistar of cerebellar cortex of the aluminium treated group (AC) (100mg/kg of aluminium chloride) showing distortion in the cytoarchitecture of the cerebellar cortex. Purkinje cell 'PK' (white line); Granular Layer (GL); Molecular layer (M), Chromatolysis (red line) 'k'; Neuronal degeneration (Perineuronal vacoulations PV 'black line') (Mag x 250 CFV).

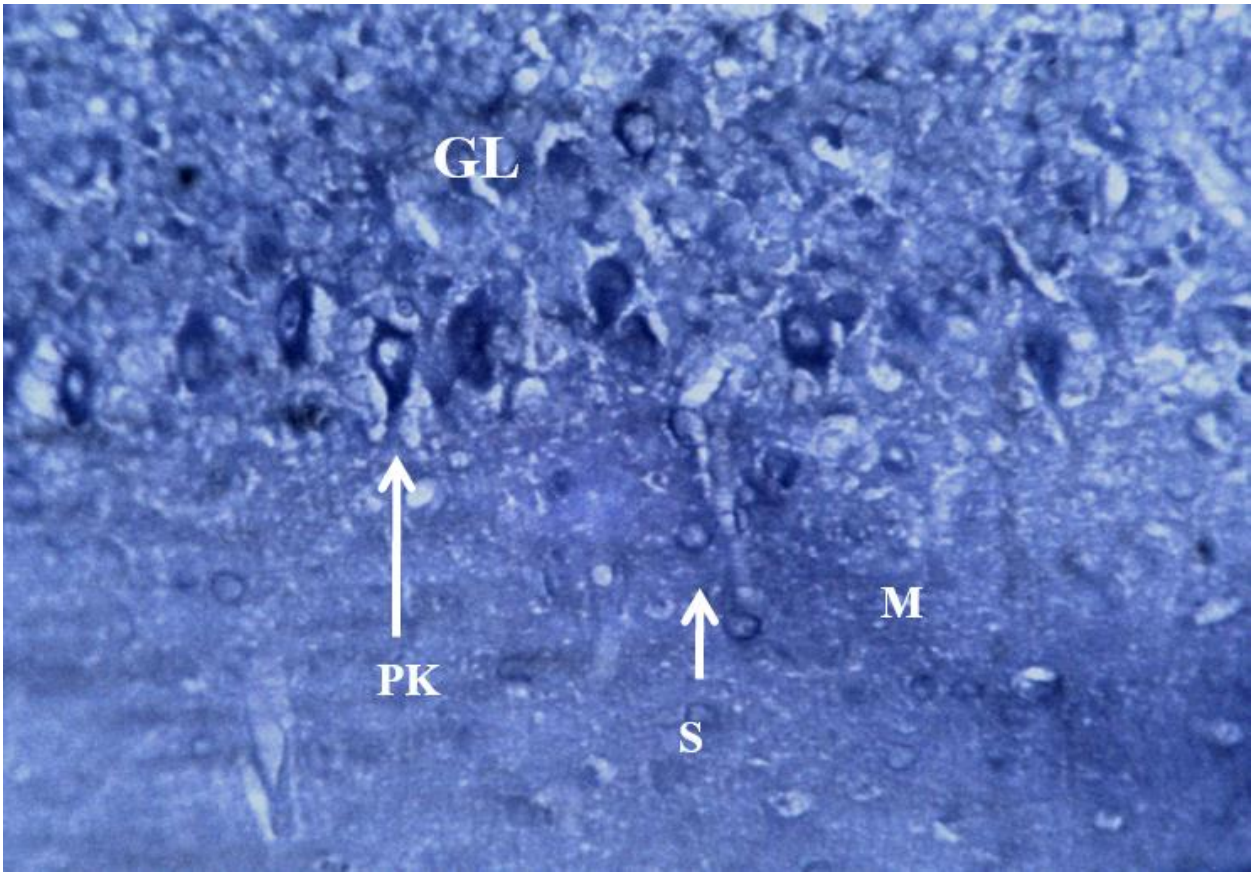


Plate 4.33: Section of Wistar rat cerebellar cortex of Group EGH+AC (300mg/kg of Eugenol and 100mg/kg of aluminium chloride) showing mild distortion in the cytoarchitecture of the cerebellar cortex with perineuronal vacoulations. Purkinje cell (PK); Stellate cell (S); Molecular layer (M); Granular layer (GL) (Mag x 250 CFV).

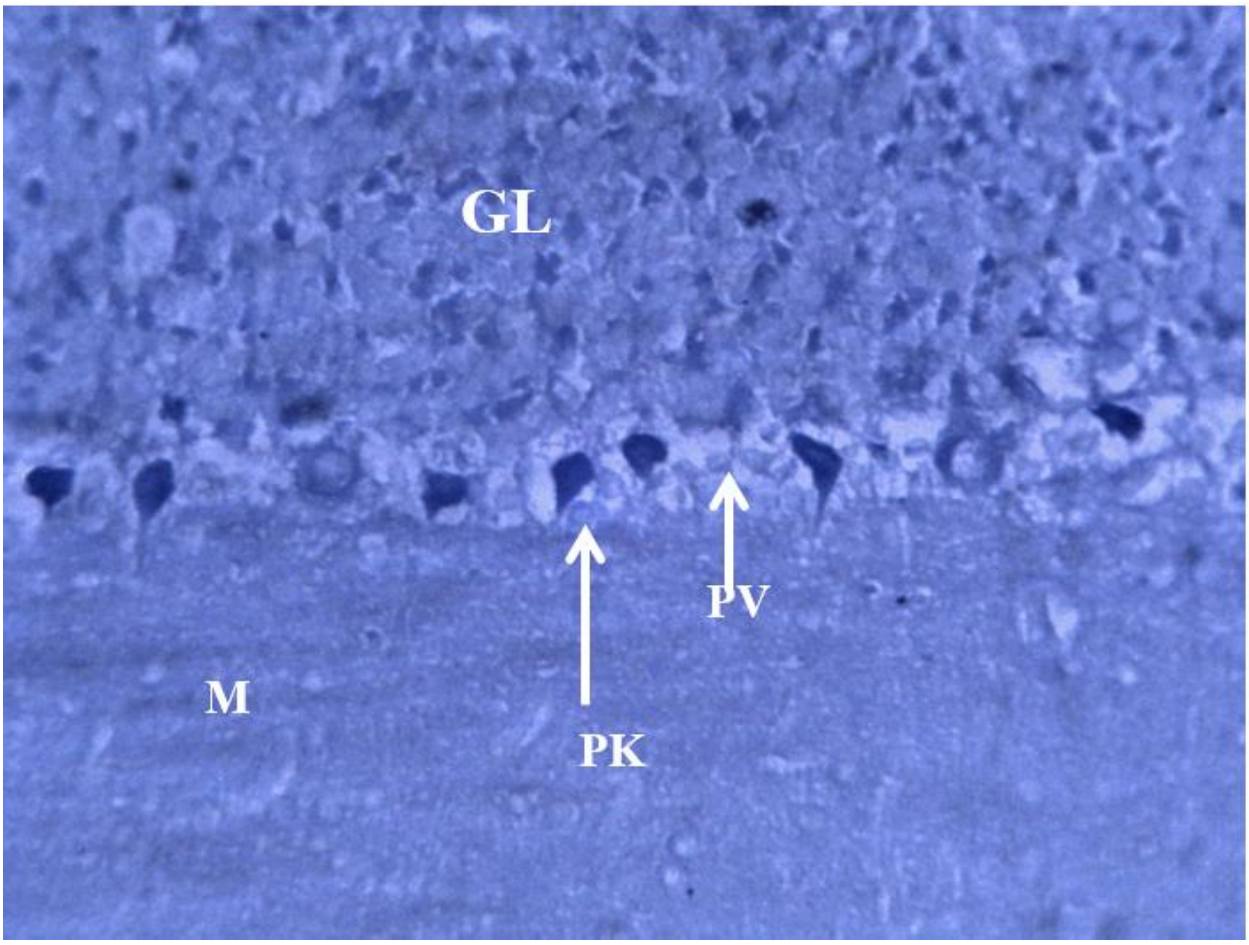


Plate 4.34: Section of Wistar rat cerebellar cortex of Group EGL+AC (150mg/kg of Eugenol and 100mg/kg of aluminium chloride) revealing a mild distortion in the cytoarchitecture of the cerebellar cortex with perineuronal vacoulations (PV). Granular Layer (GL); Purkinje layer (PK); Molecular layer (Mag x 250 CFV).

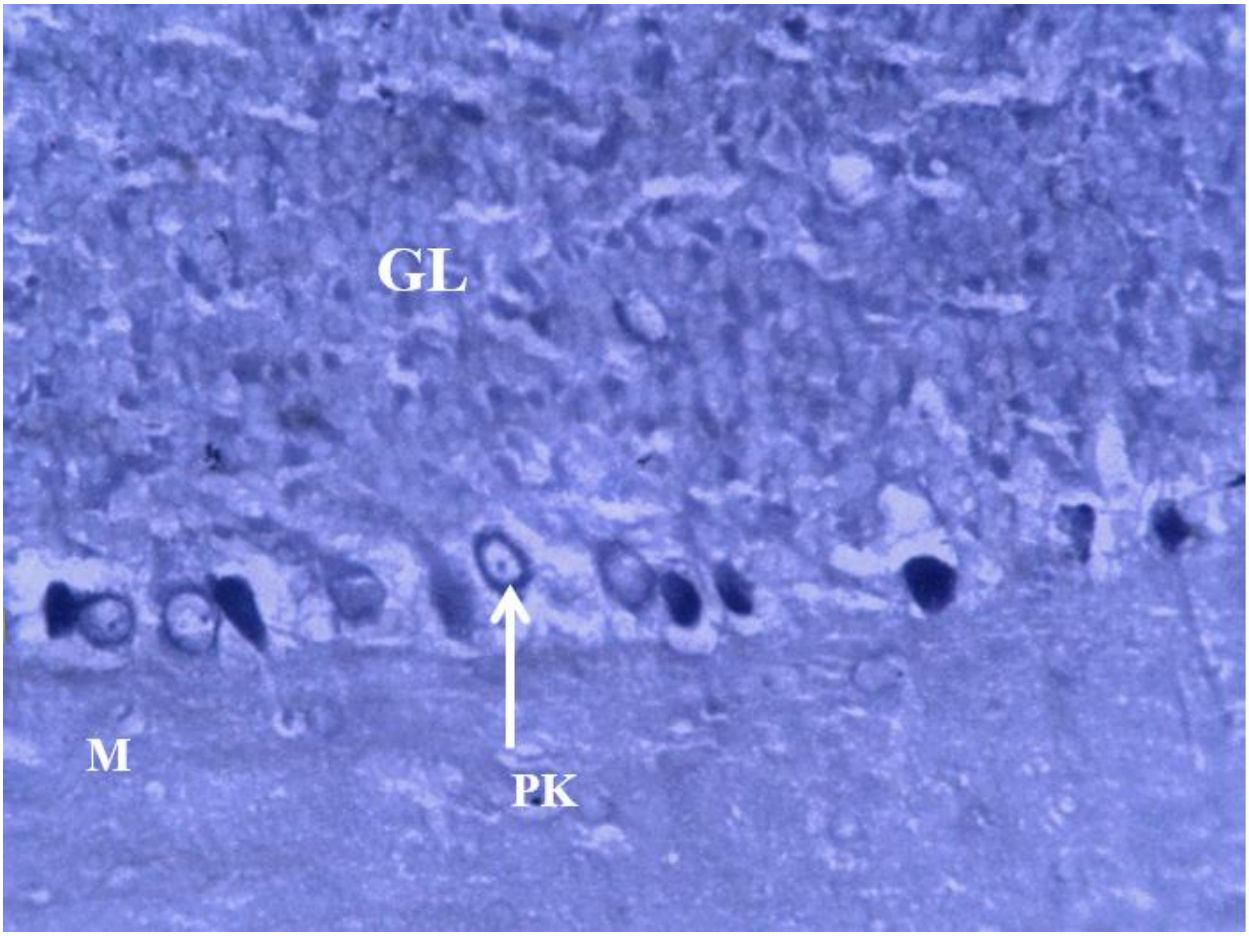


Plate 4.35: section of the cerebellar cortex of Group EGH (300mg/kg of Eugenol) revealing a normal cytoarchitecture of the cerebellar cortex. Granular Layer (GL); Purkinje cell (PK); Molecular layer (M) (Mag x 250 CFV).

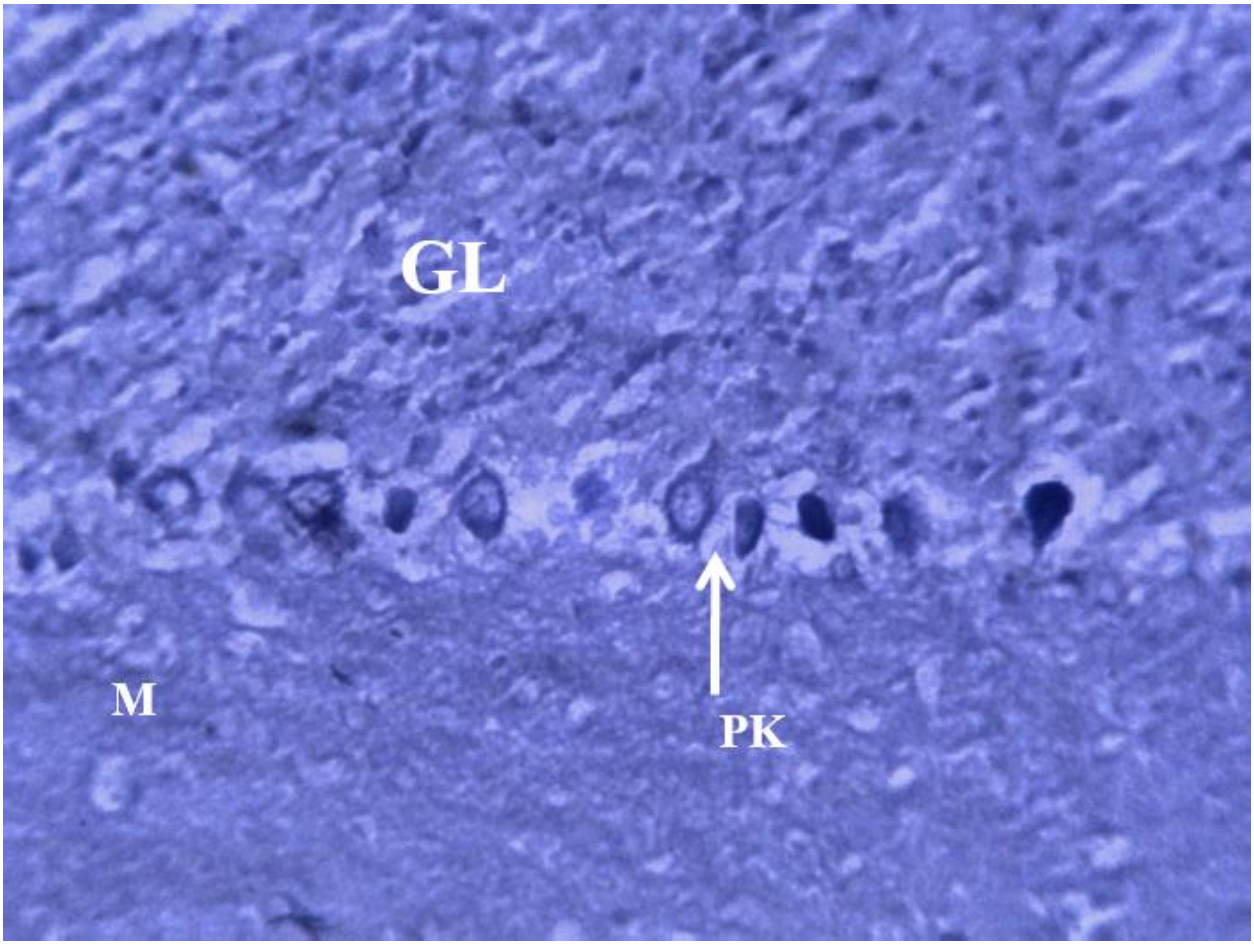


Plate 4.36: Section of Wistar rat Cerebellar cortex of Group EGL (150mg/kg of Eugenol) revealing a normal cytoarchitecture of the cerebellar cortex. Granular layer (GL); Molecular layer (M); Stellate cell(S); Purkinje cell (PK) (Mag x 250 CFV).

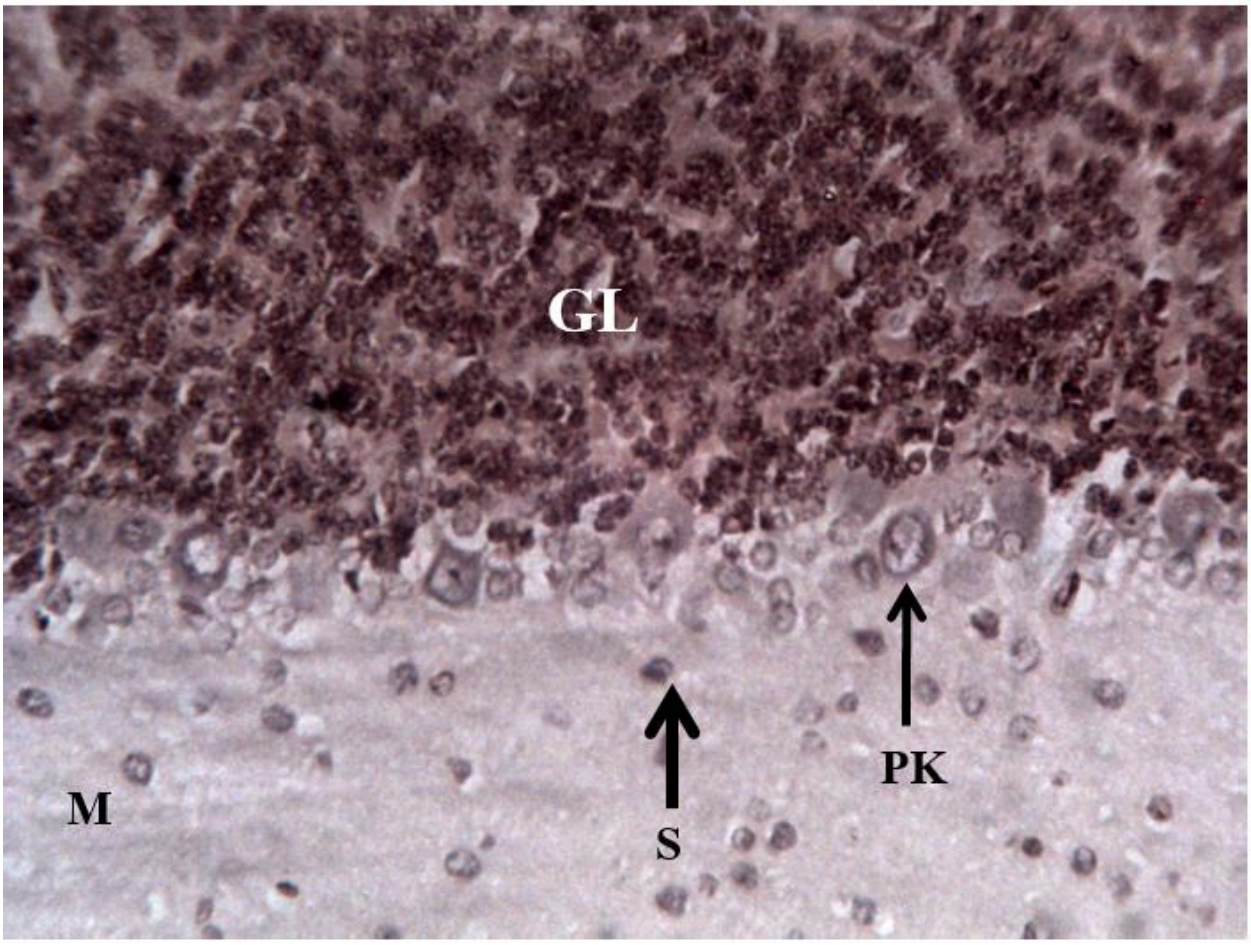


Plate 4.37: Section of Wistar rat cerebellar cortex of the control (CTRL) untreated group showing normal histology of the cerebellar cortex. Purkinje cell (PK); Granular layer (GL); Molecular layer (M); Stellate cells (S) (Mag x 250 Congo red).

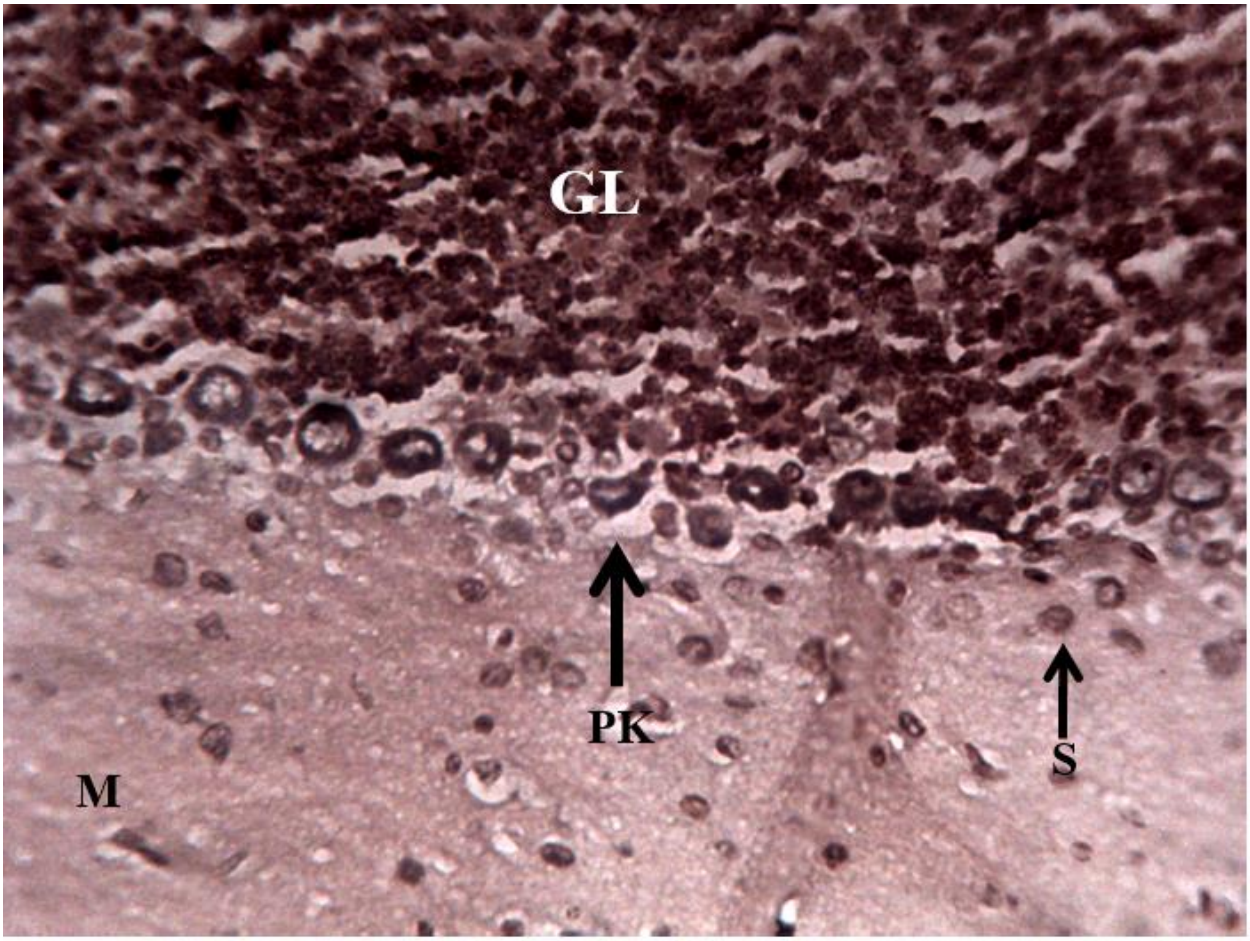


Plate 4.38: Section of Wistar rat cerebellar cortex of Group the aluminium treated (AC) group (AC) (100mg/kg of aluminium chloride), showing distortion the cytoarchitecture of the cerebellar cortex but no visible amyloid plaques. Granular Layer (GL); Purkinje cell (PK); Molecular Layer (M); Stellate cell (S) (Mag x 250 Congo).

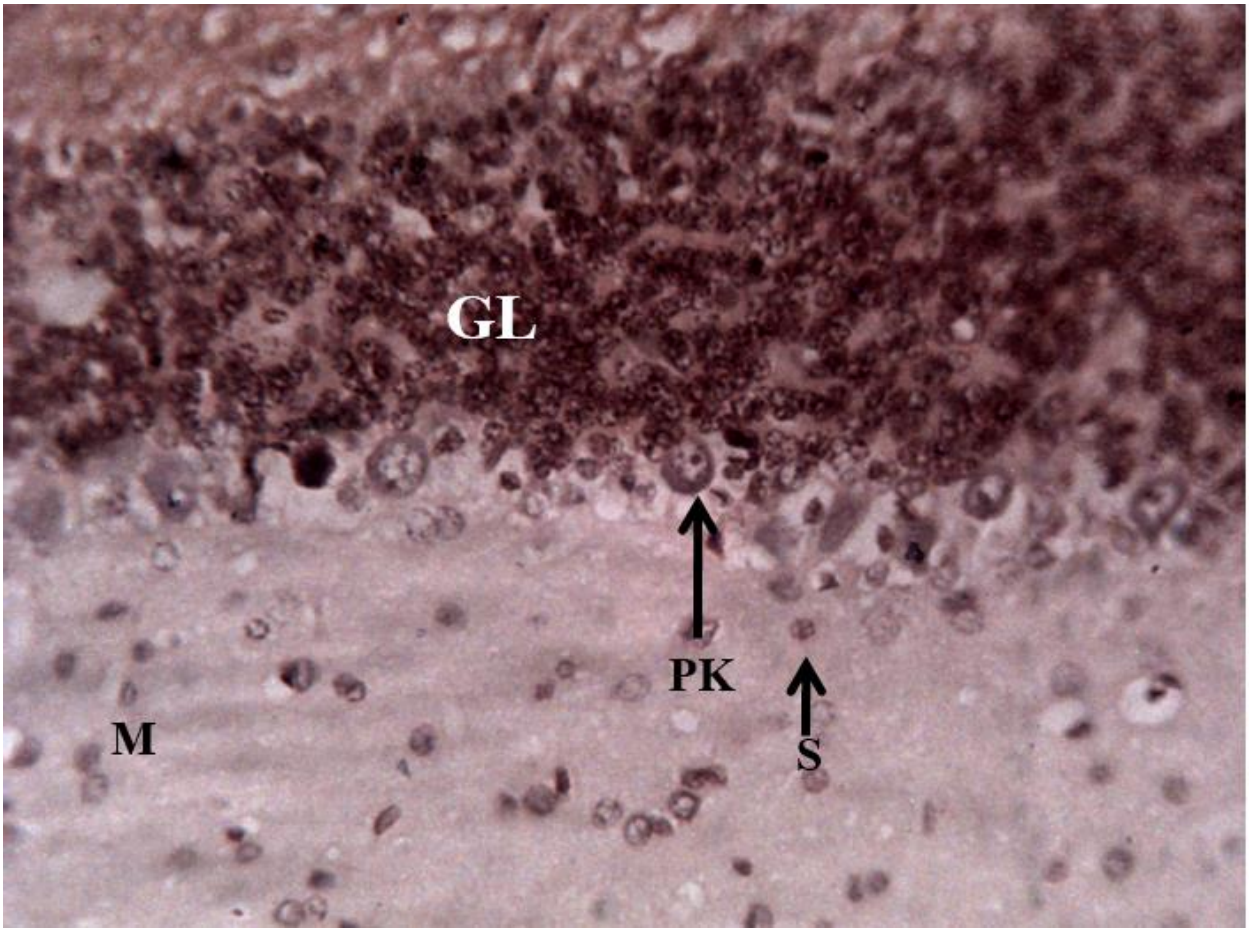


Plate 4.39: Section of Wistar rat cerebellar cortex of Group EGH+AC (300mg/kg of Eugenol and 100mg/kg of aluminium chloride) showing distortion the cytoarchitecture of the cerebellar cortex but no visible amyloid plaques. Granular Layer (GL); Purkinje cell (PK); Molecular Layer (M); Stellate cell (S) (Mag x 250 Congo).

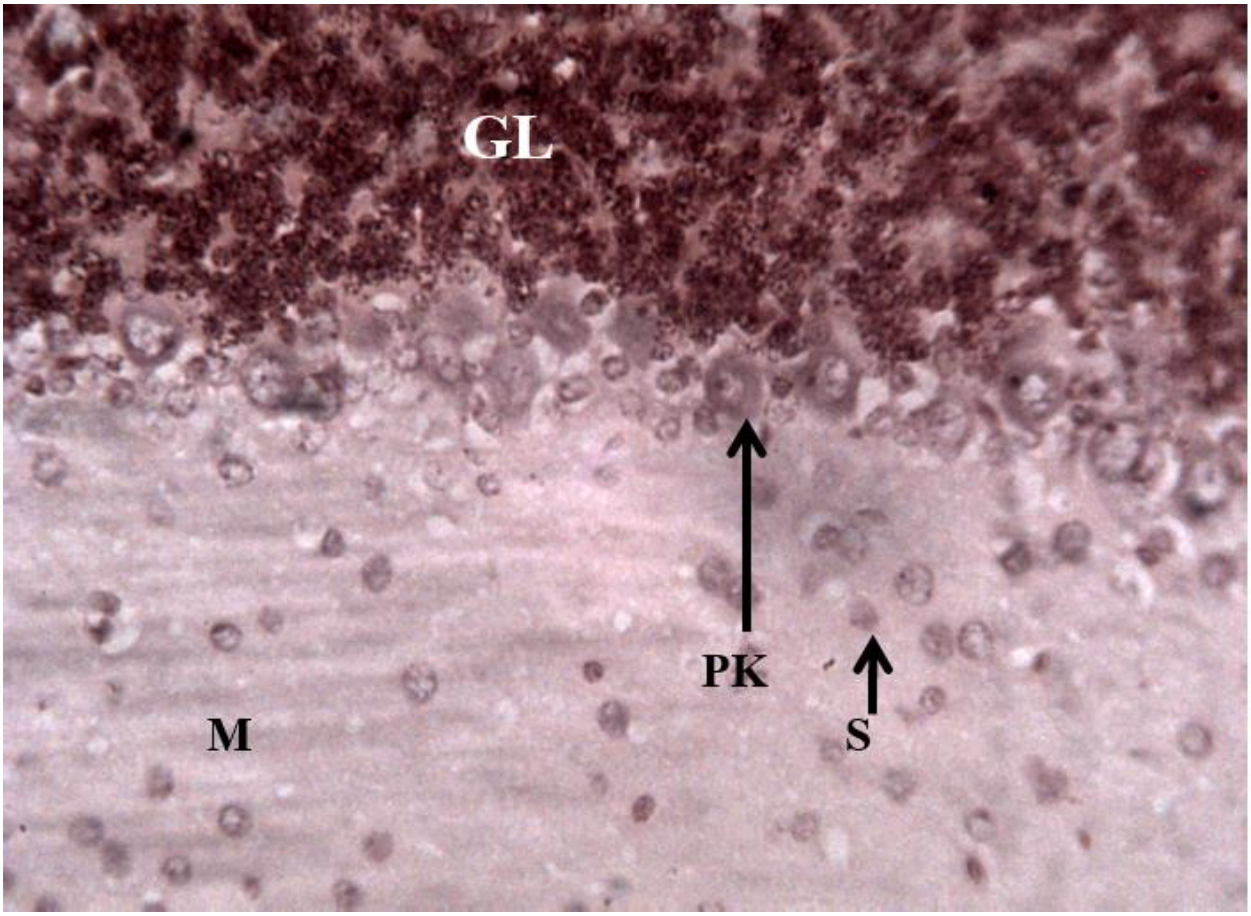


Plate 4.40: Section of Wistar rat cerebellar cortex of Group EGL+AC (150mg/kg of Eugenol and 100mg/kg of aluminium chloride) with mild distortion in the histology of the cerebellar cortex but no visible amyloid plaques. Purkinje cell (PK); Stellate cell (S); Molecular layer (M); Granular layer (GL) (Mag x 250 Congo red).

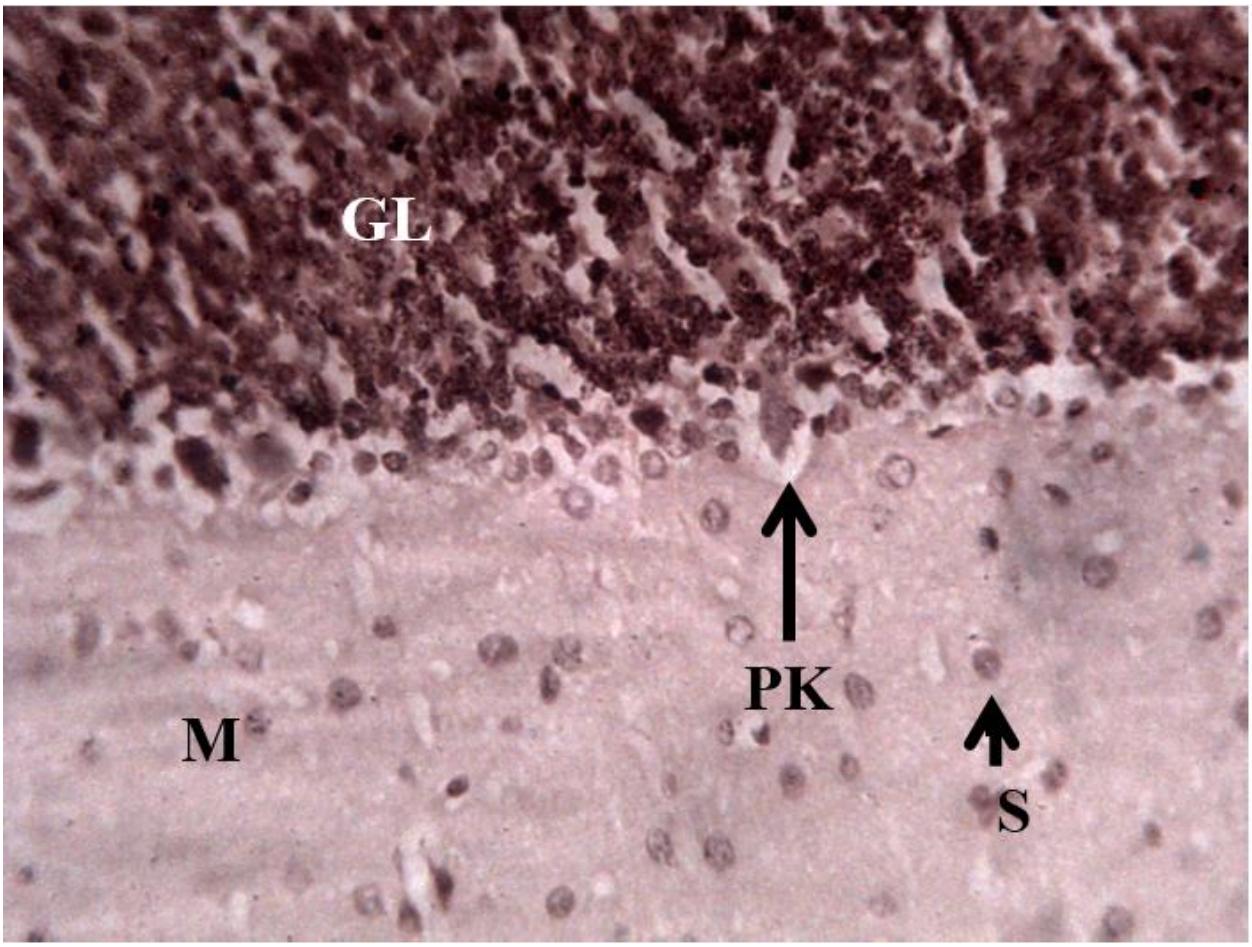


Plate 4.41: Section of the cerebellar cortex of Group EGH (300mg/kg of Eugenol) revealing a normal cytoarchitecture of the cerebellar cortex with no visible amyloid plaques. Granular Layer (GL); Purkinje cell (PK); Molecular layer (M) (Mag x 250 Congo red).

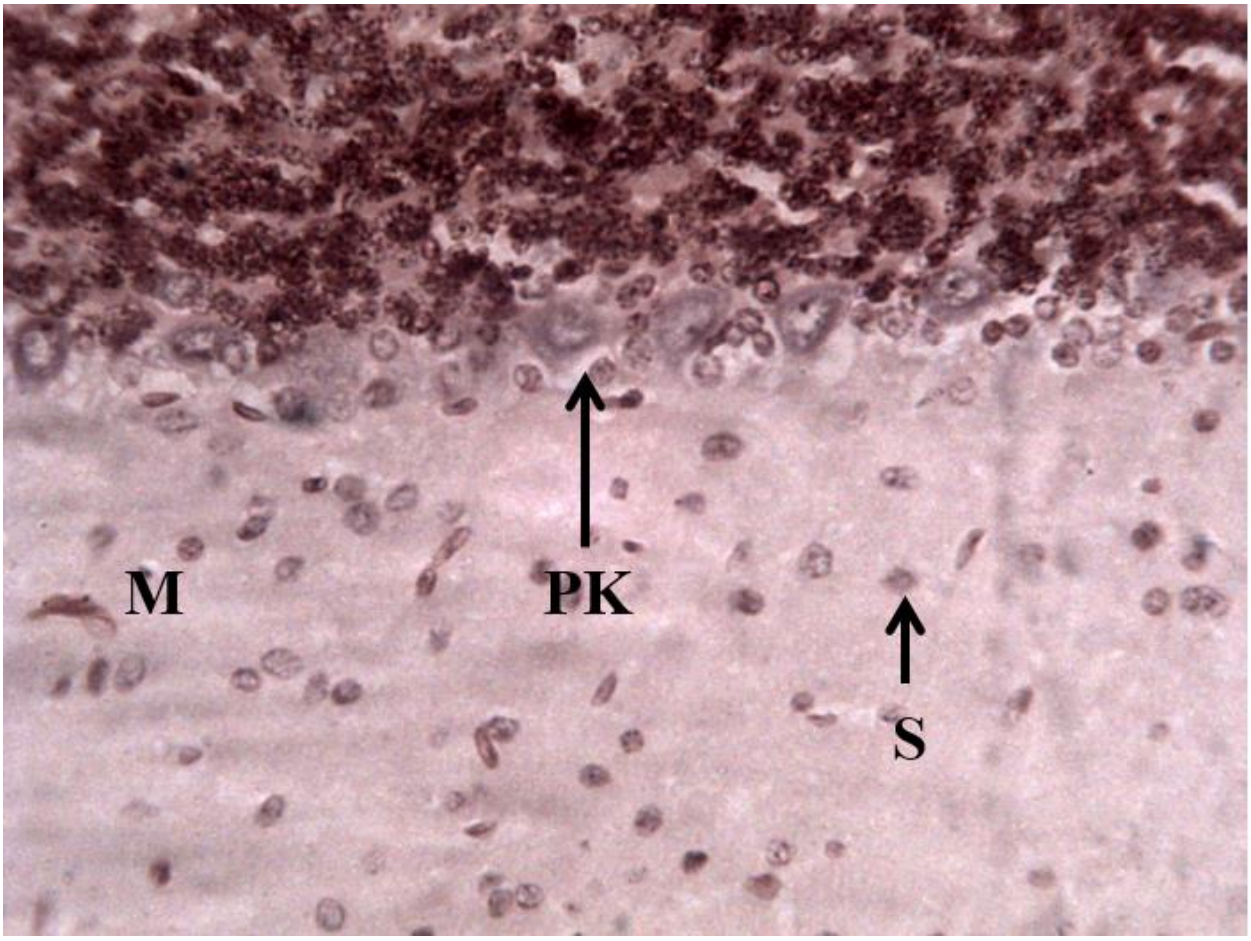


Plate 4.42: Section of Wistar rat Cerebellar cortex of Group EGL (150mg/kg of Eugenol) revealing a normal cytoarchitecture of the cerebellar cortex and no visible amyloid plaques. Granular layer (GL); Molecular layer (M); Stellate cell(S); Purkinje cell (PK) (Mag x 250 Congo red).

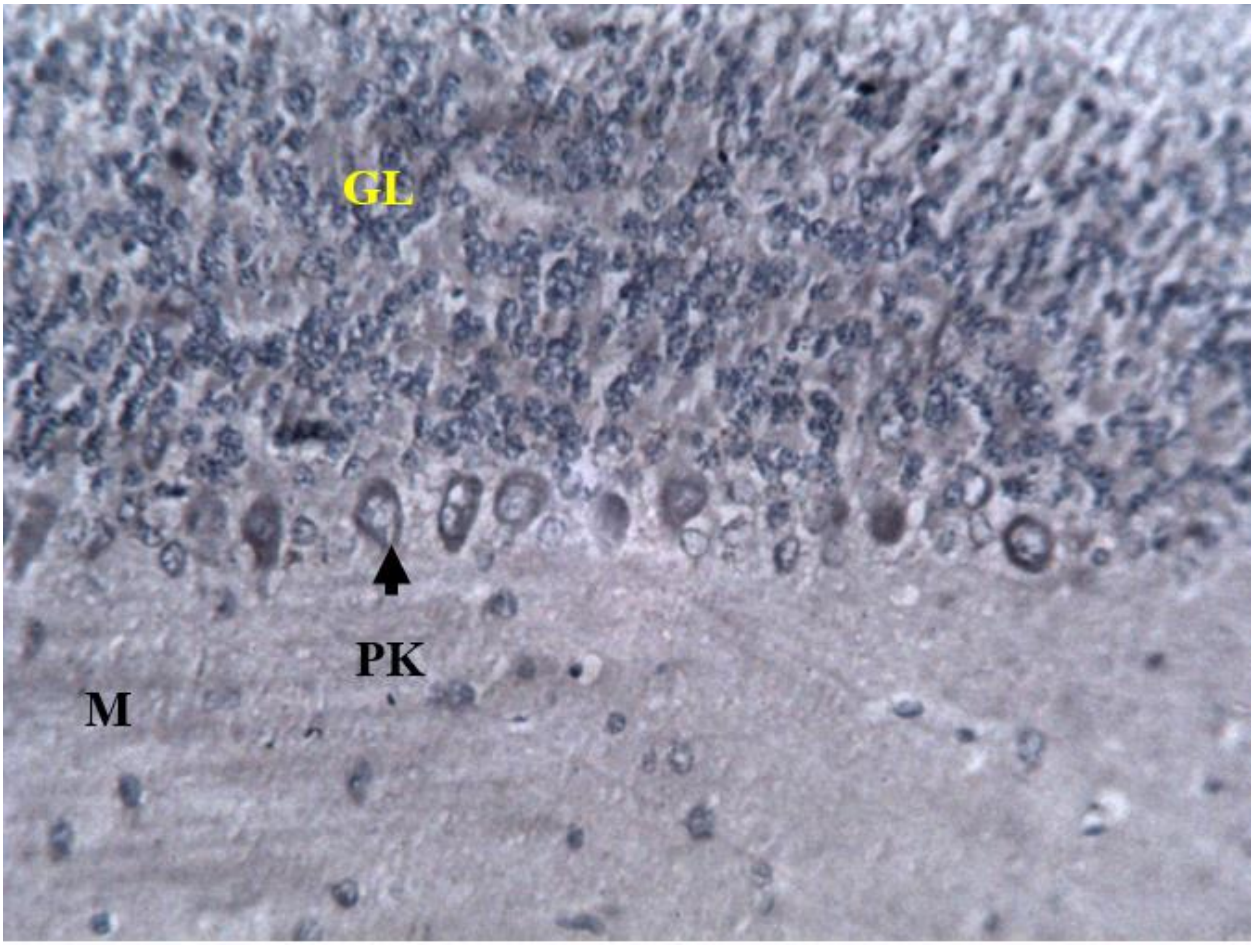


Plate 4.43: Section of Wistar rat Cerebellar cortex of the control (CTRL) (Untreated), Showing a normal ACAT-1 Immunoreactivity of the Purkinje cells of the cerebellar cortex. Granular layer (GL); Molecular layer (M); Purkinje cell (PK) (ACAT x 250).

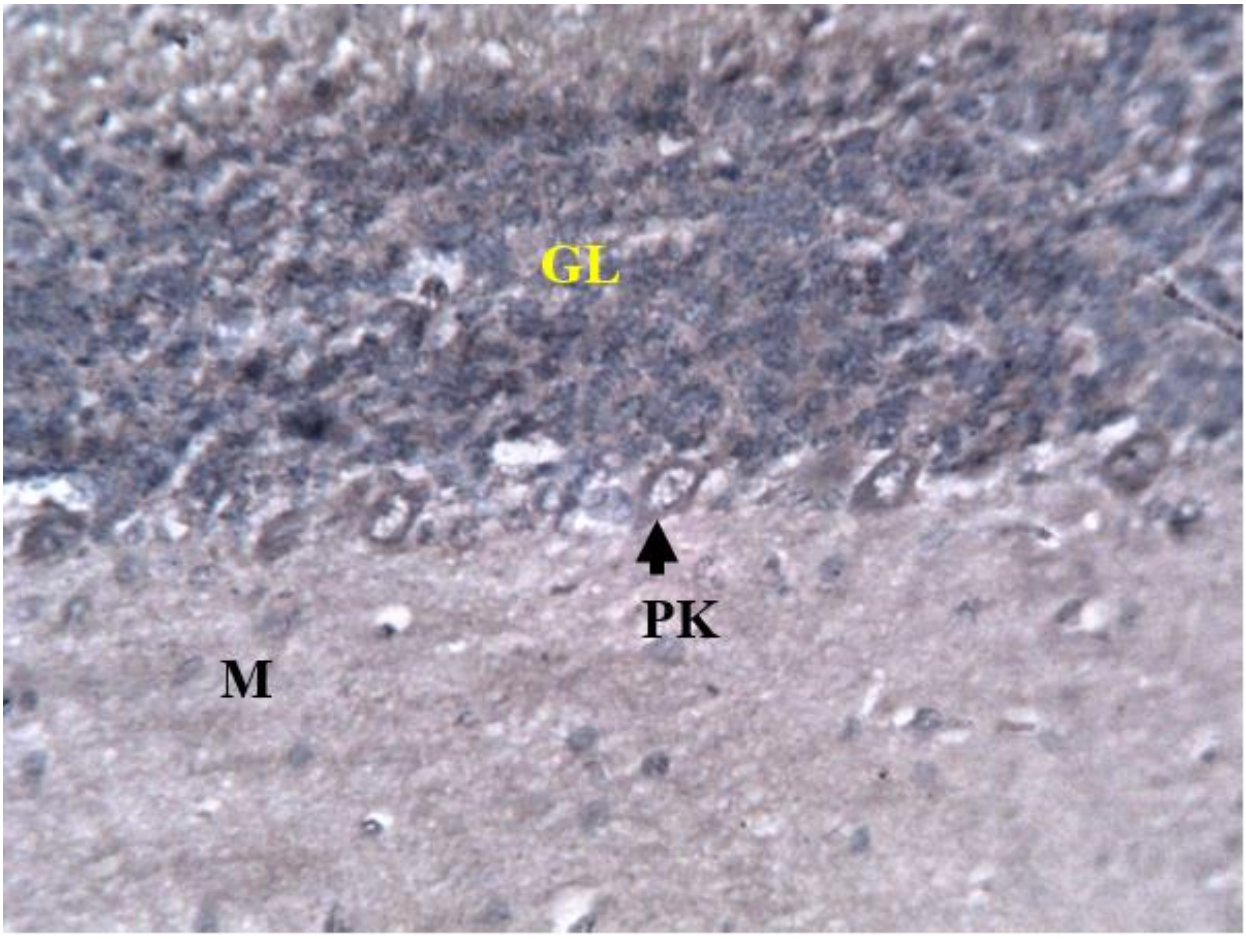


Plate 4.44: Section of Wistar rat Cerebellar cortex of the AC group (100 mg/kg Aluminium chloride) revealing a reduced ACAT-1 Immunoreactivity of the purkinje cells of the cerebellar cortex. Granular layer (GL); Molecular layer (M); Purkinje cell (PK) (ACAT x 250).

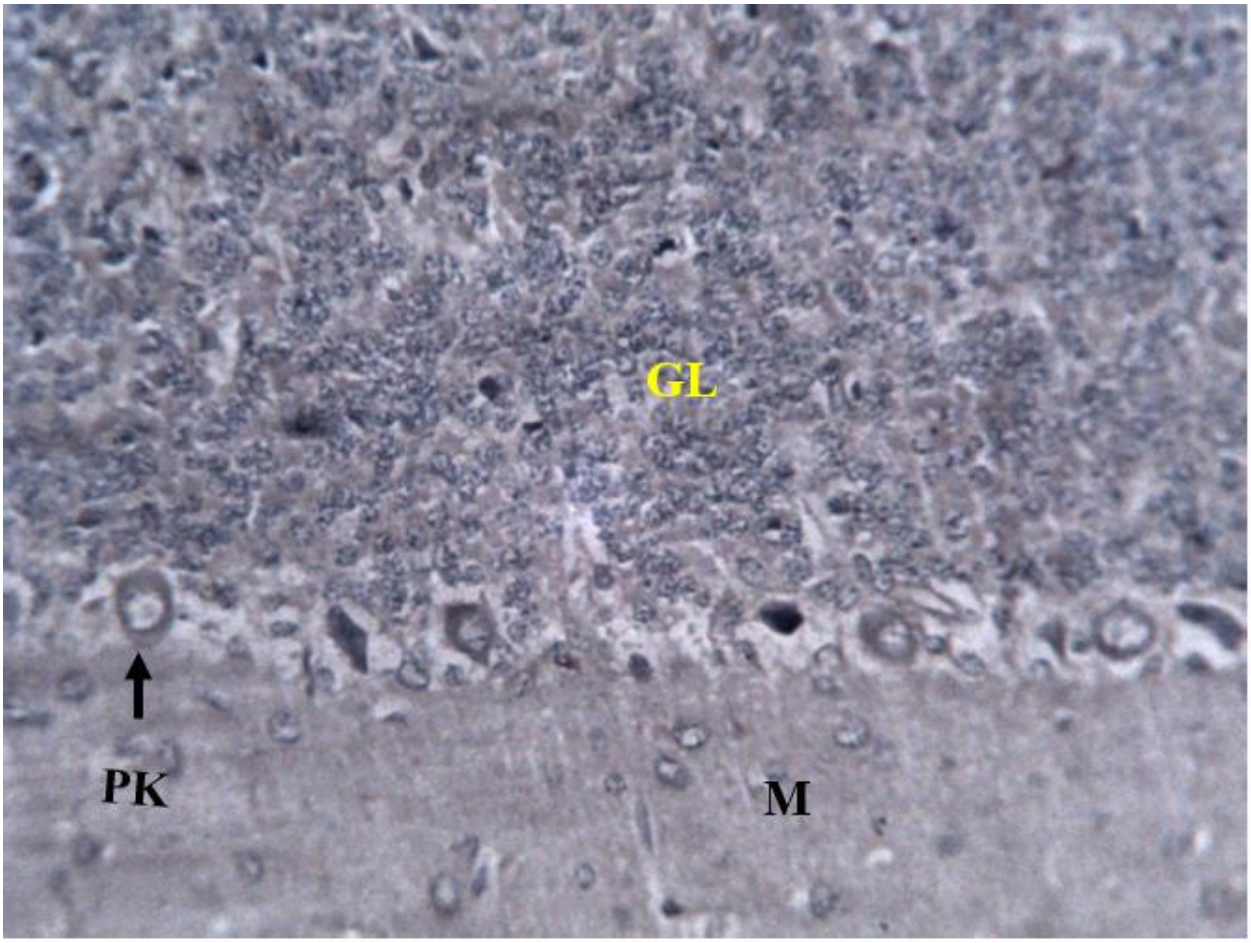


Plate 4.45: Section of Wistar rat Cerebellar cortex of the EGH+AC group (300 mg/kg Eugenol and 100 mg/kg Aluminium chloride) revealing a restored ACAT-1 Immunoreactivity of the purkinje cells of the cerebellar cortex when compared to AC. Granular layer (GL); Molecular layer (M); Purkinje cell (PK) (ACAT x 250).

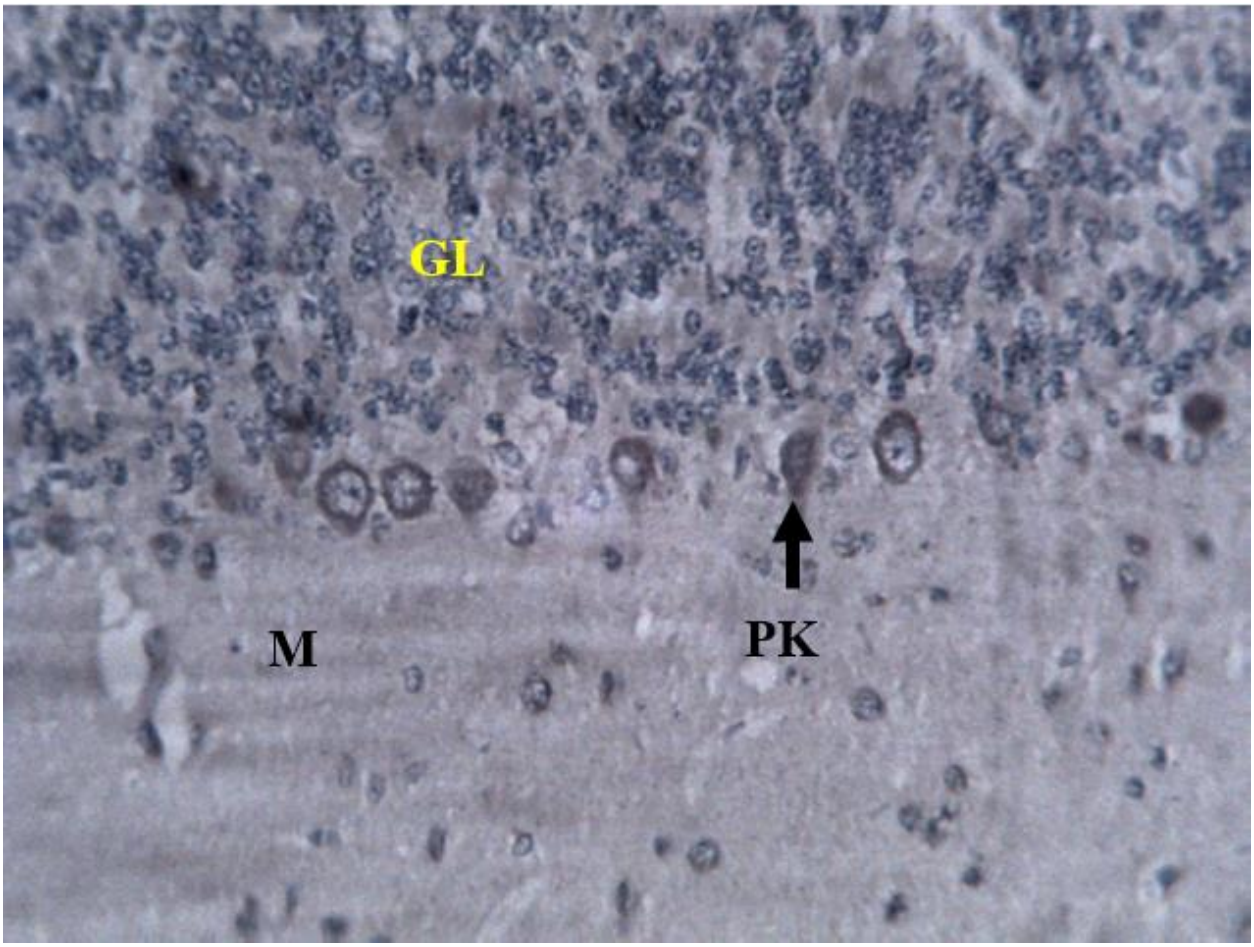


Plate 4.46: Section of Wistar rat Cerebellar cortex of the EGL+AC group (150 mg/kg Eugenol and 100 mg/kg Aluminium chloride) revealing a restored ACAT-1 Immunoreactivity of the purkinje cells of the cerebellar cortex when compared to AC group. Granular layer (GL); Molecular layer (M); Purkinje cell (PK) (ACAT x 250).

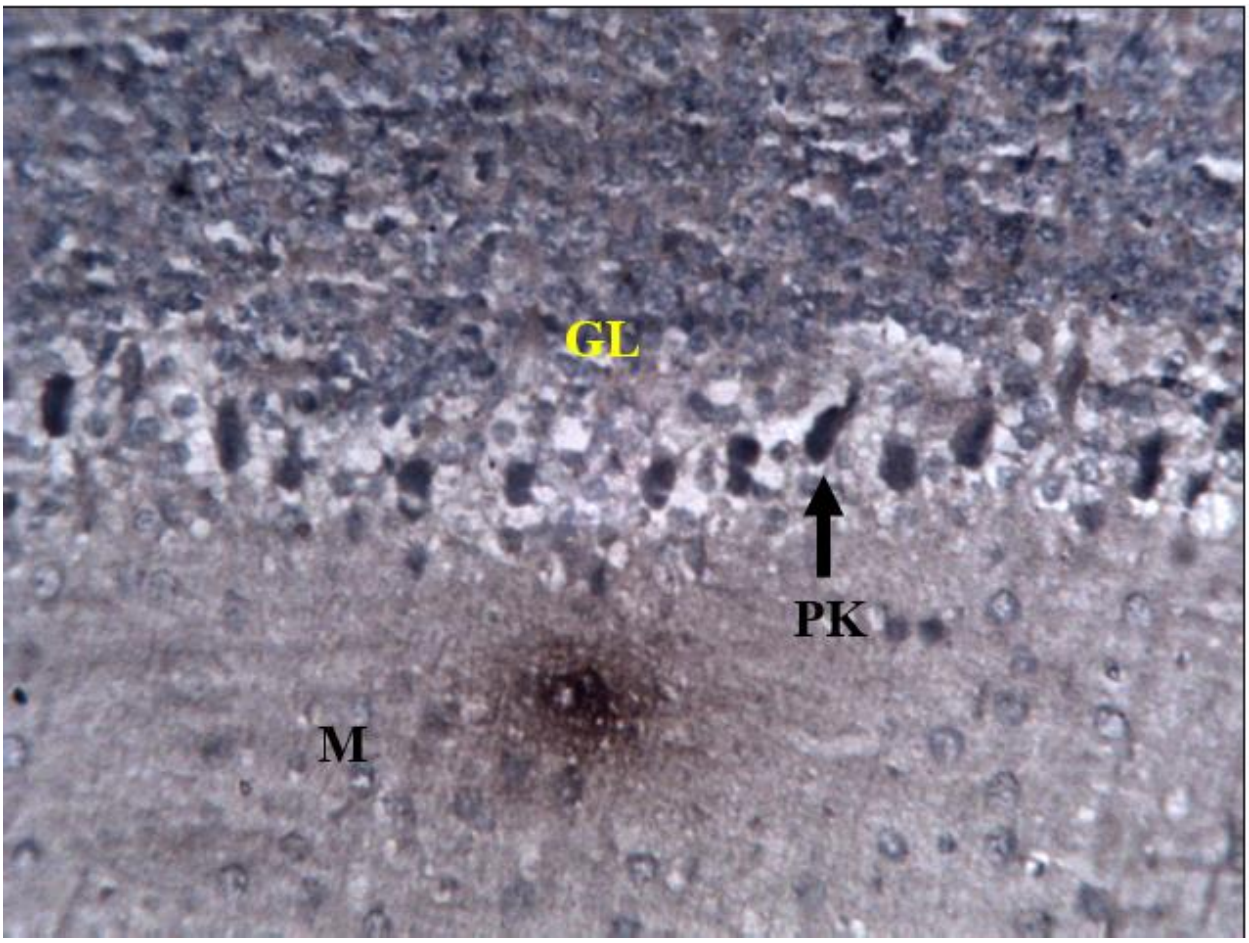


Plate 4.47: Section of Wistar rat Cerebellar cortex of the EGH (300 mg/kg Eugenol) revealing a high ACAT-1 Immunoreactivity of the purkinje cells of the cerebellar cortex when compared to AC group. Granular layer (GL); Molecular layer (M); Purkinje cell (PK) (ACAT x 250).

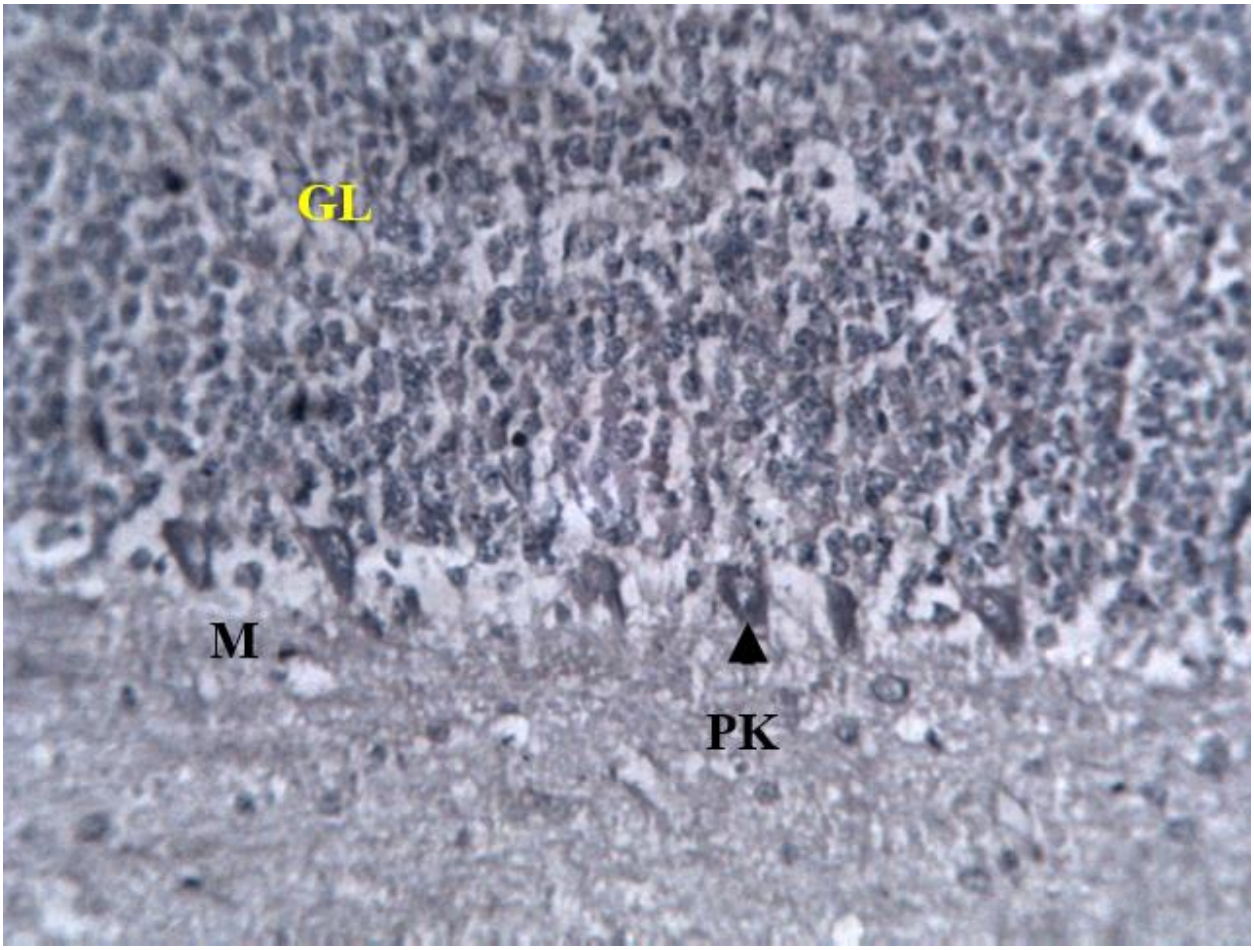


Plate 4.48: Section of Wistar rat Cerebellar cortex of EGL group (150mg/kg Eugenol), Showing a high ACAT-1 Immunoreactivity of the purkinje cells of the cerebellar cortex when compared to AC group. Granular layer (GL); Molecular layer (M); Purkinje cell (PK) (ACAT x 250).

4.4.3 Histological and Histochemical Features of the Hippocampus

The rat hippocampus (*hippocampus proprius*) is divided into four regions (CA1-CA4, CA stands for *Cornu ammonis)* according to the density, size and branching of the axons and dendrites of pyramidal cells and *stratum multiforme* (multiform layer). The continuation of CA3 in the concavity of the dentate gyrus (fascia dentate) is CA4. CA1 is characterized by densely packed medium-sized cells; CA3 is the region with large, less dense packed cells, while CA2 is the transition field between CA1 and CA3 as shown below;

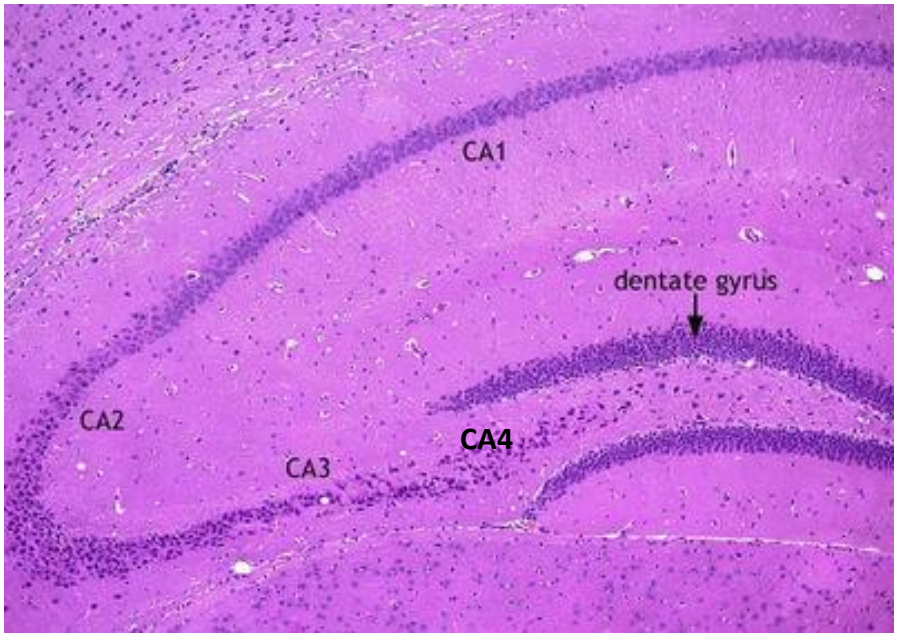


Figure 4.1: Histological Photomicrograph of the Hippocampus showing different regioms

4.4.3.1 Histological, Histochemical and Immunohistochemical Features of the Hippocampus of the Control (Untreated), Wistar rat

Histological examination of rat hippocampus (CA1 and CA3) regions. The control group showed a normal cytoarchitecture of these regions: the basic pattern of an ordered sheet of large neurones (Pyramidal and granule cells) whose cell bodies are packed together. The large neurones are the

giant pyramids of CA3 and the smaller Pyramids of CA1. Histochemical (CFV) staining for nissil bodies' revealed normal appearance and other interneurons such as fusiform cells which differ from Pyramidal and granule cells as observed in **(Plate 4.55).**

Histochemical (Congo red) staining for amyloid plaques revealed normal appearance of hippocampal neurones, but revealed no amyloidal plaques as expected for the untreated group as observed in **(Plate 4.61).** Immunostaining reaction with ACAT-1 revealed immunohistochemical localization of ACAT-1 within the neuronal cell body with emphasis on Pyramidal cells. Normal ACAT-1 immunoreactivity was seen in Pyramidal cells of the control (untreated) which is indicated by a brown outline on the purkinje cells as seen in **(Plate 4.73).**

4.4.3.2 Histological, Histochemical and Immunohistochemical Features of the Hippocampus of Treated Wistar Rats

Histological and Histochemical (CFV) examination of rat hippocampi treated with aluminium revealed cytoarchitectural distortion in the in the hippocampi regions (CA1 and CA3); neurodegenerative changes such as irregular arrangement of CA1 hippocampal neurones, Pyknotic and basophilic necrosis **(Plate 4.56).**

Histochemical (Congo red) examination of rat hippocampi treated with aluminium revealed no visible amyloidal plaques with the hippocampi across all groups **(Plates 4.61-4.66).**

Histological and Histochemical (CFV stained) examinations of the hippocampi of Eugenol treated Wistar rats revealed a normal cytoarchitecture when compared with the control **(Plates 4.59 and 4.60)**, while Wistar rats that received Eugenol followed by aluminium treatment revealed mild cytoarchitectural distortions of hippocampi regions (CA1 and CA3) **(Plates 4.57 and 4.58).**

Immunostaining reaction with ACAT-1 showed reduced Immunohistochemical localization of ACAT-1 within the neuronal cell body with emphasis on Pyramidal cells, cholinergic neurons of the group administered aluminium chloride. Reduced ACAT-1 immunoreactivity was seen in Pyramidal cells of all treated groups. Upon administration of Eugenol, an apparent restoration of ACAT-1 immunoreactivity was observed, which is indicated by the brown outline of the purkinje cells as seen in **(Plates 4.67-4.72).**

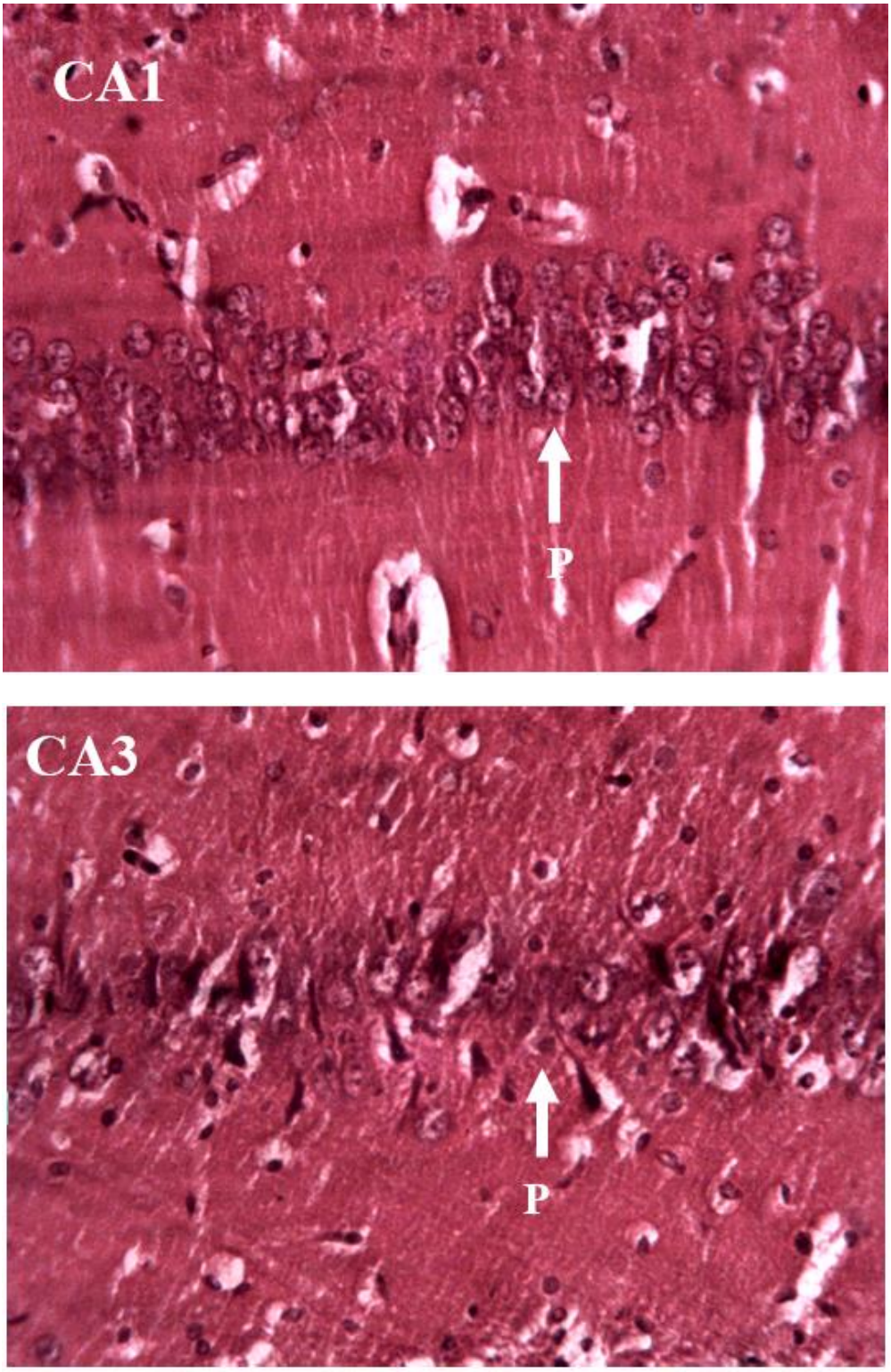


Plate 4.49: Sections of Wistar rat hippocampal regions (CA1 and CA3) of the control (CTRL) untreated group showing normal cytoarchitecture of the hippocampus. Pyramidal cell (P (Mag x 250 H&E).

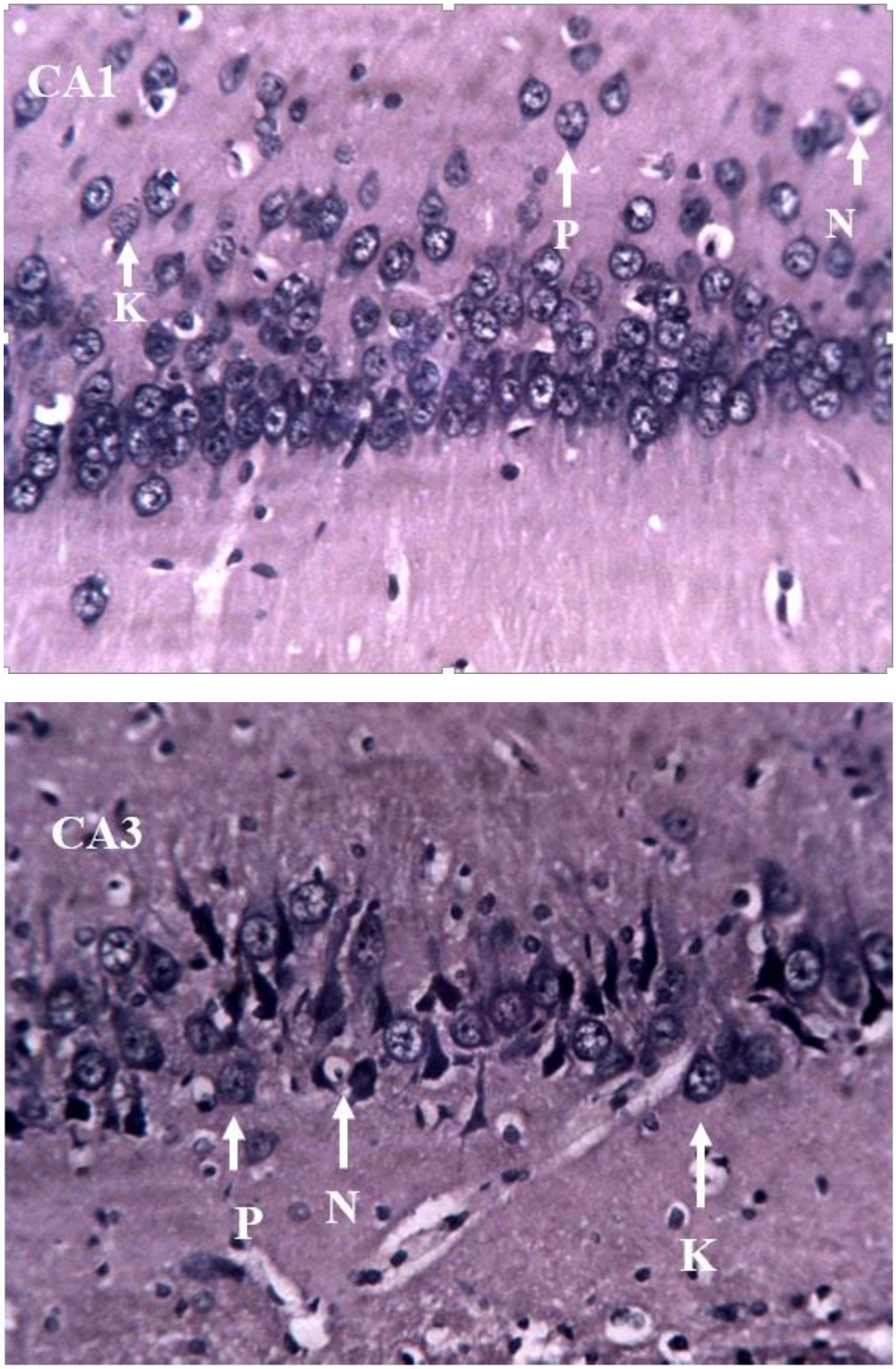


Plate 4.50: Sections of Wistar rat hippocampal regions (CA1 and CA3) of of the aluminium treated group (AC) (100mgkg of aluminium) showing distortion (Neuronal degeneration N) in the cytoarchitecture of the hippocampus. Pyramidal cell (P), Chromatolysis (K) (Mag x 250 H&E).

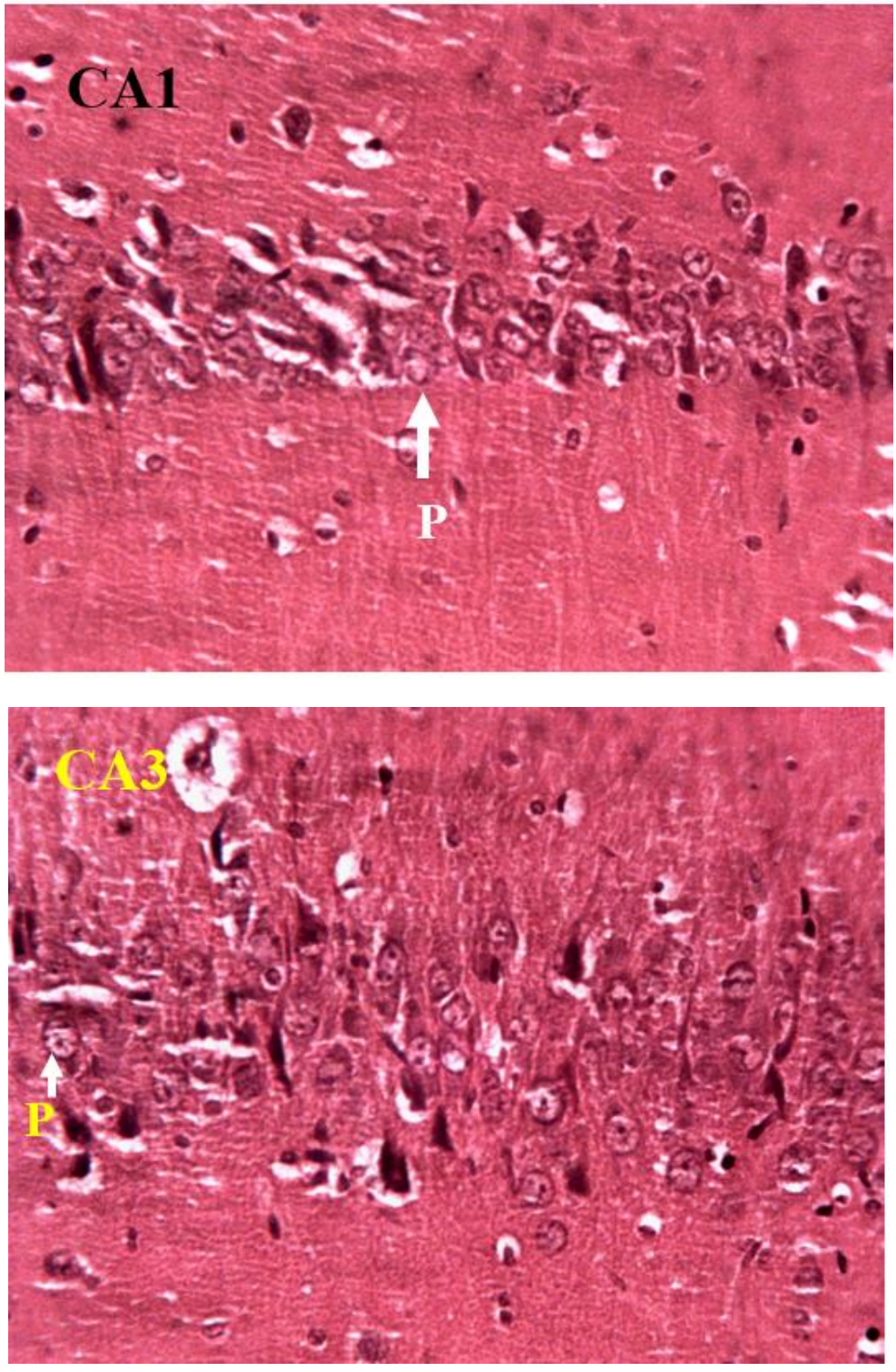


Plate 4.51: Sections of Wistar rat hippocampal regions (CA1 and CA3) of Group EGH+AC (300mg/kg Eugenol and 100mg/kg of aluminium chloride) showing mild distortion in the cytoarchitecture of the hippocampus. Pyramidal cell (P) (Mag x 250 H&E).

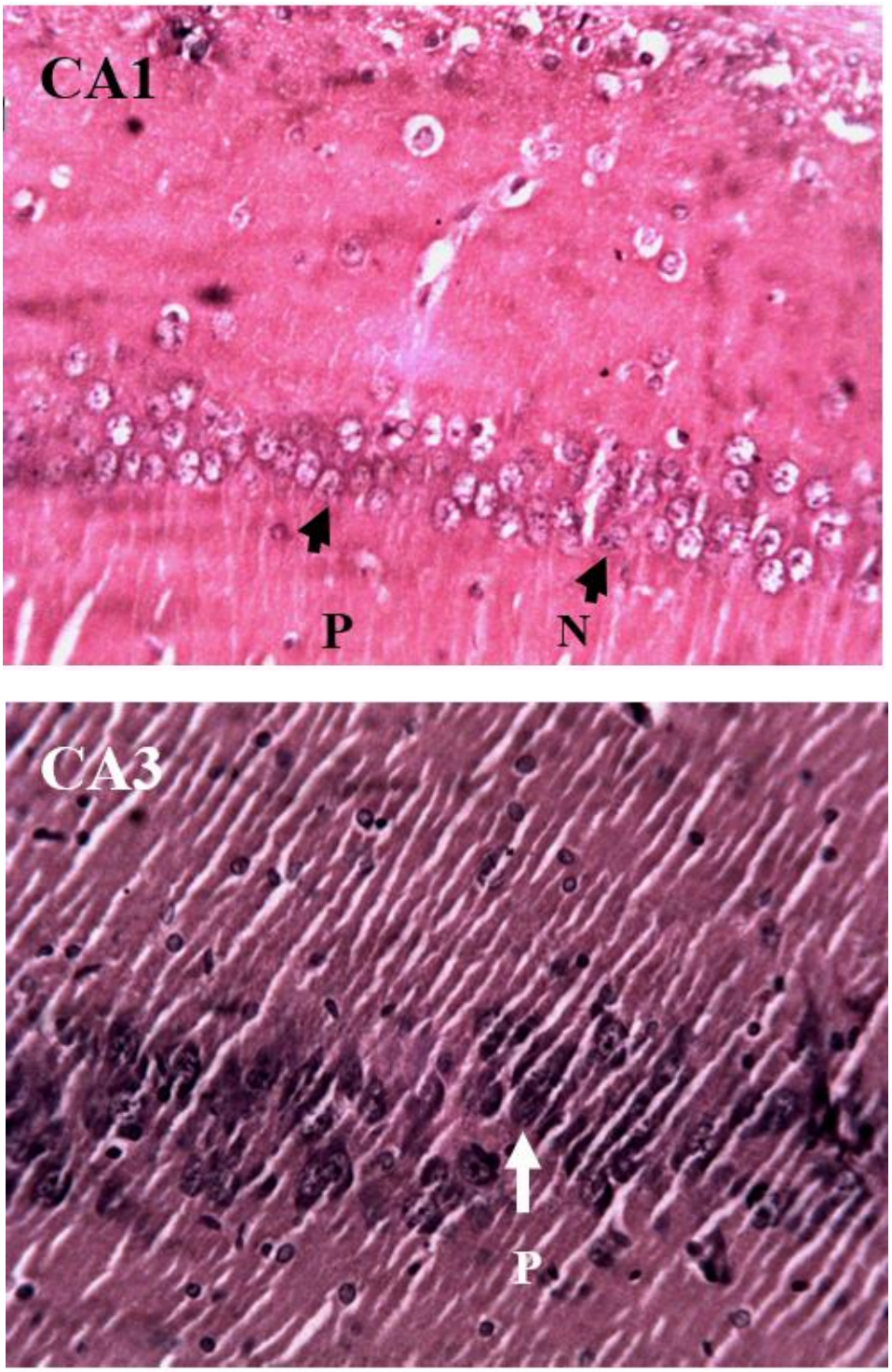


Plate 4.52: Section of Wistar rat hippocampal regions (CA1 and CA3) of Group EGL+AC (150mg/kg Eugenol and 100mg/kg of aluminium chloride) showing mild distortion with Neuronal degeneration (N). Pyramidal cell (P) (Mag x 250 H&E).

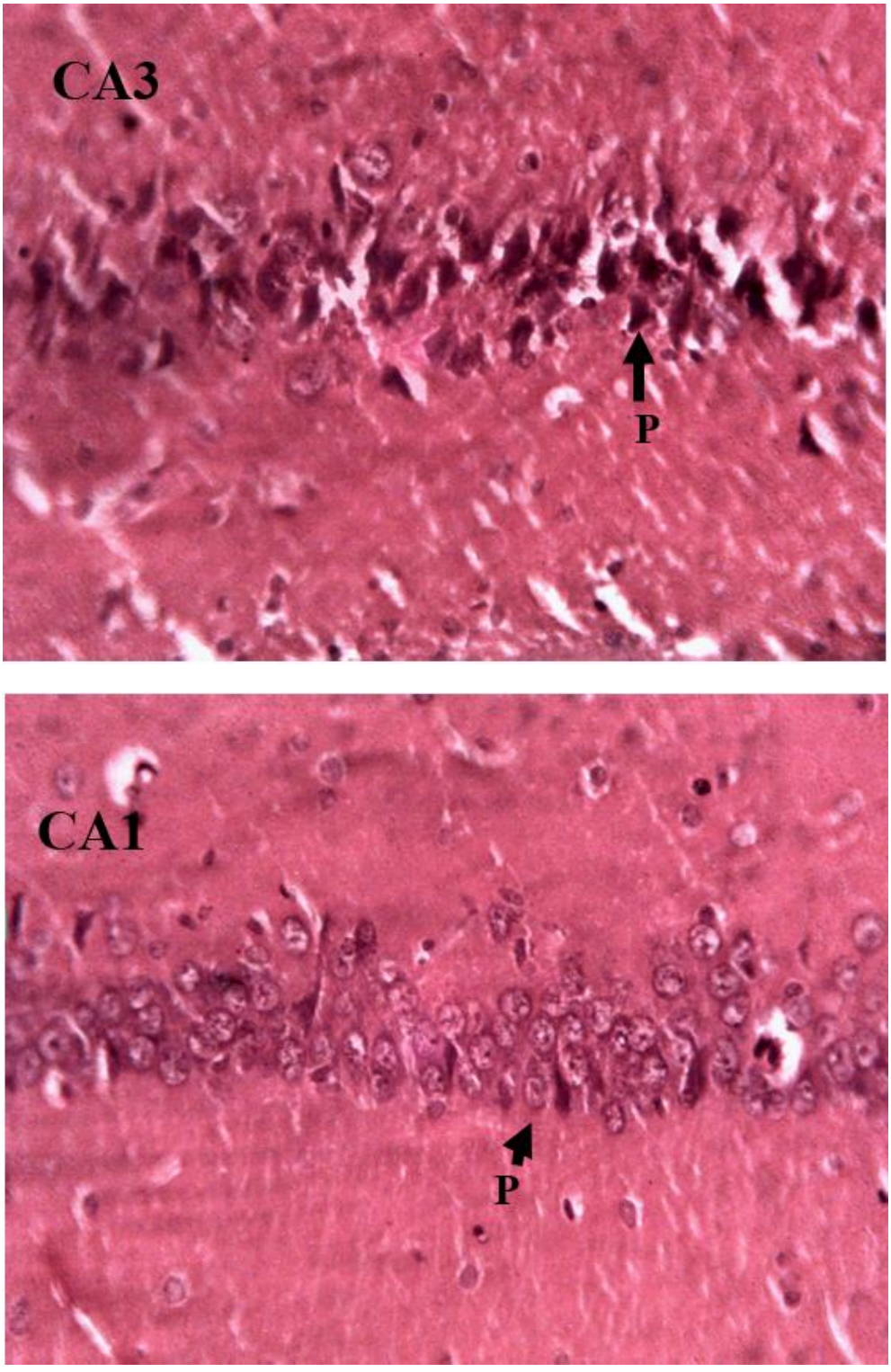


Plate 4.53: Sections of Wistar rat hippocampal regions (CA1 and CA3) regions of Group EGH (300mg/kg Eugenol) Showing a normal cytoarchitecture of the hippocampus when compared to the untreated group. Pyramidal cell (P) (Mag x 250 H&E).

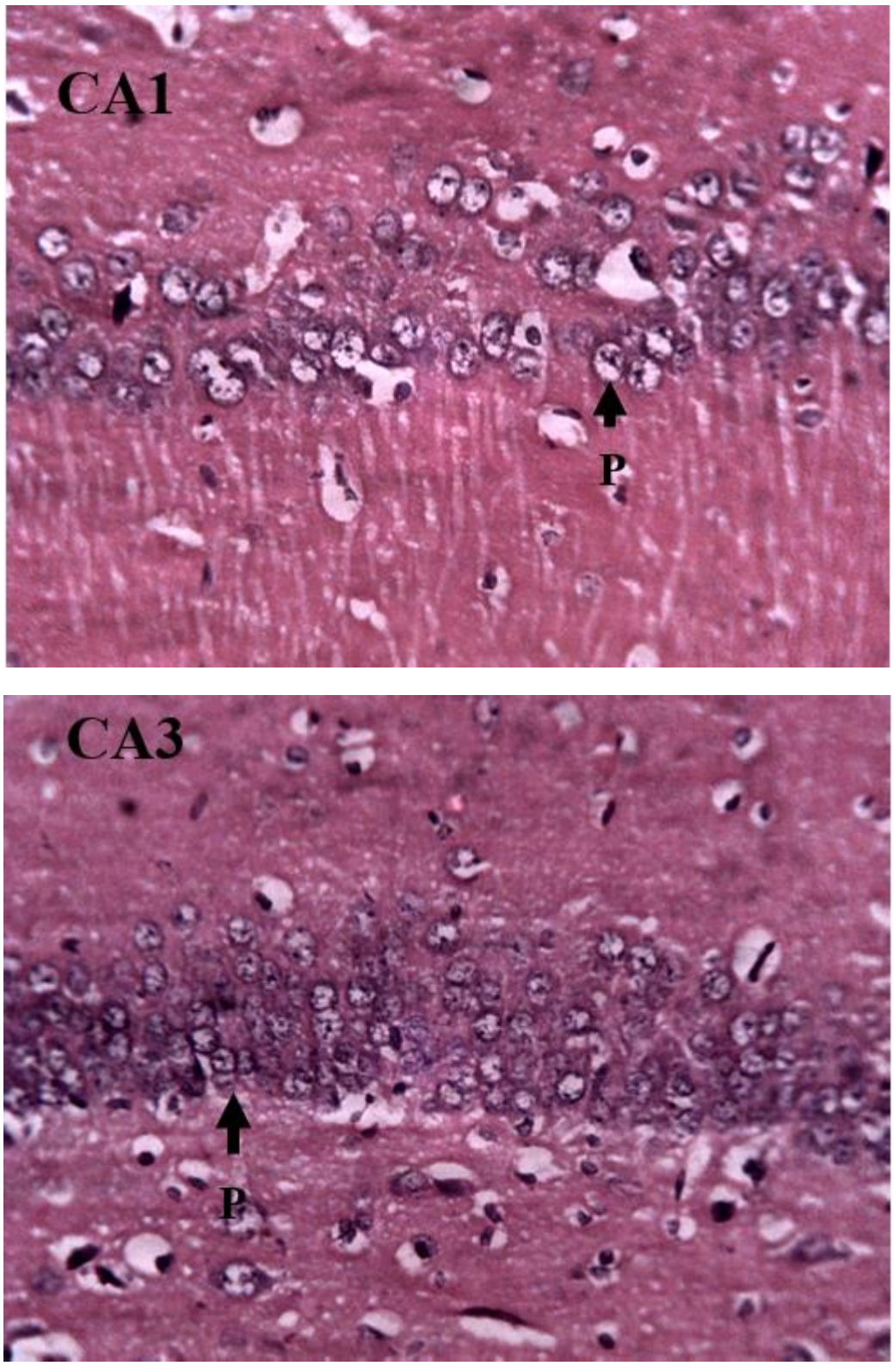


Plate 4.54: Sections of Wistar rat's hippocampal region (CA1 and CA3) of Group EGL (150mg/kg Eugenol) showing a normal cytoarchitecture when compared to the control group. Pyramidal cell (P) (Mag x 250 H&E).

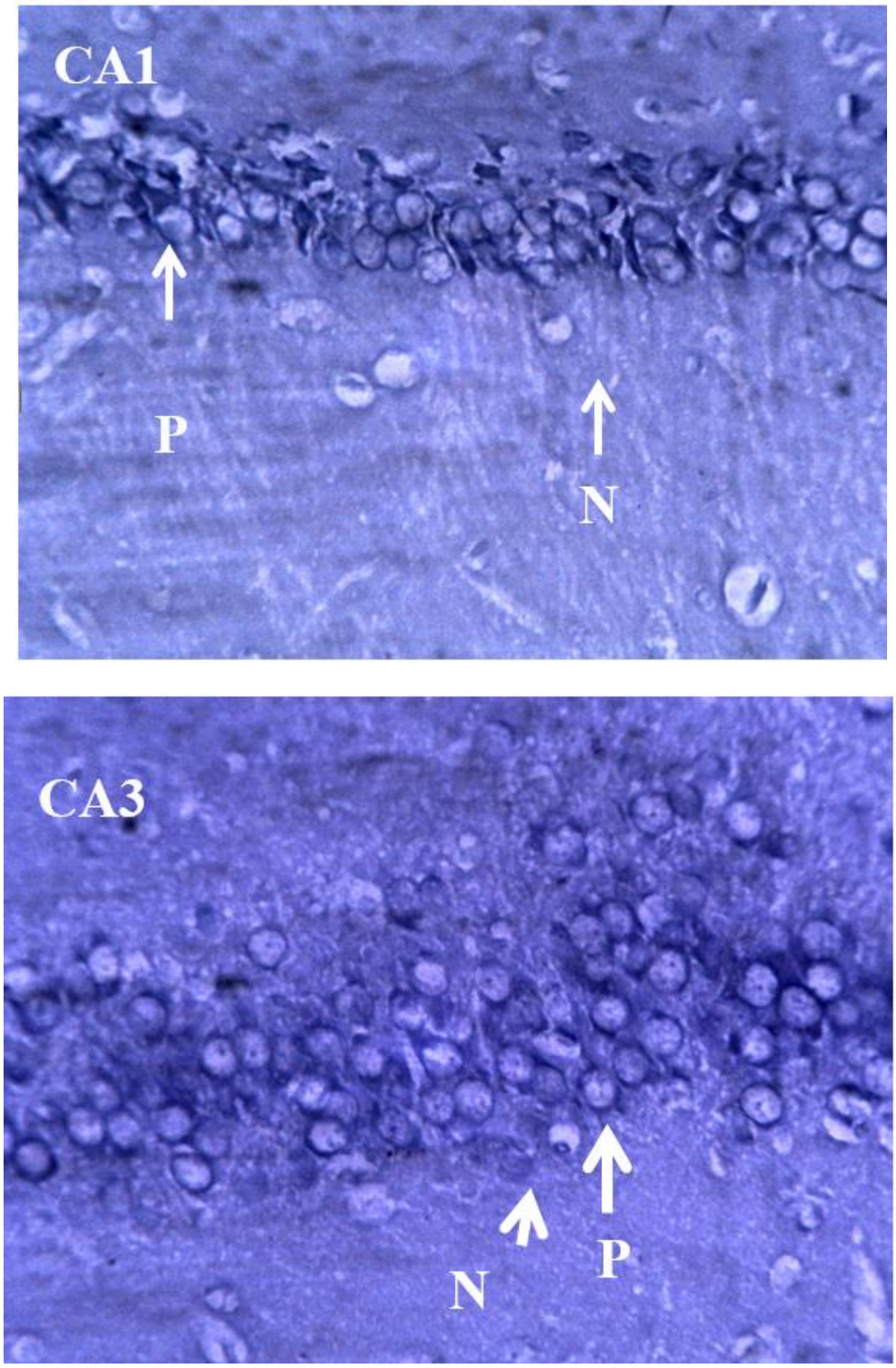


Plate 4.55: Sections of rat hippocampal regions (CA1 and CA3) of Group control (CTRL) untreated group showing normal cytoarchitecture of the hippocampus. Pyramidal cell (P); Fusiform cell (F) (Mag x 250 CFV).

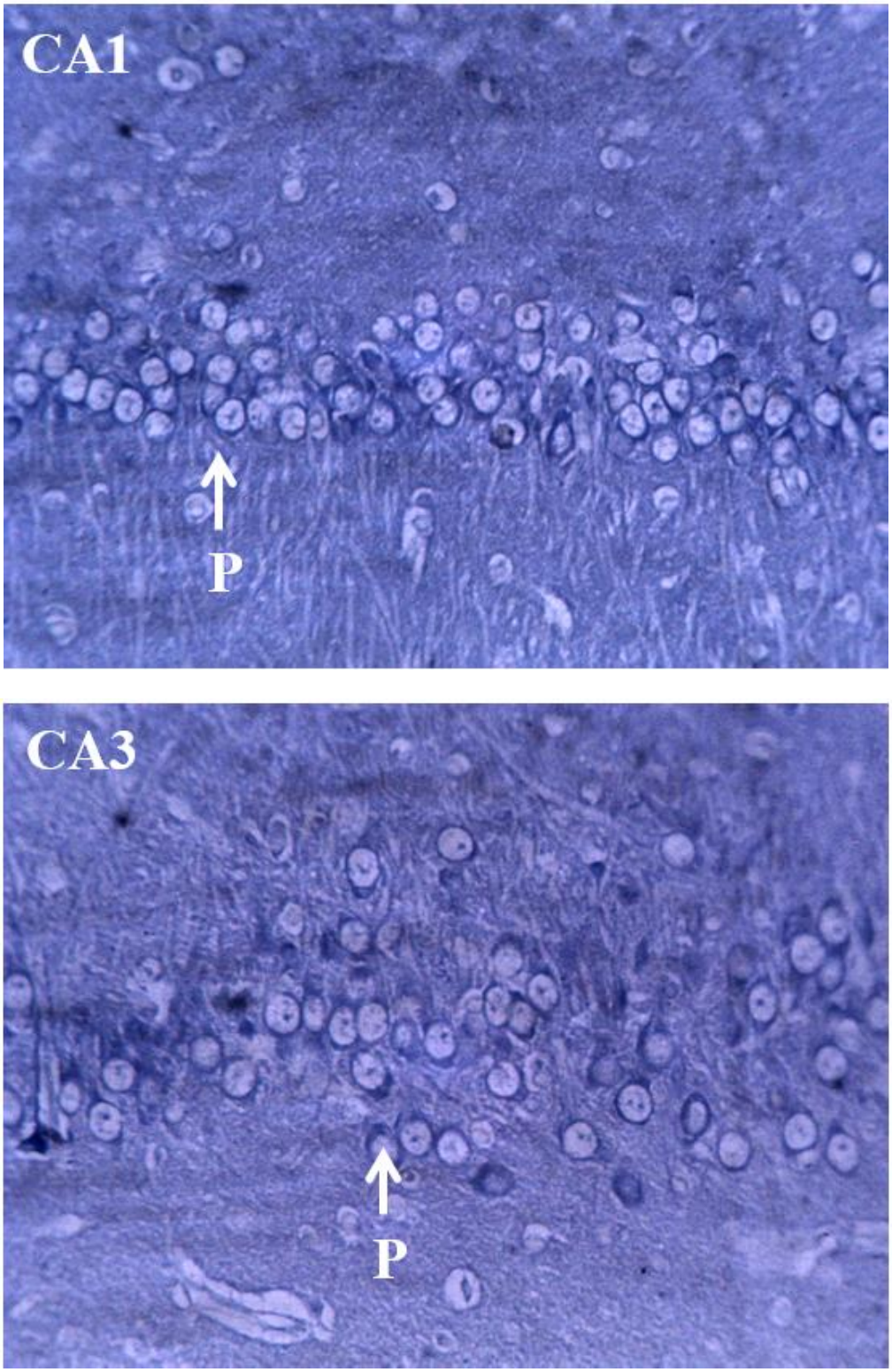


Plate 4.56: Sections of Wistar rat hippocampal regions (CA1 and CA3) of the aluminium treated group (AC) (100mg/kg of aluminium chloride) showing distortion in the cytoarchitecture of the hippocampus. Pyramidal cell (P) (Mag x 250 CFV).

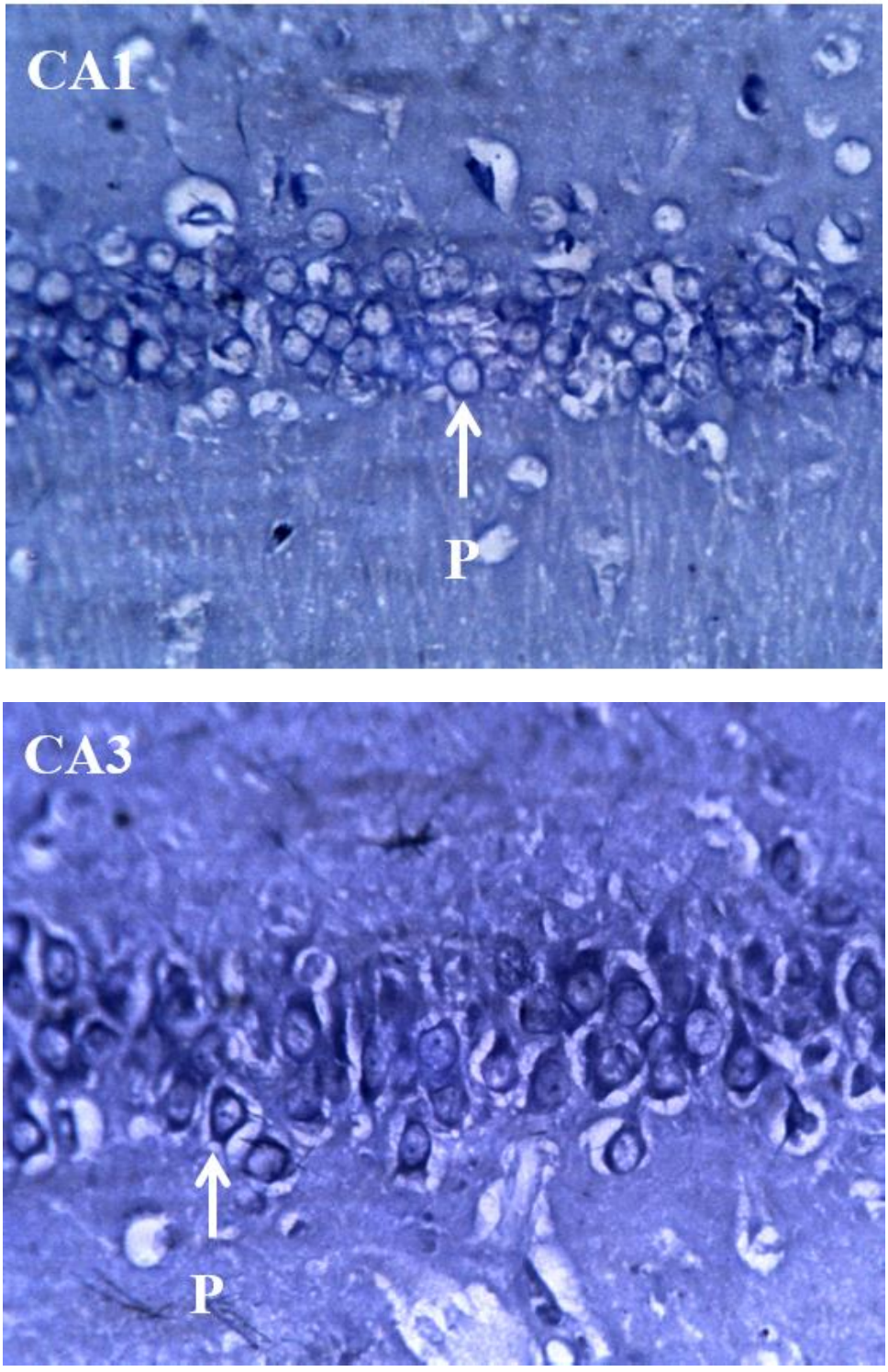


Plate 4.57: Section of Wistar rat hippocampal regions (CA1 and CA3) of Group (EGH+AC) (300mg/kg of Eugenol and 100mg/kg of aluminium chloride) showing mild distortion (Neuronal degeneration with perineuronal vacoulations N). Pyramidal cell (P) (Mag x 250 CFV).

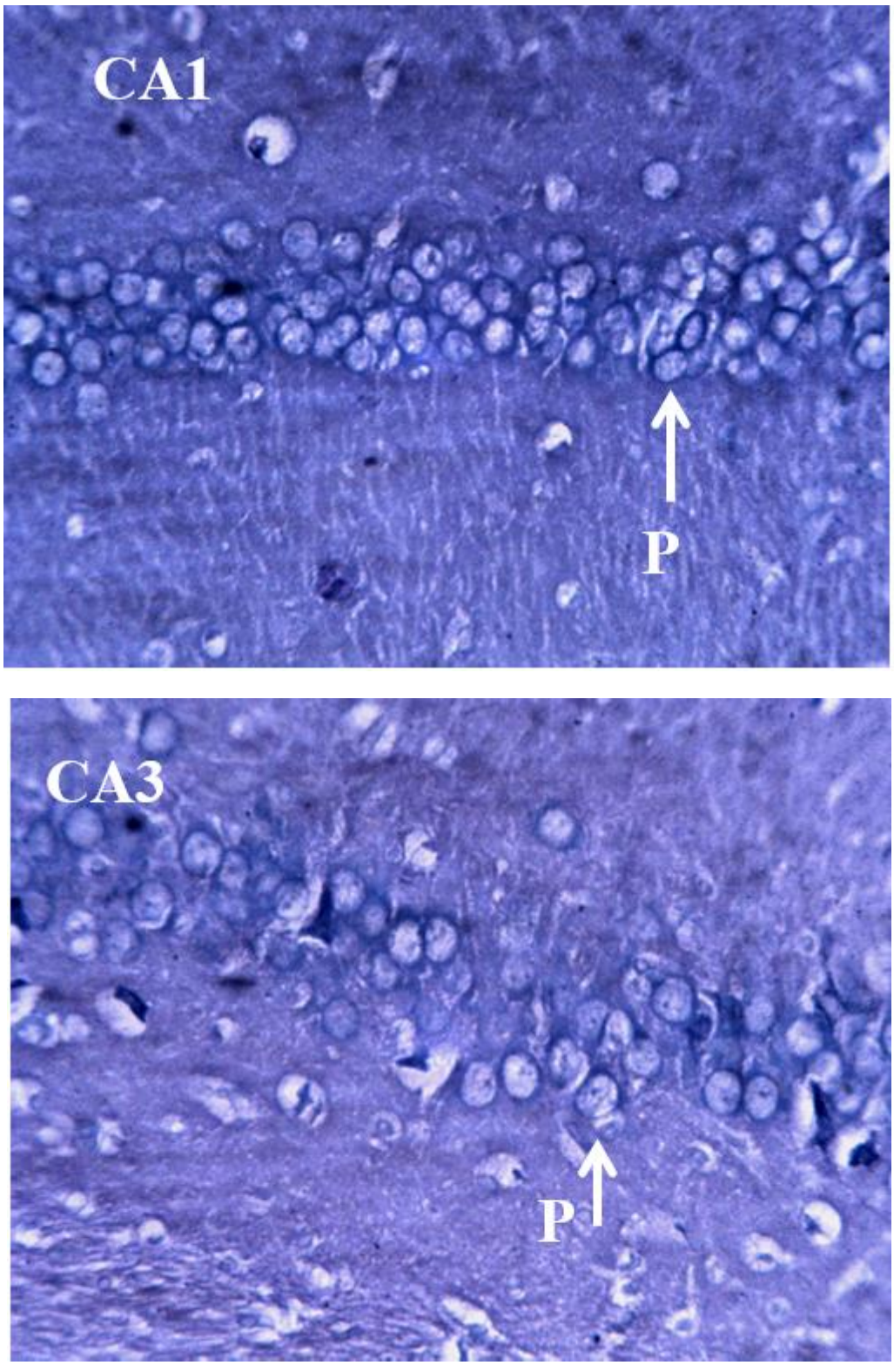


Plate 4.58: Sections of Wistar rat hippocampal regions (CA1 and CA3) of Group EGL+AC (150mg/kg Eugenol and 100mg/kg of aluminium chloride) showing mild distortion in the cytoarchitecture of the hippocampus. Pyramidal cell (P); (Mag x 250 CFV).

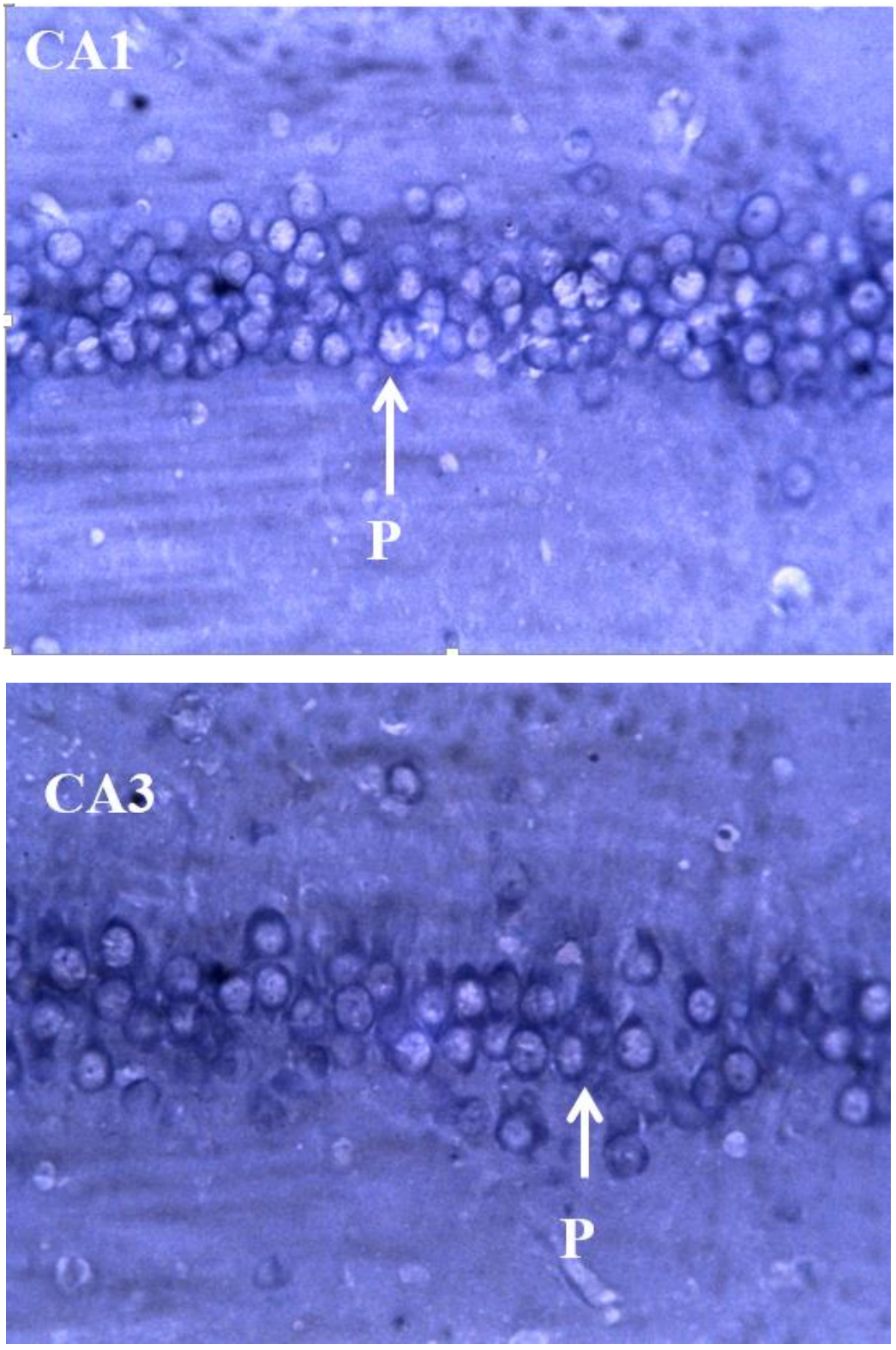


Plate 4.59: Sections of Wistar at hippocampal regions (CA1 and CA3) of Group EGH (300mg/kg of Eugenol) Showing a normal cytoarchitecture of the hippocampus when compared with the control (Untreated). Pyramidal cell (P) (Mag x 250 CFV).

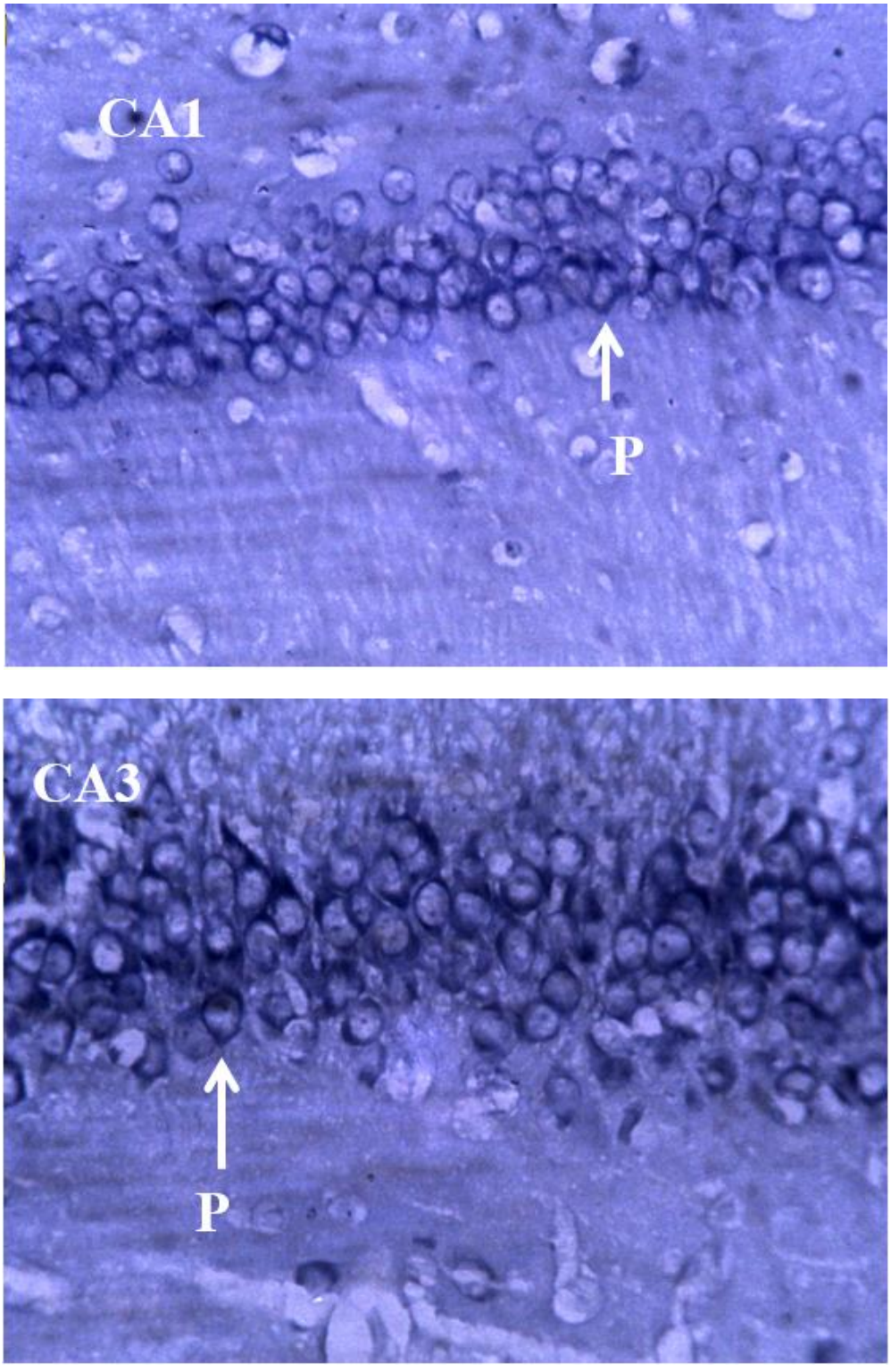


Plate 4.60: Section of Wistar rat hippocampal regions (CA1 and CA3) of Group EGL (150mg/kg Eugenol) showing a normal cytoarchitecture of the hippocampal region. (Pyramidal cell (P) (Mag x 250 CFV).

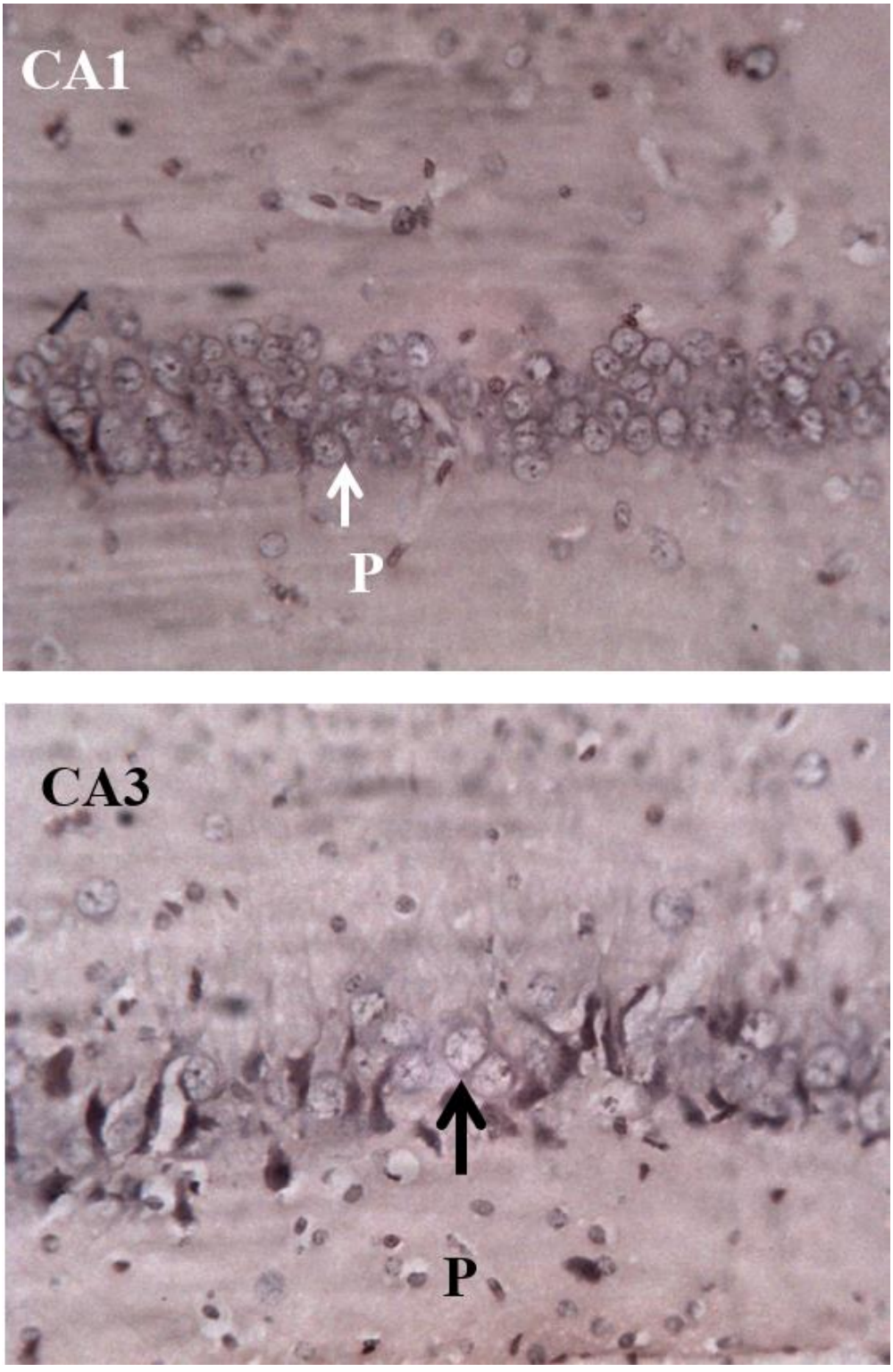


Plate 4.61: Sections of Wistar rat hippocampal regions (CA1 and CA3) of the control (CTRL) Untreated group showing a normal cytoarchitecture of the hippocampus with no visible amyloid plaques. Pyramidal cell (P) (Mag x 250 Congo red).

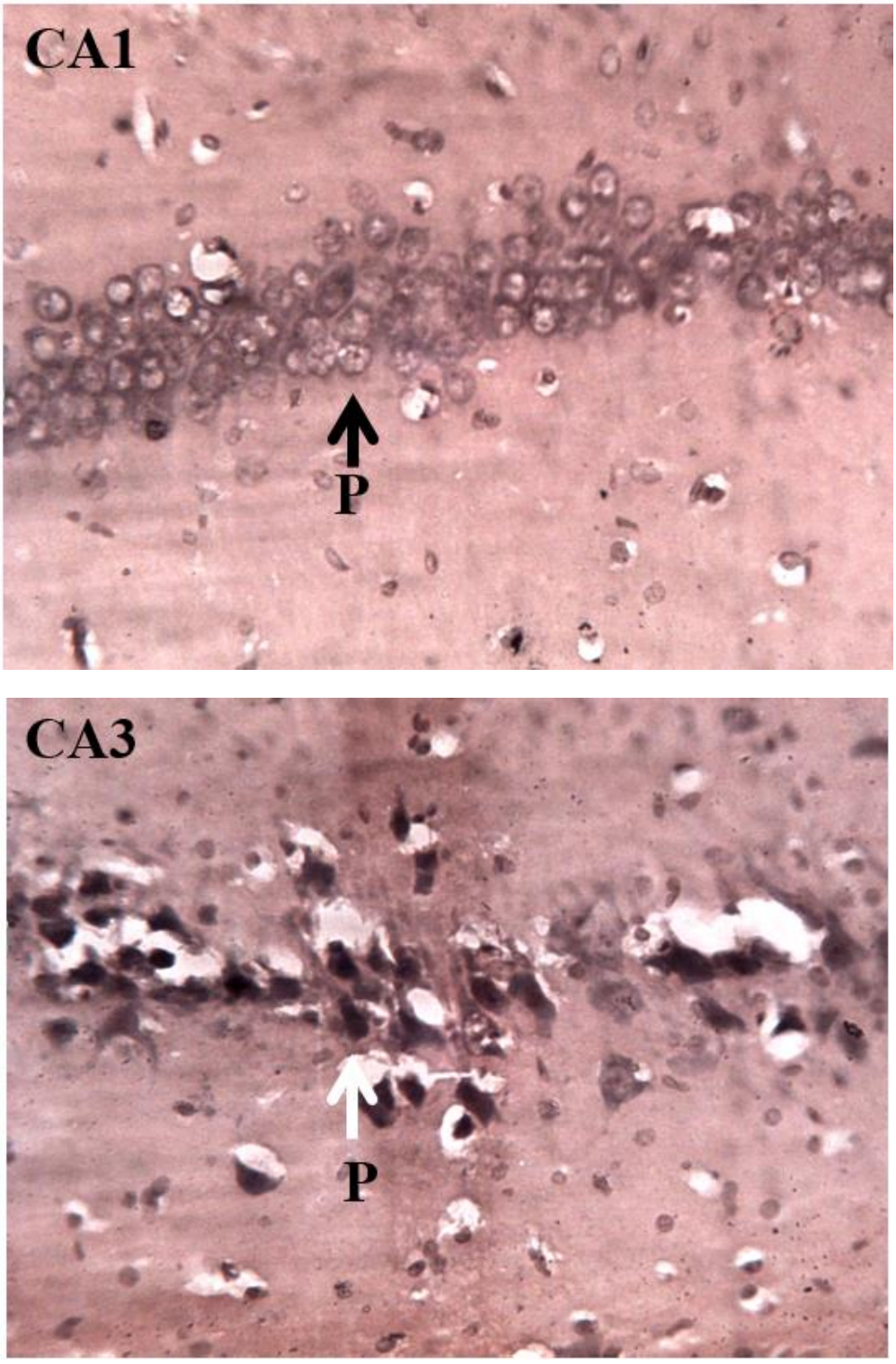


Plate 4.62: Sections of Wistar rat hippocampal regions (CA1 and CA3) of the aluminium treated group (AC) (100mg/kg of aluminium chloride) showing distortions in the cytoarchitecture of the hippocampus, but no visible amyloid plaques. Pyramidal cell (P) (Mag x 250 Congo red).

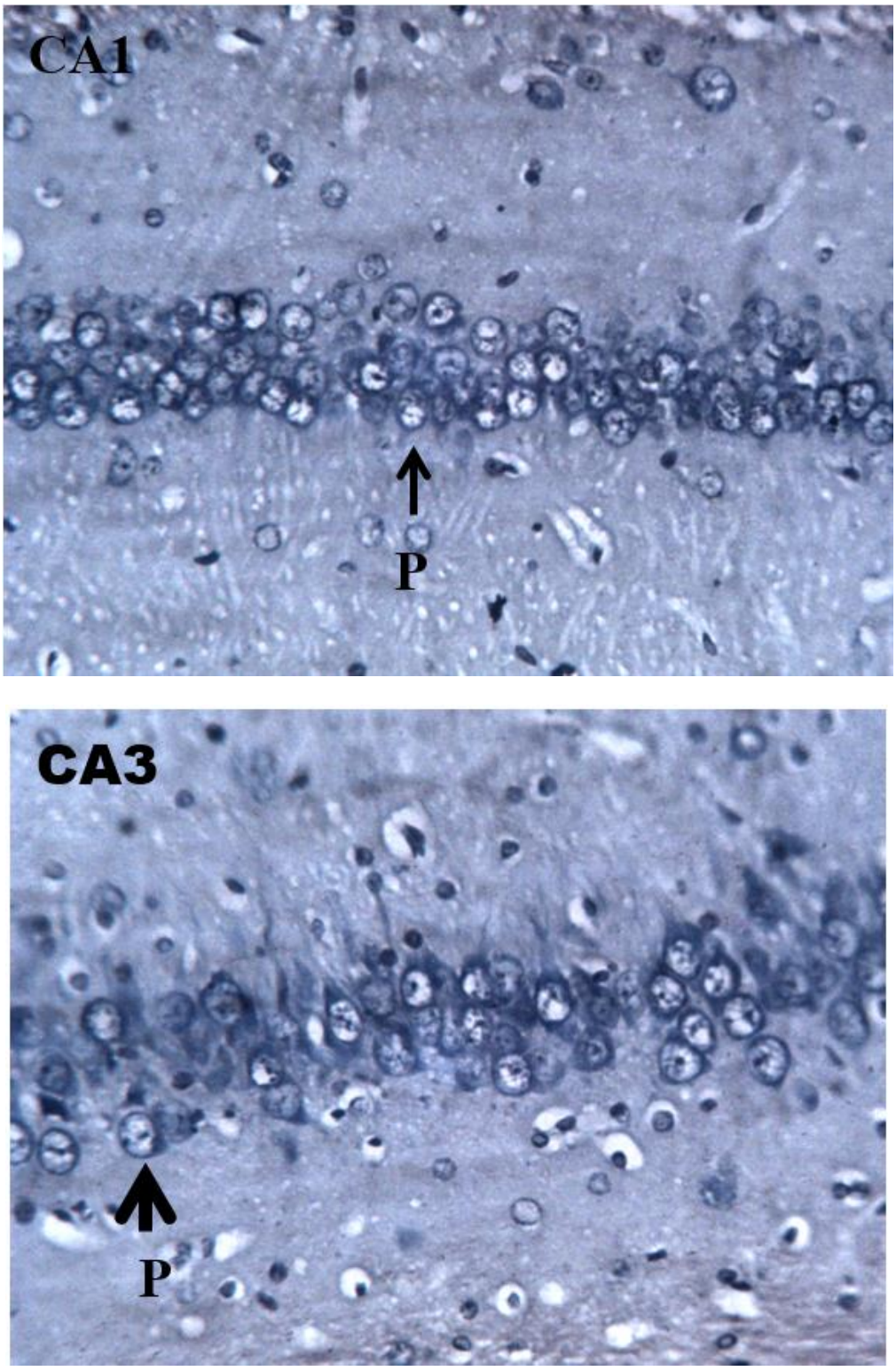


Plate 4.63: Sections of Wistar rat hippocampal regions (CA1 and CA3) of Group (EGH+AC) (300mg/kg Eugenol and 100mg/kg of aluminium chloride) showing mild distortion but no visible amyloid plaques. Pyramidal cell (P) (Mag x 250 Congo red).

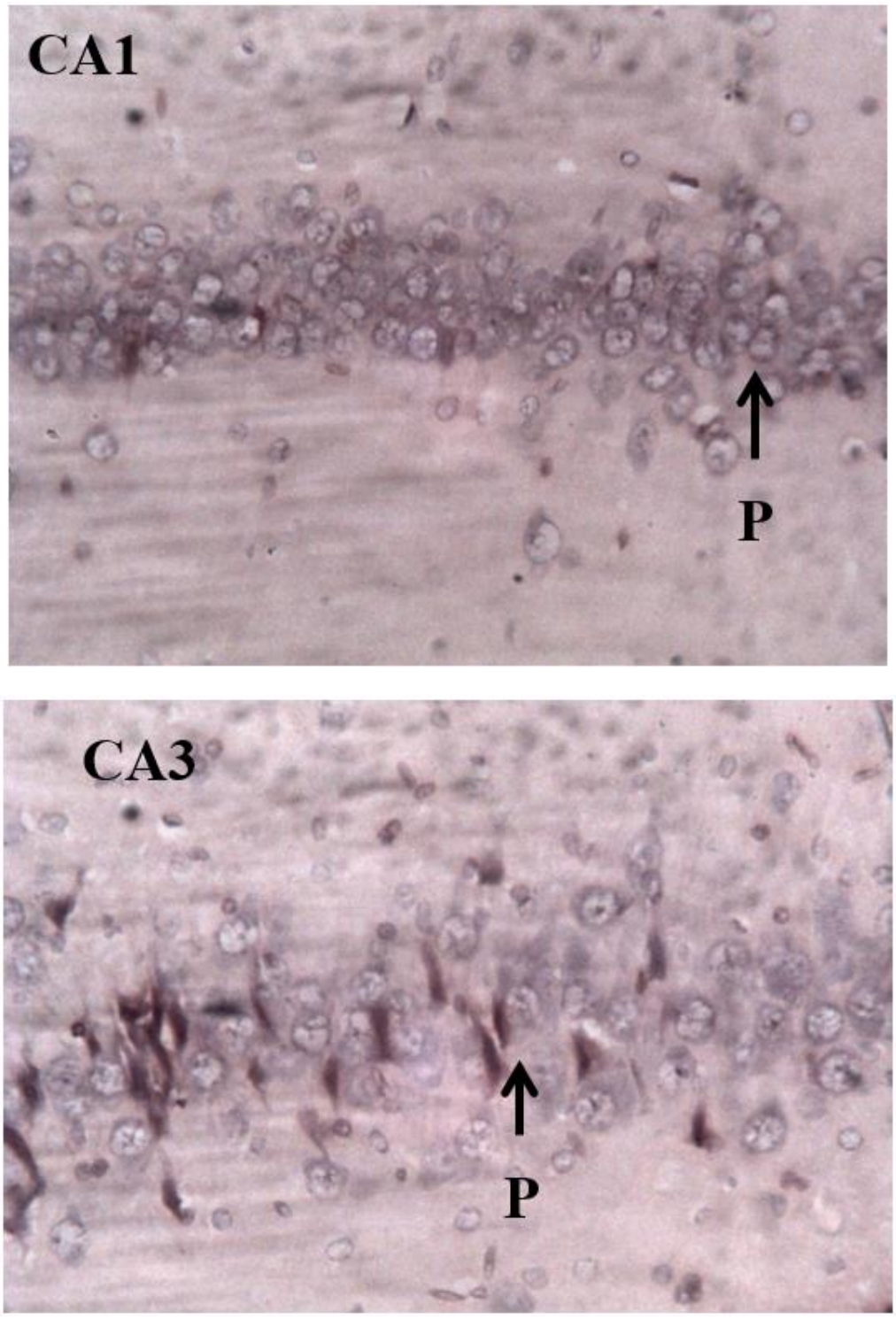


Plate 4.64: Sections of Wistar rat hippocampal regions (CA1 and CA3) regions of Group EGL+AC (150mg/kg Eugenol and 100mg/kg of aluminium chloride) with mild distortion in the cytoarchitecture of the hippocampus with no visible amyloid plaques.(Pyramidal cell (P) (Mag x 250 Congo red).

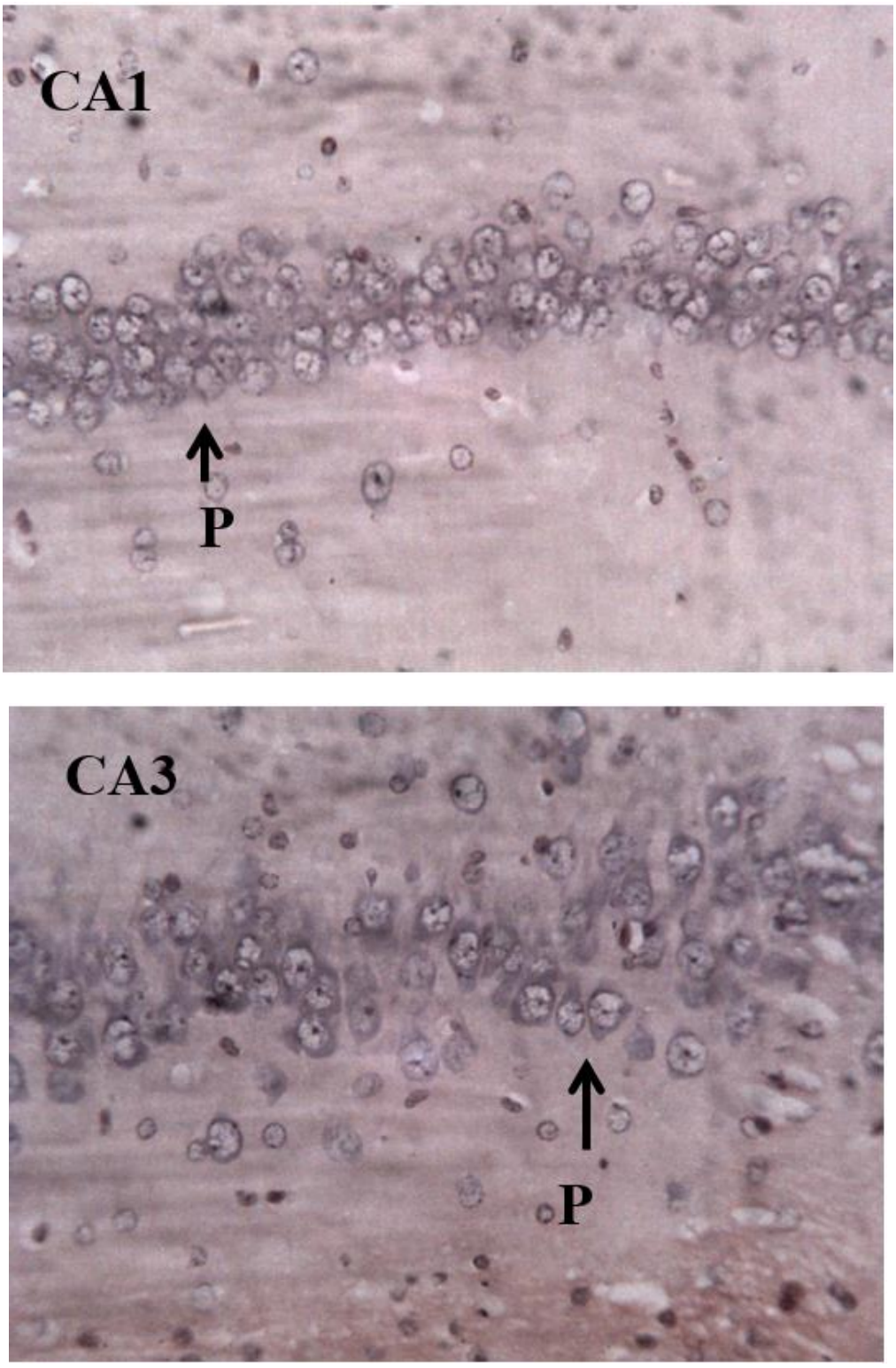


Plate 4.65: Sections of Wistar rat hippocampal regions (CA1 and CA3) of Group EGH (300mg/kg Eugenol) showing a normal cytoarchitecture when compared with the control (Untreated) with no visible amyloid plaques. Pyramidal cell (P) (Mag x 250 Congo red).

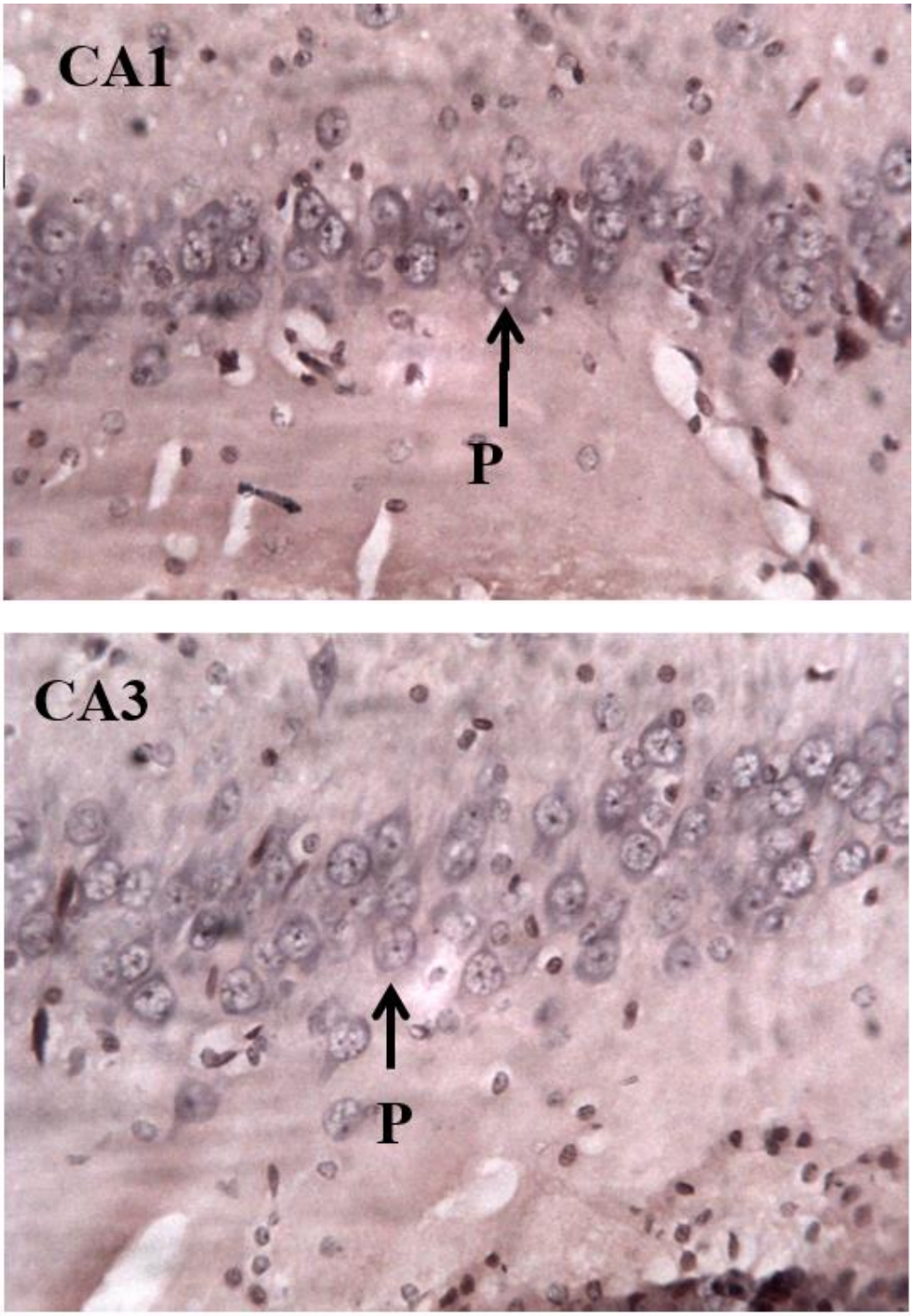


Plate 4.66: Sections of Wistar rat hippocampal regions (CA1 and CA3) of Group EGL (150mg/kg of Eugenol) showing a normal cytoarchitecture of hippocampal regions with no visible amyloid plaques. Pyramidal cell (P) (Mag x 250 Congo red).

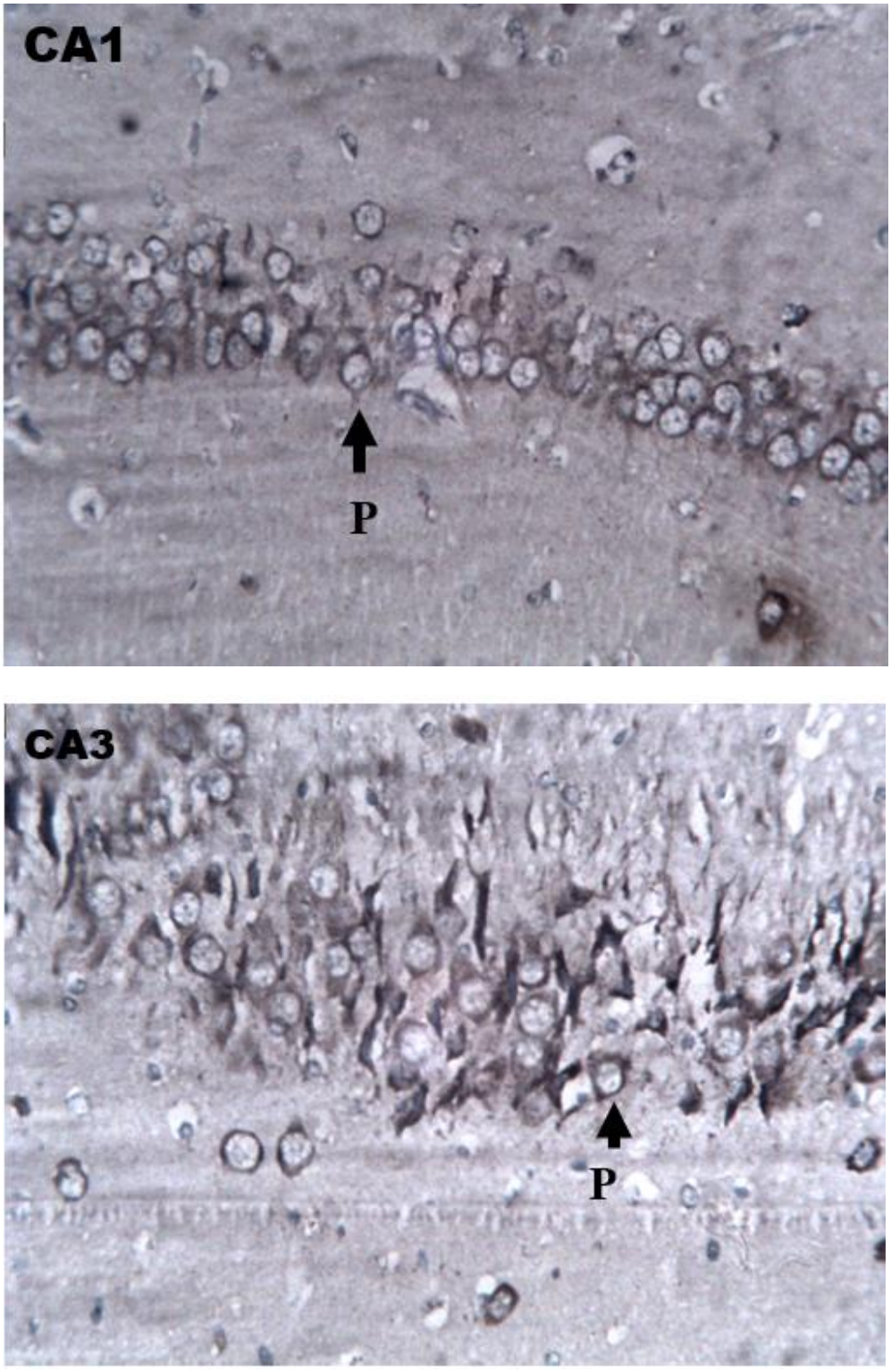


Plate 4.67: Section of Wistar rat hippocampal regions (CA1 and CA3) of Group VI (Untreated) showing a normal ACAT-1 immunoreactivity of the hippocampal region. (Pyramidal cell (P) (ACAT-1 x 250).

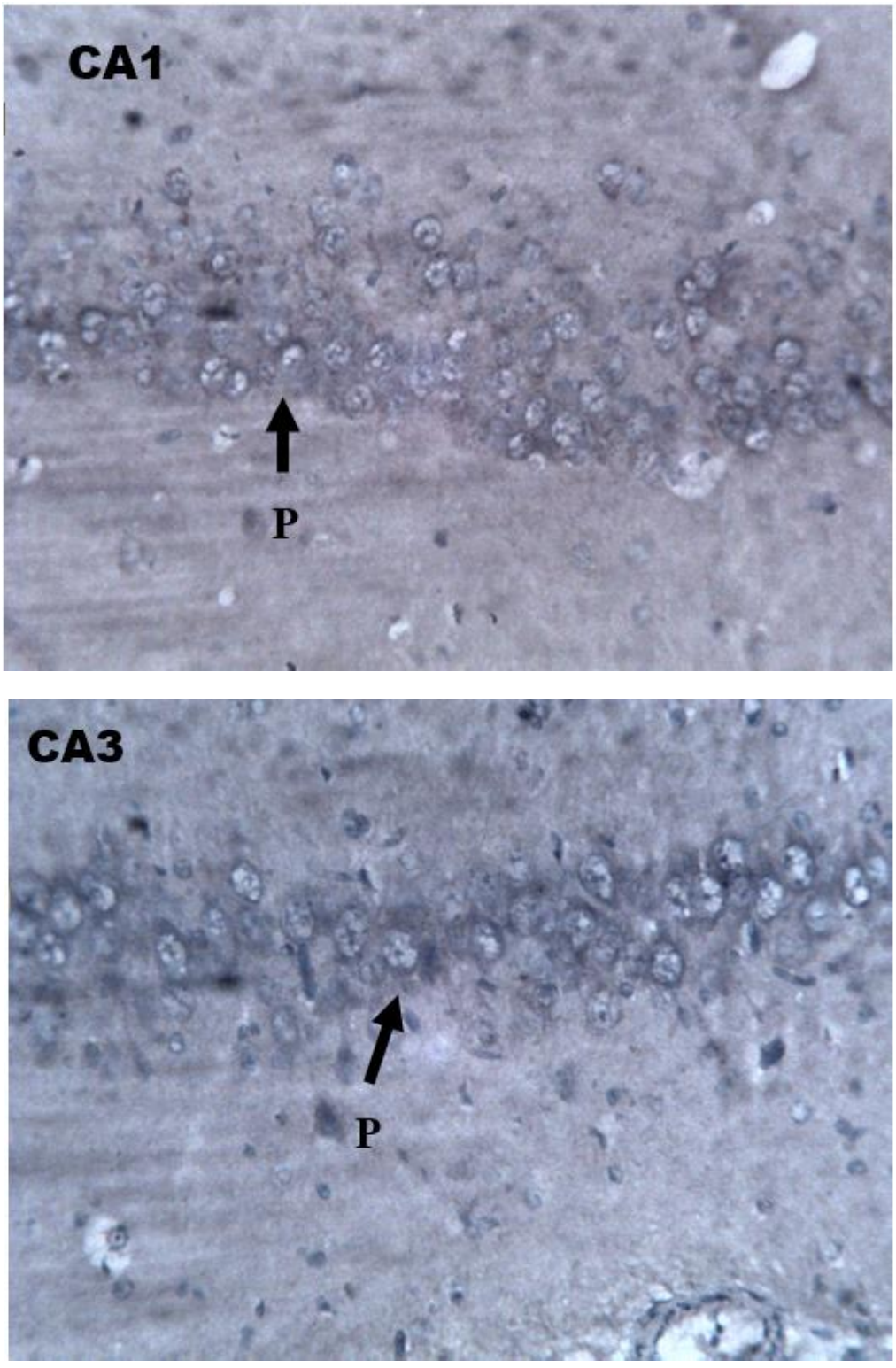


Plate 4.68: Section of Wistar rat hippocampal regions (CA1 and CA3) of Group V (100mg/kg $AlCl_3$) showing a diminished ACAT-1 immunoreactivity of the Pyramidal cells of the hippocampal region. (Pyramidal cell (P). (ACAT-1 x 250).

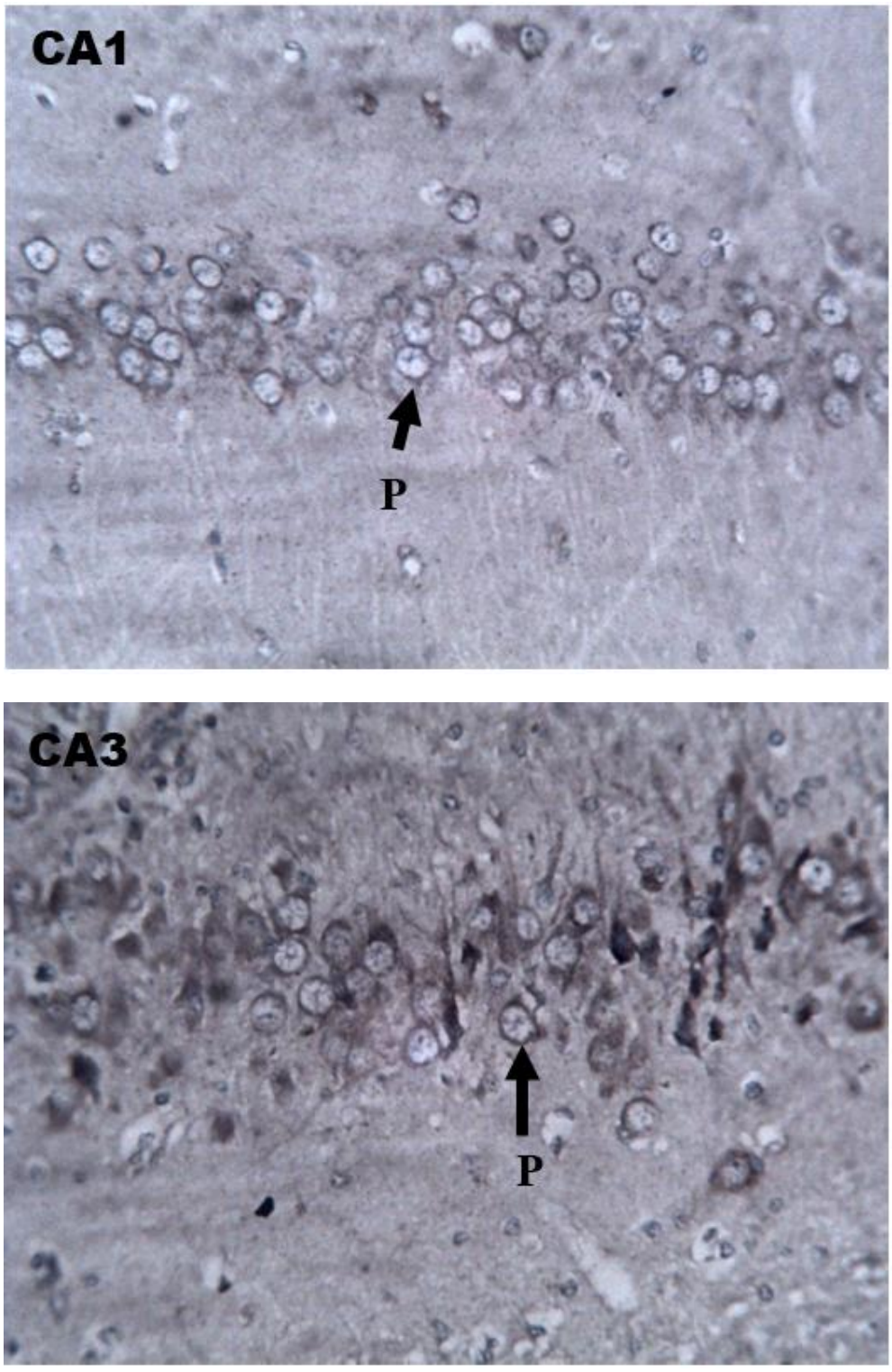


Plate 4.69: Section of Wistar rat hippocampal regions (CA1 and CA3) of Group III (300mg/kg Eugenol and 100mg/kg $AlCl_3$) revealing a restored ACAT-1 immunoreactivity of the Pyramidal cells of the hippocampal region when compared to Group V. (Pyramidal cell (P) (ACAT-1 x 250).

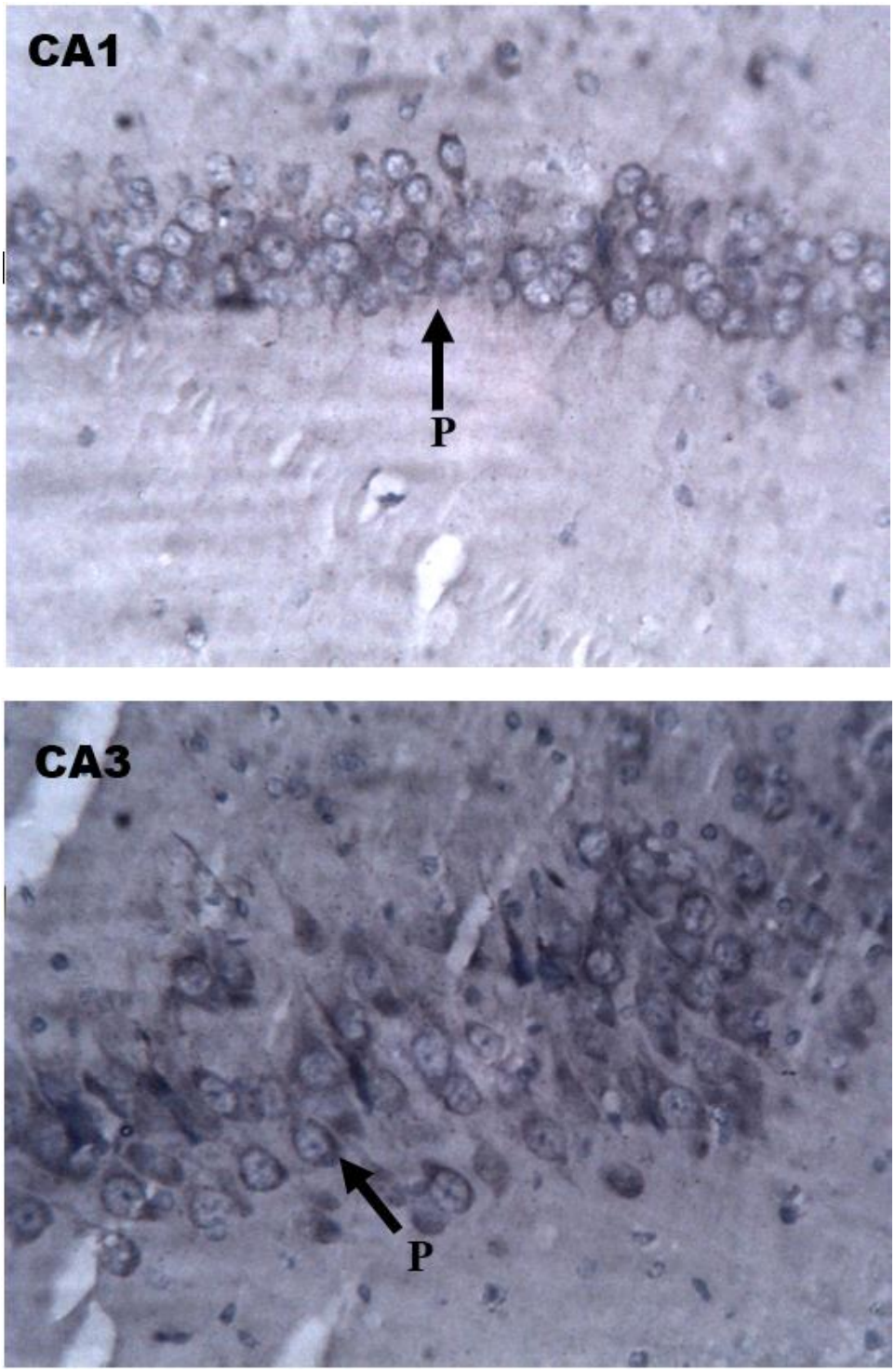


Plate 4.70: Section of Wistar rat hippocampal regions (CA1 and CA3) of Group IV (150 mg/kg Eugenol and 100mg/kg Aluminium chloride) revealing a restored ACAT-1 immunoreactivity of the Pyramidal cells of the hippocampal region when compared to Group V. (Pyramidal cell (P) (ACAT-1 x 250).

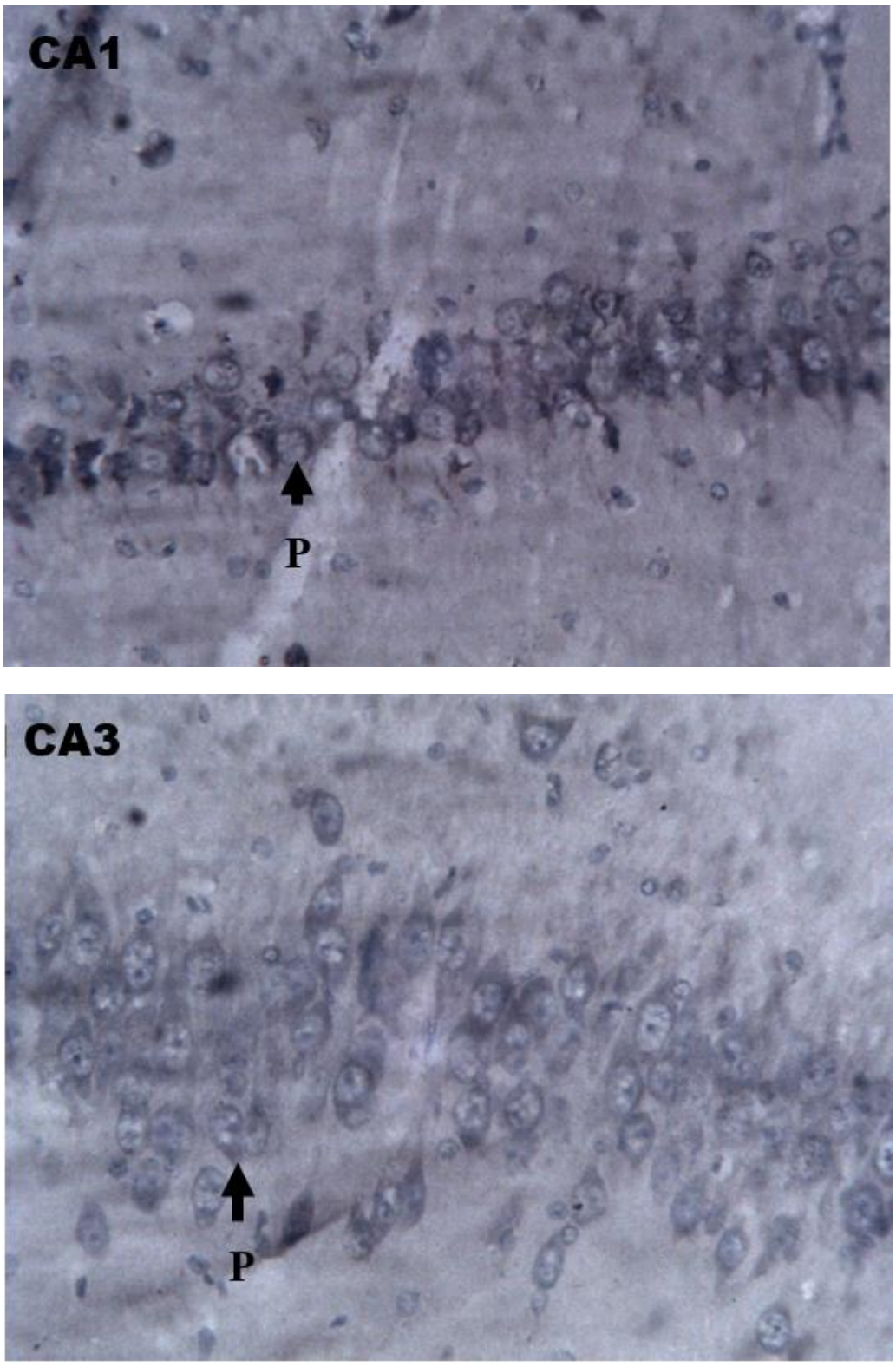


Plate 4.71: Section of Wistar rat hippocampal regions (CA1 and CA3) of Group I (300 mg/kg Eugenol) showing a normal ACAT-1 immunoreactivity of the Pyramidal cells of the hippocampal region when compared to Group V. (Pyramidal cell (P) (ACAT-1 x 250).

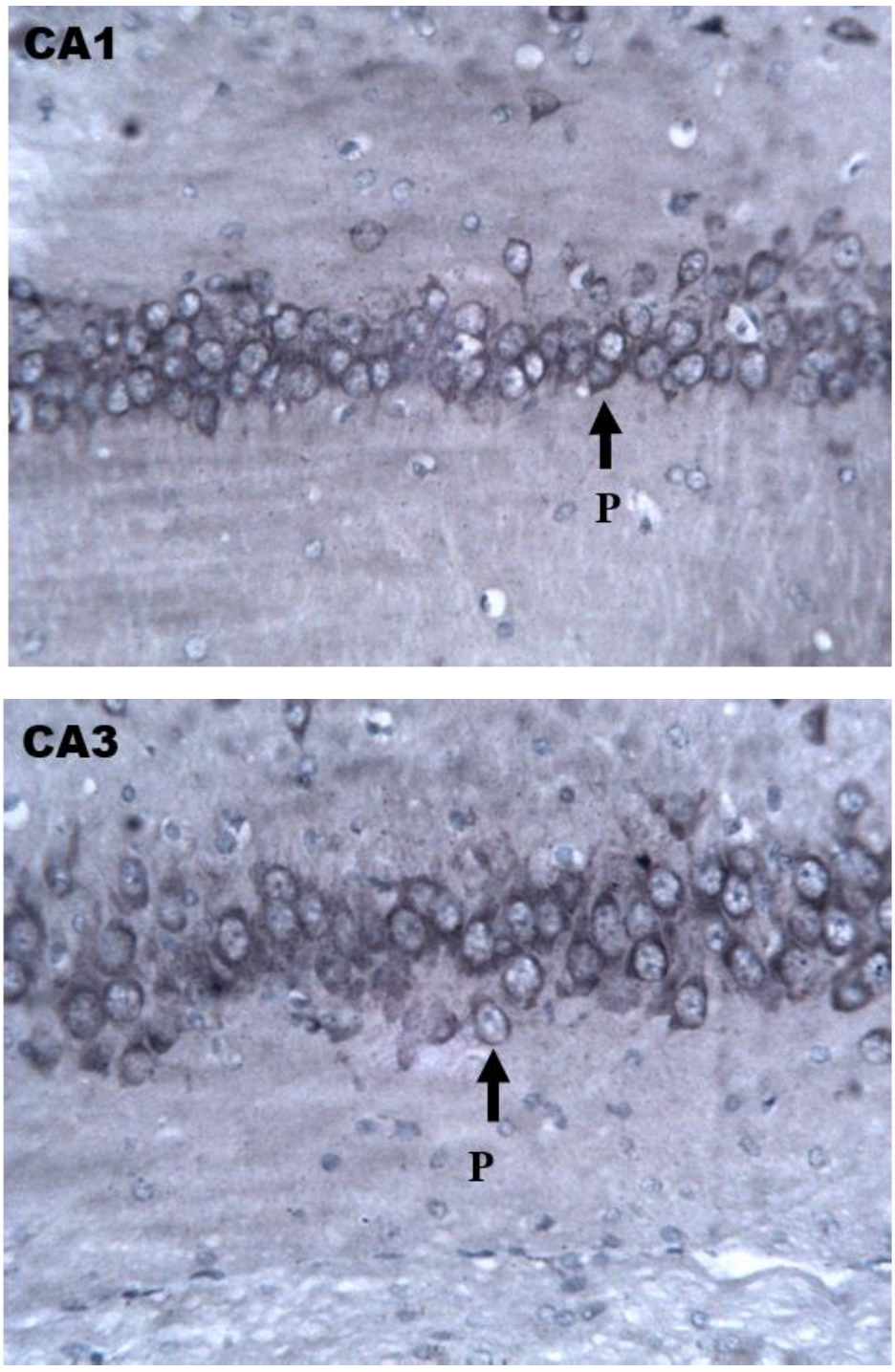


Plate 4.72: Section of Wistar rat hippocampal regions (CA1 and CA3) of Group II (150 mg/kg Eugenol) revealing a normal ACAT-1 immunoreactivity of the Pyramidal cells of the hippocampal region when compared to Group V. (Pyramidal cell (P) (ACAT-1 x 250).

4.5 Neurobehavioral Studies

A battery of neurobehavioral tests were conducted to assess a variety of endpoints, such as cognition, sensory-motor activity, and motor coordination in Wistar rats. Elevated plus maze (EPM) was used to assess anxiety-like behavior, transfer latency (TL) on EPM open arm to evaluate learning and memory; Morris water maze (MWM) for spatial learning and memory; forelimb grip strength (FGS) test to asses muscular strength in the forelimbs in rats.

4.5.1 Elevated plus Maze (EPM) Studies

In the elevated plus maze test, specific variables (time spent in open/close arms, grooming, rearing) were used to characterize the level of anxiety in rats.

4.5.1.1 EPM Open arm Duration

Open duration in EPM was used as a measurement of anxiety and was measured in seconds. Open arm duration of the control group (CTRL) showed a constant open arm duration from pretreatment through day 21. However administration of aluminium chloride resulted in significant ($p<0.05$) reduction in open arm duration on day 21. Co-administration of high dose eugenol and aluminium chloride (EGH+AC) resulted in a significant ($p<0.05$) increase in open arm duration when compared to aluminium treated group but was not significant ($p>0.05$) when compared to the control (CTRL) on day 21. Co-administration of eugenol at low dose and aluminium chloride (EGL+AC) open arm duration revealed a non-significant open arm duration when compared across the groups. Eugenol at high and low dose (EGH and EGL) resulted in an increase in open arm duration which was significant ($p<0.05$) on day 21 when compared to the aluminium treated group (AC). This is represented in **(Figure 4.5a).**

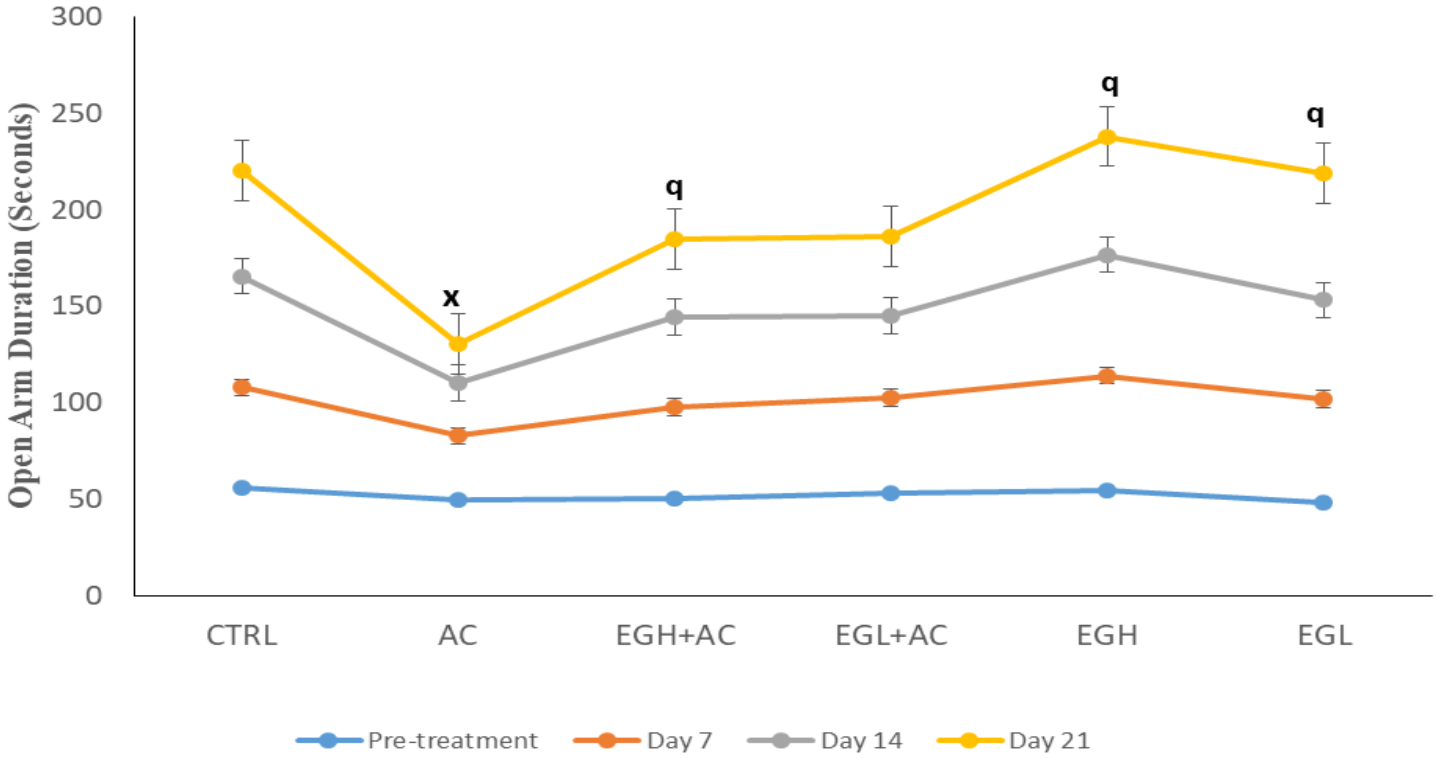


Figure 4.5a: Effect of Eugenol on Open arm duration (seconds) following administration of aluminium chloride.

n = 5; mean ± SEM; One way ANOVA with repeated measures, *LSD post hoc test* q = $p<0.05$; when compared with aluminium treated group (AC). x=$p<0.05$ compared with the control (CTRL) on day 21.

4.5.1.2 Modified Elevated Plus Maze (EPM) Close arm duration

Close arm duration was used as a measure of anxiety and was measured in seconds. Close arm duration before the commencement of this study (pretreatment), all rats had almost equal time spent in the open arm. Administration of aluminium chloride within the aluminium treated group (AC) resulted in a steady increase in open arm duration from day 7 to day 21. However, this increase was significant ($p<0.05$) on day 21 when compared to pre-treatment, when compared to day 21 within the control it was also found to be significant ($p<0.05$). Co-administration with high dose eugenol and aluminium chloride (EGH+AC) resulted in an decrease in close arm duration which was nonsignificant ($p>0.05$) when compared to control (CTRL) and aluminium treated group (AC). Co-administration of eugenol and aluminium chloride at low dose (EGL+AC) resulted in decrease in close arm duration on day 21 which was significant ($p<0.05$) when compared to day 21 in the aluminium treated group (AC) bu was nonsignificant ($p>0.05$) when compared to the control (CTRL).

Administration of high dose eugenol (EGH) only resulted in a significant ($p<0.05$) reduction in close arm duration on day 21 when compared to the aluminium treated group (AC) but non-significant ($p>0.05$) when compared to the control (CTRL), low dose eugenol (EGL), how ever resulted in significant ($p<0.05$) reduction in close arm duration on day 14 and 21 when compared to the aluminium treated group (AC). This is represented in Figure (Figure 4.5b)

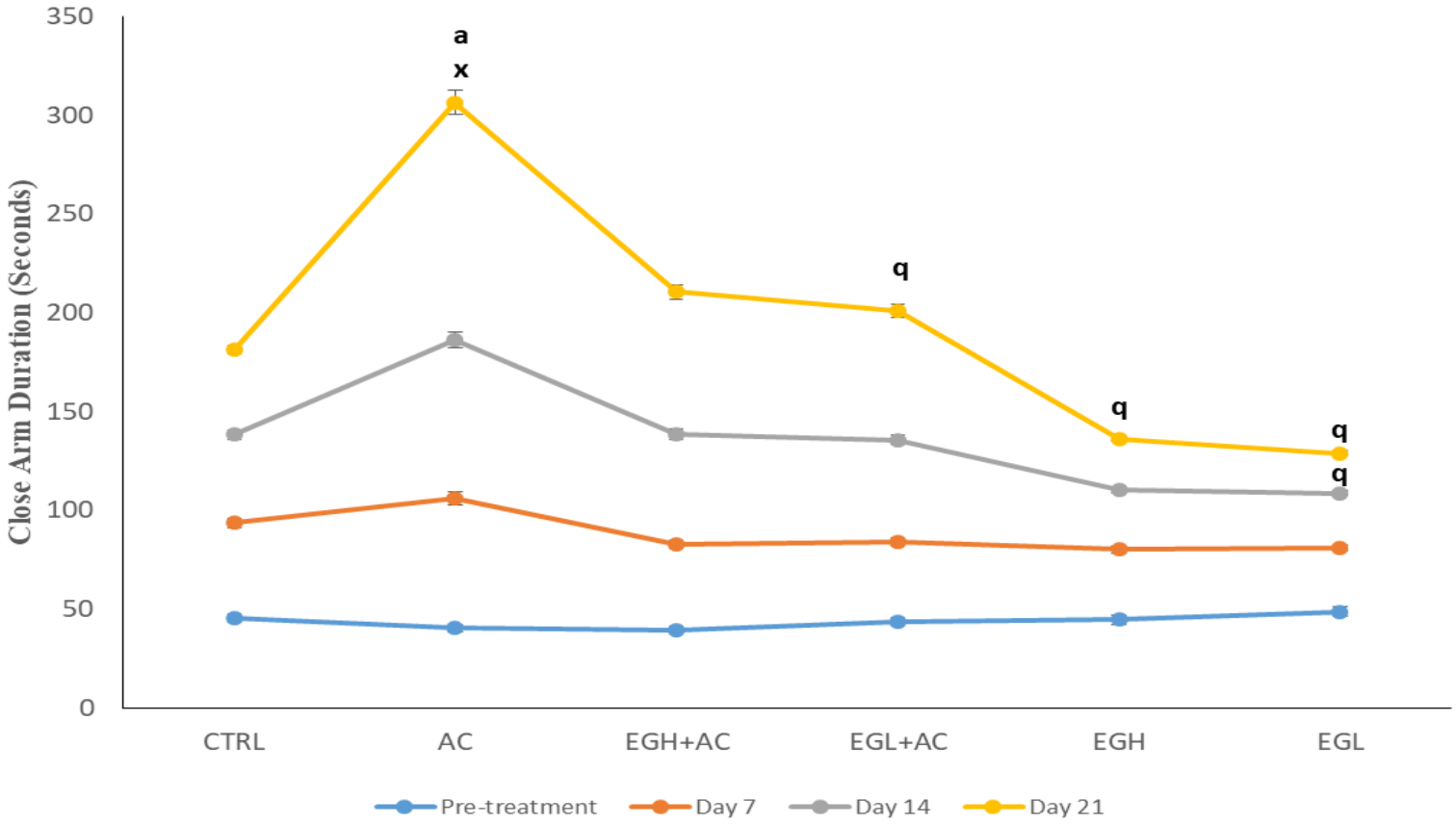


Figure 4.5b: Effect of Eugenol on Close arm duration following administration of aluminium chloride

n = 5; mean ± SEM; One way ANOVA with repeated measures, *LSD post hoc test*, a= $p<0.05$; when pretreatment is compared with day 21; q=$p<0.05$ when compared with aluminium treated group (AC) on day 14 and 21; x=$p<0.05$ when the AC treated group is compared to the control (CTRL).

4.5.1.3 Modified Elevated Plus Maze (EPM) Rearing Frequency

Rearing is an anxiety-like activity that occurs in the open arm. Rearing in the control (CTRL) was constant from pre-treatment to day21. Administration of aluminium chloride within the aluminium treated group (AC) resulted in a reduction in rearing frequency. Comparing pre-treatment within the AC group compared to day 21 resulted in a significant ($p<0.05$) reduction this reduction was significant ($p<0.05$) on day 21 when compared to day 21 in the control. Co-administration of eugenol at high dose and aluminium chloride (EGH+AC) resulted in a nonsignificant ($p>0.05$) difference across day 7 to day 21 and also non-significant when compared to control (CTRL) and aluminium treated Group (AC). Co-administration with low dose eugenol and aluminium chloride (EGL+AC) however resulted in significant ($p<0.05$) rearing frequency on day 14 when compared to pretreatment but not significant ($p>0.05$) when compared to control (CTRL) and aluminium treated groups (AC). Administration of eugenol at high and low dose (EGH and EGL), respectively, resulted in an increase in rearing frequency within the open arm and this increase was significant ($p<0.05$) on day 21 when compared to pre-treatment and also significant when compared to aluminium treated group on day 21. The increase observed on other days was not statistically significant when compared to pretreatment or when compared to the control group (CTRL) and aluminium treated group (AC). This is represented in Figure 4.5c.

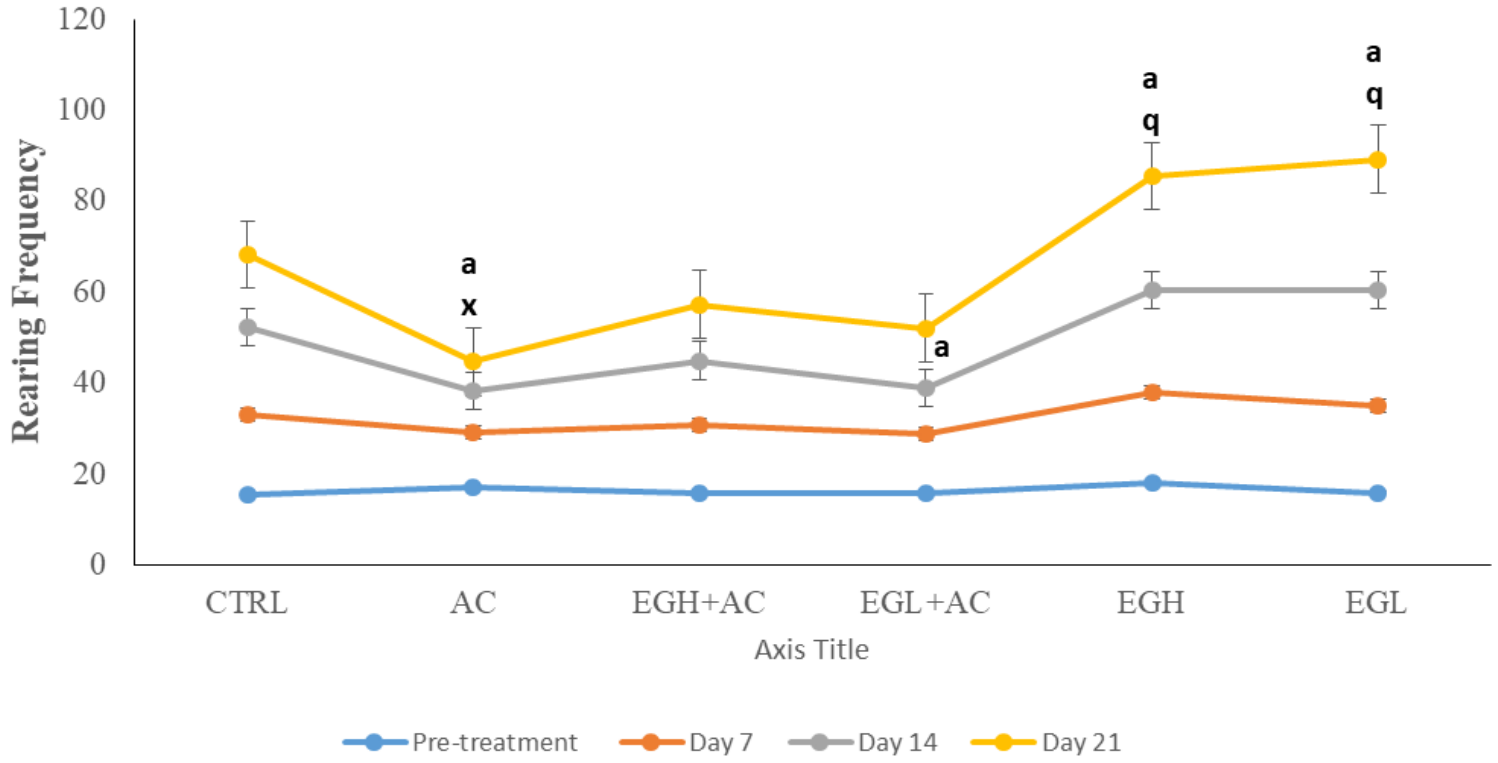


Figure 4.5c: Effect of Eugenol on rearing frequency in elevated plus maze following administration of aluminium chloride.

n = 5; mean ± SEM; One way ANOVA with repeated measures, *LSD post hoc test* a=p<0.05 when pre-treatment is compared to day 21; q=p<0.05 when compared with Aluminium treated group on day 21; x=q<0.05 when AC group is compared to the control (CTRL) group.

4.5.1.4 Grooming (cephalocaudal axis)

Grooming In the cephalocaudal axis was at almost the same frequency across all groups before the commencement of this study. Administration of aluminium chloride (AC), however, resulted in a steady decline in grooming frequency along the cephalocaudal axis. On day21, this reduction was significant ($p<0.05$) when compared to pretreatment and when compared to day 21 in the control group. Co-administration of eugenol at high dose and aluminium chloride (EGH+AC) revealed a significant ($p<0.05$) increase in grooming frequency (cephalocaudal axis) on day 21 when compared to day 21 of the aluminium treated group (AC). Co-administration of eugenol at low dose and aluminium chloride (EGL+AC) revealed a significant ($p<0.0s$) increase in grooming frequency (cephalocaudal axis) on day 21 when compared to ay 21 of the aluminium treated group (AC). Administration of eugenol at high dose (EGH) resulted in a steady increase in grooming frequency along the cephalocaudal axis, however this increase was significant on day 21 when compared to day 21 of control (CTRL). At low dose eugenol, EGL, also revealed a similar pattern of steady increase in grooming frequency. However, on day 21, this increase was found to be significant as shown in **Figure 4.5d.**

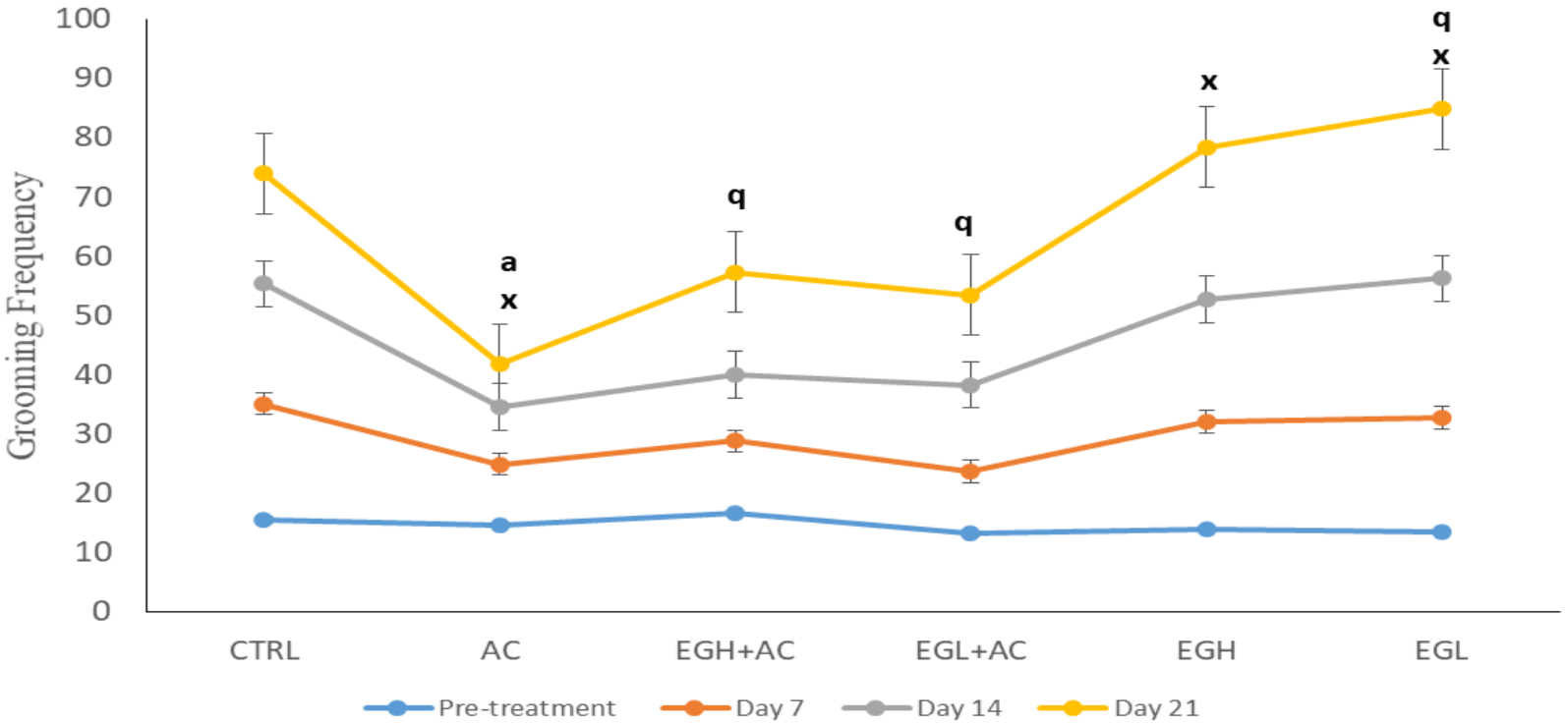


Figure 4.5d: Effect of Eugenol on Grooming following administration of aluminium chloride in Wistar rats elevated

n = 5; mean ± SEM; One way ANOVA with repeated measures, *LSD post hoc test* a=p<0.05 when pre-treatment is compared to day 21; q=p<0.05 when compared with Aluminium treated group on day 21; x=q<0.05 when AC group is compared to the control (CTRL) group.

4.5.1.5 Forelimb grip Strength Time (FGST)

Forelimb grip strength test was used as a measure of muscular strength in the forelimbs (forepaws) of the Wistar rats. Forelimb grip strength time (latency time to release grip) reflects the FGS. Foregrip strength time within the control (CTRL) group revealed an almost similar FGST from pretreatment to day-21. However administration of aluminium chloride resulted in a reduction in FGST within the aluminium treated group (AC), which was significant on day 14 when compared to pretreatment. However co-administration of eugenol at high dose with aluminium chloride (EGH+AC) resulted in a significant ($p<0.05$) increase in FGST when day 14 were compared to pretreatment and also was was found to be significant ($p<0.05$) when compared to the control on day 14. Co-administration of eugenol at low dose with aluminium chloride (EGL+AC) resulted in a non-significant increase in FGST when compared to pretreatment to day-14.

However, on day 21, FGST was found to be significant ($P<0.05$) when compared to pretreatment, when compared to control on day-21 and aluminium treated group (AC) on day-21. Administration of eugenol at high dose resulted in a steady increase in FGST which was however significant ($p<0.05$) on day 21 when compared to pre-treatment, was also significant ($p<0.05$) when day 21 were compared to day 21 in the aluminium treated group and also significant ($p<0.05$) when compared to day 21 of the control group. Eugenol at low dose (EGL) revealed a steady increase in the FGST which was significant ($p<0.05$) on day-14 when compared to pretreatment and also significant ($p<0.05$) when compared to day 14 of the control. On day 21, there was a significant ($p<0.05$) when pretreatment were compared to day 21 and

comparing day 21 on control (CTRL) and aluminium treated group (AC) showed a significant difference($p<0.05$)**(Figure-4.5e).**

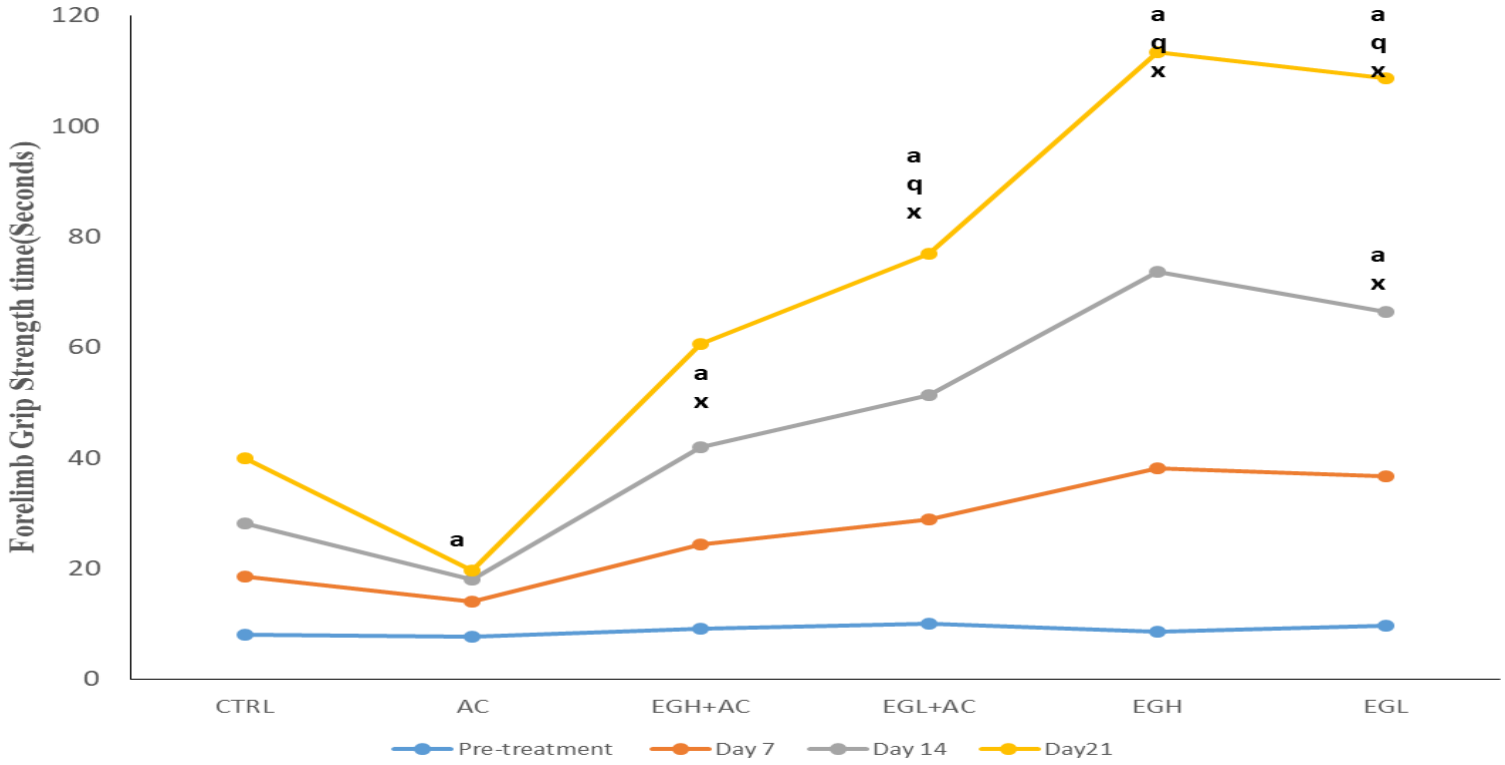


Figure 4.5e: Effect of Eugenol on Forelimb grip strength following exposure to aluminium chloride in Wistar rats

n = 5; mean ± SEM; Paired sample t-test, a, b and c = $p<0.05$ when compared with pre-treatment. Repeated measure ANOVA LSD post hoc test, x = $p<0.05$ when compared with the control (at day-14).

4.5.1.6 Morris Water Maze Studies (MWM)

Morris Water, a well validated test for spatial learning and memory, was used to assess learning and memory in experimental animals (Wistar rats). Performance in the training/habituation sessions revealed reduced latency (latency time) to find the hidden platform day-1 to day-4 of the training sessions (Figure 4.5f).

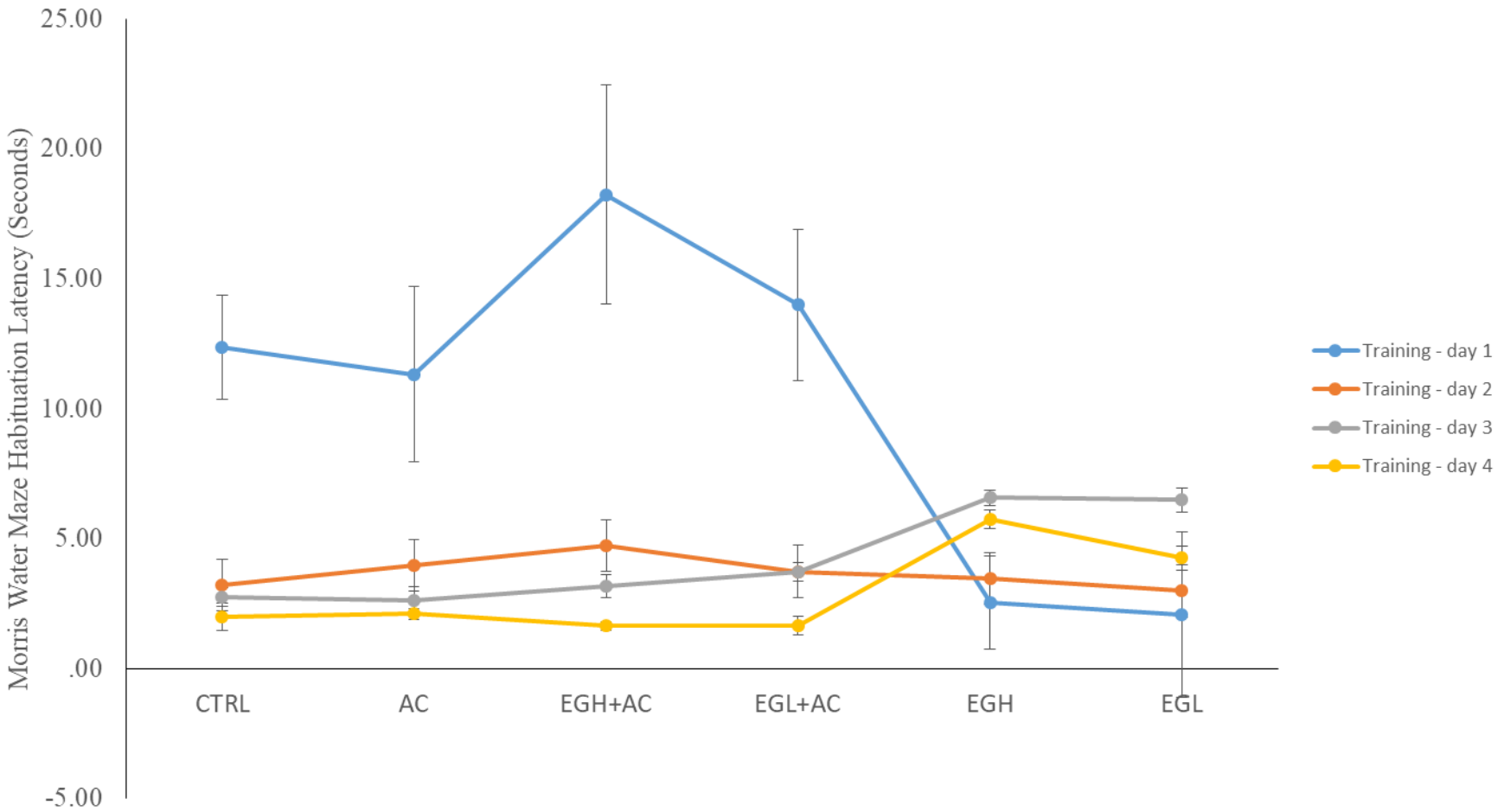


Figure 4.5f: Transfer Latency of Wistar rats on Morris water maze habituation.

Figure 4.5f reveals the training latency time in seconds for rats spanning a four-day period. Day one shows the time taken for rats to locate the escape platform (latency time). From days 2, 3 and 4 shows a reduced latency time across all groups and similar time taken to find the escape platform. **Figure 4.5g** reveals latency time to locate the escape platform at pretreatment, days-7, 14, and 21. Pre-treatment latency times across all groups are similar before commencement of the study. However on day 7 there was a significant ($p<0.05$) increase in latency time in the aluminium (AC) treated group when day-7 were compared to pretreatment. In the aluminium treated group (AC) on day-14, there was a significant ($p<0.05$) increase in latency time when day-14 were compared to pre-treatment and also significant ($p<0.05$) when compared to day- 14 in control (CTRL). Latency time on day-21 for AC treated group was found to be nonsignificant when compared to pretreatment and when compared to day-21 on control (CTRL) group.

Co-administration of high dose eugenol and aluminium chloride (EGH+AC) revealed a significant ($p<0.05$) reduction in latency time when pretreatment were compared to day-21, however this reduction was not significant ($p>0.05$) when compared to the control. Co-administration of eugenol at low dose and aluminum chloride (EGL+AC) resulted in a significant ($p<0.05$) increase in latency time on day-7 when compared to pretreatment but was not significant ($p>0.05$) when compared to the control (CTRL). On day 14 however, there was a nonsignificant ($p>0.05$) increase in latency time. On day 21, there was a significant reduction in latency time when day 21 were compared to pretreatment.

Latency time for eugenol high dose (EGH) was not significant ($p>0.05$) when day7, 14 and 21 were compared to pre-treatment and when compared to the control.

Administration of low dose eugenol (EGL) there was a significant increase ($p<0.05$) on day 14 when compared to pretreatment but not significant when compared to control (CTRL) and aluminium treated group (AC).

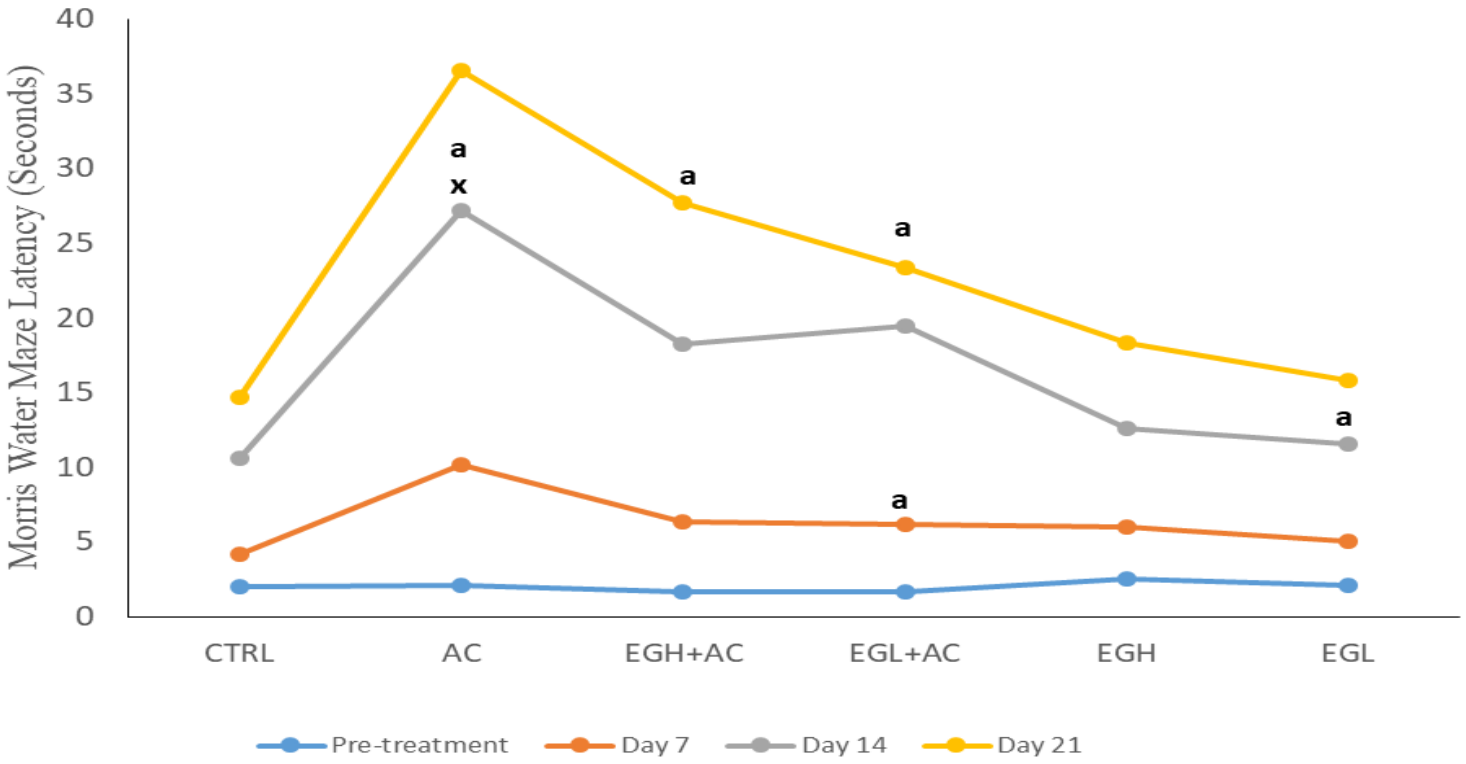


Figure 4.5g: Effect of Eugenol on Cognition (Morris water maze) following administration of aluminium chloride.

n = 5; mean ± SEM; Paired sample t-test, a = $p<0.05$ b = $p<0.01$; c = $p<0.001$ when compared with pre-treatment. One way ANOVA LSD post hoc test, x = $p<0.05$ when compared with the control (at day-14).

4.6 Neurochemical and Biochemical Studies

Neurochemical analysis for metal estimation was assessed for the concentration of neuro-trace elements (Iron, Fe; Manganese, Mn; Magnesium, Mg; and Aluminium) in the tissue (brain) homogenate.

Biochemical analysis for lipid peroxide levels and antioxidant enzyme activity (malondialdehyde, MDA; superoxide dismutase, SOD; catalase CAT; glutathione peroxidase GPx) were assessed using brain homogenate and endogenous enzymatic activity of acetylcholinesterase.

4.6.1 Neurochemistry of Neuro-trace Elements

A Significantly ($p<0.05$) reduced level of Iron (Fe) concentration in the brain tissue of rats was observed in the aluminium-treated (AC) group when compared to the control (CTRL).

Eugenol treated groups (EGH, EGL, EGH+AC, EGL+AC) showed a significantly ($p<0.05$) increased level of Iron when compared to aluminium treated group (AC). A nonsignificant ($p>0.05$) increase was observed in EGH and EGL when compared to control (CTRL) **(Figure 4.6a).**

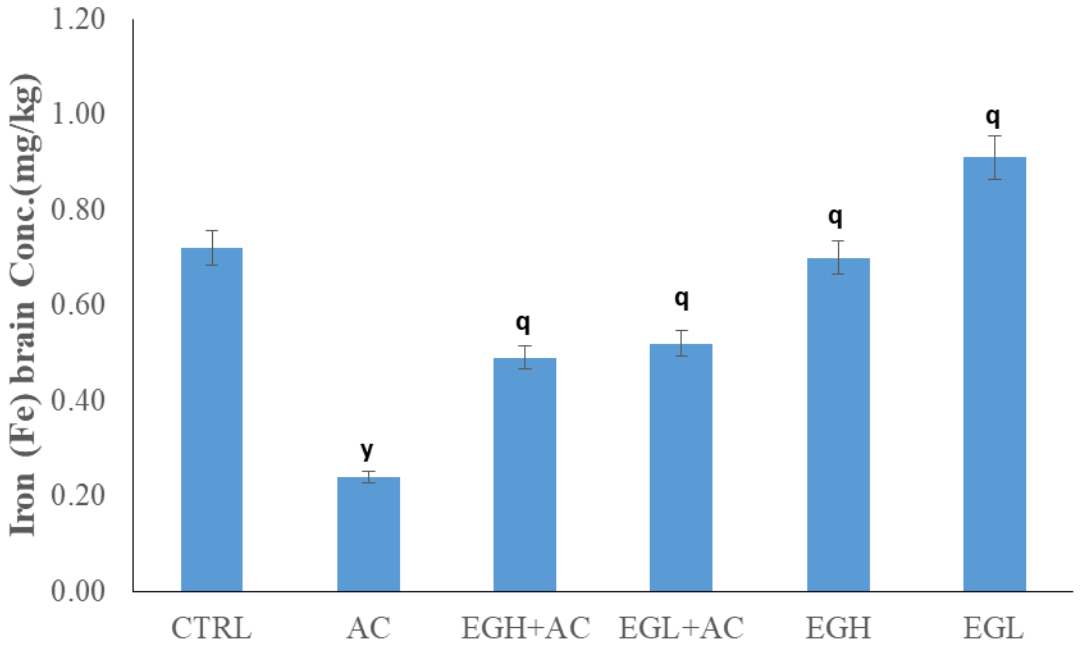


Figure 4.6a: Effect of Eugenol on Neurotrace Brain element (Iron Fe) following administration of aluminium chloride on Wistar rats.

n = 5; mean ± SEM One way ANOVA *LSD post hoc test*: q= $p<0.05$ when compared with aluminium chloride (AC) treated group. x=$p<0.05$ when aluminium (AC) treated group is compared to control (CTRL) group.

Manganese (Mn) levels in EGH and EGL shows a non-significant ($p>0.05$) reduced Mn level when compared to the control (CTRL), but EGH+AC and EGl+AC revealed slightly elevated Mn levels which was not significant ($p>0.05$) when compared to the control. Alumiumium treated group (AC) showed a significant ($p<0.05$) increase in the levels of Mn when compared to the control (CTRL). This is represented in **Figure 4.6b.**

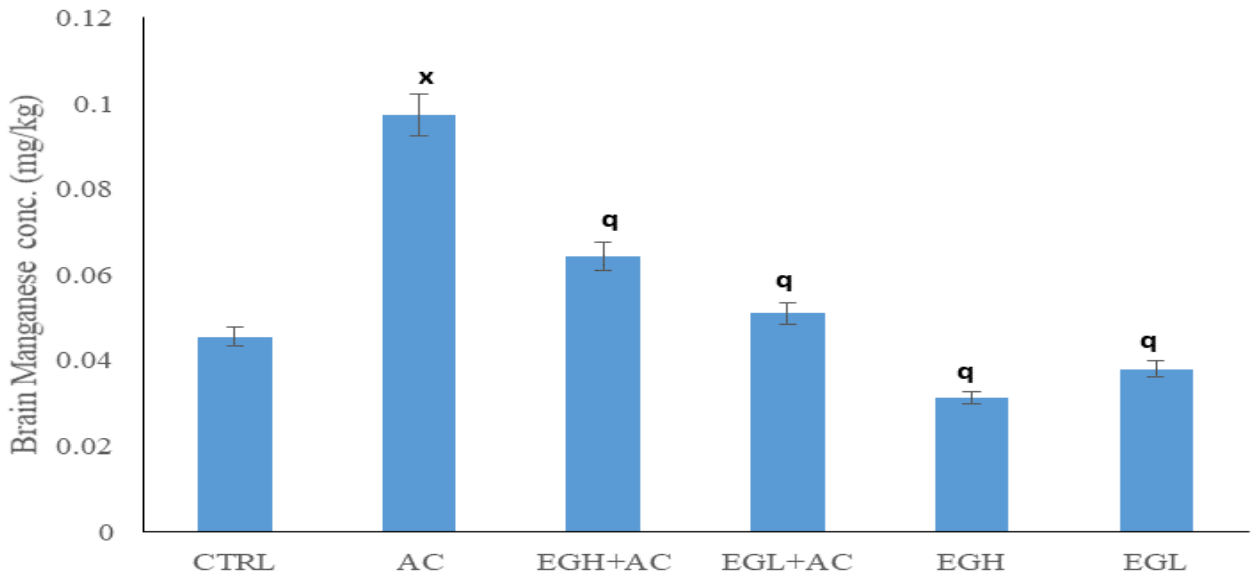


Figure 4.6b: Effect of Eugenol on Neurotrace Brain element (Manganese Mn) following administration of aluminium chloride on Wistar rats.

n = 5; mean ± SEM One way ANOVA *LSD post hoc test*: q= $p<0.05$ when compared with aluminium treated (AC) group. x=$p<0.05$ when compared to the control (CTRL) group.

Significantly ($p<0.05$) reduced level of Magnesium was observed in the aluminium treated group when compared to the control (Group V). In the Eugenol the salvaged groups (EGH+AC and EGL+AC) revealed a significant ($p<0.05$) increase in magnesium level when compared to AC. EGH and EGL also revealed a nonsignificant ($p>0.05$) increase in Magnesium levels when compared to control (CTRL). This is represented in **figure 4.**6c.

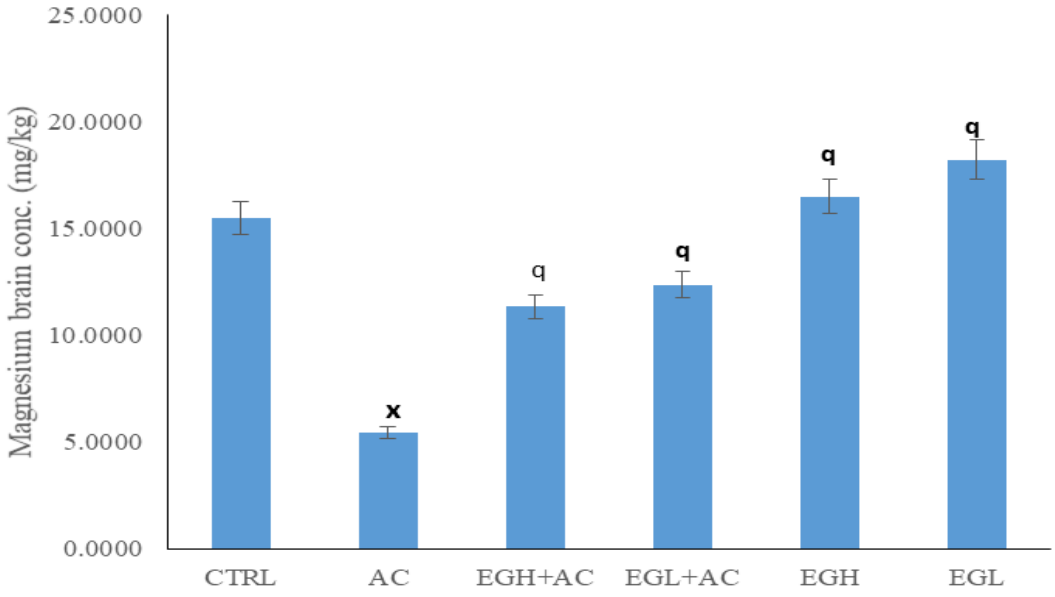


Figure 4.6d: Effect of Eugenol on Neurotrace Brain element (Magnesium Mg) following administration of aluminium chloride on Wistar rats

n = 5; mean ± SEM One way ANOVA *LSD post hoc test*: q= $p<0.05$; x=$p<0.05$ when compared with aluminium chloride (AC) and the control group respectively.

Aluminium (Al) concentration levels was significantly ($p<0.05$) elevated when the aluminium treated (AC) group is compared to the control (CTRL). Co-administration of eugenol in the EGH+AC and EGL+AC resulted in a significant ($p<0.05$) reduction of aluminium levels when compared to the AC and control group, respectively as shown in **figure 4.6d.**

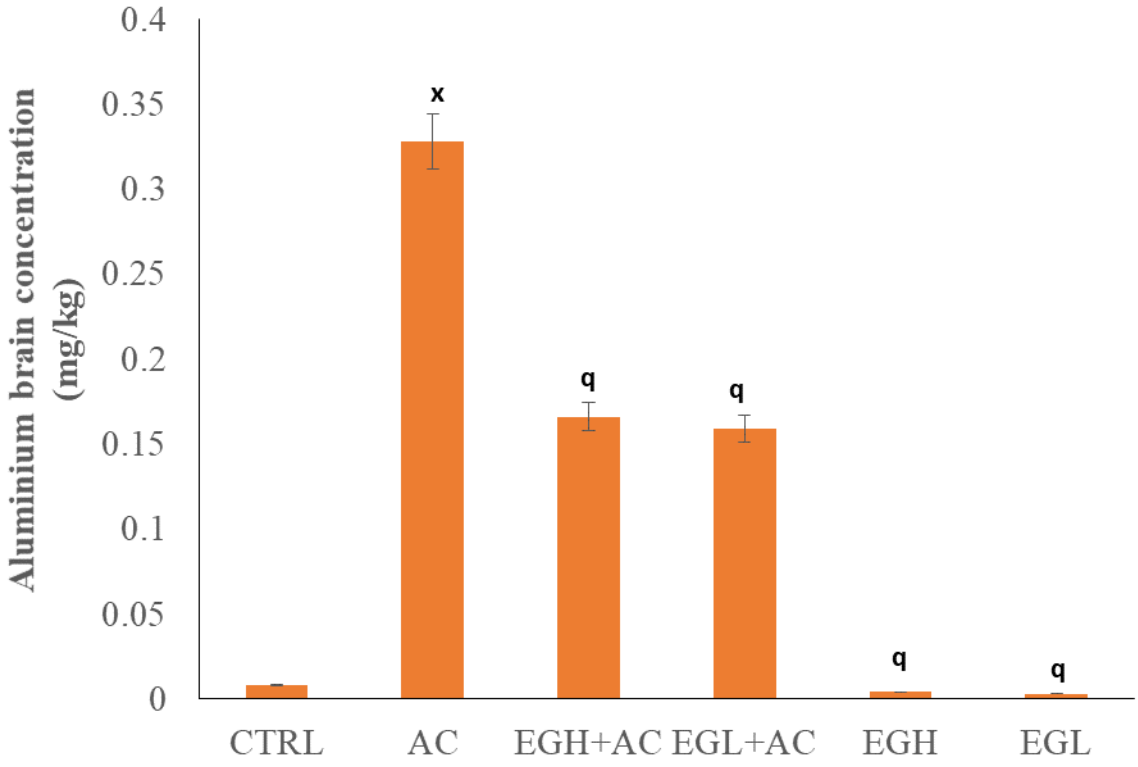


Figure 4.6c: Effect of Eugenol on accumulation of aluminium in the Brain element following administration of aluminium chloride on Wistar rats.

n = 5; mean ± SEM One way ANOVA *LSD post hoc test*: q= $p<0.05$; x= $p<0.05$ when compared with the aluminium chloride (AC) and the control group respectively.

4.6.2 Biochemistry of Lipid Peroxide Levels and Antioxidant Enzyme Activity

The malondialdehyde (MDA) or thiobarbituric acid-reactive –substances (TBARS) assay was used to estimate the lipid peroxidation levels, while antioxidant enzymatic activity was estimated by assaying for superoxide dismutase (SOD), catalase (CAT), and glutathione peroxidase (GPx) activities in brain tissue.

Tissue MDA activity levels in CTRL, AC, EGH,+AC, EGL+AC, EGH and EGL were 334.05 ± 18.12, 684.28 ± 15.21, 405.43 ± 19.08, 382.64 ± 21.21, 300.56 ± 20.01 and 285.59 ± 17.01 respectively. This result showed a significant ($p<0.05$) increase activity levels of MDA in aluminium treated group AC when compared with the control group (CTRL). Co-administration of eugenol and aluminium chloride (EGH+AC, EGL+AC) revealed a significant ($p<0.01$) reduction in the tissue levels of MDA when compared to aluminium treated group (AC). This was however not significant ($p>0.05$) when compared to the control (CTRL). Administration of eugenol only (EGH and EGL) resulted in significant ($p<0.05$) reduced tissue activity of MDA when compared to the aluminium treated group (AC). This reduction was nonsignificant when compared to the control (CTRL) group. This is presented in **figure 4.6e.**

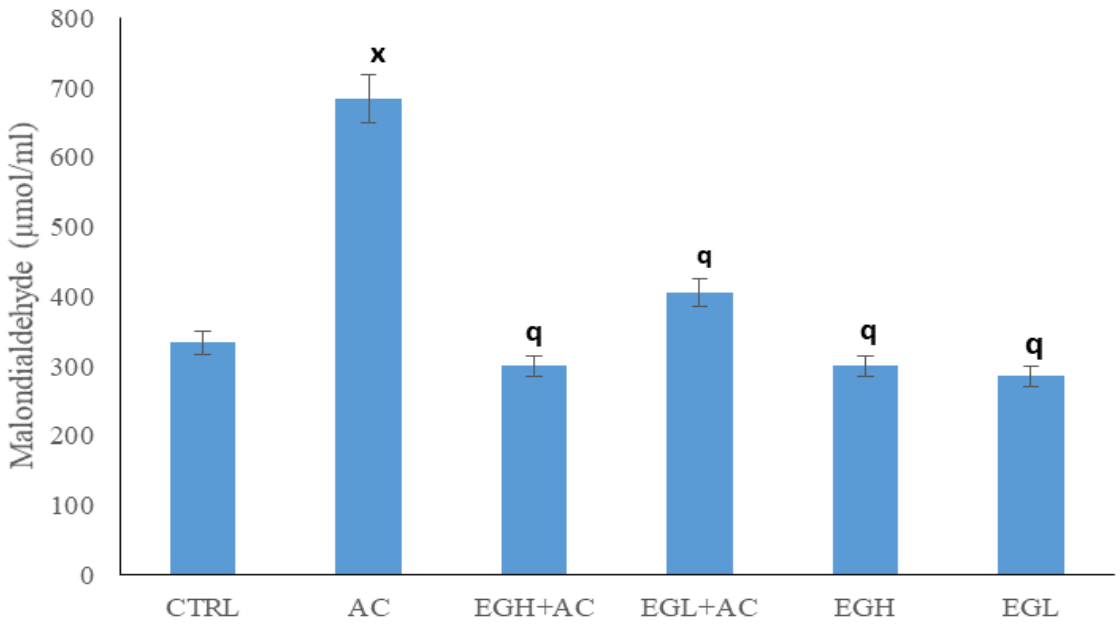


Figure 4.6e: Effect of Eugenol on tissue (brain) MDA concentration following administration of aluminium chloride in Wistar rats.

n = 5; mean ± SEM One way ANOVA *LSD post hoc test*: q=p<0.05; when compared with aluminium treated group (AC). x=p<0.05 when AC is compared to the control (CTRL).

Tissue SOD activity levels in CTRL, AC, EGH+AC, EGL+AC, EGH and EGL were 2.09 ± 0.25, 0.82 ± 0.29, 1.45 ± 0.22, 1.66 ± 0.33, 3.95 ± 0.57 and 3.17 ± 0.45, and respectively. This result shows a significant ($p<0.05$) reduction in the activity levels of SOD in the aluminium treated group (AC) when compared to the control group (CTRL). Co-administration of eugenol and aluminium chloride (EGH+AC, EGL+AC) resulted in significant ($p<0.05$) increase in tissue activity of SOD when compared to the aluminium treated group (AC). Administration of eugenol only (EGH and EGL) resulted in a significant ($p<0.05$) elevation in the tissue activity of SOD when compared to control (CTRL) and aluminium treated groups (AC). This is presented in **figure 4.6f**

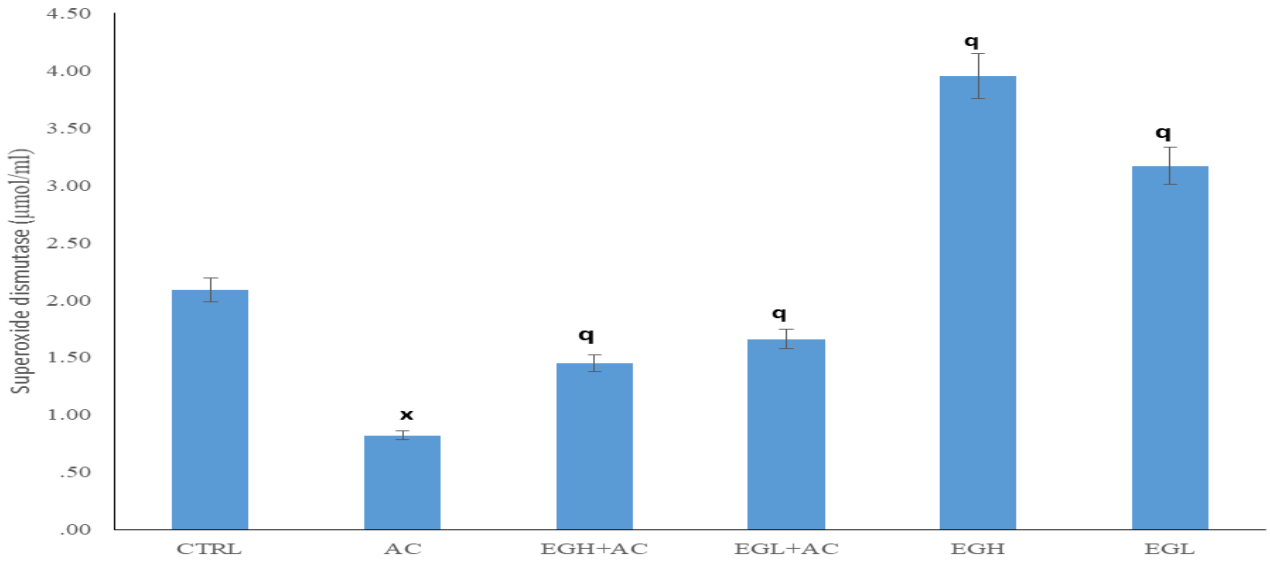


Figure 4.6f: Effect of Eugenol on tissue (brain) SOD concentration following administration of aluminium chloride in Wistar rats.

n = 5; mean ± SEM One way ANOVA *LSD post hoc test*: q = $p<0.05$; when compared with aluminium (AC) treated group (AC) x=$p<0.05$ when compared with the control (CTRL)

Tissue CAT activity levels in CTRL, AC, EGH+AC, EGL+AC, EGH and EGL were42.46 ± 4.21, 15.09 ± 3.58, 27.46 ± 3.21, 25.49 ± 3.02, 45.68 ± 3.45 and 50.90 ± 4.17 respectively. This result shows a significant ($p<0.05$) reduction in the activity levels of CAT in the aluminium treated group (AC) when compared to the control group (CTRL). Co-administration of eugenol and aluminium (EGH+AC) resulted in a significant ($p<0.05$) increase in the tissue activity of catalase when compared to the AC group, however this increase was not significant in the EGL+AC group when compared to the AC group. Administration of eugenol only (EGH and EGL) resulted in significant ($p<0.05$) increased tissue activity of CAT when compared to the AC group but was nonsignificant ($p>0.05$) when compared to the control group (CTRL). This is presented in **figure 4.6g.**

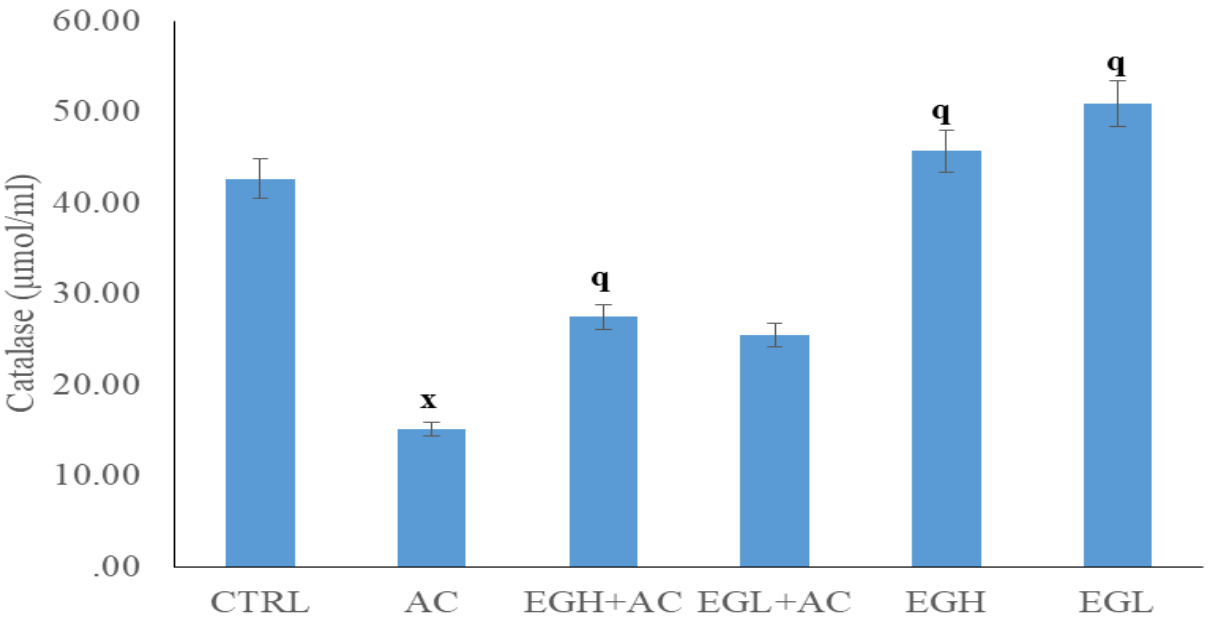


Figure 4.6g: Effect of Eugenol on tissue (brain) CAT concentration following administration of aluminium chloride in Wistar rats.

n = 5; mean ± SEM One way ANOVA *LSD post hoc test*: q = $p<0.05$ when compared with aluminium treated group (AC). x=$p<0.05$ when the aluminium treated group (AC) is compared to the control.

Tissue GPx activity levels in CTRL, AC, EGH,,,,+AC, EGL+AC, EGH and EGL were 35.10 ± 1,.83, 15.98 ± 2.61, 27.10 ± 2.98, 29.65 ± 0.44, 35.57 ± 1.85 and 40.98 ± 4.78 respectively. This result shows a significant ($p<0.05$) reduction in the activity levels of CAT in the aluminium treated (AC) group when compared to the control (CTRL). Co-administration of eugenol and aluminium chloride (EGH+AC, EGL+AC) resulted in a significant ($p<0.05$) increase in tissue activity of GPx when compared to the AC group. This increase was however not significant ($p>0.05$) when compared to the control. Administration of eugenol only (EGH and EGL) resulted in a significant ($p<0.05$) increase in tissue activity of GPx when compared to the AC group but non-significant ($p>0.05$) when compared to the control (CTRL) group.This presented in figure (**Figure 4.6h)**.

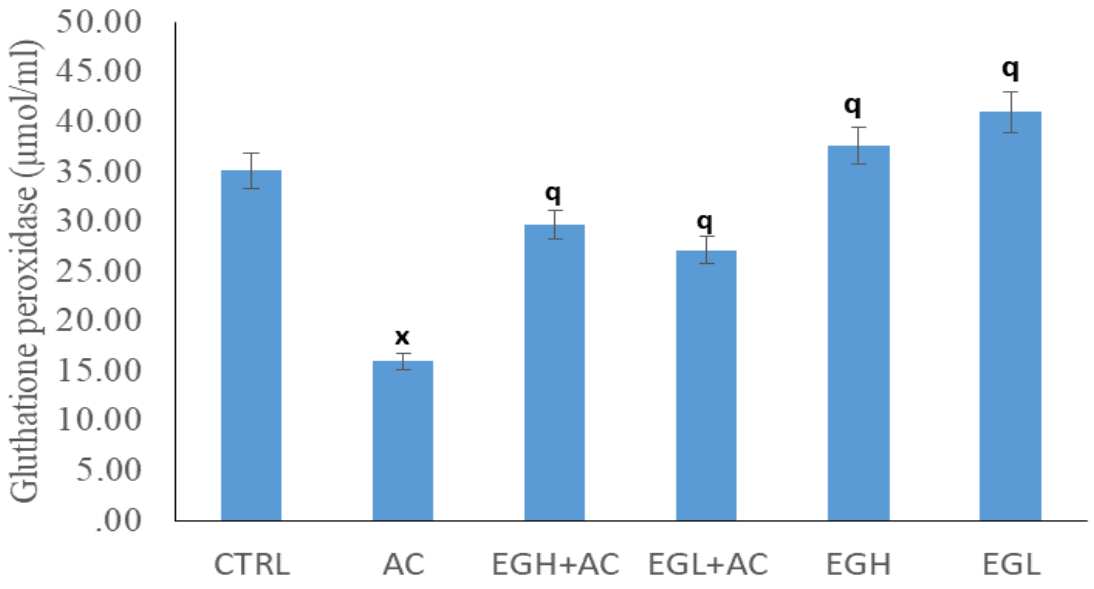


Figure 4.6h: Effect of Eugenol on tissue (brain) GPx concentration following administration of aluminium chloride in Wistar rats.

n = 5; mean ± SEM One way ANOVA *LSD post hoc test*: q = $p<0.05$ when compared with aluminium treated group (AC). x=$p<0.05$ when the aluminium treated group (AC) is compared to the control.

4.6.3 Intramitochondrial accumulation of 8-Hydroxy-2-deoxyguanosine (8-OHdG)

The Intramitochondrial accumulation of 8-OHdG is used as a biomarker to assess oxidative damage to mtDNA within biological systems. In this study, administration of aluminium chloride resulted in a significant ($p<0.05$) increase in the levels of 8-OHdG when compared to the control (CTRL). However co-administration of eugenol with aluminium chloride (EGH+AC and EGL+AC) significantly ($p<0.05$) prevented the increase in the tissue level of 8-OHdG. Within the group administered eugenol only (EGH and EGL), levels of 8-OHdG was significantly ($p<0.05$) reduced when compared with the aluminium (AC) treated group but these levels resulted in nonsignificant ($p>0.05$) levels when compared to the control. This is represented in **Figure 4.7.**

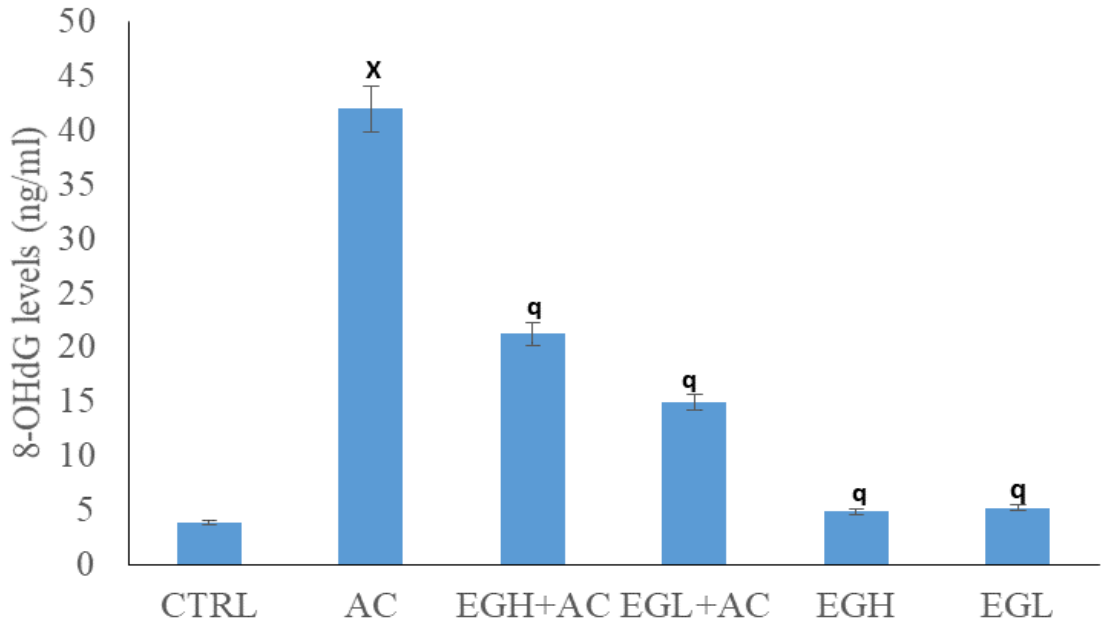


Figure 4.7: Effect of eugenol on intramitochondrial accumulation of 8-OHdG levels following exposure to aluminium chloride (AC).

n=5 mean ± SEM One way ANOVA *LSD post hoc test* q=$p<0.05$ when compared with the aluminium chloride treated group. x=$p<0.05$ when compared with the control (CTRL).

4.6.4 Effect of Eugenol on Caspase- 3 proteins following administration of aluminium chloride.

Caspase-3 is known as an executioner caspase in apoptosis because of its role in coordinating the destruction of cellular materials such as DNA fragmentation. In this study, administration of aluminium chloride resulted in significant ($p<0.05$) levels of apoptosis inducing caspase-3 when compared to the control. Co-administration of eugenol and aluminium chloride (EGH+AC) resulted in a non-significant ($p>0.05$) reduction of caspase-3 levels when compared to the AC treated group. Co-administration of eugenol with aluminium chloride at low dose (EGL+AC) resulted to a significantly ($p<0.05$) reduced level of caspase-3 levels when compared to the aluminium treated group (AC) and control (CTRL). Tissue level of caspase-3 in the group administered eugenol only (EGH and EGL) was found to be significant ($p<0.05$) when compared to the aluminium treated (AC) group. Comparison with the control, however, was found not to be significant ($p>0.05$) when compared to the control (CTRL). This is represented on **figure 4.8.**

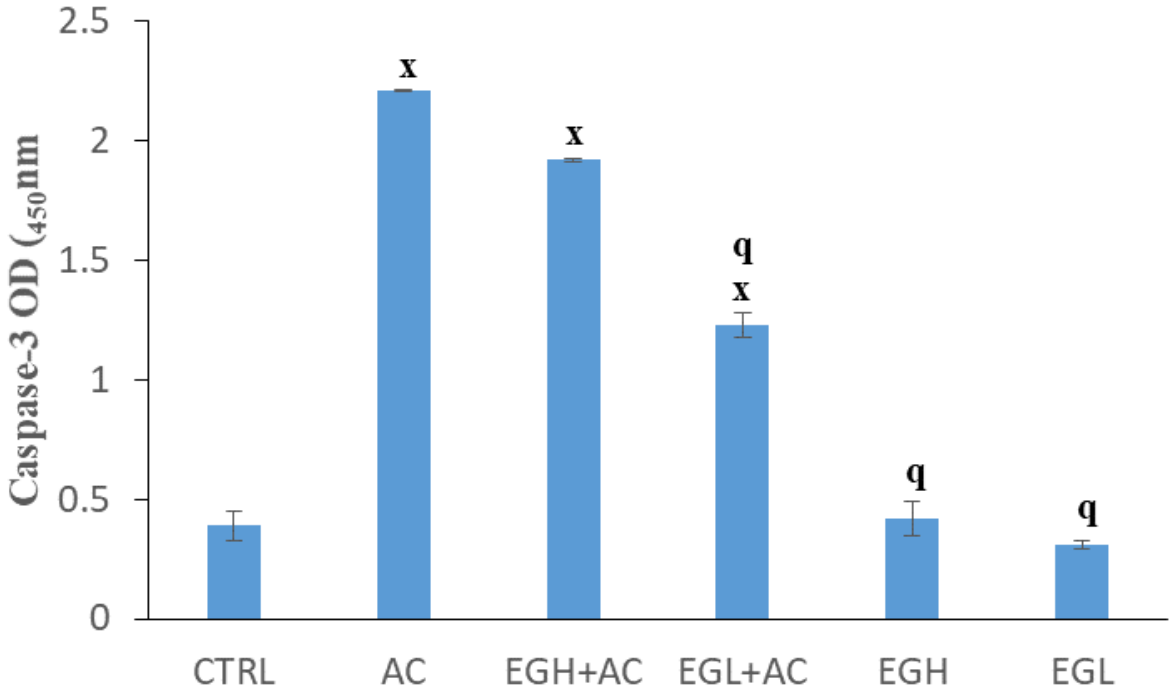


Figure 4.8: Effect of eugenol on brain caspase-3 levels following administration of aluminium chloride in Wistar rats.

n = 5; mean ± SEM One way ANOVA *LSD post hoc test:* q=p<0.05; when compared to the aluminium (AC) treated group. x=p<0.05; when compared to the control (CTRL).

4.6.5 Effect of Eugenol on proapoptotic (Bax) and antiapoptotic (Bcl-2) protein following administration of aluminium chloride.

In this study, administration of aluminium chloride resulted in significant ($p<0.05$) increased levels of proapoptotic protein Bax when the aluminium treated group (AC) is compared to control (CTRL). Co-administration of eugenol and aluminium chloride (EGH+AC and EGL+AC), resulted in a significant ($p<0.05$) reduction in the levels of Bax when compared to the control (CTRL) and aluminium treated group (AC). Tissue level of Bax was however significant ($p<0.05$) when compared to the aluminium treated group (AC) and a non-significant ($p>0.05$) when compared to the control. Administration of aluminium chloride also resulted to a significant ($p<0.05$) reduction in the tissue levels of antiapoptotic protein (Bcl-2) when the aluminium treated group (AC) is compared to the control (CTRL). Co-administration of euenol and aluminium chloride (EGH+AC) in high dose resulted in a nonsignificant ($p>0.05$) increase when compared to the aluminium treated group (AC) but significant ($p<0.05$) when compared to the control (CTRL). Co-administration of eugenol at low dose with aluminium chloride (EGL+AC) resulted in significant ($p<0.05$) increase in tissue levels of Bcl-2 when compared to the aluminium treated (AC) and control (CTRL) group. In the group administered eugenol at high and low dose (EGH and EGL), levels of Bcl-2 was significant ($p<0.05$) when compared to the aluminium treated group (AC) but non-significant ($p>0.05$) when compared to the control (CTRL).

Bax/Bcl-2 ratio reveals the susceptibility of a cell to apoptosis. In this study administration of aluminium chloride resulted significant ($p<0.05$) elevated Bax/Bcl-2 ratio when compared to the control. Co-administration of eugenol and aluminium chloride at low and high doses (EGH+AC and EGL+AC) reduced the ratio of Bax/Bcl-2 and these leves was significant ($p<0.05$) when

compared to both aluminium treated (AC) and control (CTRL) groups respectively. Administration of Eugenol only at high and low dose (EGH and EGL) resulted in a Bax/Bcl-2 ratio level that was significant ($p<0.01$) when compared to the aluminium treated group but non-significant ($p>0.05$) when compared to the control (CTRL). This is represented in **table 4.4.**

Table 4.4: Effect of eugenol on proapoptotic and antiapoptotic proteins following administration of aluminium chloride in wistar rats

Pro/Antiapoptotic proteins	CTRL (0.6 ml)	AC (100 mg/kg)	EGH+AC (300 mg/kg + 100 mg/kg)	EGL+AC (150 mg/kg + 100 mg/kg)	EGH (300 mg/kg)	EGL (150 mg/kg)
Bcl-2	17.06 ± 062	5.12 ± 0.12^{x}	6.02 ± 0.72^{x}	9.02 ± 0.45^{qx}	13.25 ± 0.21^{qx}	15.25 ± 0.21^{q}
Bax	3.21 ± 0.82	19.52 ± 0.60^{x}	15.21 ± 0.81^{qx}	12.21±0.71^{qx}	4.36±0.37^{q}	2.41 ± 0.82^{q}
Bax/Bcl-2	0.19 ± 0.01	3.81 ± 0.05^{x}	2.53 ± 0.09^{qx}	1.35 ± 0.03^{qx}	0.32 ± 0.05^{q}	0.16 ± 0.06^{q}

n= 5; mean ± SEM One way ANOVA *LSD post hoc test:* q=p<0.05 when compared with aluminium (AC) treated group. x=p<0.05; when compared to the control (CTRL) group.

4.6.6 Biochemistry of Endogenous Enzyme Activity

Endogenous enzyme was estimated by assaying acetylcholinesterase (AchE) activity in brain tissue of Wistar rats. AchE activity level was found to have significantly ($p<0.05$) increased in aluminium AC) treated group when compared to control group (CTRL). Co-administration of eugenol and aluminium chloride (EGH+AC and EGL+AC) significantly ($p<0.05$) reduced the activity of acetylcholinesterase when compared to the aluminium treated group (AC). This reduction was however not significant when compared to the control. Administration of eugenol only (EGH and EGL) significantly ($p<0.05$) prevented elevation in tissue activity of acetylcholinesterase when compared to the aluminium treated group, but these levels where however not significant ($p>0.05$) when compared to the control (CTRL). This is represented in **Figure 4.6I**.

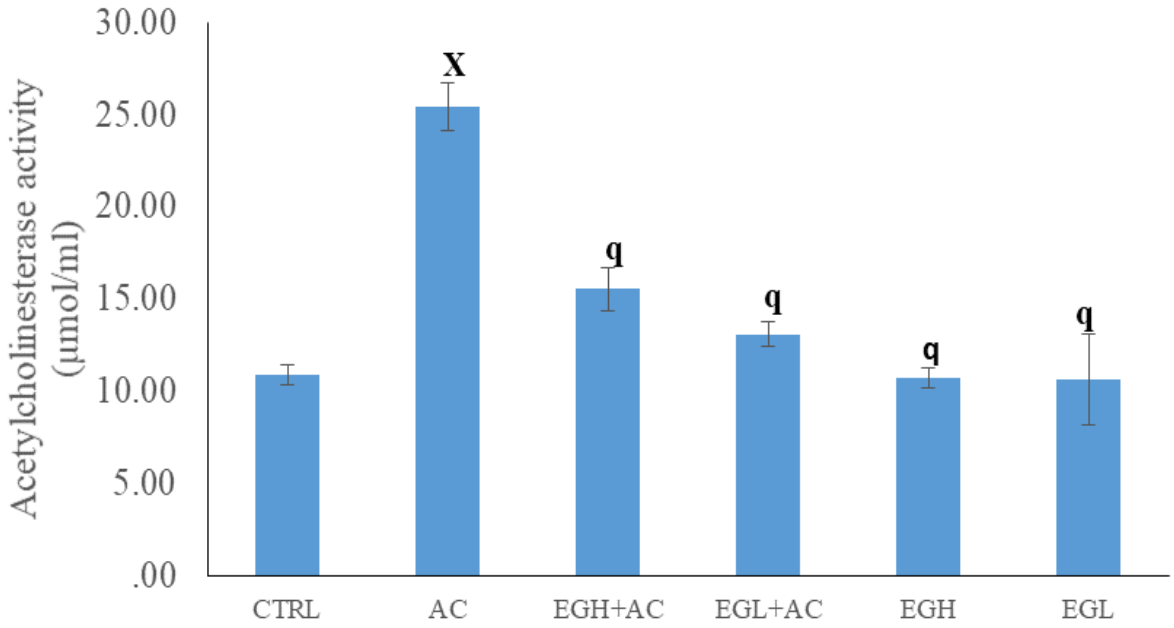


Figure 4.6I: Effect of Eugenol on tissue (brain) AchE concentration following administration of aluminium chloride in Wistar rats.

n = 5; mean ± SEM One way ANOVA *LSD post hoc test*: q= $p<0.05$ when compared to the aluminium chloride (AC) group; x= $p<0.05$; when compared with control (CTRL). **AchE**= Acetylcholinesterase.

CHAPTER FIVE

5.1 Discussion

In this study, the effects of Eugenol on aluminium-induced cerebral cerebellar and hippocampal neurotoxicity in Wistar rats was assessed using morphologic and histometric, histologic, histochemical, immunohistochemical neurobehavioural, neurochemical and biochemical investigations was carried out.

5.2 Physical Observation

Aluminium treated rats, showed no apparent reduction in their physical activity. Reduced physical activity can be manifested as sluggishness and loss of appetite, which are indicators that are associated with metal toxicity (Toma *et al.*, 2009; Salawu *et al.*, 2009). The increase in body weight as observed in this study is in concordance with Kumar, 1998 who carried out a study for 60 days observing an increase in weight at 21. This is also in agreement with the report of Azzaoui *et al*., 2008, who reported a remarkable increase in the weight of animals exposed to aluminium chloride.

Body weight changes serve as a sensitive indicator of the general health status of an animal. Animals usually exhibit a normal increment in body weight as a result of food intake. It can be stated that aluminium chloride during this study did not interfere with the normal metabolism of the rats. The significant increment in food and water intake is considered as being responsible for augmentation in body weight gain. (Salawu *et al*., 2009).

5.3 Morphological Studies

Morphometry in this study involves studying changes in brain size among groups. Evaluation of size changes in the brain is a key step in the development of new rodent models, the monitoring of different pathologies and assessing the effect of various environmental influences (Scheenstra *et al.*, 2010).

In this study, morphometry of brain dimensions and the relative organ weights were computed and compared with the control. Relative organ weight significantly increased in the the group administered aluminium chloride relative to control and this is indicative of treatment related toxicity.

Increased relative brain weight associated with aluminium intoxication was reported by Kumar, 1998.

Azzaoui *et al*. (2008) reported macroscopic brain lessions of rats treated with aluminium chloride appeared edematous, with congested blood capillaries. Relative organ weight of the groups that were co-administered eugenol and aluminium chloride reduced when compared to the aluminium treated group. Eugenol's ability to prevent macroscopic brain lessions of rats might be responsible for its ability to restore relative organ weight of rats in this study.

Histometry provides a sound basis for the comparison of histological observations. It offers objectivity, increases precision compared with direct visual appraisal, and makes statistical analysis easier. It improves assessment of certain histological changes, which, although may be recognizable by eye, are accurately graded and their progression better appreciated by histometric quantization (Ahmad *et al*., 1989; Asuquo *et al*., 2007; Huda and Zaid, 2007).

In this study, histometry of the cell area and perimeter of neurons (pyramidal cells of the cerebral cortex; layer III, V, CA1 and CA3 hippocampal regions and Purkinje cells of the cerebellar cortex) of the Wistar rats were conducted.

Histometric analysis of the soma area of pyramidal cells within the layer III of the cerebral cortex revealed a significant increase in the cell area of the aluminium chloride treated group when compared to the control group. The associated increase in cell soma area is due to aluminum's ability to initiate dissolution of lipid bilayer of the neuronal membrane and before this dissolution aluminium causes the cell membrane to swell and this swelling is associated with several cascades of events within the cell. This increase in the neuronal soma area is part of the cascade of events, finally culminating in the decline of cognitive and spatial navigation skills of rats. Co-administration of eugenol and aluminium chloride, however, prevented the changes associated with aluminium chloride by enhancing the various protective mechanisms of the neuronal cells such as preventing lipid peroxidation that will result in the dissolution of the cell membrane.

Perimeter can be described as the distance around the outside shape of an object (in this instance soma of a neuron). In this study, neuronal soma perimeter of pyramidal neurons in layer III and V revealed an increase in the perimeter of the soma of pyramidal neurons when compared to the control and co-administration of eugenol and aluminium chloride resulted in a reduction in the perimeter of the cell soma when compared to the group that was administered aluminium chloride only. Histometric analysis of the soma of Purkinje cells within the cerebellar cortex of rats administered aluminium chloride resulted in an increase in soma cell area when compared to the control and a decrease in soma perimeter when compared to the control. Pyramidal neurons

within the CA1 and CA3 region of the hippocampus are vulnerable to hypo-ischemic events, toxicants and inflammatory assaults (Seidman, 2011).

The ability of aluminium to undergo redox reactions and also produce reactive radicals, accounts for the degenerative changes in histometric features such as changes such as shrinkage of neurons and deeply stained Pyknotic nuclei (Namekata *et al.*, 1997; Crichton *et al.*, 2002; Duce *et al.*, 2010; Mohammad *et al*., 2012).

5.4 Histological and Histochemical Studies

In this study, light microscopic examination of histological sections routinely (Haematoxylin and Eosin, H&E) and histochemically (Cresyl Fast Violet, Congo red and Silver-Golgi) stained histological sections of Wistar rat brain regions: Cerebral cortex –layers III and V, Cerebellar cortex and Hippocampus were conducted.

Neurodegneration is a process involved in both neuropathological conditions and brain ageing (Kumar and Khanum, 2012). Histoarchitectural distortions of neural tissue manifesting as neuronal degenerative changes are indicative of neurotoxicity in the central nervous system (Nahla *et al*., 2011; Kalantariapour *et al.*, 2012). In this study, degenerative changes were observed such as cortical neuronal shrinkage, perineuronal vacoulations, loss of pyramidal neurone process, necrosis and chromatolysis in sections of brain studied regions of aluminium-treated rats compared to the control, which indicates treatment (aluminium) related neurotoxicity. This is in concordance to the findings of previous researchers on aluminium, who reported that this metal may have the capacity to induce nervous tissue damage (Frank, 2006; Ouafa and Djebli, 2008; Buraimoh *et al.*, 2012).

Ouafa and Djebli, 2008, reported that aluminium can cause a massive cellular depletion in the hippocampal formation with neurofibrillary degeneration and showed numerous ghosts like neurons with cytoplasmic and nuclear vacoulations, which were thought to be due to the accumulation of aluminium in these regions. Manal *et al.*, 2010, also demonstrated that administration of aluminium chloride cause marked histophathological alterations in the brain tissue which were represented by focal as well as diffuse gliosion in the cerebral cortex, odema and inflammatory cell infiltration and pericellular odema in the cerebral cortex, encephalomylacia with neuronal degeneration.

Neuronal injury may result in irreversible cell damage or cell death (Seilhean *et al.,* 2004). Cell death has also been reported to result from neuronal degeneration (Waters *et al.,* 1994). Cell death may also result from necrosis, a pathologic type of cell death that occurs from extrinsic insults to the cells or after abnormal stress such as toxins, chemical injury, thermal and mechanical factors (Kumar *et al*., 2009).

In the present study, mild cytoarchitectural distortions such as chromatolysis, necrosis, satellitosis/gliosis, indistinct neurons due to reduced staining intensity and loss of neuronal processes compared to the control group observed in the cerebral sections of rats treated with Eugenol followed by administration of aluminium chloride is indicative of aluminium induced neurotoxicity.

Chromatolysis (central chromatolysis) is a histopathologic change observed in the cell body of a neurone, where the chromatin and cell nucleus are pushed to the cell periphery, in response to neuronal axonal injury (Holland, 1996); it is a morphologic manifestation of a reparative

response to injury (Seilhean *et al.,* 2004) and response is associated with increased protein synthesis to accommodate for axonal sprouting (Holland, 1996).

Necrosis is an indication of treated related toxicity (Kumar *et al,* 2009). Cresyl fast violet (CFV) is stain for Nissl bodies (essentially rough endoplasmic reticulum RER). Degenerating neurons can stain very poorly (with low staining intensity) with CFV as a result of dissociation of ribosomes from RER which occurs in the early stage of cell degeneration (Garman, 2011).

Eugenol is a known antioxidant compound (Ou *et al*., 2006). In this study, histological features of the Eugenol treated group were comparable to the control. Thus indicates neuroprotection. This finding is in consistence with Sara and Mahmoud, 2017; Said and Abd, 2017, Eugenol ameliorated aluminium induced cerebral cortex damage antioxidant molecules are thought to play a crucial role in counteracting free radical induced damage to macromolecules and has been found to heel the free radical mediated cell damage (Flora, 2002).

Treatment of rats with Eugenol in this study, showed a preserved parenchyma of the cerebral cortex and cytoarchitectural preservation of neuronal cell Nissl substance. This implies that Eugenol could have a protective effect against aluminium-induced neurotoxicity. Results from this study are in consistence with the report on the neuroprotective effects of Eugenol against aluminium-induced toxicity (Said and Abd, 2017) observed that Histological examination revealed a neuroprotective potential of eugenol against aluminium induced toxicity as demonstrated by reducing neuronal cell damage of the cerebral cortex.

Purkinje and granule cells are the most important targets in cerebellum for toxic substances (Fonnum and Lock, 2000). Neurodegenerative changes such as perineuronal vacoulations, neuronal cytoplasmic shrinkage, gliosis, and swelling of neuronal cytoplasm. Purkinje and

internal granule cell necrosis and indistinct neurones due to reduced staining intensity observed in aluminium-treated Wistar rats. Findings are in agreement with the studies related to aluminium chloride and enlarged cell bodies (Akirinade *et al.,* 2013).

Aluminium is known to accumulate in the mitochondria and disrupt a number of mitochondrial functions leading to an energy deficit, which by itself may not result in sufficient neuronal dysfunction or damage (Kumar *et al,* 2008; Mohan *et al,* 2009).

Studies revealed that reductions in neuronal energy can dramatically amplify excitotoxic injury. Impairment of mitochondrial function and energy metabolism by aluminium would thus be expected to increase the sensitivity of neurons to excitotoxicity and accelerate and potentiate neuronal damage within the regions of the brain such as the cerebrum, cerebellum hippocampus etc (Greenamyre, 1991; Storey *et al*, 1992; Ludolph *et al*, 1993).

Oral administration of aluminium chloride has been reported to induce cerebellar cellular degeneration (Akirinade *et al,* 2013). These degenerative changes could occur in ways such as suppressesion of neuronal energy production, especially mitochondrial energy production, greatly enhancing excitotoxic sensitivity (Henneberry, 1989; Nicholls and Budd, 1998; Beal *et al*., 1993).

Aluminium is also known to inhibit cellular energy producing enzymes, including mitochondrial electron transport enzymes (Blaylock and Ridgeland, 2004). The clinical importance of neuronal energy suppression by aluminium lies in the fact that mitochondrial energy suppression is intimately connected as an early event to neurodegenerative diseases such as Alzheimer's dementia, and Parkinson's disease (Meltzer *et al*., 1996; Schapira *et al*., 1998; Gibson *et al*., 1999). Hence neuronal energy suppression is one of the basis for cellular degeneration within the central nervous system.

Rough endoplasmic reticulum and free ribosomes appear as basophilic granular areas (Nissl bodies) on CFV staining under light microscopy. Reduction in Nissl Bodies has been reported in relation to neuronal degeneration: loss of Nissl bodies with consequent reduced staining intensity of the Nissl substances in the cerebellar section of the aluminium treated rats in this study is in concordance with reports of earlier findings of Akinrinade *et al.,* 2013 and Ibrahim and Heba, (2013) reporting loss of Nissl substance within the cerebellar neurones and shrinkage of the nucleus following aluminium induced toxicity.

Mild histoarchitectural distortions, such as perineuronal vacoulations, satelliotosis or gliosis compared to the control observed in cerebellar sections of rats treated with Eugenol followed by the administration of aluminium chloride suggest aluminium-induced neurotoxicity.

The brain is made up of neurones and neuroglia, the neurones have been responsible for sending and receiving nerve impulses or signals. Microglia and astrocytes are essential for ensuring the proper functioning of neurones and are quick to intervene when neurones become injured or stressed. As they are sentinels of neurons well-being, pathological impairment of microglia or astrocytes could have devastating consequences for brain function. It is presumed that neuroglial activation is mainly determined by neuron signals (Halliwell, 1992). Satellitosis, a condition marked by the accumulation of neuroglia cells around damaged or necrosed neurones of the central nervous system, often as a prelude to neuronphagia (Manickam *et al.,* 2009), as observed in this study is indicative of treatment related toxicity . Acute injury causes neurones to generate signal that inform neuroglia about the neuronal status. Depending on the degree of severity of the neuronal injury, neuroglia will either nurse the injured neurons into regeneration or kill them if they are not viable. These types of neuroglia responses are considered to represent normal physiological and neuroprotective responses (Kumar and Khanum, 2012).

Administration of Eugenol showed a preserved neuronal cell Nissl substance in Wistar rats. This implies that eugenols have a protective effect against aluminium induced neurotoxocity. Results from this study are in agreement with the report on the neuroprotective of eugenol (Said and Abd, 2017).

Said and Abd (2017), reported Protection against Aluminium chloride induced brain toxicity with eugenol was evident by reducing karyopyknotic neuronal cells of the cerebellar cortex.

Aluminium has been implicated in the deposition of amyloid beta and tau protein, which precedes by years the clinical manifestation of dementia. Aluminium has been shown to be causative agent and shown to increase the accumulation of amyloid beta in the brain. This evidence has led to the Amyloid beta (Aβ) cascade hypothesis of AD (Gómez *et al.,* 2008). Transgenic mice lack neurofibrillary tangles (NFT) formation. Requirement of an additional tau mutation for Amyloid beta protein plaques transgenic mice to form NFT1 suggests that Amyloid beta accumulation is an accelerating factor that enhances tau abnormality, which is primarily caused by some distinct, age-related factors (Praticó *et al.,* 2002; Ribes *et al.*, 2008).

In this study administration of aluminium chloride to rats, did not reveal any amyloidal plaques at the administered dose and duration using Congo red stain (to detect amyloidal plaques). This is in agreement with previous studies that was carried out on Long-term oral intake of aluminium and zinc did not accelerate deposition of aluminium in transgenic model of Alzhemier's disease mice model (Haruhiko *et al.,* 2011).

Haruhiko *et al.* (2011) observed that long-term oral intake of Al does not accelerate AD pathology in transgenic mouse models and does not promote the deposition of amyloid plaques in mouse models. Oral ingestion of aluminium did not accelerate the deposition of amyloid plaques throughout the duration of the study, hence no visible amyloid plaques in brain sections

of the experimental animals. Fang *et al.* (2013) reported no visible amyloid plaques following oral administration of aluminium chloride for the duration of a three week study within the cerebral, cerebellar cortex and hippocampus of Wistar rats.

Majority of orally administered Al is considered absorbed from the intestines and the vast majority of absorbed Al is excreted via the kidney. The extent to which Al in the blood passes the blood–brain barrier is undetermined and may be limited probably due to the blood brain barrier; however, the occurrence of Al encephalopathy provides evidence that Al does enter the brain from the blood (Haruhiko *et al.,* 2011).

Neuroprotection refers to the relative preservation of neuronal structure and/or function (Casson *et al.,* 2012). Relative preservation of neuronal integrity implies an amelioration in the rate of neuronal damage in the presence of a neurotoxicant such as aluminium.

Findings are in consistence with reports related to the neuroprotective activity of plants which also contain eugenol (Wantanabe *et al*., 2001; Levites *et al*, 2002; Kim *et al*., 2008).

Most of this studies attribute the neuroprotective effects to the antioxidant properties (Norfaizatul *et al.,* 2010; Hwang *et al*., 2012).

Observed histoarchitectural distortion of the hippocampal region (CA1 and CA3), such as irregular arrangement of CA1 hippocampal neurons, pyknosis, and basophilic necrosis is indicative of treatment associated with administration of aluminium chloride induced neurodegenerative changes. Findings were in accordance to previous reports on aluminium-induced neurotoxicity (Buraimoh *et al.,* 2011).

Hippocampal CA1 neurons, are characteristically packed together; arranged in one or two very dense rows (Slomianka, 2011). Histoarchitecture of CA1 region is important because of the particular vulnerability of the neurones to in the pyramidal layer to toxic events (Seidman, 2011). Irregular arrangement of CA1 neurones in this study implies degenerative changes. Towfighi *et al.* (2004) reported a degeneration of deep CA1 pyramidal cells was observed during early postnatal development in rabbits as a consequence of pilocarpine induced seizures.

A higher incidence of depolarizing responses to anoxia has been found in rat deep CA1 pyramidal cells when compared to superficial cells (Morris *et al.*, 1995). Differential effects of ischemia on CA1 pyramidal cells have also been reported (fan *et al.*, 2005; Ruan *et al.*, 2007). Basophilia of the cytoplasm and pyknosis of neurones, which histologically characterizes neuronal atrophy (Mena *et al*., 2004) as observed in this study is indicative of treatment related toxicity. Neuronal atrophy, a descriptive term given to a wide variety of irreversible neuronal injuries resulting in slow cell death. These occurs in many degenerative disorders (Seilhean *et al.*, 2004; Susan, 2007).

Mild neurodegenerative changes in CA1 and CA3 regions of the hippocampus, such as irregular arrangement of CA1 hippocampal neurones, chromatolysis, Pyknotic necrosis, and perineuronal vacoulations compared to the control in rats treated Eugenol followed by administration of aluminium suggest aluminium induced neurotoxicity. Acute neuronal necrosis occurs in a variety of acute injuries such as ischemia and anoxia (Seilhean *et al.*, 2004). Neurodegenerative changes have been reported as direct toxic effect of aluminium chloride as anoxic poison (Ding and Yang, 2010; Buraimoh *et al.*, 2011; Akirinade *et al.*, 2013). Acute neuronal necrosis involves cytoplasmic organelles and the cell membrane, which leads to ruptures, leading to cell death.

Features include neuronal cytoplasmic shrinkage, disappearance of Nissl bodies and intense eosinophilia (red neurone) (Mena *et al.,* 2004; Seilhean *et al.,* 2004).

In this study, administration of eugenol had a neuroprotective effect against aluminium-induced hippocampal damage. Result is in concordance with previous studies on neuroprotective activity of eugenol following intoxication with aluminium chloride (Said and Abd, 2017).

Said and Abd (2017) observed neurodegenerative such as pyramidal cells of the hippocampus, showed darkened nuclei, changes in the hippocampus (CA1 and CA3) of aluminium exposed animals were less severe in Eugenol treated animals. Treatment with Eugenol ameliorated aluminium-induced hippocampal damage by conferring histoarchitectural preservation of the hippocampus, especially with a dose of 150 mg/kg Eugenol compared to the control. Neuroprotection refers to the relative preservation of neuronal integrity and implies a reduction in the rate of neuronal damage in the presence of a neurodegenerative insult such as aluminium (Esparaza *et al.*, 2019).

Amyloidal plaques is one of the numerous results of long term exposure to aluminium. These plaques are key in the progression of neurodegenerative diseases and are components of histological sections of different brain regions which include the hippocampus (Yan *et al.,* 2003; Zhang *et al.,* 2005). In this study, oral administration of aluminium chloride did not lead to deposition of amyloid beta and this is in concordance to the study by Fang *et al.,* 2013, who reported that after three weeks of oral administration of aluminium chloride among rats did not reveal the deposition of amyloid plaques using Congo red as a staining technique.

Haruhiko *et al.,* 2011 showed that long-term oral intake of Al or Zn does not accelerate AD pathology in transgenic mouse models.

The evidence in this study does indicate that oral intake of Al is not a risk factor in accelerating AD. Rearing is an exploratory behavior induced by novelty, such as exposure to an open field. Stimulation of certain brain (Hippocampus) regions by certain substances (such as phenolics) can induce rearing. Brain excitability is controlled by gamma-aminobutyric acid (GABA) inhibitory neurotransmission through its ionotropic GABAA/allosteric benzodi- azepine site. Drugs that decrease GABAA receptor fast inhibitory neurotransmission induced could reduce the frequency of rearing (Rosana *et al*., 2012). Administration of aluminium chloride could have inactivated GABA receptor sites and hence a reduction in rearing frequency was observed and co-administration with eugenol at high and low doses prevented the inactivation of this receptor sites.

Rats naturally are aversive to open spaces and will naturally prefer the protection offered by closed spaces. This behaviour is due to the natural fear of predators and an increase in open arm duration not accompanied by defecation or urination can be used as a measurement of decreased anxiety accompanied with other behaviours such as rearing and grooming. An increased duration within the close arm is used as an indication of increased anxiety. An increase in time spent and proportion of the entry into the open arms without changing locomotor activity is regarded as a powerful marker for an anxiolytic substance effect (Pellow *et al.,* 1985). In this study, Administration of Eugenol remarkably decreased anxiety levels by a remarkable increase in open arm duration,, and reduced close arm duration showing eugenol as an anxiolytic agent. The result in this study was also in agreement where rats showed preference for being in open arms over closed arms was calculated to measure anxiety-like behaviour and an increase in open arm activity (duration and/or entries) reflected anti-anxiety behaviour. Results of this study showed that the rats treated with aluminium chloride had increased number of times crossing close arm

entries and increased average time spent in close arms. However they show decreased time (lesser time) spent in the open arm of the maze when compared to the control group. This implied that the aluminium-treated groups expressed more anxiety-related behaviour than the control groups in exploration of their activities on the EPM. Finally they concluded that aluminium chloride exposure has negative effects on anxiety related behaviour of rats as indicated by increased rate of anxiety in Alumiminium treated rats (Buraimoh *et al.,* 2011; Tripathi and Modi, 2012).

Memory is an organism's mental ability to store, retain, and recall information (Chakravarthi *et al.,* 2012). In the present study, morris water maze served as an exteroceptive behavioural model to evaluate learning and memory in Wistar rats (Kulkarni *et al.,* 2011; Veni Bharti *et al.,* 2013).

Learning behaviour in Wistar rats can be reflected by the duration of transfer latency (TL) of the first day (pre-treatment) and retention of information or memory reflected by the transfer latency of day-7, day-14 and day-21 of treatment. Administration of Eugenol remarkably improved learning and memory by reduction of TL when compared to pretreatment and to the control.

The Morris water maze is one of the most widely used tasks in behavioural neuroscience for studying the psychological process and neural mechanisms of spatial learning and memory (Brandies *et al.,* 1989; He *et al.,* 2011). Learning and memory of rats is reflected by escape latency compared to the performance at the pretreatment session to day 21 throughout the duration of this study.

Increased escape latency as observed with aluminium treatment at day-7, 14, and 21 is an indication of learning and memory impairment. Memory forms can be classified as declarative or explicit (ability to recall past events deliberately) and are hippocampus dependant; and non-

declarative or procedural (implicit), defined by unconsciously performed skills (motor or cognitive) that are mainly dependent on the straitum and cerebellum (Packard and McGaugh, 1992).

The hippocampus and the cerebral cortex are the key structures of memory formation. Because the hippocampus is especially indispensable in the integration of spatial information, a decline in learning ability may be induced by the deterioration of hippocampal function (Munoz and Feldman, 2000). The brain regions particularly affected by Al neurotoxicity include those involved in memory and learning. This may be due to the specific distribution of transferrin receptors (tfrs) and neuroanatomical connections between brain regions important for cognitive processes (Veer *et al.*, 2005). Ouafa and Djebli (2008) reported that exposure to aluminium chloride induced memory deficits and correlated cognitive dysfunction to accumulation of aluminium chloride in the hippocampus.

The hippocampus plays an important role in learning and memory (Chakravarthi *et al.*, 2012). Results are in accordance with Tripathi and Modi. (2012) that inferred acute and chronic doses of aluminium induced cognitive damage in rat model.

Eugenol treatment showed a decrease in latency time when compared to the aluminium treated group, and administration of Eugenol especially at day-21 of treatment had a neruprotective effect on aluminium intoxication by decreased latency. Zhibin *et al.* (2013) also reported that Eugenol can increase learning and memory, using MWM to assess learning and memory.

Memory enhancing of action by eugenol is by the increased supply of oxygen, and free radical elimination from the body, thereby improving memory (Zhinbin *et al.*, 2013).

Nutraceuticals (Eugenol as a member) have been demonstrated to limit neurodgeneration, decrease neuroinflamation, and prevent or reverse age related dependent lose in cognitive performance (Park and Kim, 2002). Results from this study suggest that Eugenol is a potential neuroprotective agent against chemical-induced cognitive dysfunction.

The motor cortex has long been viewed to play an important role in fine motor control and fractionation of movement (Evarts *et al.,* 1983), sensorimotor integration, and higher order cognitive motor movements (Sanes and Donoghue, 2000). In this study, muscular strength in the forelimbs (forepaws) of rats was assessed using forelimb grip strength (FGS) test. Time to release grip (forelimb grip strength time) reflect FGS.

Forelimb grip strength decline was has been reported with aluminium intoxication in rats (Colomina *et al.,* 2005). Golub *et al.* (2000) reported a forelimb grip strength decline in animals exposed to aluminium.

Administration of eugenol at a dose of 300mg/kg improved FGS which was not significant when compared to the control and aluminium treated groups across the period of study. Several antioxidants such as curcumin, ocimum, and clove which contains Eugenol as an active component have been used to protect cells from oxidative stress and muscle cell damage (Halliwell and Gutteridge, 1999; Zoppi *et al.,* 2006).

The cerebellum is involved in the control of movements, particularly those linked to the voluntary nervous system and movements where timing is an important aspect. It coordinates the different muscle groups so that the muscle exerts movements fluently and precisely. The cerebellum receives continuous feedback information about the intended movement and actual movements. The cerebellum should be regarded as a stabilizing control system which receives

the forewarning of each motor impulse. Atrophy of the cerebellum is accompanied by different forms of ataxia and unstable gait (Fonnum and Lock, 2000).

5.5 Neurochemical/ Biochemical Studies

Trace elements are of widespread neurological importance and have critical actions in neurodevelopment, neurotransmitter synthesis, energy metabolism, antioxidant defence, and DNA synthesis. Thus trace elements are important for cognitive function (Jones *et al.,* 2008; Dauncey, 2009).

Antioxidants have been suggested to be useful in conditions associated with oxidative stress (Halliwell and Gutteridge, 1999; Norfaizatul *et al*., 2010). Oxidative stress, which occurs due to the imbalance between the production and detoxicification of reactive oxygen species (ROS), has also been implicated in many neurodegenerative diseases such as Parkinson's and Alzheimer's disease (Gilgun-Sherki *et al.,* 2001; Trushina and Mcmurray, 2007). The brain is more susceptible to oxidative stress due to its high oxygen consumption, relatively low antioxidant capacity, and high content of lipids. Increased oxidative stress stress will further lead to lipid peroxidation, DNA damage,, protein, damage and induction of apoptosis (Halliwell and Gutteridge, 1999; Crichton *et al.,* 2007).

The role of oxidative stress in neuronal degeneration is a widely discussed concept, and understanding on the role of aluminium in mediating neuronal oxidative stress may help to clarify the role of aluminium in brain damage. Although aluminium has no redox capacity in biological systems it can induce oxidative damage through multiple mechanisms (Verstraeten, 2008). It can bind to negatively charged brain phospholipids, which contain polyunsaturated fatty acids and are easily attacked by ROS such as O^{-2}, H_2O_2, and OH^- (Exley, 2004; Halliwell and

Gutteride., 2007). Further, this element stimulates iron-initiated lipid peroxidation in the redox reaction, which causes ROS production and Fe^{+3} formations (Exley, 2004). Reactive oxygen species may also cause cellular damage by oxidizing amino acid residues on proteins, forming protein carbonyls suggesting for aluminium to have catalytic activity to produce free radicals (Verstraeten, 2008). Furthermore, the main mechanism of Aluminium toxicity involves the disruption of the homeostasis of metals, such as magnesium (Mg), calcium (Ca), iron (Fe), and manganese (Mn). The physical and chemical properties of Aluminium allow it to effectively mimic these metals in their respective biological functions and trigger biochemical abnormalities. Aluminium has been shown to replace Mg and bind to phosphate groups on the cell membrane, DNA and ATP (Kawahara and Kato, 2011).

In this study, there was an increase in the levels of Aluminium (Al), Magnesium (Mg), and Iron (Fe) in the aluminium treated group compared to the control.

Excess iron (Fe) accumulation affects the CNS. Increased Fe has been observed in the lesionsite of a number of neurodegenerative disorders and models of neurodegeneration (Olanow *et al.,* 1990). Increased Fe deposits in regions of the brain have been implicated in Parkinson's disease (PD) (Watts, 1990). Fe levels are also increased at sites of degeneration in Alzheimer disease (AD); detected in the hippocampus, nucleus basilis, frontal cortex and motor cortex of A.D patients (Connor *et al.,* 1992; Richardson, 1993).

Although Al cannot change its redox state, it exacerbates free radical damage and lipid peroxidation initiated by iron. This can be attributed to the fact that, like iron, Al binds to the iron regulatory protein (IRP), which influences the expression of iron-binding proteins. This

causes further stabilisation of iron in its ferrous (Fe^{+2}) state that promotes Fe^{+2}-induced LPO by the Fenton reaction, modifying therefore the biophysical properties of membranes.

Oxidative damage resulting from aluminium and deregulated iron is in-dissociable in aluminium-loaded neurons, where their combined activity provides an oxidative environment (Kawahara and Kato, 2011; Zatta *et al.*, 2003; Parekh *et al.*, 2013).

Aluminium is neither required by biological systems nor is it known to participate in any essential biological processes. While today all living organisms contain some aluminium, there is no scientific evidence that any organism uses aluminium for any biological purpose. There is similarly no evidence from the proteome or genome that any organism has utilized aluminium at any time in the evolutionary record. Aluminium's abundance and paradoxical lack of biological function remains a biochemical enigma (Exley, 2009).

It has also been shown that aluminium in combination with other trace metals in the body (e.g., copper, zinc Iron Magnesium) additively increases brain inflammation (Becaria *et al.*, 2006)

Manganese is an essential mineral for maintaining brain function, manganese toxicity in humans is associated with Parkinsonian-like symptoms such as ataxia, and altered balance may develop (Watts, 1990). Exposure to aluminium has been shown to induce changes in the cerebral, cerebellar, and hippocampal levels of neurotrace elements (Said and Abd, 2017).

In this study, exposure to aluminium resulted in increased levels of manganese and this increase was higher than the control group. Increases in the levels of manganese within the brain also act as a prooxidant and hence a toxicant to the brain (elevated amounts) and these could most likely account for the elevated levels of oxidative stress markers in rats.

Magnesium (Mg) is known to play an essential role in supporting brain plasticity, this primes the brain for optimal learning, memory, and cognitive function. Increasing brain magnesium levels has been shown to restore critical brain plasticity and thus improve cognition (Slutsky *et al.*, 2010)

In this study, decreased Mg brain levels as observed in the aluminium treated group might be responsible for the low cognition that was observed in the aluminium treated group. This is in tandem with the study of Slutsky *et al.*, 2010. Eugenol was able to salvage the reduction in the Mg levels that was induced by Aluminium resulting to an increase in Mg levels when compared to the control group. EGH and EGL also had increased elevated Mg levels when compared to the control group (CTRL). Eugenol's ability to increase brain Mg levels might be responsible for its cognitive improving properties.

Iron deficiency is not perceived as a life-threatening disorder. However, Lowered levels of Iron (Fe) have resulted in impaired behaviours including learning as was reported by Youdim, 2008.

Iron affects synthesis and signalling of the neurotransmitter dopamine and the brain requires iron to generate ATP via electron transport chain within the mitochondria. Within the mitochondria, mitochondrial enzyme requires iron and hence deficiency of mitochondrial enzymes can damage mitochondrial DNA. Reduced mitochondrial efficiency results in elevation of of biomarkers of oxidative stress which initiates the intrinsic apoptotic pathway. Diminished brain iron levels in this study might be one of the trigger factors for the initiation of the apoptosis as observed in this study.

Results from this study revealed reduced brain iron levels in AC group when compared to control. Also Eugenol salvaged groups (EGH and EGL) showed an increase in Fe levels when

compared to the aluminium treated group. Rats that received eugenol showed increased levels of Fe When compared to the control group. Reduced Fe levels in rat brains (AC treated) might be responsible for cognitive deficits associated with aluminium toxicity due to the fact that iron affects the synthesis and signalling of the neurotransmitter dopamine and dopamine plays a vital role in memory. The brain requires iron to generate ATP by the electron transport chain which occurs within the mitochondria of neurons and asa result iron deficiency can result in damage to mitochondria DNA which can in turn result in elevation of biomarkers of oxidative stress. Elevated levels of aluminium in the brain have been associated with neurological diseases such as Alzheimer's or Parkinsonism (Exley *et al.,* 2010), which has been attributed to the accumulation of such metals in the brain of affected individuals (Walton, 2012).

Oral exposure to aluminium results in accumulation within the hippocampus of the brain and thus affects some essential elements (Fe, Zn, Cu, Mn, and Mg) contents in the hippocampus at varying levels (Kruck *et al*, 2004). Previous studies have correlated neurological disorders with accumulation of aluminium chloride in the brain of Wistar rats (Said and Abd, 2017; Lukiw *et al.*, 2005; Sies and Jones, 2007). Thus, findings of this study corroborate reports on trace element toxicity with aluminium toxicity.

In this study, administration of eugenol restored the changed levels of the studied neuro-trace elements concentrations. Findings are in agreement with studies related to the neuroprotective activity of eugenol (Zhang *et al*., 2017)

Phenolics share the same general structure as they are composed of an aromatic hydroxyl nucleus and exist in an approximated number of 8000 in nature (Karaman *et al.,* 2009). So far, plant phenolics constitute one of the major groups of compounds acting as primary antioxidants or free

radical terminators. Plant polyphenols are multifunctional in the sense that they can act as reducing agents, hydrogen atom donators, and singlet oxygen scavengers. Certain polyphenols are also effective as antioxidants capable of chelating transition metal ions, which may otherwise induce Fenton-type oxidation reactions in their free states (Karaman *et al.,* 2009; Rice-evans *et al.,* 1996).

Eugenol, a major phenolic component from clove oil (Eugenia caryophyllata), has demonstrated several biological activities, such as anti-inflammatory activity by inhibiting the enzyme cyclooxygenase-II (Son *et al.,* 1998), analgesic activity due to selective binding at the capsaicin receptor, anti-oxidation activity (Ou *et al.,* 2006) and antibacterial activity against both gram-positive and gram-negative microorganisms (Laekeman *et al.,* 1990; Kalemba and Kunicka, 2003). In addition, it has been widely used as a fragrant and flavouring agent in a variety of food and cosmetic products (Atsumi *et al.,* 2001). However, at high concentrations, eugenol has adverse effects, including inflammatory and allergic reactions, possibly due to the formation of phenoxyl radicals and, subsequently, of quinine intermediates, via its pro-oxidant activity (Fujisawa *et al.,* 2002).

The brain has a large potential oxidative capacity but a limited ability to counteract oxidative stress. Oxidative stress has been implicated in mechanisms leading to neuronal cell injury in various pathological states of the brain, including neurodegenerative disorders. Although the brain accounts for less than 2% of the body weight, it consumes about 20% of the oxygen available through respiration. Therefore, because of its high oxygen demand, the brain is the most susceptible organ to oxidative damage (Weiss and Fintelmann, 2000).

In this study, malondialdehyde (MDA) or thiobarbituric acid-reactive substances (TBARS) were assayed by using the estimation of lipid peroxidation levels, while antioxidant enzymatic activity was estimated by assaying for superoxide dismutase (SOD), catalase (CAT) and glutathione peroxidase (GPx) activities in the brain tissue.

Tissue MDA levels increased remarkably in AC group, when compared to the control, however co-administration of Eugenol in EGH and EGL resulted in reduced tissue MDA levels when compared to AC group. Elevated tissue MDA levels, suggest enhanced lipid peroxidation, leading to tissue damage and failure of the antioxidant defence mechanism to prevent the formation of excessive radicals (Himakar *et al.*, 2010). Lipid peroxidation is a free radical related process, which is potentially harmful because it is uncontrolled self-enhancing process which causes disruption of membranes, lipids and other cell components. It is also involved in oxidative stress which plays a major role in neuronal degeneration (Rao and Purohit, 2011). Abnormally high levels of lipid peroxidation and simultaneous decline of antioxidant defence mechanism can lead to destruction of various cellular organelles and as a result lead to oxidative stress (Mahboob *et al.*, 2005).

Results of this study demonstrated that treatment of rats with aluminium chloride had a significant enhancement of TBARS levels, indicative of the generation of lipid peroxides (LPO). Enhanced Lipid peroxidation levels were also reported in aluminium toxicity by Manal *et al.* (2010) and Yang *et al.* (2006).

Al^{+3} has been reported to induce lipid peroxidation and to alter physiological and biochemical characteristics of biological systems (Sies and Jones, 2007). Polyunsaturated fatty acid peroxides

generate malondialdehyde (MDA) upon decomposition and measurement of the concentration of MDA used as an indicator of lipid peroxidation (Okutan *et al.,* 2005).

This elevation of MDA could be attributed to the ability of Al itself and its different salts to accelerate oxidative damage to biomolecules like lipids, proteins, and this element can be able to cross the blood-brain barrier and is deposited in to brain and increases LPO. Therefore, the estimation of free radical generation and antioxidant defense has become an important aspect of investigation in mammals (Verstraeten, 2008).

Biological systems protect themselves against the damaging effects of reactive oxygen species by several means. These include free radical scavengers and chain reaction terminators, enzymes such as SOD, CAT and GPx systems (Semiz and Sen, 2007; Uma *et al.,* 2012).

Superoxide dismutase (SOD) belongs to the members of enzymatic antioxidative defense mechanisms against reactive oxygen species (ROS), and protects macromolecules, cells and cell membranes from peroxidative damage. SOD catalyses the dismutation of the superoxide anion radical into oxygen and hydrogen (Kankofer, 2002).

The activity of SOD is a sensitive index of oxidative damage as it scavenges the superoxide anion to form hydrogen peroxide leading to diminishing toxic effects (Khan *et al.,* 2012).

In this study, tissue SOD activity levels decreased in the aluminium treated group and increased in the eugenol treated group, which was significant among the 150mg/kg and 300mg/kg eugenol only group. Aluminium has been reported to reduce anti-oxidative enzymes such as catalase, SOD, and glutathione reductase (Yuan *et al.,* 2012; Ivana *et al.,* 2009).

Aluminium results in an imbalance between the production and neutralization of reactive oxygen species, which may occur when anti oxidative system is not efficient enough, leading to peroxidative damage of macromolecules and as a consequence the disturbance of metabolic pathways, injury of tissues (Kankofer, 2002).

Administration of eugenol in this study maintained an elevated level of SOD activity. This is in consistence with with the reports of Debapriya *et al.* (2015). Eugenol is believed to have an aromatic ring. This phenolic group stabilized a radical formed on a-carbon with conjugation to the eugenol molecule. It has been reported that the main mechanism of action of phenolic antioxidants was considered the scavenging of free radicals, although other mechanisms may be involved (Nenandis *et al.*, 2003).

Eugenol treatment has a neuroprotective function on aluminium induced decrease in SOD activity due to its antioxidant and free radical scavenging effect through its abilty to maintain levels of manganese and manganese is a cofactor to SOD within the inner mitochondrial membrane and hence enhance the free radical scavenging property of SOD.

Glutathione peroxidase (GPx) is an enzyme family with peroxides activity whose main biological role is to protect the organism from oxidative damage and helps to prevent lipid peroxidation of cellular membrane by removing the free peroxides in the cell. Oxidative stress has been implicated in the pathogenesis of a number of disorders and its extent of injury is generally related to an increase or decrease of one or more free radical scavenging enzymes of which GPx is one (Kankofer, 2002).

The activity of GPx is coupled with glutathione reductase (GSSG-R), which maintains reduced glutathione (GSH) levels (Bompart *et al.,* 1990). Using glutathione (GSH) as a reducing reagent,

the GPx enzymes catalyse the reduction of H_2O_2 and organic peroxides (R-O-O-H) to water and the corresponding stable alcohol thus inhibiting the formation of free radicals (Khan *et al.*, 2012). Aluminium –induced increase in GPx activity indicates the occurrence of oxidative stress in wistar rat brain. The finding is in line with the report of Yuan *et al.* (2012) and is not in line with the reports of Manal *et al.* (2010) who reported a decrease in GPx activity levels following administration of aluminium chloride. However administration of eugenol seemed not to have any significant effect on GPx activity levels, But the group administered 300mg/kg eugenol plus 100mg/kg aluminium chloride showed comparable activity levels which were almost the same levels as the control. Other doses seem not to show any improvement on GPx levels.

Catalase is a key component of the antioxidant defence system. Inhibition of these protective mechanism risks in enhanced sensitivity to free radical-induced cellular damage (Young and Woodside, 2001).

In this study, tissue CAT activity levels in all treated groups showed remarkable difference, except in the EGL group (150 mg/kg eugenol and 100 mg/kg aluminium) treated groups compared to the control. The result obtained from this research is in concordance with the reports of Said and Abd. (2007), Catalase (CAT) can catalyse the decomposition of hydrogen peroxide to oxygen and water. It does not require a special donor of organisms but can protect the bodies from reactive oxygen species. Therefore, it is an essential antioxidase and exists in most living cells (Liu *et al.*, 2011).

5.6 Intramitochondrial accumulation of 8-OHdG

Mitochondria, a key organelle of most eukaryotic cells, are not only essential for cellular energy generation but also important for calcium metabolism and apoptotic cell signaling (Milane *et al*., 2015). Like the nucleus, both mitochondria and chloroplasts contain their own DNA, and mitochondrial DNA (mtDNA) damage has been frequently implicated in several diseases including neurodegeneration, cancer, stroke, and aging-related disorders (Mishra and chan, 2014).

Mitochondrial DNA (mtDNA) is very susceptible to undergo oxidation; it is quite possible that generation of ROS can attack mtDNA, leading to more than 20 products of oxidized bases (Cooke et al., 2003; Ratan et al., 1994). Among the many types of DNA damage caused by ROS, the formation of 8-OHdG is the most common one (Cheng et al., 1992). Thus, the amount of 8-OHdG in mtDNA may be an index for cellular oxidative damage. In this present study, administration of aluminium chloride resulted in increased levels of 8-OHdG and hence resulting in oxidative damage to mtDNA, which is in agreement with the a study performed by Kumar *et al*., 2008; Kumar *et al*., 2009 and Ding and Yang, 2010. However, treatment with eugenol prevented the generation of 8-OHdG, which confers a neuroprotection of the and this might also postulate the ability of eugenol to penetrate the inner mitochondrial membrane to prevent this deleterious process and in agreement with Ozkan and Erdogan, 2019.

Ding and Yang, 2010, postulated that a decrease in SOD activity and increase in MDA level may suggest the involvement of oxidative stress in the accumulation of 8-OHdG within the mitochondria.

5.7 Proaoptotic and Antiapoptotic Proteins (Bax and Bcl-2)

The process of programmed cell death, or apoptosis, is generally characterized by distinct morphological characteristics and energy-dependent biochemical mechanisms (Elmore, 2007). Apoptosis is considered a vital component of various processes including normal cell turnover, proper development and functioning of the immune system, hormone-dependent atrophy, embryonic development and chemical-induced cell death. Inappropriate apoptosis (either too little or too much) is a factor in many human conditions including neurodegenerative diseases, ischemic damage, autoimmune disorders, and many types of cancer (Elmore, 2007).

Mitochondria-mediated apoptotic intrinsic pathway is regulated by the proapoptotic (Bcl-2) group of proteins. The Bcl-2 protein family can be classified mainly into two subclassifications which are according to structural homology. The balance between the proapoptotic and antiapoptotic proteins is pivotal in determining the fate of a cell. Bcl-2 may function to negate the damaging effects of ROS by reducing the levels of different ROS within the cytosol (Akifusa *et a*l., 2009). Bcl-2 was discovered to inhibit the release of cytochrome c within the mitochondrial membrane. In contrast to Bcl-2, Bax on the other hand, monitors apoptosis by controlling the release of cytochrome c into the cytosol, resulting in caspase-3 activation (Cai *et al*., 2011).

In this study, oral administration of aluminium chloride resulted in elevation of the proapoptotic protein Bax and co-administration of eugenol and aluminium chloride (EGH+AC, EGL+AC) however resulted in reduction in the levels of Bax. Bcl-2 is an antiapoptotic protein which was reduced in the group administered aluminium chloride and coadministration with eugenol resulted in an increase in Bcl-2 which suggests neuroprotection within neuronal cells. This increase in Bcl-2 might have resulted from increased in oxidative stress biomarkers and

accumulation of 8-OHdG within the inner mitochondrial membrane. Oxidative stress is one of the triggers of apoptosis. Intramitochondrial accumulation of 8-OHdG could be a likely trigger for the apoptosis in this study. Bax/Bcl2 ratio can act as a rheostat which determines cell susceptibility to apoptosis, the lower this ratio the higher the susceptibility to apoptosis (Raisova *et a*l., 2001; Ehsan et al., 2014). Co-administration of eugenol and aluminium chloride resulted in reduction of Bax/Bcl-2 ratio, which implies a higher survival probability for neuronal cells of rats within this group.

5.8 Caspase -3 activation

Reactive oxygen species increase the permeability of the mitochondrial membrane and therefore results in mitochondrial failure (Huang *et al*., 2008). The membrane of the mitochondria permeability is dependent upon the level of mitochondrial permeability transition pore; these result in the release of cytochrome c from the inner mitochondrial membrane into the cytosol within the cytoplasm (Yang *et al*., 2014). Once cytochrome c is released from the mitochondrial membrane, cytochrome c then binds to Apaf-1 within the cytoplasm; these results in a complex that will activate caspase-9, and hence activation of apoptosis-inducing caspase-3 (Ghribi *et al.*, 2002*).* In this study, oral administration of aluminium chloride resulted in elevation in the level of apoptosis inducing caspase-3 and this elevation is correlated to the increased level of proapoptotic protein Bax in the group administered aluminium chloride. Result from this study is in line with the study carried out by Fuji et al., 2019, Coadministration of eugenol and aluminium chloride resulted in reduced levels of caspase-3 activation which infers a neuroprotective function. Activation of caspase-3 is is an irreversible indicator of apoptosis and correlated to a reduction in tissue levels of MnSOD as indicated of the result in this study.

5.9 Acetylcholinesterase

Acetylcholine (Ach), the first neurotransmitter to be characterized, has a very significant presence in the brain; it was determined that acetylcholine is essential for learning and memory (Winkler *et al.,* 1995); that is the central cholinergic system is essential for the regulation of cognitive functions (Khan *et al.,* 2012). Acetylcholine deficit, an extensive loss of cholinergic neurones, among other factors, has been held responsible for senile dementia and other degenerative cognitive disorders, including Alzheimer's disease (Kumar and Khanum, 2012). Acetylcholinesterase metabolizes acetylcholine to choline and acetyl-CoA which exist in asymmetric form and globular forms (Lane *et al.,* 2006).

Acetylcholinesterase is a significant biological component of the membrane that contributes to its integrity. Induction of Acetylcholinesterase activity causes faster acetylcholine degradation and consequent lowered stimulation of acetylcholine receptors, which produces a reduction of diverse cholinergic (learning and memory), as well as non-cholinergic (cell proliferation and neurite outgrowth) functions (Singh and Panwar., 2014; Prasad and Muralidhara., 2013).

In this study, endogenous enzyme was estimated by assaying acetylcholinesterase (AchE) activity in brain tissue of rats. Elevated AchE activity levels was observed in the (Group V) aluminium treated group Aluminium chloride has been shown to increase acetylcholinesterase activity in rat and mouse brain (Singh and Goel. 2015). Aluminium chloride has been shown to have a biphasic effect on acetylcholinesterase activity with an initial increase and then a decrease in the brain acetylcholinesterase activity (Kumar, 1998). This might be responsible for the increase as observed in this study as this might be the initial response to aluminium chloride onslaught. This is in concordance with the study by Al-otaibi *et al*., 2018.

Bilkei-Gorzo. (1993) has suggested the effect of aluminium on AChE activity was a direct action of aluminium. Since brain aluminium accumulation increased with the increase in duration of treatment. Decrease in AChE activity at longer duration (60 days) of exposure may be due to the high concentration of aluminium accumulated (Kumar, 1998).

Gulya *et al*. (1990) have suggested that increase in AChE activity following aluminium exposure was due to allosteric interaction between the cation in the brain and a peripheral anionic site of the enzyme molecule.

Decreased activity levels was observed in the eugenol salvaged groups (Groups III and IV) when compared to aluminium treated group (Group V). This was however in agreement with the study carried out by Garabadu *et al.* (2011) who reported eugenol to reverse the stress-induced changes of serotonin and AchE levels in all rat brain regions and such modulation in brain function is attributed to the ability of eugenol to regulate voltage-gated cation channels and the release of neurotransmitters. Groups administered with eugenol only (Group I and II), however showed no significant difference in the activity of acetylcholinesterase when compared with Group VI (control group). Many anticholinergic agents/ drugs cause learning and memory deficits in a variety of cognitive animal models (Zimmerman and Soreq, 2006). Agonist of cholinergic receptors and inhibitors of AchE have been extensively used to increase endogenous acetylcholine levels and thus overcome cognitive deficits. Medicinal plant bioactive metabolites play a key role in the slowing of many pathogenesis and neurodegenerative disorders such as Alzheimer and dementia (Dai *et al.,* 2006). Beneficial effects of these metabolites are proposed to associate with potentiating of antioxidant defences, which is linked to normal aging and neurodegenerative diseases (Morris *et al.,* 2006). Phenolic compounds have anticholinesterase activities, which might be valuable for the treatment of AD (Tumiatti *et al.,* 2008).

In this study, Eugenol was able to restore AchE levels close to the control which might be due to a decrease in gene transcription, translation, and enhanced cholinergic activity thereby increasing cognitive function (Shahidi *et al.,* 2008). Findings are in accordance to studies related to the neuroprotective role of eugenol (Said and Abd, 2017) indicating ameliorative role against aluminium-induced elevated levels of AchE activity and its potential in the attenuation of the severity of neurodegenerative disease, such as Alzheimer's disease.

5.10 Immunohistological and Immunohistochemical Studies

In this study, light microscopic examination of ACAT-1 stained Immunohistochemical sections of Wistar rat's brain regions: cerebral cortex- layer III and V, cerebellar cortex and hippocampus (CA1 and CA3) were conducted.

Acetylcholine (ACh) is a neurotransmitter. Acetylcholine in vertebrates is the major transmitter at neuromuscular junctions, autonomic ganglia, parasympathetic effector junctions, a subset of sympathetic effector junctions, and at many sites in the central nervous system (Hozumi *et al.*, 2011). Its physiological and pharmacological effects, metabolism, release, and receptors have been well documented in several species. ACh has been considered an important excitatory neurotransmitter in the carotid body (CB). Various nicotinic and muscarinic ACh receptors are present in both afferent nerve endings and glomus cells (Hozumi *et al.,* 2011; Rosler *et al.,* 2001) Therefore, ACh can depolarize or hyperpolarize the cell membrane depending on the available receptor type in the vicinity. Binding of ACh to its receptor can create a wide variety of cellular responses including opening cation channels (nicotinic ACh receptor activation), releasing Ca2+ from intracellular storage sites (via muscarinic ACh receptors), and modulating the activities of K+ and Ca2+ channels. Interactions between ACh and other neurotransmitters (dopamine, adenosine, nitric oxide) have been known, and they may induce complicated

responses. Cholinergic biology in the CB differs among species and even within the same species due to different genetic composition. Development and environment influence cholinergic biology (Raskind *et al.,* 1999). Pharmacological data clearly indicate that both muscarinic and nicotinic acetylcholine receptors have a role in the encoding of new memories. Localized lesions and antagonist infusions demonstrate the anatomical locus of these cholinergic effects, and computational modeling links the function of cholinergic modulation to specific cellular effects within these regions. Acetylcholine has been shown to increase the strength of afferent input relative to feedback, to contribute to theta rhythm oscillations, activate intrinsic mechanisms for persistent spiking, and increase the modification of synapses (Tsuruoka *et al.,* 2013). These effects might enhance different types of encoding in different cortical structures. In particular, the effects in entorhinal and perirhinal cortex and hippocampus might be important for encoding new episodic memories. The role of ACh in attention has been repeatedly demonstrated in several tasks. Acetylcholine is linked to response accuracy in voluntary and reflexive attention and also to response speed in reflexive attention. It is well known that those with Attention-deficit/hyperactivity disorders tend to be inaccurate and slow to respond (Bocca *et al.,* 2005; Jia *et al.,* 2004).

Impairment of cognitive capacity of the brain and preferential degeneration of cholinergic neurons are characteristic features of several degenerative diseases of the central nervous system. They include Alzheimer's disease, dialysis, alcohol, and postischemic encephalopathy as well as some forms of Parkinson's disease (Guela and Mesulam, 1988).

Cholinergic neurons, unlike other brain cells, utilize acetyl-CoA not only for energy production but also for acetylcholine (ACh) synthesis. Therefore, suppression of acetylCoA metabolism by different neurotoxic inputs may be particularly harmful for this group of cells.

Toxicants such as heavy metals and other metals have the capacity to reduce the synthesis of acetylcholine, hence its effect on memory (Szutowicz *et al.,* 2000).

In this study we studied the effect of aluminium intoxication and the neuroprotective effect of eugenol on Immuno-histochemical studies of hippocampus (CA1 and CA3), cerebellar and cerebral cortex using anti-ACAT-1.

Administration of rats with aluminium chloride revealed decreased immunoreactivity with ACAT-1 and reduced ACAT-1 expression within the pyramidal cells of the hippocampus (CA1 and CA3), Cerebral cortex and Purkinje cells of the cerebellar cortex region when compared to the control (untreated), which could be responsible for the high level of acetylcholinesterase activity in aluminium treated group.

Lower expression of acetylcholine in the hippocampus of the coupled with poor performance in Morris water maze for memory and learning and high levels of acetylcholinesterase activity and diminished fore grip strength time can be as a result of the administration of aluminium as a neurotoxicant. Szutowicz *et al.,* 2000, reported loss of cholinergic neurones due to administration of aluminium which resulted in memory loss.

Treatment with eugenol resulted in enhanced immunoreactivity and hence enhanced ACAT-1 when compared to the control group.

CHAPTER SIX

Summary, Conclusion and Recommendation

6.1 Summary

In this study, evaluation of the neuroprotective effects of Eugenol on aluminium-induced neurotoxicity in adult rats, the results revealed that exposure to aluminium ($Alcl_3$) resulted in neurotoxicity, which was evident in morphologic, histometric, histological, histochemical and Immunohistochemical alterations in the brain of Wistar rats. Aluminium induced anxiety-related responses, short-and long-term memory impairments and motor deficits in neurobehavioural assessment and altered levels of neurochemical and biochemical constituents which could be related, at least in part, to the cortical and hippocampal Aluminium content that may interfere with local homeostasis.

Findings of the present study reveal the potential of eugenol as a neuroprotective agent in the following studies:

1. Morphologic features of the brain and histometric characteristics of brain regions (cerebral, cerebellar corticies and hippocampus) were preserved relative to the control.

2. Aluminium-induced anxiety-related responses, short-and long-term memory impairments and motor coordination in neurobehavioral assessment were ameliorated relative to the control. Thus eugenol possesses anxiolytic, cognitive/motor and memory enhancing properties.

3. Alterations in the concentration levels of neurotrace elements (Fe, Mn and Mg), MDA and endogenous antioxidants (SOD, CAT, GPx) and endogenous enzyme (AchE) activity levels

and neurotransmitter levels Acetylcholine (Ach) were moderately ameliorated relative to the control which protect neurones against reactive oxygen species (ROS).

4. Prevented the generation of 8-OHdG within the inner mitochondrial membrane, hence preventing oxidative stress within the mitochondria.

5. Prevented reduction in antiapoptotic protein (Bcl-2) levels in the brain of rats and reduced the tissue level proapoptotic protein (Bax).

6. Prevented the activation of caspase-3 within the intrinsic pathway of apoptosis

All these evidences explain the importance of plants in neurodegenerative disorders management in modern day health care. The results of this study revealed that eugenol has neuroprotective properties. These properties explain the rationale for the efficacy for the use of plant based nutriceuticals as a neuroprotective agent in the traditional practice of medicine.

6.2 Contribution to knowledge

The present study has examined the neuroprotective effects of eugenol against aluminium-induced toxicity on the cerebrum, cerebellum and hippocampus in adult Wistar rats. Based on the findings from the present study, the following are contributions to existing knowledge.

1. The results showed that eugenol has an anxiolytic property when the mean values of the time spent (seconds) in the open arm of the elevated plus maze apparatus, of which an increase in time spent in the open arm indicates a low level of anxiety. The mean values on day 21 are 54.62±6.62, 40.21±3.02, 41.22±4.05, 61.31±5.01 and 65.62±3.25 for Groups CTRL, EGH+AC, EGL+AC, EGH and EGL respectively when compared to AC with mean

value of 20.32±4.45.The eugenol treated Groups had a significantly increased time in the open arm when compared to AC group.

2. Eugenol ameliorates the cognitive deficit produced by oral administration of aluminium chloride. Comparing mean values of MWM (seconds) on the 21st day between Group CTRL, EGH+AC, EGL+AC, EGH, EGL includes 4.14±1.33, 9.44±2.91, 3.88±0.18, 5.74±1.23, 4.26±1.02 when compared to the aluminium treated group (AC) 9.39±0.77.

3. Eugenol prevented the intramitochondrial accumulation of 8-Hydroxy-2deoxyguanosine, which can trigger the intrinsic pathway of apoptosis. Mean values obtained from 8-OHdG (ng/ml) includes 3.92±0.03, 21.25±2.01, 15.01±1.15, 4.91±0.32 and 5.25±0.42 for group CTRL, EGH+AC, EGL+AC, EGH and EGL respectively when compared to 42.01±3.32 for AC group.

4. Eugenol prevented apoptosis by preventing the reduction in tissue levels of Bcl-2. Mean values obtained from Bcl-2 (ng/ml) included 17.06±0.62, 6.02±0.72, 9.02±0.45, 13.25±0.21, and 15.25±0.21 for group CTRL, EGH+AC, EGL+AC, EGH and EGL respectively when compared to 5.12±0.12 for AC group.

5. Eugenol prevented activation of apoptosis inducing protein caspase-3. Mean values obtained from Caspase-3 (OD $_{(405}$ nm) included 0.39±0.062, 1.92±0.008, 1.23±0.052, 0.42±0.072 and 0.31±0.015 for group CTRL, EGH+AC, EGL+AC, EGH and EGL respectively when compared to 2.21±0.003 for AC group.

6.3 Conclusion

The result of the present study suggests that eugenol is effective in ameliorating aluminium-induced alterations in the brain (cerebral and cerebellar cortices and hippocampus) of Wistar rats.

The neuroprotective property of eugenol is attributed to its antioxidant properties and ability to mop up reactive oxygen species (ROS). Therefore eugenol is a potential candidate for application in the management and treatment of reactive ROS-induced neurodegenerative diseases such as Alzheimer's disease and Parkinson's disease.

Neuroprotection by eugenol in this study were optimal at 150 mg/kg and this dose showed a maximal efficacy.

6.4 Recommendation

Consumption of plants such as cinnamon, clove, ocimum sanctum, soya bean etc which contains high percentage of eugenol is highly recommended

Further studies are required to investigate the most appropriate and efficacious dose with best neuroprotective activity and in depth studies (such as, ultra-microscopy, stereology, DNA and mitochondrial DNA) are required to confirm findings of the study.

Further long duration studies are required to determine the efficacy of eugenol against amyloid plaques generated by administration of aluminium. Further studies are required using cell culture mediums. Further studies are required as to the mechanism how eugenol is able to prevent apoptosis via the intrinsic pathway. Further studies are required about the efficacy of eugenol with regards to the extrinsic pathway of apoptosis.

Eugenol could be used as a possible treatment for neurotoxicity induced by aluminium chloride

REFERENCES

Ahmad, K.N., Lennox, B. and Mack, W.S. (1989). Estimation of the volume of Leydig cells in man. *Lancet* 2:461.

Ahmed Saad A., Ali F.B., Alaa Naji S. and Ahmed Saad Correspondence (2018). Histological and histometrical characteristics of the vesicular gland in non-breeding rams. *Journal of Entomology and Zoology studies*. 6(1): **1218**-122.

Akifusa S., Kamio, N. Shimazaki,Y. Yamaguchi,N. Nishihara, T and Yamashita, Y. (2009). Globular adiponectin-induced RAW 264 apoptosis is regulated by a reactive oxygen species-dependent pathway involving Bcl-2. *Free Radical Biology & Medicine*, 46(9):1308–1316.

Akinrinade, I. D., Ogundele, O. M., Memudu, A. E., and Obia S. (2013) Cytoarchitecture of the cerebellum in fluoride and aluminium toxicity. *Journal of Cell and Animal Biology*. 7(6) 67-72.

Al-Azemi, M. and Omu, F.E. Kehinde, E.O.Anim,J.T.Oriowo, M.A. and Omu, A.E. (2010).Lithium protects against toxic effects of cadmium in the rat testes. *Journal of assisted reproduction and genetics.* 27(8):469-476.

Al-Otaibi, Sooad Saud and Arafah, Maha Mohamad and Sharma, Bechan and Alhomida, Abdullah Salih and Siddiqi and Nikhat Jamal (2018). Synergistic Effect of Quercetin and alpha-Lipoic Acid on Aluminium Chloride Induced Neurotoxicity in Rats 2018: 300-308.

Alfrey, A.C., LeGendre, G. R. and Kaehny D. (1976). The dialysis encephalopathy syndrome and Possible aluminium intoxication. *The New England Journal of Medicine*. 294(4): 184–188.

Altmann, P., Cunningham, J., Dhanesha, U., Ballard, M., Thompson, J. Marsh F. (1999). Disturbance of cerebral function in people exposed to drinking water contaminated with aluminium sulphate: retrospective study of the Camelford water incident. *British Medical Journal*. 319(7213): 807–811.

Amaral, D. and Lavenex, P. (2007). Hippocampal neuroanatomy.The hippocampus book (first ed.). *New York: Oxford University Press*. p. 37.

Ambreen M., Andrew K., Claire T., and Christopher E. (2017). Aluminium in brain tissue in familial Alzheimer's disease. *Journal of trace element in medicine and Biology.* 40:30-36.

Andersen, B.B. and Pakkenberg, B. (2003). Stereological quantitation in cerebellar of people With Schizophrenia. *British journal of Psychiatry*, 182:354-361

Andersson Maud. (1988). Toxicity and tolerance of aluminium in vascular plants. *Water, Air, & Soil Pollution Trends in Plant Science*. 39 (3–4): 439–462.

Anil, K., Samirata, D., Atish, P. (2009). Protective effect of curcumin (*curcuma longa)* against aluminium toxicity: Possible behavioural and biochemical alterations in rats. *Behavioural brain research* 205: 384-390.

Aremu, D.A. and Meshitsuka, S. (2006). Some aspects of astroglial functions and aluminum Implications for neurodegeneration. *Brain Research Reviews*, 52(1):193-200.

Ashubhantiku, S., Abraham, K., and Rosaheb, K. (2004). Eugenol as an in-vivio radioprotective agent. *Journals of Radiant Research* 45, 435-440.

Asuquo, O.R., Igiri, A.O., Olawoyin, O.O. and Eyong, E.U. (2007). Correlation of histological and histometric changes in rats testes treated with chloroquine phosphate. Nigerian *Journal of Physiological Sciences*, 22 (1-2): 135-139.

Atsumi, T., Iwakura, I., Fujisawa, S., Ueha, T. (2001). Reactive oxygen species generation and photo-cytotoxicity of eugenol in solutions of various pH. *Biomaterials*; 22:1459–1466.

Azzaoui FZ, Ahami A.O, Khadmoui A (2008). Impact of sub-chronic on body weight and recognition memoryof Wistar rat. *Pakistan journal of biological sciences* 11(14):1830-1834.

Barros, H.M., Tannhauser, S.L., Tannhauser, M.A., Tannhauser, M. (1994). The effects of GABAergic drugs on grooming behavior in the open field. *Pharmacology and Toxicology*, 74:339–344.

Bayer, S.A. and Altman, J. (1974). Hippocampal development in the rat. Cytogenesis and morphogenesis examined with autoradiography and low level X-irradiation. *Journal of Comparative Neurology*, 158:55-80.

Beal, M.F., Hyman, B.T., Koroshetz, W. (1993). Do defects in mitochondrial energy metabolism underlie the pathology of neurodegenerative diseases? *Trends in Neurosciences*, 16:125-131.

Becaria, A., Bondy, SC., Campbell, A. (2003). Aluminium and copper interact in the promotion of Oxidative but not inflammatory events: implications for Alzheimer's disease. *Journal of Alzheimer's Disease*, 5:31 – 38.

Becaria, A., Lahiri, D.K., Bondy, S.C., Chen, D., Hamadeh, A., Li, H., Taylor, R and Campbell, A. (2006). Aluminium and copper in drinking water enhance inflammatory or oxidative events specifically in the brain. *Journal of Neuroimmunology* 176: (1-2): 16-23.

Bilkei-Gorzo, A. (1993) .Neurotoxic effect of enteral aluminium. *Food and Chemical Toxicology*. 31 (5) 357–361.

Bingham E. and Cohrssen B. (2012). Patty's Toxicology, 6 Volume Set. *John Wiley & Sons*. p. 244.

Bishop, N.J., Morley, R., Day, J.P., Lucas, A. (1997). Aluminium neurotoxicity in preterm infants receiving intravenous-feeding solutions. *New England Journal of Medicine*; 336: 1557 – 1561.

Blaylock, R.L., Ridgeland, M.S. (2004). Excitotoxicity: A Possible Central Mechanism in Fluoride Neurotoxicity. Fluoride. *Research and Reports*. 37(4):264– 277.

Bocca, B., Forte, G., Petrucci, F., Pino, A., Marchione, F., Bomboi, G., Senofonte, O., Giubilei, F., Alimonti, A. (2005): Monitoring of chemical elements and oxidative damage in patients affected by Alzheimer's disease. *Annali dell'Istituto Superiore di Sanità*; 41(2):197-203.

Bolles, R.C. (1960). Grooming behavior in the rat. *Journal of Comparative Physiological Psychology*, 53:306–10.

Bompart, G.J., Prevot, D.S. and Bascands, J.L. (1990). Rapid automated analysis of glutathione reductase, peroxidase and S-transferase activity. *Clinical Biochemistry* 23:501-504.

Brandies, R., Brandys, Y. and Yehuda, S. (1989). The use of Morris water maze in the study of memory and learning. *International journal of Neuroscience*, 48:29-69.

Burrell, S.A., Exley, C. (2010). There is (still) too much aluminium in infant formulas. *BMC Pediatrics*, 10:63.

Burt, S. (2004). Essential oils, their antibacterial properties and potential applications in Foods-a review. *International of food Microbiology*, 94(3):223-53.

Buraimoh, A., Ojo, S., Hambolu, J. And Adebisi, S. (2011). Effects of oral administration of Aluminium Chloride on the Histology of the Hippocampus of Wistar rats. Current Research, *Journal of Biological Sciences*, 3(5): 509-515.

Buraimoh, A., Ojo, S., Hambolu, J. And Adebisi, S. (2011). Behavioural endpoints of adult Wistar rats, following Aluminium chloride exposure. *Journal of Pharmacology & Toxicology*, 2: 273-276.

Buraimoh, A., Ojo, S., Hambolu, J., and Adebisi, S. (2012). Effects of Aluminium Chloride exposure on the Cerebral Cortex of Adult Wistar Rats Were Not Transferable to the Offspring. *Journal of Biology and Life Science*, 2: 8-10.

Burton, N.C and Guilarte, T.R. (2009). Manganese neurotoxicity, lessons learned from longitudinal studies in nonhuman primates. *Environmental Health Perspectives*, 117, (3), 325-332.

Cai, X. Zhang, H. Tong, D. Tan, Z. Han, D. Ji, F. and Hu, W. (2011). Corosolic acid triggers mitochondria and caspase-dependent apoptotic cell death in osteosarcoma MG-63 cells," *Phytotherapy Research.* 25(9):1354–1361.

Campbell, A. (2002).The potential role of aluminium in Alzheimer's disease. *Nephrology Dialysis and Transplantation*; 17(2): 17 – 20.

Campbell, A., Becaria, A., Lahiri, D.K., Sharman, K., Bondy, S.C. (2004). Chronic exposure to Aluminium in drinking water increases inflammatory parameters selectively in the brain. *Journal of Neuroscience Research*, 75, (4), 565-572.

Carson, B.L. (2000). Aluminum compounds. Review of toxicological literature, Abridged Final Report: 84 p. *integrated laboratory Systems, Research Triangle Park*, North Carolina.

Casson R.J., Chidlow G., Ebneter A., Wood J.P., Crowston J and Goldberg I. (2012). Translational neuroprotection research in glaucoma: a review of definitions and principles. *Clinical and Experimental Ophtalmology*. 40(4): 350-357.

Chaieb, K., Hajlaoui, H., Zmantar, T. (2007). The chemical composition and biological activity of clove essential oil, *Eugenia caryophllata* (Syzigium aromaticum L Myrtaceae): A short review. *Phytotherapy Research*, 21(6):501-6.

Chakravarthi, k.k., Ramakrishna, A., Narayan R.S. (2012). Effect of Glycyrrhiza glabra root extract on learning and memory Albino Wistar rats. *International journal of Biological and Medical Research*, 3(3): 2059-2064.

Cheng, K.C., Cahill, D.S., Kasai, H., Nishimura, S., Loeb, L.A., 1992. 8-Hydroxyguanine, an abundant form of oxidativeDNA damage, causes G™T and A™C substitutions. *Journal of Biological Chemistry* 267, 166–172.

Christmas, A. J. and Maxwell, D. R. A. (1970) comparison of the effects of some benzodiazepines and other drugs on aggressive and exploratory behavior in mice and rats. *Neuropharmacology* 9:17-29.

Chusid, J.G., Pacella, B.L., Kopelof, L.M. and Kopeloff, N. (1951). Chronic epilepsy in the Monkey following multiple intracerebral injection of alumina cream. *Proceedings of the Society for Experimental Biology and Medicine*, 78:53–54.

Colbern, D.L., Gispen, W.H. (1988). Neural mechanisms and biological significance of Grooming behavior. *Annals of New York Academy of Sciences New York*; 426: 123-145.

Colomina T., Roig J., Terrente M., Dominigo J. and Paloma V. (2005).

Concurrent exposure to aluminum and stress during pregnancy in rats: Effects on postnatal development and behavior of the offspring, *Neurotoxicology and Teratology* 27(4):565-74.

Connor, J., Snyder B., Beard J., Fine, R. and Mufson, EA Histochemical study of Iron, transferrin and ferritin in Alzheimer's disease brains. *Journal of Neuroscience Research,* 31:327-335.

Cooke, M.S., Evan, M.D., Dizdarogev, R.J., Wine, C.J., (2003). Oxidative DNA damage: mechanisms, mutation and disease. *FASEB Journal*. 17, 1195–1214.

Costall, B., Jones B., Kelly M., Naylor R., Tomskins D. (1989). Exploration of mice in a black and white test box: Validation as a model of anxiety. *Pharmacology Biochemistry and Behavior*, 32:777-785.

Couette, M., Boisse, M.F., Maison, P., Brugieres, P., Cesaro, P., Chevalier, X., Gherardi, R.K., Bachoud-Levi, A.C., Authier, F.J. (2009). Long-term persistence of vaccine-derived aluminum hydroxide is associated with chronic cognitive dysfunction. *Journal of Inorganic Biochemistry.* 103(11):1571-1578.

Crichton, R.R., Wilmet, S. Legssyer, R., and Ward R. J, (2002). Molecular and cellular mechanisms of iron homeostasisand toxicity in mammalian cells. *Journal of Inorganic Biochemistry*, 91(1):9–18.

Critchon, R.R., Dexter D.T. and Ward R.J. (2007). Metal based neurodegenerative diseases from molecular mechanism to therapeutic strategies. *Coordination Chemistry reviews*, 1:1-11.

Crusio, W. E. (2001). Genetic Dissection of Mouse Exploratory Behavior. *Behavioural Brain Research,* 125(1-2):127-132.

Cryan, J and Holmes, A. (2005). The ascent of mouse: advances in modelling human depression and anxiety. *Nature reviews and drug discovery,* 4:775-790.

Cunat, L., Lanhers, M.C., Joyeux, M., and Burnel, D. (2000). Bioavailability and intestinal absorption of aluminum in rats: effects of aluminium compounds and some dietary constituents. *Biological Trace Element Research.* 76(1):31-55.

Cunningham, C., Campion, S., Lunnon, K., Murray, C.L., Woods, J.F., Deacon, R.M., Rawlins, J.N., Perry, V.H. (2009). Systemic inflammation induces acute behavioural and cognitive changes and accelerates neurodegenerative disease. *Biological Psychiatry* 65, (4):304-312.

D'hooge R and De Deyn P. (2001). Applications of Morris water maze in the study of learning and memory. Brain Research review, 36:60-90.

Dai Q., Borenstein A.R., Wu Y., Jackson J.C and Larson E.B. (2006). Fruit and Vegetable

juices and Alzheimer's disease: The kame project. *American Journal of Medicine*. 119:751-759.

Dantzer, R.; Kelley, K.W. (2007).Twenty years of research on cytokine induced sickness behavior. *Brain Behaviour and Immunity.* 21(2):153-160.

Darbre, P. D. (2006). Metalloestrogens: an emerging class of inorganic xenoestrogens with Potential to add to the oestrogenic burden of the human breast. *Journal of Applied Toxicology*, 26 (3): 191–7.

Dauncey, M.J. (2009). New insights into nutrition and cognitive neuroscience; symposium On early nutrition and later disease: current concepts, research and implications. *Proceedings of the Nutrition Society*, 68:408-415.

Debapriya Garabadu., Ankit Shah., Sanjay Singh and Sairam Krishnamurthy. (2015). Protective effect of eugenol against restraint stress-induced gastrointestinal dysfunction: Potential use in irritable bowel syndrome, *Pharmaceutical Biology*, 53(7):968-974.

Deloncle, R., Guillard, O., Huguet, F., Clanet, F. (1995). Modification of the blood-brain barrier through chronic intoxication by aluminum glutamate. Possible role in the etiology of Alzheimer's disease. *Biological Trace Element Research*: 47(1-3):227-233.

Ding R. and Yang Y. (2010). Aluminum chloride induced oxidative damage on cells derived from hippocampus and cortex of ICR mice. *Brain research journals* 1324: 96 – 102.

Dohmeier, C., Loos, D., and Schnöckel, H. (1996). Aluminum and Gallium Compounds: Syntheses, Structures, and Reactions. *Angewandte Chemie International Edition*. 35: 129–149.

Dolara Piero. (2014). Occurrence, exposure, effects, recommended intake and possible dietary Use Of Selected trace compounds (aluminium, bismuth, cobalt, gold, lithium, and nickel, silver). *International Journal of Food Sciences and Nutrition*. 65 (8): 911–924.

Drapeau E., Mayo W., Aurousseau C., Moal M., Piazza P., and Abrous D.N. (2003). Spatial memory performances of aged rats in water maze predict levels of hippocampal neurogenesis. *Proceedings of the national academy of sciences*, 100(24):14385-14390.

Drury, R.A.B., Wallington, E.A., Cameron, S.R. (1967). Carleton's Histological technique. 4th ed., *oxford university*, *New York.*

Duce J.A., Tsatsanis, A., Cater M.A. (2010). Iron-export ferroxidase activity of β-amyloid precursor protein is inhibited by zinc in Alzheimer's disease. *Cell*. 142(6):857–867.

Durrant P.J. and Durrant. K. (2014). *Introduction to Advanced Inorganic Chemistry, Longman, London,* 2014, p. 532.

Edwards, M., Kent, T.A., Rea H.C., Wei J., Quast, M., Izumi, T., Mitra S., Perez-Polo J.R. (1998). APE/Ref-1 responses to ischemia in rat brain. *Neuroreport* 1998(9):4015–4018.

Ehsan K. Narges J. Farid F. Behnam K. and Massoud H. (2014). Is Bax/Bcl-2 ratio considered as a prognostic Marker with age and tumor Location in Colorectal Cancer? *Iranian Biomedical Journal* 19(2): 69-75

Elif Inan-Eroglu and Aylin Ayaz. (2018). Is aluminum exposure a risk factor for neurological disorders? *Journal of Research in Medical Sciences*. 23: 51-65.

Elmore S. (2007). Apoptosis: a review of programmed cell death,*Toxicologic pathology*, 35(4):495-516

EMMI, (1997). Biological tissues; Analytical Methods for Determining Copper in environmental Samples. *Analytical methods,* p.196.

Esparza Jos.L and Gomez Mercedes and Domingo Jos (2019). Role of Melatonin in Aluminum-Related Neurodegenerative Disorders: a Review. *Biological trace element research*, 188(1):60-67.

Evans, P.H., Yano, E., Klinowski, J., Peterhans, E. (1992). Oxidative damage in Alzheimer's dementia, and the potential etiopathogenic role of aluminosilicates, microglia and micronutrient interactions. *Experimentia Supplementum*, 62:178-189.

Evarts, E.V., Fromm, C., Kroller, J., and Jennings, V.A. (1983). Mortor cortex control of Fibely graded forces. *Journal of Neurophysiology*, 49:1199-1215.

Exley, C. (2011). Reflections upon and recent insight into the mechanism of formation of hydroxyaluminosilicates and the therapeutic potential of silicic acid. *Coordination Chemistry Reviews;* 256(1–2):82–88.

Exley, C. (2009). Darwin, natural selection and the biological essentiality of aluminium and silicon. *Trends in Biochemical Sciences* 34:589–593.

Exley, C. (2009). Aluminium and medicine. Molecular and supramolecular bioinorganic Chemistry: applications in medical sciences. *New York F: Nova Biomedical Books*; 2009. p. 45–68.

Exley, C. (2004). The pro-oxidant activity of aluminium. *Journal of Free Radical Biology and Medicine, 36*(3):380-387.

Exley, C., Siesjo, P., Eriksson, H. (2010). The immunobiology of aluminium adjuvants: how do they really work? *Trends in Immunology*, 31(3):103-109.

Exley, C., Korchazhkina, O., Job, D., Strekopytov, S., Polwart, A.,Crome, P.(2006). Non-invasive therapy to reduce the body burden of aluminium in Alzheimer's disease. *Journal Alzheimer's disease*, 10(1):17–24; *discussion* 29-31

Exley, J.R. (2006). Aluminum in hippocampal neurons from humans with Alzheimer's disease. *Neurotoxicology*; 27(3):385–94.

Fan Y., Zou B., Ruan Y., Pang Z., and XU Z.C. (2005). In *vivo* demonstration of a late depolarizing postsynaptic potential in CA1 pyramidal neurons. *Journals of Neurophysiology*, 93: 7598-7609.

Fang, F., Ning Y, Zhanhui, F., Xiangqin, L., Zheng, X., Ming, W., Hua, H., Yong, Y. (2013). Alzheimer's disease Animal Model by Aluminum, Beta-Amyloid and Transforming Growth Factor Beta-1. *Aging and Neurodegeneration*, 1(1): 15-19.

Feibo X. Yanfen L., Hansong Z. and Kaiyuan Y. (2017). Aluminum chloride caused liver dysfunction and mitochondrial energy metabolism disorder in rat. *Journal of inorganic biochemistry*. 10(3): 1002-1018.

Fentress, J.C. (1988). Expressive contexts, fine structure and central mediation of rodent grooming. *Annals of New York Academy of Sciences*;525:18–26.

File, S. E. (1985). Models of anxiety. *British Journal Clinical Practice* 38:15-20.

Flarend, R.E., Hem, S.L., White, J.L., Elmore, D.; Suckow, M.A., Rudy, A.C., Dandashli, E.A. (1997). In vivo absorption of aluminium containing vaccine adjuvants using 26Al. *Vaccine.* 15(12- 13):1314-1318.

Flaten, T. P. (2001). "Aluminium as a risk factor in Alzheimer's disease, with emphasis on drinking water, *Brain Research Bulletin*, 55(2):187–196.

Flora S.J.S. (2002). Nutritional Components Modify Metal Absorption, Toxic Response and Chelation therapy. *Journal of Nutrition Environmental Medicine*: 12:51-65.

Fonnum, F. and Lock, E.A. (2000). Cerebellum as a target for toxic substances. *Toxicology letters*, 112-113:9-16.

Forbes, W. F. and McLachlan, D. R. C. (1996). Further thoughts on the aluminium—alzheimer's disease link, *Journal of Epidemiology and Community Health*, 50(4):401–403.

Frank, H. (2006). Aluminum a Toxic Element Link to many Diseases in Humans.

Frank, W.B. (2009). *Aluminum.* Ullmann's Encyclopedia of Industrial Chemistry. *Wiley-VCH* pg 30-33.

Frecker M.F. (1991). "Dementia in Newfoundland: identification of a geographical isolate? *Journal of Epidemiology and Community Health*, 45(4):307–311.

Frey, A., Neutra, M.R., Robey, F.A. (1997). Peptomer aluminium oxide nanoparticle conjugates as systemic and mucosal vaccine candidates: synthesis and characterization of a conjugate derived from the C4 domain of HIV-1MN gp120. *Bioconjugate Chemistry. 8*, (3), 424-433.

Fujii, M., Kishibe, M., Honma, M., Anan, T. and Ishida-Yamamoto, A. (2019). Aluminum Chloride–Induced Apoptosis Leads to Keratinization Arrest and Granular Parakeratosis. *The American Journal of Dermatopathology*, doi:10.1097/dad.0000000000001513

Fujimura M., Morita-Fujimura Y, Narasimhan P.J, Copin C., Kawase M., Chan P.H. (1999). Copper-zinc superoxide dismutase prevents the early decrease of apurinic/apyrimidinic endonuclease and subsequent DNA fragmentation after transient focal cerebral ischemia in mice. *Stroke declocle*, 30:2408–2415.

Fujisawa, S., Atsumi, T., Kadoma, Y. (2001). Radical generation, radical-scavenging activity, and cytotoxicity of eugenol compounds. *Toxicology in Vitro*, 13(4):269-79.

Fujisawa, S., Atsumi, T., Kadoma, Y., Sakagami, H. (2002): Antioxidant and pro-oxidant action of Eugenol-related compounds and their cytotoxicity. *Toxicology*: 177:39–54.

Garabadu, D., Shah, A., Ahmad, A., Joshi, V.B., Saxena, B., Palit, G., Krishnamurthy, S. (2011) Eugenol as an anti-stress agent: modulation of hypothalamic-pituitary-adrenal axis and brain monoaminergic systems in a rat model of stress. *Stress*; 14:145-55.

Garay, P.A., McAllister, A.K. (2010). Novel roles for immune molecules in neural development:implications for neurodevelopmental disorders. *Frontiers in Synaptic Neuroscience* 2, 136.

Garcıa, J. L., Esparza, M., Giralt, M., Romeu, J. L., Domingo, M. and Gomez M. (2010). Protective role of melatonin on oxidative stress status and RNA expression in cerebral cortex and cerebellum of a*β*pp transgenic mice after chronic exposure to aluminum," *Biological Trace Element Research*, 135(1–3):220–232.

Garman, R.H. (2011). Histology of the Central Nervous System. *Toxicologic pathology*, 39: 22-35.

Ghribi,O. Herman, M. and Savory, J. (2002).The endoplasmic reticulum is the main site for caspase-3 activation following aluminum-induced neurotoxicity in rabbit hippocampus, *Neuroscience Letters*, 324(3):217–221.

Gibson, G.E., Park, L.C., Zhang, H., Sorbi, S., Calingasan, N.Y. (1999). Oxidative stress and a key metabolic enzyme in Alzheimer brains, cultured cells, and an animal model of chronic oxidative deficits. *Annals New york Academic Sciences*. 893:79-94.

Gilbert, P.E., and Brushfield A.M. (2009). The role of the CA3 hippocampal sub region in spatial memory. A process oriented behavioral assessment. *Progres in Neuropsychopharmacology and Biological Psychiatry*; 33:774–81.

Gilgun-Sherki Y., Melamed, E., and Offen, D. (2001). Oxidative stress induced Neurodegenerative diseases: the need for antioxidants that penetrate the blood brain barrier. *Neuropharmacology* 40: 959-975.

Gilliams-Francis K. L., Quaye A. A., Naegele J. R. (2003). PARP cleavage, DNA fragmentation, and pyknosis during excitotoxin-induced neuronal death. *Experimental Neurology* . 184(1):359–372

Gluck, M., Mercado, E., Myers, C. (2014). *Learning and Memory from Brain to Behavior Second Edition. New York: Kevin Feyen*. p. 416.

Greenamyre, J.T. (1991). Neuronal bioenergetic defects, excitotoxicity and Alzheimer's disease: "use it and lose it". *Neurobiology of Aging*.12(4):334-336; *discussion* 352-335.

Griswold W.R., Reznik, V., Mendoza, S.A., Trauner, D., Alfrey, A.C. (1983). Accumulation of aluminium in a nondialysed uremic child receiving aluminium hydroxide. *Pediatrics*; 71:56 – 8.

Golub, M.S., Keen, C.L., Han, B. and Gershwin, M.E. (2000). Effects of dietary aluminum Excess and manganese deficiency on neurobehavioral endpoints in adult mice. *Toxicology and Applied Pharmacology* 112(1):154-60.

Gómez, M., Esparza, J.L., Cabré, M., García, T., Domingo J.L. (2008). Aluminum exposure through the diet: metal levels in AbPP transgenic mice, a model for Alzheimer's disease. *Toxicology*; 249: 214–219.

Gómez M, Esparza JL, Nogués MR, Giralt M, Cabré M, Domingo JL (2005). Pro-oxidant activity of aluminum in the rat hippocampus: gene expression of antioxidant enzymes after melatonin administration. *Free Radical Biology and Medicine*; 38: 104-11.

Gordon Klein (2005). Aluminum: new recognition of an old problem. *Current opinion in pharmacology*. 5(6):637-640.

Guela. C., and Mesulam, M.M. (1988). Cholinergic system and related neuropathological Predilection patterns in Alzhcimer's disease. In: Terry, R.D., Katzman, R,, and Bick, K.L., (eds), *Alzheimer Disease, Raven Press, New York*, pp. 263-291.

Gulya, K., Rakonczay, Z., Kasa, P. (1990). Cholinotoxic effects of aluminium in rat brain. *Journal of Neurochemistry* 54(3):1020-1026.

Guénette, S.A., Ross, A., Marier, J.F. (2007). Pharmacokinetics of eugenol and its effects on Thermal hypersensitivity in rats. *European Journal of Pharmacology*; 562(1-2):60-67.

Halliwell B., (1992). Reactive Oxygen species and central nervous systems. *Journal of Neurochemistry*. 59:1609-1623.

Halliwell, B. and Gutteridge, J.M.C. (1999). Free Radicals in Biology and Medicine (3rd ed.), *Oxford Science Publications*. New York

Halliwell, B., Gutteride J.M. (2007). Free radicals in biology and medicine. 4th edition. New York: *Oxford University Press*; 2007.

Harrison, F., Reiserer, R., Tomaken., McDonald, M. (2006). Spatial and non-spatial escape strategies in Barnes maze. *Learning and Memory* 13:809-819.

Haruhiko, A., Masato, H., Fuyuki, K., Hiromi, K., Momoko, C., Masako, F., and Takeshi, T. (2011). Long-term oral intake of aluminium or zinc does not accelerate Alzheimer pathology in AbPP and AbPP/tau transgenic mice. *Neuropathology* 1440-1789.

He, L., Shi, H., Liu, T., Xu, Y., Ye, K., and Wang, S. (2011). Effects of extremely low frequency magnetic field on anxiety level and spatial memory of adult rats. *Chinese Medical journal*. 124(20):3362-3366.

Henneberry, R.C. (1989). The role of neuronal energy in neurotoxicity of excitatory amino acids. *Neurobiology of aging*, 10:611-613.

Hewitt, C.D., Savory, J., Wills M.R. (1990). Aspects of aluminium toxicity. *Clinics in Laboratory Medicine.* 10:403 – 422.

Hihara, B., Lloyd, H., Adler-Ralph P.I., Latanision-Ronald, M. (2013). Environmental Degradation of Advanced and Traditional Engineering Materials. *CRC Press.*

Himkar R.K., Tharanath V., Nagi, Reddy K.B., Sharma, P.V., and Reddy O.V. (2010). Studies on hepatoprotective effect of hexane extract of hexane extract of *Dillenia indica* against CCl_4 induced toxicity and its safety evaluation in Wistar albino rats. *Research Journal of Pharmaceutical, Biological and Chemical Sciences*. 1(3):441-450.

Hirata-Koizumi M, Fujii S, Ono A, Hirose A, Imai T, Ogawa K, Ema M, Nishikawa A.(2011). Evaluation of the reproductive and developmental toxicity of aluminium ammonium sulfate in a two-generation study in rats. *Food and chemical toxicology*, (49):1948-59

Holland, G.R. (1996). Experimental trigeminal nerve injury. *Critical reviews in oral Biology and Medicine*. 7(3): 237-258.

Holleman, E., Wiberg, N., Wiberg, Lehrbuch derAnorganischen Chemie, Walter de Gruyter Berlin. (1995). Royal Danish Academy of Sciences and Letters *(1827).* Det Kongelige Danske Videnskabernes Selskabs philosophiske og historiske afhandlinger *The philosophical and historical dissertations of the Royal Danish Science Society (in Danish). Popp. pp*. XXV–XXVI.

Hozumi, I., Hasegawa, T., Honda, A., Ozawa, K., Hayashi, Y., Hashimoto, K., Yamada, M., Koumura, A., Sakurai, T., Kimura, A., Tanaka, Y., Satoh, M., Inuzuka, T. (2011): Patterns of levels of biological metals in CSF differ among neurodegenerative diseases. *Journal of Neurological Sciences*.15; 303(1-2):95-9.

Huang, S.H, Lin, C. M and Chiang, B. H. (2008). Protective effects of Angelica sinensis extract on amyloid beta-peptide-induced neurotoxicity, *Phytomedicine*, 15(9):710-721.

Huda, M.A., and Zaid, A.A. (2007). Photo-histometry a modified computer assisted Morphometric measurement program. *Journal of Faculty of Medicine, Baghdad*, 49(1):139-145.

Hussain, A., Brahmbhatt, K., and Priyani, A. (2011). Eugenol enhances the chemotherapeutic potential of gemcitabine and induce anticarcinogenic and anti-inflammatory activity in human cervical cancer cells. *Cancer Biotheraphy Radiopharmaceuticals*; 26(5):519-27.

Hwang S., Shih, P., and Yen, G. (2012). Neuroprotective Effects of citrus Flavonoids. *Journal Of Agricultural and Food Chemistry*, 60 (4): 877-885.

Ibrahim, K. and Heba, K. (2013). Effects of aluminum on rat cerebellar cortex and the possible protective role of Nigella sativa: a light and electron microscopic study. *The Egyptian Journal of Histology*, 36:210-213.

Ige S.F., Akhigbe R.E., Edeogho O., Owolabi O.Q., Oyekunle O.S., Ajayi A.F. (2011). Hepatoprotective activities of *allium cepa* in cadmium-treated rats. *International journal of Pharmaceutical Sciences* 3(5):60-63.

Indebir Singh (2018).Human Embryology. 11th edition *Jaypee Brothers Medical Publishers (P)*

Ltd. Pg 55

Ivana, D., Marina, D., Ankica J. And Miodrag, C. (2009). Effects of L-NAME, a non-Specific nitric oxide synthase inhibitor, on AlCl3induced toxicity in the rat forebrain cortex. *Journal of veterinary science*, 10(1):15-22.

Iversen, S. D. (1970). Animal models of anxiety and benzodiazepine actions. *Arzneimittel-Forschung*: 30:862-868.

Izumi, T., Wiederhold, L.R., Roy, G., Roy, R., Jaiswal, A., Bhakat, K.K., Mitra, S., Hazra, T.K. (2003). Mammalian DNA base excision repair proteins: their interactions and role in repair of oxidative DNA damage. *Toxicology*, 193:43–65.

Jelsing, J., Gundersen, H., Nielsen, R., Hemmingsen, R., and Pakkenberg B. (2006). The postnatal development of cerebellar Purkinje cells in the Gottingen minipig estimated with a new stereological sampling technique- the vertical bar fractionators. *Journal of anatomy*. 209:321-331.

Jia, J.P., Jia, J.M., Zhou, W.D., Xu, M., Chu C.B., Yan, X., Sun, Y.X. (2004). Differential acetylcholine and choline concentrations in the cerebrospinal fluid of patients with Alzheimer's disease and vascular dementia. *Chinese Medical Journal* 117(8):1161-1164.

John, M S. (2010). Schematic drawing of elevated Plus Maze (EPM) experiment for behavior tests with rats. *Psychopharmacology* 92:325-385.

Jones, L.C., Beard, J.L., and Jones, B.C. (2008). Genetic analysis reveal polygenic influences on Iron, copper and zinc in mouse hippocampus with neurobiological implications. *Hippocampus.* 18: 398-410.

Kalantariapour, T.P., Asadi-Shekaari., Basri, M., Gholaamhosseinian N.A. (2012). Cerebroprotective effect of date seed extract (*Phoenix dactylifera)* on cerebral ischemia in male rats. *Journal of Biological Sciences* 12:180-185.

Kalueff, A.V., Tuohimaa, P. (2004). Contrasting grooming phenotypes in C57Bl/6 and 129S1/SvImJmice. *Brain Research*, 1028:75–82.

Kaizaki, A., Tien, L., Pang, Y., Cai, Z., Tanaka, S., Numazawa, S., Bhatt, A.J and Fan L. (2003). Celecoxib reduces brain doperminergic neuronal dysfuction and improves sensorimotor behavioural performance in neonatal rats exposed to lipopolysaccharide. *Journal of neuroinflamation*, 10(45): 1-14.

Kalemba, D., Kunicka, A. (2003): Antibacterial and antifungal properties of essential oils. *Current Medicinal Chemistry*, 10:813–829.

Kankofer, M. (2002). Superoxide dismutase and glutathione peroxidase activities in bovine

placenta spectrophotometric and electrophoretic analysis. *Journal of Véternary medicine*, 153(2):121-124.

Karaman, S.X., Tu¨tem, E., Baskan, K.S., Apak, R. (2009): Comparison of total antioxidant capacity and phenolic composition of some apple juices with combined HPLC-CUPRAC assay. *Food Chemistry*, 120:1201–1209.

Karl, A., Schaefer, M., Malta, L.S., Dörfel, D., Rohleder, N., Werner, A. (2006). A meta-analysis of structural brain abnormalities in PTSD. *Neuroscience and Biobehavioral Reviews*. 30 (7):1004–31.

Katayama, T., and Nagai, I. (1960). Chemical significance of the volatile compounds of spices in the food preservative viewpoint-IV. Structure and antibacterial activity of terpenes. *Bulletin Japanese Society Science Fisheries*, 26(1):29-33.

Kawahara, M., Kato-Negishi, M. (2011). Link between aluminum and the pathogenesis of Alzheimer's disease: the integration of the aluminum and Amyloid cascade hypothesis. *International Journal of Alzheimer's disease*, 276393.

Khan, R.A., Khan, M.R., and Sahreen, S. (2012). Brain antioxidant markers, cognitive Performance and acetylcholinesterase activity of rats: efficiency of *Sonchus asper*. *Behavioural and Brain functions*. 8:21 p1-7.

Khare, P., Yadav, G., Chuadhary, S., and Singh, L. (2014). Investigation on the protective effects of *cressa cretica* extract on scopolamine induced memory impairment. International journal of Pharmacology and Toxicology, 2(1): 13-16.

Kim, S., Nah, S.Y., and Rhim, H. (2008). Neuroprotective effects of Ginseng saponins against L-type Ca^{2+} channel-mediated cell death in rat cortical neurons. *Biochemical and Biophysical Research Communications*, 365(3): 399-405.

Kruck, T.P.; Cui, J.G.; Percy, M.E.; Lukiw, W.J. (2004). Molecular shuttle chelation: the use of ascorbate, desferrioxamine and Feralex-G in combination to remove nuclear bound aluminium. *Cell and Mollecular Neurobiology*. 24(3):443-459.

Kochenborger, L., Levone, B.R., Da silva, E.S. (2014). The microinjection of a cannabinoid agonist into the accumbens shell induces anxiogenesis in the elevated plus-maze. *Pharmacology Biochemistry and Behaviour*, 124:160-166.

Koehl, M., Abrous, DN. (2011). A new chapter in the field of memory: Adult hippocampal neurogenesis. *European Journal of Neuroscience*, 33:1101–1114.

Kulkarni, P.D., Ghaisas,M.M., Chivate, N.D., Sankpal, P.S. (2011). Memory enhancing Activity of *Cissampelos pariera* in mice. *International journal of Pharmacy and Pharmaceutical sciences*, 3(2): 206-211.

Kumar, S. (1998). Biphasic effect of aluminium on cholinergic enzyme of rat brain *Neuroscience letters*, (248) 121-123.

Kumar, V., Bal, A., Gill, K.D., 2008. Impairment of mitochondrial energy metabolism in different regions of rat brain following chronic exposure to aluminium. Brain Res. 1232, 94–103.

Kumar, V., Bal, A., Gill, K.D., (2009). Susceptibility of mitochondrial superoxide dismutase to aluminium induced oxidative damage. *Toxicology* 255, 117–123.

Kumar, G.P., and Khanum, F. (2012). Neuroprotective potential of Phytochemicals. *Pharmacognosy review*, 6(12) 81-90.

Kumar, V., Abbas, A.K., Aster, J.C., and Fausto, N. (2009). Cell death. In. Robbins and cotran Pathologic basis of Disease. 8th ed., *Philadephia-W.B Saunders Company*. P.4-5.

Kumar, V., Bal, A., Gill, K.D. (2008). Impairment of mitochondrial energy metabolism in different regions of rat brain following chronic exposure to aluminium. *Brain Research,* 1232, 94-103.

Kurian R, Arulmozhi DK, Veeranjaneyulu A. (2006). Effect of eugenol on animal models of nociception. *Indian Journal Pharmacology*; 38(5):341-5.

Laekeman, S.M., Hoof, V.L., Haemers, A. (1990): Eugenol A valuable compound for in vitro experimental research and worthwhile for further in vivo investigation. *Phytotherapy and Research*, 4:90–96.

Lai, P.C., Huang, Y.T., Wu, C.W., Lai C., Wang, P.G., and Chiu, T.H. (2011). Ceftriaxone attenuates hypoxic-ischemic brain injury in neonatal rats. *Journal of Biomedical Science,* 18(69): 1-10.

Lane, R.M., Potkin, S.G., and Enz, A. (2006). Targeting acetylcholinesterase and butyrlcholinesterase in dementia. *International Journal of Neuropsyco-pharmacology*. 9: 101-124.

Leugeb, S., Leutgeb, J.K., Treves, A., Moser, M.B., and Moser, E.I. (2004). Distict ensemble codes in the hippocampal areas CA3 and CA1. *Science*, 305(5688): 1295-1298.

Levites, Y., Amit, T., Youdim, M.B., and Mandel, S. (2002). Involvement of Protein kinase C - activation and cell survival/ cell cycle genes in green tea polyphenol epigallocatechin 3-gallate neuroprotective action. *Journal of Biological chemistry*, 277(34): 30574-30580.

Li, J.M., Shah, A.M., (2004). Endothelial cell superoxide generation: regulation and relevance for cardiovascular pathophysiology. *American Journal* of *Physiology* Regulatory, *Integrative and Comparative* Physiology 287, 1014–1030.

Li, X., Zheng, H., Zhang, Z., Li, M., Huang, Z., Schluesener, H.J., Li, Y., Xu, S. (2009). Glia activation induced by peripheral administration of aluminum oxide nanoparticles in rat brains. *Nanomedicine: 5*(4):473-479.

Lister, R.G. (1987). The use of a plus maze to measure anxiety in the mouse. *Psychopharmacology*, 92: 180-185.

Liu, X., Yi, S.L., Gao, S.P .(2011). Effect of the Lead Stress on the Activity of SOD-POD and CAT in Fragrant Plantain lily Seedling with Purple Calyx. *Journal of Anhui Agricultural Sciences*, 14:8244-8246.

Liu, Y., Wen, T., Feng, J.D. (2001). Effects of eugenol on PEG-2 and cAMP contents in arcuate nucleus brain tissue of pyrogeneous rabbits. *Zhong Guo Yi Ke Da Xue Xue Bao* 30(5):339-41.

Lory Alton and Staff Writer. (2017). High levels of aluminium in 8 percent of people tested for toxicity. *Natural 365.com*.

Lu, S.M., Chen, Z.L., Chen, J.X. (2008). A study on in vitro bacteriostatic action of eugenol. *Shi Pin Ke Xue*; 29(9):122-4.

Ludolph, A.C., Riepe, M., Ullrich, K. (1993). Excitotoxicity, energy metabolism and neurodegeneration. *Journal of Inherited Metabolic. Disorders*, 16(4):716-723.

Machado, M., Dinis, A.M., Salgueiro, L. (2011). Anti-giardia activity of Syzygium aromaticum essential oil and eugenol: Effects on growth, viability, adherence and ultrastructure. *Experimental Parasitology*, 127(4):732-9.

Machmud, Edy, Jubhari, Eri Hendra, & Ardiansyah, Muchammad. (2019). Histometry Analysis of Osteoclasts, Osteoblasts and Fibroblasts in Immediate Placement Implants with Addition of Aloe Vera Extract. Pesquisa Brasileira em Odontopediatria e Clínica Integrada, 19, e4537. Epub October 31, 2019.https://doi.org/10.4034/pboci.2019.191.74

Mahboob, M., Rahman, M.F., and Grover, P. (2005). Serum lipid peroxidation and oxidant Enzyme levels in male and female diabetic patients. *Singapore Medical Journal*, 46(7):322-334.

Manal, S., Azza, H. And Eman, T. (2010). The Protective Effect of Vitamin E against the neurotoxic Effect of Aluminum Cholorid in Male Albino Rat. *Journal of American Science*, 6(10): 978-991.

Mander, P., and Brown, G.G. (2005). Activation of microglial NADPH oxidase is synergistic With glial iNOS expression in inducing neuronal death: a dual-key mechanism of inflammatory neurodegeneration. *Journal of Neuroinflammation*, 2: 10.1186/1742-2094-2-20.

Mantha, A.K., Dhiman, M., Taglialatela, G., Perez-Polo, R.J., Mitra, S. (2012). Proteomic study of Amyloid beta (25–35) peptide exposure to neuronal cells: Impact on APE1/Ref1's protein-protein interaction. *Journal of Neuroscience Research*, 90:1230–1239.

Marcus Ferrone and Mathew Geracci (2007). A Review of the Relationship between Parenteral and Metabolic Bone Disease. *Nutrition in clinical practice*. Vol 22(3): 329-339.

Martin, J.H. (2003). Limbic system and cerebral circuits for emotions, learning, and memory. Neuroanatomy: text and atlas (third ed.). *McGraw-Hill Companies*. p. 382.

Martin, J.P., Dailey, M., and Sugarman, E. (1987). Negative and Positive assays of superoxide dismutase based on hematoxylin autoxidation. *Archives of Biochemistry and Physics*, 255:329-336.

Martyn, C.N., Osmond, J. A. Edwardson, D. J. P. Barker, E. C. Harris, and R. F. Lacey. (1989). "Geographical relation between Alzheimer's disease and aluminium in drinking water," *The Lancet*, vol. 1, no. 8629, pp. 59–62, 1989.

Masae, I., Keiko, M., Masataka, Y. (2005). Antioxidant action of eugenol compounds: role of metal ion in the inhibition of lipid peroxidation. *Food Chemical Toxicology*, 43(3):461-6.

Mathew M., Dorcars U., Andrew K. and Christopher E. (2018). Aluminium in brain tissue in autism. *Journal of trace elements in medicine and biology*.46: 76-82.

Matthew Mold, Agata Chmielecka, Maria Raquel Ramirez Rodriguez, Femia Thom, Caroline Linhart, Andrew King, and Christopher Exley. (2018). Aluminium in Brain Tissue in Multiple Sclerosis. *International journal of Environmental research and public health.* 15(18):177-185

Matsugami, T.R., Tanemura, K., Mieda, M., Nakatomi, R., Yamada, K., Kondo, T., Ogawa, M., Obata, K., Watanabe, M., Hashikawa, T., Tanaka, K. (2006).From the Cover: Indispensability of the glutamate transporters GLAST and GLT1 to brain development. *Proceedings of National Academy of Sciences*, 103(32):12161-12166.

McKee, A.S., Munks., M.W., MacLeod, M.K., Fleenor, C.J., Van Rooijen, N., Kappler, J.W., Marrack, P. (2009). Alum induces innate immune responses through macrophage and mast cell sensors, but these sensors are not required for alum to act as an adjuvant for specific immunity. *Journal of Immunology*, 183(7):4403-4414.

Meija, J. (2016). Atomic weights of the elements 2013. IUPAC Technical Report. *Pure and Applied Chemistry*. 88(3): 265–91.

Manickam, B., Sajitha, I.S., Lakshmi, R., and Nair, N.D. (2009). Prevelance, gross and Histopathological study of brian disorders in Cattle-Kerala state, India. *International journal of Tropical Medicine,* 4(1):9-20.

Mecocci,P. MacGarvey, U. and Beal, M.F. (1994). Oxidative damage to mitochondrial DNA is increased in Alzheimer's disease, *Annals of Neurology,* 36(5):747–751.

Meltzer, C.C., Zubieta, J.K., Brandt, J., Tune, L.E., Mayberg, H.S., Frost, J.J. (1996). Regional hypometabolism in Alzheimer's disease as measured by positron emission tomography after correction for effects of partial volume averaging. *Neurobiology of Disease*, 47:452-461.

Mena, H., Cadavid, D., and Rushing, E.J. (2004). Human cerebral infact: A proposed Histopathologic classification based on 137 cases. *Acta Neuropathologica,* 108:524-530.

Micheal H. Ross and Wojeich Pawlina (2019). Histology and Text Atlas with correlated cell and molecular biology 6th edition *Lipincot Williams and wilkins.*

Milane L. Trivedi M. Singh A.Talekar, M. and Amiji, M. (2015).Mitochondrial biology, targets, and drug delivery. *Journal of controlled release*; 207: 40-58.

Mishra P, Chan D.C. (2014). Mitochondrial dynamics and inheritance during cell division, development and disease. Nature Reviews Molecular Cell Biology; 15(10): 634–646.

Mitra, S., Izumi, T., Boldogh, I., Bhakat, K.K., Hill, J.W., Hazra, T.K. (2002). Choreography of oxidative Damage repair in mammalian genomes. *Free Radical Biology and Medicine*, 33:15–28.

Mjad Khan, Tahir Ali, Shafiq Ur Rehman, Muhammad Sohail Khan, Sayed Ibrar Alam, Muhammad Ikram, Tahir Muhammad, Kamran Saeed, Haroon Badshah and Myeong Ok Kim (2018). Neuroprotective Effect of Quercetin Against the Detrimental Effects of LPS in the Adult Mouse Brain. *Ethnopharmacology*. 9(10):1324-1348

Mohan, N., Alleyne, T., Adogwa, A. (2009). The effects of ingested aluminium on brain cytochrome oxidase activity, *West Indian Medical Journal.* 58 (5):422-427.

Mohammad, H., Ibrahim, E., and Ali, H. (2012). The effect of prenatal exposure to restraint Stress on Hippocampal granule neurons of Adult rat offspring. *Iranian Journal of Basic Medical Sciences,* 15(5):1060-1067.

Moreira-Lobo, D.C., Linhares-Siqueira., E.D., Cruz, G.M. (2010). Eugenol modifies the excitability of rat sciatic nerve and superior cervical ganglion neurons. *Neuroscience Letters*; 472(3):220-4.

Morris, M.C., Evans, D.A., Tangney, C.C., Bienias, J.L., and Wilson, R.S. (2006). Associations of Vegetable and fruit consumption with age related cognitive change. *Neurology*, 67:1370-1376.

Morris M.E., Baimbridge K.G., El-Beheiry., Obrocea G.V and Rosen A.S. (1995). Correlation of anoxic neuronal responses and calbindin-D $_{28k}$ localization in the stratum pyramidale of rat hippocampus. *Hippocampus* 5:25-39.

Morris, R., Garrud P., Rawlins, J., O'Keefe J. (1982). Place navigation impaired in rats with hippocampal lessions. *Nature,* 297 (5868): 681-683.

Morris, R. (1984). Development of a water maze procedure for studying spatial learning in the rat. Journal of Neuroscience Methods, 11:47-60.

Mosca, F., Tritto, E., Muzzi, A., Monaci, E., Bagnoli, F., Iavarone, C., O'Hagan, D., Rappuoli, R., De Gregorio, E. (2008). Molecular and cellular signatures of human vaccine adjuvants. *Proccedings of the National Academy of Sciences*, 105(30):10501-10506.

Moser, V.C. (2001). Neurobehavioral screening in rodents. *Current protocols in toxicology*, (11):243-255.

Moser, V.C. (1991). Applications of neurobehavioral screening battery. *Journal of American College of Toxicology*, 10:661-691.

Moore, K.L and Persaud, T.V.N. (2008). Development of the brain. The developing human, clinically oriented embryology. 8th ed. *Philadephia, WB Saunders*. 17: p392-399.

Moore, K.L., Dalley, A.F., and Agur, A.M.R. (2014). The Brain. Clinically Oriented anatomy. 7th ed. *Lippincott Williams & Wilkins, Philadephia* 7: p1060.

Munoz, D.G., and Feldman, H. (2000). Causes of Alzheimer's disease. *Canadian Medical Association*: 162:65-72.

Murakami, K., and Yoshino, M. (2004). Aluminium decreases the glutathione regeneration by the inhibition of NADP-isocitrate dehydrogenase in mitochondria. *Journal of Cellular. Biochemistry, 93*, (6), 1267-1271.

Nagababu E, Rifkind JM, Boindala S and Nakka L (2010). Assessment of antioxidant activity of eugenol in vitro and in vivo. *Methods of molecular Biology*. 610:165-180.

Nahla, A.G., Refat, A., and Abass, M.A. (2011). Efficacy of myrrh extract to reduce lead acetate toxicity in albino Wistar rats with special reference to cerebellum and testes. *Life Science Journal*, 8:406-414.

Nakamura, H., Rose, P.G., Blumer, J.L., Reed, M.D. (2000). Acute encephalopathy due to aluminium toxicity successfully treated by combined intravenous deferoxamine and hemodialysis. *Journal of Clinical Pharmacology*, 40: 296 – 300.

Nayak Prasunpriya (2002). Aluminum: impacts and disease. *Journal of Environmental research*. Vol: 89(2):101-105, Elsevier.

Nenandis, N., Boyle, S., Bakalbassis, E.G., Tsimidou, M. (2003): An experimental approach to Structure-activity relationships of caffeic and dihydrocaffeic acids and related monophenols. *Journal of American oil Chemist*, 80: 451–458.

Namekata, K., Magawa, M., Terashi, A., Ohta, S., Oyama, F., and Ihara, Y. (1997). Association of transferrin C2 allele with late-onset Alzheimer's disease. *Human Genetics*, 101(2): 126–129.

Neri, L.C., and Hewitt, D. (1991). Aluminium, Alzheimer's disease, and drinking water. *The Lancet*, 338(8763):390.

Nicholls, D.G., Budd, S.L. (1998). Mitochondia and neuronal glutamate excitotoxicity. *Biochemistry and Biophysica Acta*, 1366:97-112.

Norfaizatul, S.O., Zetty, Akmal C.Z. Noralisa, A.K., and Then S.M. (2010). Dual effects of plant antioxidants on neuron cell viability, *Journal of Medicinal Plants*, 9 (6): 133-132.

Nosek, K., Dennis, K., Andrus, B.M. (2008). Context and strain-dependent behavioral Response to stress. *Behavioral and Brain Functions*, 8(4):23-35.

Olanow, C.W., Jenner, P., and Youdim, M. (1990). Neurodegeneration and neuroprotection in Parkinson's disease; United States Edition Published *by Academic Press Inc. San Diego*, CA 92101.

Oliverio, A., Eleftheriou, B. E., Bailey, D.W. (1973).Exploratory activity: Genetic analysis of its modification by scopolamine and amphetamine. Physiology and Behavior. 10:893-899.

Olopade, F.E, Shokunbi, M.T., and Siren, A. (2012). The relationship between ventricular

dilation, neuropathological and neurobehavioral changes in hydrocephalic rats. *Fluids and Barriers of the CNS*, 9:19:1-10.

O'Keefe, J., and Recce, M.L. (1993). Phase relationship between hippocampal place units and the EEG theta rhythm. *Hippocampus*. 3 (3): 317–30.

Okutan Huseyin, Ozcelik Nurten, Yilmaz Ramazan and Uz, Efkan (2005). Effects of caffeic acid phenethyl ester on lipid peroxidation and antioxidant enzymes in diabetic rat heart. *Journal of clinical biochemistry*. 38(2):191-196.

Ou H.C., Chou F.I., Lin T.M. (2006). Protective effects of eugenol against oxidized LDLinduced cytotoxicity and adhesion molecule expression in endothelial cell. *Food Chemical Toxicology*; 44(9):1485-595.

Ouafa, R. And Djebli, E. (2008). Chronic Exposure to Aluminum Chloride in Mice: Exploratory Behaviors and Spatial Learning. *Journal of Biological Research*, 2 (1-2): 26-33.

Ozkan A. and Erdogan A. (2013).Membrane and DNA damaging/protective effects of eugenol, eucalyptol, terpinen-4-ol, and camphor at various concentrations on parental and drug-resistant H1299 cells.*Turkish Journal of Biology*, 37(4):405-413.

Packard, M.G. and McGaugh, J.L. (1992). Double dissociation of fornix and caudate nucleus lesions on acquisition of two water maze tasks: Further evidence for multiple memory systems. *Behavioural Neuroscience*, 106:439-446.

Pandey, R., Kalra, A., Tandon, S. (2000). Essential oil compounds as potent source of nematicidal compounds. *Journal of Phytopathology*, 148(7-8):501-2.

Parekh, K.D., Dash R.P., Pandya, A.N., Vasu, K.K., Nivsarkar, M. (2013). Implication of novel bis-imidazopyridines for management of Alzheimer's disease and establishment of its role on protein phosphatase 2A activity in brain. *Journal of Pharmacy Pharmacology*, 65:1785-95.

Park, K.A, Vasko M.R. (2005). Lipid mediators of sensitivity in sensory neurons. Trends in *Pharmacological Sciences*, 26:571–577.

Park, S.Y., Kim, D.S. (2002). Discovery of natural products from Curcuma longa that protect Cells from beta-amyloid insult: a drug discovery effort against Alzheimer's disease. *Journal of Natural Products*, 65:1227–1231.

Pellow, S., Chopin, P., File, S., Briley, M. (1985). Validation of open /closed arm entries in elevated plus maze as a measure of anxiety in the rat. *Journal of Neuroscience methods*, 14:149-167.

Percy, M.E., Kruck, T.P., Pogue, A.I., Lukiw, W.J. (2011).Towards the prevention of potential Aluminium toxic effects and an effective treatment for Alzheimer's disease. *Journal of Inorganic Biochemistry*; 105: 1505 – 12.

Pessoa, L.M., Morais, S.M., Bevilaqua, C.M. (2002). Anthelmintic activity of essential oil of Ocimum gratissimum Linn and eugenol against Haemonchus contortus. *Veterinary Parasitology*, 109(1-2):59-63.

Peter N Alexandrov, Aileen I Pogue, and Walter J Lukiw (2018). Synergism in aluminum and mercury neurotoxicity. *Journal of integrated food and Nutrition.*5(3):1054- 1078.

Prakash, P., and Gupta N. (2005). Therapeutic uses of *Ocimum sanctum* Linn (Tulsi) with a note On eugenol and its pharmacological actions: a short review. *Indian Journal of Pharmacology*; 49(2):125-31.

Prasad, S.N., and Muralidhara. (2013). Neuroprotective efficacy of eugenol and isoeugenol in Acrylamide-induced neuropathy in rats: behavioral and biochemical evidence. *Neurochemical Research*, 38:330-45.

Pratico, D., Uryu, K., Sung, S., Tang, S., Trojanowski, J.Q., Lee, V.M. (2002). Aluminium modulates Brain amyloidosis through oxidative stress in APP transgenic mice. *Journal of Federation of American Societies for Experimental Biology*, 16:1138–1140.

Raisova M, Hossini AM, Eberle J, Riebeling C, Wieder T, Sturm I, Daniel PT, Orfanos CE and Geilen CC (2001). The Bax/Bcl-2 ratio determines the susceptibility of human melanoma cells to CD95/Fas-mediated apoptosis. *The Journal of Investigative Dermatology*. 117(2):333-40.

Rao, M.V., and Purohit, A.R. (2011). Neuroprotection by melatonin on Mercury induced Toxicity in the Rat Brain. *Pharmacology and Pharmacy*, 2:375-385.

Raskind, M.A., Peskind, E.R., Holmes, C., Goldstein, D.S. (1999). Patterns of cerebrospinal fluid catechols support increased central noradrenergic responsiveness in aging and Alzheimer's disease. *Biological Psychiatry*, 15; 46(6):756-65.

Ratan, R.R., Murphy, T.H., Baraban, J.M., 1994. Oxidative stress induced apoptosis in embryonic cortical neurons. *Journal of Neurochemistry*. 62, 376–379

Ribes, D., Colomina, M.T., Vicens, P., Domingo, J.L. (2008). Effects of oral aluminum exposure on Behavior and neurogenesis in a transgenic mouse model of Alzheimer’s disease. *Experimental Neurology*, 214:293–300.

Rice-Evans C.A., Miller, N.J., Paganga, G. (1996). Structure-antioxidant activity relationships of flavonoids and phenolic acids. *Free Radical Biology and Medicine*; 20:933–956.

Richardson, J.S. (1993). Free radicals in the genesis of Alzheimer’s disease.

Annals of the New York Academy of Sciences, 695: 73-76.

Rita, G., Manonmani, G., William, L. (2009). Combination of 2-methocyestradiol (2-ME2) and eugenol for apoptosis induction synergistically in androgen independent prostatecancer cells. *Journal of Steroid Biochemistry and Molecular Biology*, 113(1-2):25-35.

Rondeau, V., Jacqmin-Gadda, H., Commenges, D., Helmer, C., and. Dartigues, J. F. (2009). Aluminum and silica in drinking water and the risk of Alzheimer's disease or cognitive decline: findings from 15-year follow-up of the PAQUID cohort," *American Journal of Epidemiology*, 169(4):489–496.

Rosana A., José G., Marco A. (2012). High- and Low-Rearing Rats Differ in the Brain Excitability Controlled by the Allosteric Benzodiazepine Site in the GABAA Receptor. *Journal of Behavioral and Brain Science*. 2012(2):315-325.

Rosler, N., Wichart, I., Jellinger, K.A. (2001). Clinical significance of neurobiochemical profiles in the lumbar cerebrospinal fluid of Alzheimer's disease patients. *Journal of Neural Transmission (Vienna*), 108(2):231-46.

Rothwell, N., Allan, S., Toulmond, S. (1997). The role of interleukin 1 in acute neurodegeneration and stroke: pathophysiological and therapeutic implications. *Journal of Clinical Investigation*, 100(11):2648- 2652.

Ruan, Y.W., Zou, B., Fan, y., Li Y., Lin N., Zhang Y. and Xu, Z.C. (2007). Morphological Heterogeneity of CA1 Pyramidal neurones in response to ischemia. *Journal of Neuroscience Research*, 85: 193-204.

Rubenstein John. (2013). Patterning and Cell Type Specification in the Developing CNS and PNS: Comprehensive Developmental Neuroscience. *Elsevier Science & Technology* p135.

Sachs, B.D. (1988). The development of grooming and its expression in adult animals. *Annals of New York Academy of Sciences*, 525:1–17.

Said, M.M., and Abd Rabo, M.M. (2017). Neuroprotective effects of eugenol against aluminium-induced toxicity in the rat brain. *Archives of Industrial Hygiene and Toxicology*, 68:27-37.

Salawu, O.A., Chindo, B.A., Tijani, A.Y., Obidike, T.A., and Akingbasote, A.J. (2009). Acute and subacute toxicologicalevaluation of the methanolic stem bark extract of *Crossopteryx febrifuga* in rats. *African journal of Pharmacy and Pharmacology* 3:621-626.

Salusky, I.B., Coburn, J.W., Paunier, L., Sherrard, D.J., Fine, R.N. (1984). Role of aluminium

hydroxide in raising serum aluminium levels in children undergoing continuous ambulatory peritoneal dialysis. *Journal of Pediatrics*; 105: 717 – 20.

Samsonovich, A.V. and Ascoli, G.A. (2005) A simple neural network model of the hippocampus suggesting its path finding role in episodic memory retrival. *Learning and memory*, 12:193-208.

Sanes, J.N., and Donoghue, J.P. (2000). Plasticity and primary mortoe cortex. *Annual review of Neuroscience*, 23: 393-415.

Sara Joushi, Mahmoud Elahdadi Salmani. (2017). Effect of eugenol on lithium-pilocarpine Model of epilepsy: behavioral, histological, and molecular changes. *Iranian Journal of Basic Medical Sciences.* 20:745-752.

Savory, J., Exley, C., Forbes, W.F., Huang, Y., Joshi, J.G., Kruck, T., McLachlan, D.R., Wakayama I. (1996). Can the controversy of the role of aluminium in Alzheimer's disease be resolved? What are the suggested approaches to this controversy and methodological issues to be considered? *Journal of Toxicology and Environmental Health;* 48: 615 – 35.

Schapira, A.H., Gu, M., Taaman, J.W., Tabrizi, S.J., Seaton, T., Cleeter, M. (1998). Mitochondria in The etiology and pathogenesis of Parkinson's disease. *Annals of Neurology*. 44(1):S89-S98.

Scheenstra, A.E.H., Dijkstra, J., and Van der Weerd, L. (2010). Morphometry on rodent brain, volumetry and other quantitative measurements to assess the rodent brain in- vivo NMR imaging methods and protocols. *Humana press, USA. Ed. C. Faber and Schroeder in press.*

Schiller, D., Eichenbaum, H., Buffalo, E.A., Davachi, L., Foster, D.J., Leutgeb, S., Ranganath, C. (2015). Memory and Space: Towards an Understanding of the Cognitive Map. *The Journal of Neuroscience*, 35 (41): 13904–13911.

Schmitz, C. and Holf, P.R. (2005). Design based stereology in neuroscience, *Neuroscience* (130):813-831.

Seidman, R.J. (2011). Normal gross brain and microscopy. *Neuropathology, Department of Pathology stony brook university.*

Seilhean, D., De Girolami, U. and Gray, F. (2004). Basic Pathology of Central Nervous system in textbook of Escourolle and *Poirier Manual of Basic Neuropathology 4th ed. Butterworth Heinemann an imprint of Elsevier, Philadephia*.

Semiz, A., and Sen, A. (2007). Antioxidant and chemoprotective properties of *Momordica charantia L.* (Bitter melon) fruit extract. *African Journal of Biotechnology*, 6(3): 273-277.

Setton Kenneth (1976). The papacy and the Levant: The thirteenth and fourteenth centuries. *American Philosophical Society* (1): 204-1571.

Shahidi, S., Komaki, A., Mahmoodi, M., Atrvash, N., Ghodrati, M. (2008). Ascorbic acid supplementation could affect passive avoidance learning and memory in rat. *Brain Research Bulletin*, 76:109-113.

Shakhashiri, B.Z. (2008). *Chemical of the Week Aluminum . University of Wisconsin. Archived from the original (PDF) on* 9 May 2012.

Shaw, C.A., Petrik, M.S. (2009). Aluminium hydroxide injections lead to motor deficits and motor neuron degeneration. *Journal of Inorganic Biochemistry*, 103, (11), 1555-62.

Shirabe, T., Irie, K., Uchida, M. (2002). Autopsy case of aluminium encephalopathy. *Neuropathology*, 22(3):206-210.

Shweta Thakur, Bibekananda Sarkar, Ravi P Cholia, Nandini Gautam, Monisha Dhiman, and Anil K Mantha. (2014). APE1/Ref-1 as an emerging therapeutic target for various human diseases: phytochemical modulation of its functions. *Experimental and molecular medicine*. 46(7):106.

Sies, H., Jones, D. (2007). Oxidative Stress. In: *Fink G (ed) Encyclopedia of stress. Elsevier, San Diego*, pp 45–4.

Singh T and Goel R.K (2015). Neuroprotective efect of *Allium cepa* L. in aluminium chloride induced neurotoxicity, *Journal of NeuroToxicology*, 49:1–7.

Singh, V., Panwar, R. (2014). In vivo antioxidative and neuroprotective effect of 4-allyl-2-methoxyphenol against chlorpyrifosinduced neurotoxicity in rat brain. *Molecular Cellular Biochemistry*, 388:61-74.

Singh J, Bikram, Jit. (2014). A Key To Optimize Machining. Multi response Optimization of CNC turning with AL-7020 alloy. *Anchor Academic Publishing* pg 55.

Skelly, M.J., and Weiner, J.L. (2014). Chronic treatment with with prazosin or duloxetine lessens concurrent anxiety like behaviour and alcohol intake: evidence of disrupted noradrenagic signalling in anxiety relaxed alcohol use. *Brain and Behaviour* 4: 468-483.

Slanina, P., French, W., Ekström, L.G., Lööf, L., Slorach, S., Cedergren, A. (1986). Dietary citric acid enhances absorption of aluminum in antacids. *Clinical Chemistry*. **32** (3): 539–541.

Slomianka, L. (2011). Hippocampal pyramidal cells: the re-emergence of cortical

lamination. *Brain Structure and Function* 216(4): 301-317.

Slutsky L, Abumaria N, Wu LJ (2010). Ehancement of learning and memory by elevating brain magnesium levels. *Neuron*: 65(2):165-167.

Snell, R.S. (2010). Introduction and organization of the nervous system. Clinical Neuroanatomy, 7th ed. *Philadephia, lipincott Williams and Wilkins*. 1:p2.

Son, K.H., Kwon, S.Y., Kim, H.P., Chang, H.W., Kang, S.S. (1998). Constituents of *Syzigium aromaticum Merr. ET Perry*. *Natural Product Sciences*, 4:263–267.

Soudry, Y., Lemogne, C., Malinvaud, D., Consoli, S.M., Bonfils, P. (2011). Olfactory system and Emotion: Common substrates. *European Annals of Otorhinolaryngol Head Neck Diseases*; 128:18–23.

Sousa, F.C., Melo, C.T., Monteiro, A.P. (2004). Antianxiety and antidepressant effects of riparin III from *Aniba riparia (Nees) Mez (Lauraceae)* in mice. *Pharmacology Biochemistry and Behavior*, 78:27–33.

Spofforth. J., Edin, I.R.C., and Eng., M. R. C. (1921). Case of aluminium poisoning. *The Lancet*, 197(5103):1301-1310

Spruijt, B.M., van Hooff, J.A., Gispen, W.H. (1992). Ethology and neurobiology of grooming behavior. *Physiological Reviews*, 72:825–52.

Standring, S., Borley, N.R., Collins, P., Crossman, A.R., Gatzoulis, M.A., Healy, J.C., Johnson, D., Mahadevan, V., Newell, R.L.M and wigley, C. (2008). Hippocampus; Lombic lobe:Gray's Anatomy; The anatomical basis of clinical practice. 40th *ed Cóchill Livingstone/ Elsevier.* 23 (3).

Stephen C. Bondy and Arezoo Campbell. (2018). Water Quality and Brain Function. *International journal of Environmental research and public health*. 15(1):2.

Storey, E., Hyman, B.T., Jenkins, B., Brouillet, E., Miller, J.M., Rosen, B.R., Beal, M.F. (1992). 1-Methyl-4-phenylpyridinium produces excitotoxic lesions in rat striatum as a result of impairment of oxidative metabolism. *Journal of Neurochemistry*, 58(5):1975-1978.

Suarez-Fernandez, M.B., Soldado, A.B., Sanz-Medel, A., Vega, J.A., Novelli, A. (1999). Fernandez-Sanchez, M.T. Aluminium-induced degeneration of astrocytes occurs *via* apoptosis and results in neuronal death, *Brain Research. 835*(2):125-136.

Susan elmore (2007). Apoptosis: A review of programmed cell death. *Toxicologic pathology*. 35(4): 495–516.

Szutowicz, A., Tomaszewicz, M., Jankowska, A., Madziar, B., and Bielarczyk, H. (2000).

Acetyl-CoA Metabolism in Cholinergic Neurons and Their Susceptibility to Neurotoxic Inputs. *Metabolic Brain Disease*, 15(1): 29-44.

Takeuchi, H. (2010). Neurotoxicity by microglia: mechanisms and potential therapeutic strategy. *Journal of Clinical and Experimental Neuroimmunology*. 1:12-21.

Tamashiro, K., wakayama, T., Blanchard, R., Blanchard, C., Yanagimachi, R. (2000) Post natal growth and neurobehavioral development of mice cloned from adult cumulus cells. *Biology Reproduction*. 63:328-334.

Tell, G., Damante, G., Caldwell, D., Kelley, M.R. (2005). The intracellular localization of APE1/Ref-1: more than a passive phenomenon? *Antioxidant and Redox Signalling*, 7:367–384.

Thorsten Stahl, Sandy Falk, Alice Rohrbeck, Sebastian Georgii, Christin Herzog, Alexander Wiegand, Svenja Hotz, Bruce Boschek, Holger Zorn, and Hubertus Brunn. (2017). Migration of aluminum from food contact materials to food a health risk for consumers? Part I of III: exposure to aluminum, release of aluminum, tolerable weekly intake (TWI), toxicological effects of aluminum, study design, and methods. *Environmental Sciences Europe*. 29(9):19.

Toma, I., Karumi, Y., and Geidam, M.A. (2009). Phytochemical screening and toxicity of aqueous Extract of the pods pulp of *Cassia sieberianaI* DC. (*Cassia Kotchiyana Oliv.). African Journal of Pure and Applied Chemistry*, 3:26-30.

Tomljenovic, L. (2011). Aluminum and Alzheimer's disease: after a century of controversy, is there a plausible link? *Journal of Alzheimers Disease*. 23(4):567-598

Tomljenovic, L., Shaw, C.A. (2011) Do aluminum vaccine adjuvants contribute to the rising Prevalence of autism? *Journal of Inorganic Biochemistry*, 105(11):1489–99.

Tomljenovic, L., Shaw, C.A. (2011) Aluminum vaccine adjuvants: are they safe? *Current Medicinal Chemistry*, 18(17):2630–2637.

Towfighi, J., Housman, C., Brucklacher, R., and Vannuci, R.C. (2004). Neuropathology of Seizures in the immature rabbit. *Developmental Brain Research*. 152: 143-152.

Town, T., Nikolic, V., Tan, J. (2005). The microglial activation continuum: from innate to adaptive responses. *Journal of Neuroinflammation*, (2) 24-35.

Tsunoda, M., Sharma, R.P. (1999). Modulation of tumor necrosis factor alpha expression in Mouse brain after exposure to aluminium in drinking water. *Archives of Toxicology* 73, (8-9):419-426.

Tsuruoka, M., Hara, J., Hirayama, A., Sugimoto, M., Soga, T., Shankle, W.R., Tomita, M. (2013).Capillary electrophoresis-mass spectrometry-based metabolome analysis of serum and saliva from neurodegenerative dementia patients. *Electrophoresis*, 34(19):2865-2872.

Tripathi, S. And Modi, D. (2012). Alteration in Thyroid Hormones and Vitamins as Early Markers of Aluminum Induced Neurodegeneration in Rats. *International Journal of Pharmacology*, 2:137-150.

Trushina, E., and Mcmurray, C.T. (2007). Oxidative stress and mitochondrial dysfunction in neurodegenerative diseases. *Neuroscience*, 144:1233-1248.

Tumiatti, V., Bolognesi, M.L., Minarini, A., Rosini, M., Milelli, A. and Matera, R. (2008). Progress in acetylcholinesterase inhibitors for Alzheimer's disease: *an update Expert Opinion on Therapeutic Patents*, 12:45-56.

Uma, C., Poornima K., Surya S., Ravikumar, G., and Gopalakrishan, V.K. (2012). Nephroprotective Effect of Etahnolic Extract of Tabernaemontana Coronaria in Mercuric Chloride Induced Renal Damage In Wistar Albino Rats. *International Journal of Chemical Engineering and Applications*, 3(4): 269-273.

Van Abeelen, J. H. F. (1975). Genetic Analysis of Behavioural Responses to Novelty in Mice. *Nature*, 254(5497):239-24.

VanElzakker, M., Fevurly, R.D., Breindel, T., Spencer, R.L. (2008). Environmental novelty is associated with a selective increase in Fos expression in the output elements of the hippocampal formation and the perirhinal cortex. *Learning & Memory*, 15(12): 899–908.

Veer, Bala., Gupta, S., Anitha, M.L., Hegde, L., Zecca, R.M., Garruto, R., Ravid, S.K., Shankar, R., Stein, P., Shanmugavelu, K.S., Jagannatha, Rao. (2005). Aluminium in Alzheimer's disease: are we still at a crossroad? *Cellular and Molecular Life Sciences*, 62:143–158.

Veni Bharti K., Sharma S.K. and Singh S. (2013). Evaluation of memory and learning improving effects of *Benincasa hispida* seed in mice. *Pharmacoloia*, 4(3): 249-253.

Verstraeten, S. (2008). Aluminium and lead: molecular mechanisms of Brain Toxicity. School of Pharmacy and Biochemistry, a review article: *University of Buenos Aires, Argentina*, 82:789–802.

Walf, A.A., and Frye, C.A. (2007). The use of elevated plus maze as an assay of anxiety related behaviour in rodents. *Nature Protocols*, 2:322-328.

Walton, J.R. (2012). Aluminium disruption of calcium homeostasis and signal transduction resembles change that occurs in aging and Alzheimer 's disease. *Journal of Alzheimer's disease,* 29: 255 – 73.

Walton, J.R. (2007). An aluminum-based rat model for Alzheimer's disease exhibits

Oxidative damage, inhibition of PP2A activity, hyperphosphorylated tau, and granulovacuolar degeneration. *Journal of Inorgarnic Biochemistry* 101(9):1275-1284.

Walton, J.R., Wang, M.X. (2009). APP expression, distribution and accumulation are altered by aluminum in a rodent model for Alzheimer's disease. *Journal of Inorganic Biochemistry*, 103(11):1548–1554.

Wantanabe, C.M.H., Wolffram, S., Ader, P., Rimbach, P., Packer, L., Maguire, J.J., Schultz, P.G., and Gohil, K. (2001). The *in vivo* neuromodulatory effects of the herbal medicine Ginkgo biloba. *Proceedings of the National Academy of Sciences*, 98 (12): 6577-6580.

Waters, C.M., Moser, W., Walkinshaw, G., and Mitchell, I.J. (1994). Death of Neurons in neonatal rodent and Primate globus pallidus occurs by a mechanism of apoptosis. *Neuroscience*, 63:881-894.

Watts, D.L. (1990). Trace elements and neuropsychological problems as reflected in tissue mineral analysis (TMA) patterns. *Journal of Orthomolecular Medicine*, 5(3): 159-166.

Weiss R.F and Fintelmann V. (2000). *Herbal Medicine Suttgart*: Thieme, 46(2):3-20.

Wills, M.R., and Savory, J. (1989). Aluminum and chronic renal failure: sources, absorption, transport, and toxicity," *Critical Reviews in Clinical Laboratory Sciences*, 27(1):59–107.

Winkler, J., Suhr, S.T., Gaje, F.J., Thal, L.J., and Fisher, L.J. (1995). Essential role of neocorticat acetylcholine in spatial memory, *Nature* 375: 484-487.

WHO, (1997). Aluminium. Geneva, *World Health Organization, International Program on Chemical Safety Environmental Health Criteria* 194.

Yan, Q., Zhang J, Liu H, Babu-Khan S, Vassar R, Biere AL, Citron M, Landreth G (2003): Anti-inflammatory drug therapy alters beta-amyloid processing and deposition in an animal model of Alzheimer's disease. *Journal of Neuroscience*, 23(20):7504-7509.

Yang, W.C., Ouyang, W.Q., He, X. (2008). Preparation of compound eugenol nano-emulsion and study on analgesics and anti-inflammation. *Zhong Guo Yi Yao Za Zhi*, 39(5):352-5.

Yang, W. Shi, L. Chen, L. Zhang, B. Ma, K. and Liu, Y. and Qian, Y. (2014). Protective effects of perindopril on d-galactose and aluminum trichloride induced neurotoxicity via the apoptosis of mitochondria-mediated intrinsic pathway in the hippocampus of mice, *Brain Research Bulletin*, 109:46–53

Yang, Y., Niu, Q., Niu, P. and Lou, J. (2006). Effects of Aluminium on lipid peroxidation in rat's brain and its sex-related differences, *Nature reviews*, 24(5): 281-283.

Yasmin m abd el-aziz , ali abu almaaty, nahed omar and ahmed m abdeen (2019).

Evaluation of protective effects of propolis against aluminium silicate toxicity in rats. *Genetika* 51(1): 299-312.

Yokel, R.A., McNamara, P.J. (2001). Aluminium toxicokinetics: an updated mini-review. *Pharmacology and Toxicology*, 88: 159 – 67.

Youdim Moussa B (2008). Brain iron deficiency and excess; cognitive impairment and neurodegeneration with involvement of straitum and hippocampus. *Neurotoxicity research.* 14(1):45-56.

Young, B., Heath, J.W., Stevens, A., Lowe, S.J, and Deakin, J.P. (2007) The Central nervous system: Weather's functional histology: A text and colour Atlas. 5ed. *Churchill Livingstone/Elsevier Inc*. 20(3): 392 – 399.

Young, I.S., and Woodside, J.V. (2001). Antioxidants in Health and Disease, *Journal of Clinical Pathology*, 1(2): 238-245.

Yuan, C., Hsu, G. And Lee, J. (2012). Aluminum overload increases oxidative stress in four functional brain areas of Neonatal rats. *Journal of Biomedical Science*, 19:51.

Zàdori, D., Kilvényi, P., Szalàrdy, L., Fullop, F., Toldi, J., Vécsei, L. (2012). Mitochondrial disturbances, excitotoxicity, neuroinflamation and kynurenines: Novel therapeutic strategies for neurodegenerative disorders. *Journal of the Neurological Sciences*, 322(1-2): 187-191.

Zatta, P., Lucchini, R., van Rensburg, S.J., Taylor, A. (2003). The role of metals in neurodegenerative processes: aluminum, manganese, and zinc. *Brain Research Bulletin*, 62:15-28.

Zhang, L.L Zhang, L. F. Xu, J. G. and Hu, Q. P. (2017). Comparison study on antioxidant, DNA damage protective and antibacterial activities of eugenol and isoeugenol against several foodborne pathogens," Food & Nutrition Research, vol. 61, no. 1, article 1353356, 2017.

Zhang, Z.X., Zahner, G.E., Roman, G.C., Liu, J., Hong, Z., Qu, Q.M, Liu, X.H., Zhang, X.J., Zhou, B., Wu, C.B. (2005). Dementia subtypes in China: prevalence in Beijing, Xian, Shanghai, and Chengdu. Archives of Neurology, 62(3):447-453.

Zhibin Liu, Wenmin Niu, Xiaohang Yang, Yuan Wang (2013). Effects of combined Acupuncture and eugenol on learning-memory ability and antioxidation system of hippocampus in Alzheimer disease rats via olfactory system stimulation. *Journal of Traditional Chinese Medicine*: 15:33(3): 399-402.

Zimmerman, G., and Soreq, H. (2006). Termination and beyond: Acetylcholinesterase as a modulator of synaptic transmission. *Cell and Tissue research*, 326:655-669.

Zoppi, C.C., Hohl, R., Silva, F.C., Lazarim, F.L., Antunes Neto, J.M., Stancanneli, M., and Macedo, D.V. (2006). Vitamin C and E supplementation Effects in Professional Soccer players under regular training. *Journal of International Society of Sports Nutrition*, 3(2): 37-44.

APPENDIX I

METHOD OF DETERMINING THE VARIOUS DOSES OF EUGENOL AND ALUMINIUM CHLORIDE

1. **Dosage Calculation of Eugenol solution:**

   To determine the equivalent dosage of volume in **ml** to **mg/kg** body weight (bw), the following steps were observed:

   A. Dosage in mg/kg bw (150 and 300mg/kg bw of eugenol)

   A = 150 or 300mg/kg which is the standard dosage to be administered.

   A mg ---------- 1000g

   X mg ---------- Weight of animal (g)

   X = expected amount of solute to be administered to animal of a known weight.

   X (mg) = $\frac{\text{A mg x weight of animal}}{\text{1000g}}$

   B. Dosage in ml:

   50g of eugenol was dissolved in 1000 ml (distilled water)

   Standardizing values yields

   50,000mg ---------- 1000ml

   X mg (as calculated above) ---------- Y ml (volume to be administered)

   Y ml = $\frac{\text{X mg x 1000ml}}{\text{50,000 mg}}$

2. **Dosage Calculation of aluminium chloride**

To determine the equivalent dosage of volume in **ml to mg/kg bw**, the following steps were observed.

A. Dosage in mg/kg bw (100mg/kg bw of aluminium chloride)

The dosage is calculated as follows:

100mg (standard solute) ---------- 1kg

100mg (standard solute) ---------- 1000g

A = 100mg/kg which is the standard dosage to be administered.

A mg ---------- 1000g

X mg ---------- Weight of animal (g)

X = expected amount of solute to be administered to animal of a known weight.

$$\textbf{X (mg)} = \frac{\textbf{A mg x weight of animal}}{\textbf{1000g}}$$

B. Dosage in ml:

40g of aluminium chloride was dissolved in 800 ml (distilled water)

Standardizing values yields

40,000mg ---------- 1000ml

X mg (as calculated above) ---------- Y ml (volume to be administered)

$$\textbf{Y ml} = \frac{\textbf{X mg x 1000ml}}{\textbf{40,000 mg}}$$

The calculated volume (ml) of Eugenol/toxin was then administered depending on the group and body weight of each experimental animals (Wistar rats).

APPENDIX II

HISTOMETRIC METHODS USING THE AMSCOPE MICROSCOPE CAMERA

2. Photomicrography

- Using a light microscope with a x25 objective (x 250 magnification) and computer running image processing software (Amscope MT *version* 3.0.0.5, USA) for microscopy, digital microscopic images were captured.

3. Histometry and calibration (Using the Amscope Microscope Cameras; Psi Wave function, 2009)

- Firstly a micrometer slide (microscope slide with scale on it), come as 1 mm graduated in 0.01 mm units (that is divided 10x into 100 µm units) is captured at the same magnification and quality (pixels) the micrograph was photographed
- A line tool was selected and this was used to carefully measure from start of one major line (of the captured microscope slide) to the start of the next, or end to end.
- Recorded length in pixels; in this study was 408 pixels/ 100µm or 4.08 pixel/µm.
- Next use a polygon tool to measure the area and perimeter of desired cells. Values are computed and presented automatically by the software.

A

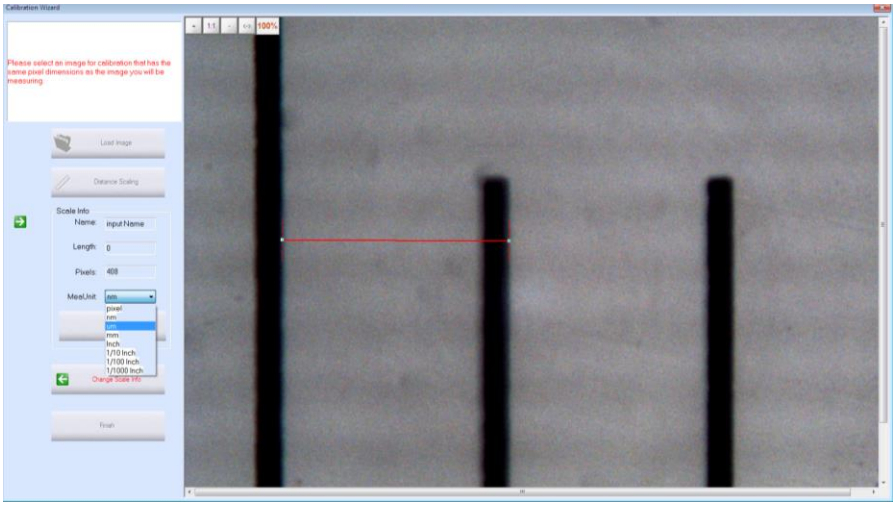


Plate 3.1a: Micrometer slide as captured by microscope at magnification x250 (using the x25 objective).

B

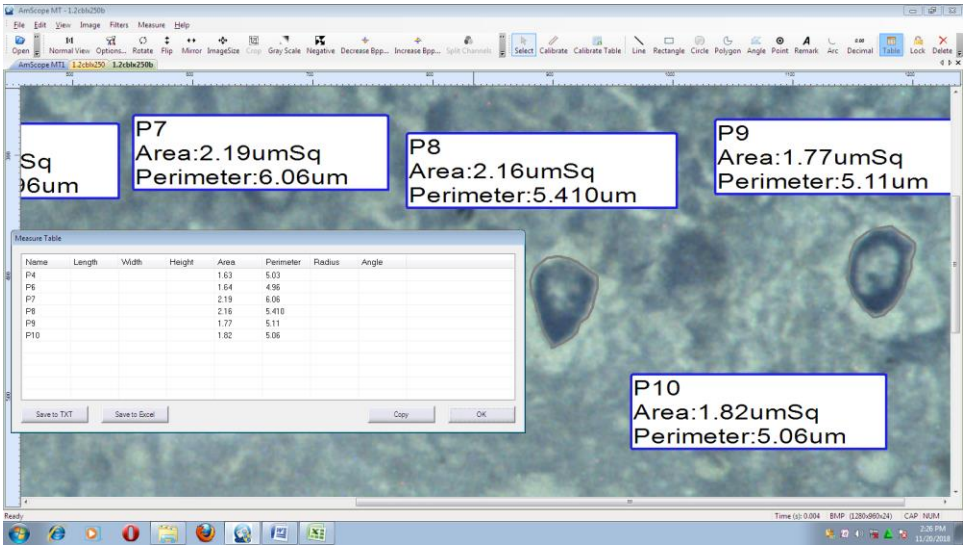


Plate 3.1b: Histometry using a Cresyl fast violet stained micrograph (digital microscopic images) with a computer running imaging software (AmScope MT version 3.0.0.5, USA)

APPENDIX III

PREPARATION OF STAINING SOLUTIONS AND STAINING

1. Haematoxylin and Eosin stains

A. Haematoxylin (Harris' (1900) Haematoxylin)

- Haematoxylin -1g
- Absolute alcohol -10ml
- Ammonium or potassium alum -20g
- Distilled water -200ml
- Mercuric oxide -0.5g

Haematoxylin was dissolved in alcohol and alum which was dissolved in water was added. The mixture was then boiled and mercuric acid added when the solution turn dark purple. It was then rapidly cooled.

B. Eosin

- Distilled water
- Crystal of thymol

5% eosin solution was made by dissolving 5g of eosin in 100ml of distilled water. To prevent growth of mould in stock solution, a crystal of thymol was added to obtain 1% staining solution, 20ml of the stock solution was diluted by making it up to 100ml.

C. Staining

- **Removal of wax with xylene**
  - Dewaxing I, 3 minutes

- Dewaxing II, 3 minutes

- **Hydration with graded alcohol**
  - Absolute alcohol, 1 minute
  - 95% alcohol, 1 minute
  - 70% alcohol, 2minutes
  - 50% alcohol, 2 minutes
  - 30% alcohol, 1minute

- **Staining Proper**
  - Haematoxylin , 10-20 minutes
  - Distilled water (washing)
  - 35% alcohol, 1 minute
  - Acid – alcohol, 30 seconds (for differentiation between nucleus and cytoplasm)
  - Distilled water 1minute
  - Staining in 1% eosin, 2 minutes

- **Dehydration** in alcohol
  - 90% alcohol , 10 – 15 seconds
  - Absolute Alcohol, 1 minute

- **Clearing**
  - Xylene-alcohol, 2 minutes
  - Pure xylene I, 3 minutes

- Pure xylene III, 3 minutes

- Mounted In DPX

(Drury, 1967)

2. CRESYL FAST VIOLET STAINING

- **Fixation** in 10% formal saline
- **Section**
- Technique
  - Dewax using xylene and take section to water
  - Staining for 1-6 hours 0.2% cresyl fast violet
  - Rinse in distilled water and differentiate in 95% alcohol
  - Dehydrate, clear and mount in mountant.

3. GOLGI STAINING (Marsland, Glees and Erikson's 1954)

- **Fixation** in 10% formal saline
- **Section**
- **Ammoniacal silver solution**

Mix 30ml of 20% silver nitrate with 20ml of absolute alcohol. Add strong ammonia drop wise until resulting precipitate dissolves. Add an afditional 5 drops of ammonia.

- **Technique**
  - Dewaxing using xylene followed by alcohol
  - Washing in distilled water

- Place in 2% silver nitrate for 15 – 60 minutes at 37°C
- Washing in10% neutral formalin for 10 – 15 seconds
- Wash off formalin with ammoniacal solution and allowed for 30 seconds
- Drain off silver solution and wash section with 10% neutral formalin for 1 minute.
- Wash in distilled water and fix in 5% sodium thiosulphate for 5 minutes
- Dehydrate, clear and mount in mountant.

(Drury, 1967

APPENDIX IV

ACAT-1 IMMUNOHISTOCHEMISTRY STAINING PROTOCOL

18. Sections were sectioned at 4 microns thick with the microtome
19. Sections were placed on electrostatically charged slides and slides were baked at 70°C for 10 minutes
20. Slides were taken to distilled water
21. Slides were blocked in hydrogen peroxide for 5 minutes
22. Slides were washed in distilled water
23. Slides were retrieved in citrate buffer pH 6.0 for 20 minutes at 95°C
24. Slides were washed in distilled water
25. Slides were covered with PBS pH 7.4
26. Slides were incubated with ACAT antibody (1/100) at RT for 90minutes
27. Slides were washed in PBS pH 7.4
28. Slides were incubated in Mouse + Rabbit HRP (DBBiotech, Slovakia), for 30 minutes
29. Slides were washed in PBS for 10 minutes
30. Slides were incubated in DAB + substrate mixture (DBBiotech, Slovakia) for 5 minutes
31. Slides were washed in distilled water
32. Slides were counter stained in Haematoxylin for 1 minute
33. Slides were washed in distilled water
34. Slides were dehydrated, cleared and mounted in DPX.

APPENDIX V

ANALYTICAL METHOD FOR DETERMINING METALS IN BIOLOGICAL TISSUES

4. **Tissue preparation/digestion** (EMMI, 1997)

- Take 1 ml (0.25g) of sample (homogenized tissue; 1g in 4ml of phosphate buffer) into boiling tube and add 2 ml of concentrated HNO_3
- Heat (100°C) for 2 hours and allow to cool
- Add 0.3 ml of 30% H_2O_2
- Heat (100°C) for 1-2 hours and allow to cool
- Filter using whatmann's filter paper.

5. **Dilution/ Deionization**

- Make volume (of digested sample) into 20ml using deionized water

6. **Analytical method:** Atomic Absorption Spectrophotometry (AAS)

7. **Computation of element concentration**

Assuming the result obtained from AAS analysis was **X** conc.ppm for sample 1. To determine the concentration of element in parts per million (ppm) or mg (of element)/kg (of tissue), the following steps were observed:

Sample = $\frac{\text{X x 20ml (disolution factor)}}{\text{0.25g (Sample weight in 1ml of homogenized tissue)}}$ = A

Blank sample = $\frac{\text{Y x 20 ml (dissolution factor)}}{\text{2.3 ml (2 ml of } HNO_3 \text{ and 0.3 ml of } H_2O_2\text{)}}$ = B

Total concentration of element in tissue (ppm or mg/kg) = A-B

APPENDIX VI

TISSUE PROCESSING- THE ROUTINE AUTOMATIC PROCESS

1. **Fixation** in formol saline/ Bouin's fluid lasted for 48 hours
2. **Washing** in running water if necessary
3. **Dehydration** in grades of alcohol
    - 70% alcohol for 3 hours
    - 90% alcohol for 3 hours
    - First change absolute (100%) alcohol for 1 hour
    - Second change absolute (100%) alcohol for 1 hour
    - Third change absolute (100%) alcohol for 2 hours
    - Fourth change absolute (100%) alcohol for 2 hours
4. **Clearing**
    - Put in pure xylene first change for 1.5 hours
    - Pure xylene second change for 2.5hours
5. **Infiltration**
    - First change in pure paraffin (wax bath) 3 hours
    - Second change in pure paraffin (wax bath) 3 hours
6. **Embed** in paraffin
7. **Microtomy**

(Drury, 1967)

APPENDIX VII

Determination of Intramitochondrial accumulation of 8-Hydroxy-2-deoxyguanosine (8-OHdG)

Intra-mitochondrial accumulation of 8-OHdG was measured as the indictor of mtDNA oxidative damage using Highly Sensitive 8-OHdG Check ELISA Kits. Mitochondrial DNA was isolated using the method of Mecocci *et al*. (1994). Hippocampus or cortex was homogenized in buffer (pH 7.5) containing 0.21 M mannitol, 0.07 M sucrose, 0.05 M Tris–HCl, 0.2 M EDTA and 3mM CaCl2. A centrifugation at 1500 ×g for 15 min was performed, the supernatant was collected and centrifuged at 1500 ×g for 10 min again, then the resulting supernatant was

again centrifuged at 14,000 ×g for 20 min. The deposit was collected and resuspended in Tris–EDTA buffer (pH 7.4). SDS (2%) and 400 μg/ml proteinase K were added to lyse the cells. Samples were incubated at 37 °C for 4 h. After three extractions with high purity distilled phenol and chloroform-isoamyl alcohol, mtDNA was precipitated with 1/10 volume of 3 M sodium acetate (pH 7.4) and 2 volumes of ethanol at −20 °C

overnight. Isolated mtDNA was digested with DNase I (200 U/mg DNA), Nuclease P1 and alkaline phosphatase (10 U/mg DNA) in the presence of 40mM Tris–HCl (pH 8.5) containing 10mM MgCl2. Samples were incubated for 4 h at 37 °C, then the kits were used to determine the level of 8-OHdG (Ding and Yang, 2010).

APPENDIX VIII

Determination of Biomarkers of Apoptosis

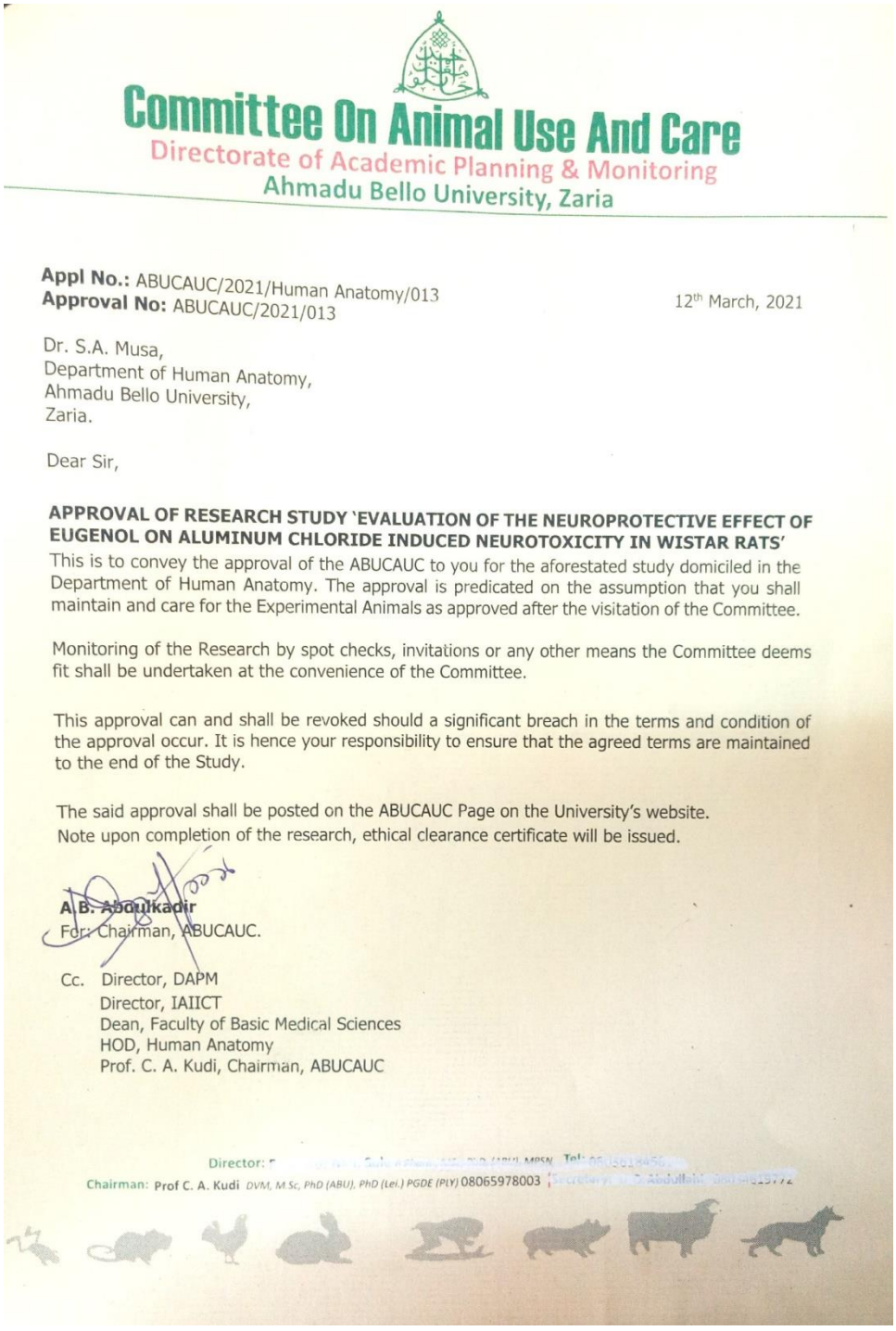
Caspase-3 enzymatic activity was measured using commercially available rat caspase-3/CPP32 colorimetric assay kit (supplied by WKEA Med Supplies Corp., China, and manufactured by Fine Test china) according to the manufacturer's instruction. The enzymatic reaction for caspase-3 activity was carried out in a 96-well microplate. Each reaction required 50 μl of sample (containing approximately 50 μg of total protein). A 50 μl of 2X Reaction Buffer (containing 10 mM DTT) was added to each sample. Then, a 5 μl of 4 mM caspase-3 substrate, DEVD-pNA (final concentration: 200 μM) was added to each reaction well. The reaction mixtures were mixed well and incubated for 2 h at 37°C. The absorbance was measured using a plate reader at a wavelength of 405 nm. Caspase-3 activity was reported as optical density (OD) measurement at 405 nm (Gilliams-Francis *et al*., 2003).

Tissue levels of Bax and BCl-2 were determined by the ELISA method according to the manufacturer's manual (R&D system Inc). Rat testis was homogenized (1/10) in normal saline and stored at −80°C. Samples were treated with cell lysis buffer modified with PMSF (phenylmethanesulphonylfluoride) and PIC (protease inhibitor cocktail) prior to the assay. Samples were further diluted in assay buffer (provided in the kit). After pipetting 100 µl assay buffer to all wells, 100 µl of sample/standard were added to the wells. The plate was sealed and incubated at room temperature on a plate shaker for 1 h. The wells were washed 5 times with wash buffer and 100 µl of Bax/Bcl-2 antibody was added to each well except blank. Following 1 hr incubation at room temperature, the plate was washed 5 times with wash buffer and 100 µl of conjugate added to all wells except blank. The plate was sealed and incubated for 30 min at room temperature. Well contents were emptied and washed 5 times in wash buffer. 100 µl of

substrate was added to each well and color allowed to develop. After 30 min, stop solution was added. The plate was read on an ELISA Plate Reader at OD 450 nm. Linear standard curves were generated in assay buffer to calculate the concentration of Bax and BCl-2 respectively (Al-Azemi et al.,2010）.

APPENDIX IX

ETHICAL APPROVAL



Committee On Animal Use And Care
Directorate of Academic Planning & Monitoring
Ahmadu Bello University, Zaria

Appl No.: ABUCAUC/2021/Human Anatomy/013
Approval No: ABUCAUC/2021/013

12th March, 2021

Dr. S.A. Musa,
Department of Human Anatomy,
Ahmadu Bello University,
Zaria.

Dear Sir,

APPROVAL OF RESEARCH STUDY 'EVALUATION OF THE NEUROPROTECTIVE EFFECT OF EUGENOL ON ALUMINUM CHLORIDE INDUCED NEUROTOXICITY IN WISTAR RATS'

This is to convey the approval of the ABUCAUC to you for the aforestated study domiciled in the Department of Human Anatomy. The approval is predicated on the assumption that you shall maintain and care for the Experimental Animals as approved after the visitation of the Committee.

Monitoring of the Research by spot checks, invitations or any other means the Committee deems fit shall be undertaken at the convenience of the Committee.

This approval can and shall be revoked should a significant breach in the terms and condition of the approval occur. It is hence your responsibility to ensure that the agreed terms are maintained to the end of the Study.

The said approval shall be posted on the ABUCAUC Page on the University's website.
Note upon completion of the research, ethical clearance certificate will be issued.

A.B. Abdulkadir
For: Chairman, ABUCAUC.

Cc. Director, DAPM
Director, IAIICT
Dean, Faculty of Basic Medical Sciences
HOD, Human Anatomy
Prof. C. A. Kudi, Chairman, ABUCAUC

Director: [illegible]
Chairman: Prof C. A. Kudi DVM, M.Sc, PhD (ABU), PhD (Lei.) PGDE (PLY) 08065978003